



Relativistic Coupled Cluster theory for excited states at a general excitation rank. Applications to diatomic molecules.

Mickaël Hubert

► To cite this version:

Mickaël Hubert. Relativistic Coupled Cluster theory for excited states at a general excitation rank. Applications to diatomic molecules.. Quantum Physics [quant-ph]. Université Paul Sabatier Toulouse III, 2013. English. ⟨NNT : TOULIII 9981635⟩. ⟨tel-01071467⟩

HAL Id: tel-01071467

<https://hal.science/tel-01071467v1>

Submitted on 14 Oct 2014

HAL is a multi-disciplinary open access archive for the deposit and dissemination of scientific research documents, whether they are published or not. The documents may come from teaching and research institutions in France or abroad, or from public or private research centers.

L'archive ouverte pluridisciplinaire **HAL**, est destinée au dépôt et à la diffusion de documents scientifiques de niveau recherche, publiés ou non, émanant des établissements d'enseignement et de recherche français ou étrangers, des laboratoires publics ou privés.



HAL Authorization



THÈSE

En vue de l'obtention du

DOCTORAT DE L'UNIVERSITÉ DE TOULOUSE

Délivré par : *l'Université Toulouse 3 Paul Sabatier (UT3 Paul Sabatier)*

Présentée et soutenue le 27/06/2013 par :

MICKAËL HUBERT

**Relativistic Coupled Cluster theory for excited states at a general
excitation rank. Applications to diatomic molecules.**

JURY

CHRISTOPH MEIER
JULIEN TOULOUSE
LUCAS VISSCHER
TIMO FLEIG

Professeur d'Université
Maître de conférence
Professeur d'Université
Professeur d'Université

Président du jury
Examineur
Rapporteur
Directeur de thèse

École doctorale et spécialité :

SDM : Physique de la matière - CO090

Unité de Recherche :

Laboratoire de Chimie et de Physique Quantique (UMR 5626)

Directeur de Thèse :

Timo FLEIG

Rapporteurs :

Lucas VISSCHER et Christof HÄTTIG

Relativistic Coupled Cluster theory for excited states at a general excitation rank. Applications to diatomic molecules.

Abstract

This thesis focuses on methodological developments of the theoretical evaluation of the quantum and relativistic energy of electronically excited states of an atom or a molecule. The wave-function method Coupled Cluster (CC) is currently one of the most accurate methods to calculate these states for many-body systems. The implementation presented is based on the many-body relativistic 4-component Dirac-Coulomb Hamiltonian and a Coupled Cluster wave function at arbitrary excitation rank. The excited states are evaluated using linear response theory by diagonalizing the Coupled Cluster Jacobian matrix. The work focuses on the evaluation of these second-quantized elements using a new commutator-based algorithm, and on its adaptation to a Dirac 4-component relativistic formalism. Finally, I present some applications of the code to challenging diatomic molecules.

—

Théorie "Coupled Cluster" relativiste pour les états excités au rang d'excitation général. Applications aux molécules diatomiques.

Résumé

Cette thèse s'articule autour de développements méthodologiques sur l'évaluation théorique des énergies quantiques et relativistes d'état électroniquement excité d'atome ou de molécule. La méthode basée sur la fonction d'onde "Coupled Cluster" (CC) est à l'heure actuelle, une des méthodes les plus précises pour calculer ces états pour les systèmes à N-corps. L'implémentation présentée est basée sur un Hamiltonien relativiste à N-corps : Dirac-Coulomb à 4 composantes et une fonction d'onde "Coupled Cluster" au rang d'excitation arbitraire. Les états excités sont évalués via la théorie de la réponse linéaire, en diagonalisant la matrice Jacobienne Coupled Cluster. L'accent des travaux se porte sur l'évaluation de ses éléments en seconde quantification via un nouvel algorithme basé sur les commutateurs, et sur son adaptation au formalisme relativiste de Dirac à 4 composantes. Enfin, des applications du code à des molécules diatomiques non triviales seront présentées.

Remerciements

Je remercie Fernand Spiegelman, directeur du Laboratoire de Chimie et Physique Quantique, pour m'avoir accueilli dans d'excellentes conditions au laboratoire pour réaliser ma thèse et pour m'avoir permis de participer à nombre d'écoles thématiques et congrès scientifiques qui ont affûté mes compétences. Je remercie également l'ensemble des membres du laboratoire pour leurs encouragements et conseils ainsi que pour leur accueil chaleureux. Je remercie aussi les doctorants et post-doctorants de l'IRSAMC avec qui j'ai eu la chance de partager de bons moments.

Je tiens à remercier également ma marraine de thèse Mai Dinh pour ses précieux conseils et ses encouragements, je te remercie aussi pour tes excellents travaux dirigés de mathématiques durant mes premières années de faculté.

Je remercie le département de génie mathématiques pour m'avoir accueilli à l'INSA en tant que moniteur, cette année d'enseignement m'a beaucoup apporté. Je remercie Marion pour cette année de vacation en école d'architecture très enrichissante, ce fût un plaisir de travailler avec toi.

Je voudrais remercier vivement mon directeur de thèse, ou devrais-je dire mon mentor, le professeur Timo Fleig qui m'a énormément apporté durant mon stage de M2 et ces quatre années de thèse, ta patience, ta pédagogie et tes grandes compétences scientifiques ont contribué à faire de cette thèse une passionnante expérience de recherche scientifique.

Of course I am thankful to Jeppe Olsen for his great help with the Coupled Cluster algorithm and well, for his kindness. I want to thank also Stefan Knecht for his help with the KRCI calculations and Lasse K. Sørensen for his help with the code and for his quick answers to my (numerous) mails. I want to thank all the **DIRAC** community for an annual stimulating meeting in Odense.

En particulier j'aimerais remercier Anthony Scemama et Radovan Bast pour leur aide précieuse en programmation et en informatique. Un grand merci également à Trond Saue pour son aide avec le formalisme des quasi-particules et pour ses nombreux encouragements et conseils. Merci à Jessica Loras pour une collaboration scientifique stimulante.

I am grateful to my thesis referees Christof Hättig and Lucas Visscher. I want to thank my defense jury for a very interesting discussion after the presentation. Je

suis également très reconnaissant envers mon examinateur Julien Toulouse pour sa lecture très détaillée du manuscrit et pour ses remarques et corrections constructives. Merci également à toute les personnes qui sont venues assister à ma soutenance de thèse et/ou au pot, j'ai apprécié votre soutien.

J'aimerais remercier les enseignants qui ont contribué à ma réussite, je leur serai à jamais reconnaissant. Je remercie chaleureusement mes parents Cathy et Hervé, ma sœur Jennifer et mon frère Yoann pour leur soutien, leur amour et pour avoir cru en moi tout au long de mes études, en particulier j'aimerais remercier ma mère pour avoir toujours essayé de me donner confiance en moi, ma chère maman je te dois ma réussite.

Ces années de thèse n'auraient pas été les même sans ces personnes en or que sont mes amis, je tiens à leur communiquer toute ma gratitude et mon affection. Merci à Paul pour ces fous-rires parfois en lieu inadapté, Emma parce que tu es 'jtée', Tof pour ses challenges toujours équilibrés et ces nombreuses soirées tonton. Merci à Cha pour ta joie de vivre quotidienne et ta gestion de l'espace personnel inégalée, merci à mon Fafounet (CUIR bzz bzz) et à mon Jipi pour ces bon moments passés ensemble. Merci à toi mon ouistiti pour ton amitié et ton humour, merci à Élise pour sa folie et sa bonne humeur, merci à Vinc' pour cette découverte des alpes à ski alimentée à la Chartreuse, bref merci à vous mes loulous. J'aimerais également remercier mes tarés de métalleux, Alex, Xavier et Flo pour ces longues années d'amitié, de rires, de Rock et d'expérience toujours saines et vertueuses, merci à Mag et Clem pour ces repas animés à l'OMP et ces concerts de type : machine à laver avec des clous. Merci à toi, mon vieil ami Yohann, pour m'avoir transmis tes névroses et ta stabilité émotionnelle.

Laurence, je te remercie du fond du cœur, j'ai passé cinq années formidables avec toi, ton soutien et ton amour m'ont tant apporté, nos chemins ce sont séparés et je te souhaite le meilleurs.

À ma mère,

CONTENTS

I. Relativistic quantum theory of the electron	6
A. The Dirac equation	6
1. The Schrödinger-like formulation	6
2. The Lorentz covariant formulation	7
B. The Dirac equation solutions	7
1. The electronic and positronic wave functions	8
2. The spatio-temporal separation of the wave function	10
C. The coupling with the electromagnetic field	11
D. The Dirac hydrogen atom	12
E. The Pauli Equation	15
II. Relativistic many body theory	20
A. The electron-electron relativistic interaction	20
1. The bielectronic interaction potential	21
2. The multi-electronic Dirac-Coulomb Hamiltonian	22
3. Spin-free and Lévy-Leblond Hamiltonian	23
B. Tools for relativistic many-body theory	24
1. Second quantization	24
2. LCAO - Basis sets	25
3. Double group point symmetry	27
4. Kramers time-reversal symmetry	28
5. Spinor strings	31
C. Methods for the relativistic many-body problem	32
1. Dirac-Hartree-Fock (DHF)	32
2. Integral transformation	33
3. Correlation energy - The correlated wave function	33
4. Generalized Active Spaces	36
5. Normal-ordered second-quantized operators	38
6. The particle-hole formalism	39
7. The contraction concept and the Wick theorem	40
8. The pure-correlation electronic Hamiltonian	41

III. Coupled Cluster Theory	44
A. Coupled Cluster wave function	44
1. General aspects	45
2. Hierarchy of excitation levels	47
3. The relativistic GAS-CC wave function ansatz	48
4. The Fermi vacuum $ \Phi\rangle$	50
5. Truncated models and equivalence FCC/FCI	52
6. The GAS parametrization	52
B. The ground state coupled cluster energy	55
1. The projected unlinked and linked equations	55
2. The energy equation	56
3. The amplitude equations	58
C. Excited-state coupled cluster energies	61
1. The Coupled Cluster Jacobian matrix	61
2. Commutator-based Coupled Cluster Jacobian implementation	62
3. Comparison with the ci-driven algorithm	66
IV. Applications	70
A. Relativistic CI-driven Coupled Cluster applications to the silicon atom and to the molecules AsH, SbH and BiH.	70
B. Spin-free commutator-based GAS Coupled Cluster applications to ScH spectroscopy.	88
C. Relativistic commutator-based GAS-CC for excited states	118
1. Carbon tests	118
D. Technical aspects - input	119
1. Spin-orbit-free or Lévy-Leblond commutator-based GAS-LRCC	120
2. Relativistic 4-component Dirac-Coulomb commutator-based GAS-LRCC	122
V. Résumé en Français	128
A. Introduction	128
B. Théorie relativiste de l'électron	130
1. L'équation de Dirac	131

2. Les solutions de l'équation de Dirac	131
3. La séparation spatio-temporelle et le champ électromagnétique externe	133
C. La théorie à N-corps relativiste	134
1. L'Hamiltonien multi-électronique de Dirac-Coulomb	135
2. Outils méthodologiques	136
D. Le modèle "Coupled Cluster"	136
1. L'opérateur CC - Hiérarchie d'excitation	138
2. La fonction d'onde CC - Le vide de Fermi	139
3. La paramétrisation des espaces actifs généralisés (GAS)	141
4. Les équations CC de l'état fondamental	143
5. Les équations CC pour les états excités	144
E. Conclusion	145
VI. Appendix for Relativistic quantum theory of the electron	150
A. The Dirac equation construction	150
1. The momentum-energy equation - The Klein-Gordon equation	151
2. The continuity equation	155
3. Lorentz covariance	156
B. The Dirac solution derivation	160
1. The free particle	161
2. The bi-spinor reformulation	162
3. Probability density	165
C. The Hydrogen-like problem	165
1. Equations of the problem	165
2. The total angular momentum	166
3. The spin-orbit coupling	166
4. The relativistic analog of the azimuthal quantum number : κ	168
5. Operator 4-component generalization	169
6. The 4-spinor ansatz	170
7. The angular wave functions	171
8. The radial stationary Dirac equation	171
9. Energy Eigenvalue	178

D. The Pauli Equation	179
VII. Appendix for relativistic many body theory	185
A. The pure correlation electronic Hamiltonian	185
VIII. appendix for Coupled Cluster theory	188
A. The Baker-Campbell-Hausdorff truncation	188
Références	190

Introduction

Electronically excited states of small molecules containing heavy atoms play an important role in many research areas of modern physics. In the (ultra-)cold molecular sciences [1] there is an increasing interest in experimentally generating molecules in their electronic and rovibrational ground state by photoassociation *via* an electronically excited state [2]. In astrophysics of stars [3], the understanding of collision processes in stellar atmospheres [4] involves the knowledge of molecular excited states, including both main group and transition metal atoms. As an example from fundamental physics, various extensions to the standard model of elementary-particle physics postulate electric dipole moments (EDM) of leptons [5]. Modern experiments search for the electron EDM in an electronically excited state of diatomic molecules and molecular ions containing a heavy atom [6]. The accurate determination of the electronic structure in excited states of the relevant molecules is of crucial importance in all of these and other research fields.

At present many theories are available for treating electronically excited states, with always a compromise between accuracy and applicability. For large scale calculation the Time-Dependent-Density-Functional-Theory (TD-DFT) method can address excitation energies [7], but for a high accuracy treatment wave function theories (WFT) are more adapted. Among the main WFT methods we distinguish Configuration Interaction (CI), Multi-Configuration Self-Consistent Field (MCSCF), Coupled Cluster (CC), and Perturbation Theory (PT) [8]. The most accurate electronic-structure approach to the calculation of electronically excited states in atoms and molecules to date is the Coupled Cluster (CC) method. Recent progress, including developments for excited states [9], has been documented in a monograph [10] covering this highly active field of many-body theory.

Numerous implementations using truncated wave operators exist, typically at the excitation rank of CC Doubles or sometimes CC Triples and Quadruples excitations for the ground-state cluster amplitudes. Some representative examples are Fock-Space (FS) CC [11], Equation-Of-Motion (EOM) CC [12], Complete Active Space (CAS) state-specific CC [13], CC3 response theory [14], or the CC2-R12 model [15]. CC approaches of general excitation rank for molecular excited-state calculations are less abundant. Such implementations have been reported by Kállay et al. [16] and Hirata et al. [17]. CC methods capable of including full iterative Triple (and higher) excitations are of great interest in molecular physics, for example, when

complete potential-energy curves of diatomic molecules are sought for which cannot be obtained with the CCSD(T) method [18]. A viable alternative is CC models which allow for active-space selected higher excitations while keeping the number of external particles limited in the cluster operators [19].

When turning to the treatment of heavy elements where relativistic generalizations of these methods are required, the general challenge of implementing such methodology becomes manifest in their scarcity (see [8] and references therein). To date, the only relativistic CC methods for the treatment of molecular excited states are the Intermediate Hamiltonian Fock-Space CC method (IH FSCC) [20, 21] by Vischer, Eliav, and co-workers and higher-order correlation methods [22] by Hirata and co-workers using the Equation-of-Motion (EOM) CC formalism [23, 24]. IH FSCC is limited in that it is not generally applicable and the treatment of excitation ranks higher than Doubles in the wave operator is currently not possible. The method of Hirata et al. is restricted to the use of two-component valence pseudospinors based on a Relativistic Effective Core Potentials (RECP) including spin-orbit interaction [25]. Such an approach lacks both the rigor and the flexibility of all-electron four-component methods, the latter use a frozen-core approximation for the electrons of atomic cores.

The developments presented in this manuscript aim at a rigorous assessment of the electronically excited states of small molecules including heavy elements, a general challenge in the relativistic electronic many-body problem until today [8]. Central elements of our methodology are a rigorous treatment of special relativity using four-component all-electron Dirac Hamiltonians at all stages of the calculation, methods of general excitation rank in the wave operator, and methods based on expansions of the wavefunction in a basis of strings of particle creation operators in second quantization, so-called string-based methods [26–28]. The use of Linear Response (LR) theory mixed with the Generalized Active Space (GAS) framework brings a significant flexibility to treat excited states. Elaborate wave functions can be set up which allow for quasi multi-reference treatments with only a single reference determinant. These methods are called Single-Reference Multi-reference Coupled Cluster (SR-MRCC) [13, 29] thereby we avoid many problems arising from a true MRCC method like redundancy problems, (over-) or under-specification of the equation system. We thus benefit with our single-reference formalism from a number of

equations that is equal to the number of CC amplitudes and the commutation of the cluster excitation operators. Finally, successful applications to diatomic molecular systems of interest are demonstrated in our references.

The manuscript is organized as follows : in the first chapter, I will introduce the relativistic quantum theory for one electron, in particular I will focus on the Dirac equation and discuss its properties. Then I will discuss its solutions, some new arising concepts compared to standard quantum physics and its coupling with an external electromagnetic field. I will finish this first chapter by discussing the Dirac hydrogen atom and the Pauli equation to show what is hidden in the four-component formalism. In the second chapter, many-body theory is discussed at a relativistic level. I will start by presenting our approximation to treat electron-electron interaction and I will show the related relativistic many-body Hamiltonian. Then I will briefly present some typical tools used in many-body theory and I will finish this chapter with a quick presentation of the methods we employed to address the many-electron problem. The third chapter is devoted to the GAS-CC theory. I will present the CC wave function and our way to solve the ground-state equations. Then I will focus on the main purpose of this project, the excitation energies and the commutator-based CC algorithm, I will finish with a comparative discussion between the new and the previous algorithm. Chapter four reports our two publications, the last part is about the very recently implemented relativistic commutator-based GAS-CC algorithm for excited states. I will show some preliminary tests on the carbon atom with the new method. The reader can find some details about the relativistic formalism and on various mathematical proofs in the appendix.

Chapter I

Relativistic Quantum Theory of the Electron

I. RELATIVISTIC QUANTUM THEORY OF THE ELECTRON

The Coupled Cluster many-body method implemented and presented in this manuscript aims to describe electronic excitation energies for molecules by taking into account relativistic effects. Such effects are responsible for spin-orbit splitting of Russell-Saunders ^{2S+1}L states in atoms, *i.e.* of the fine structure which becomes more and more important in systems with heavy nuclei. These effects can of course be treated separately with perturbation theory in an additive manner by using Schrödinger equation but one will miss the coupling between the relativistic effects and the electronic correlation. The correlation-relativity coupling can represent several hundreds of cm^{-1} for differential energies of excited state in heavy systems. The Dirac theory of the electron [30] provides a perfectly suited framework for this purpose, it combines a proper quantum mechanical description with special relativity principles. The methodological developments will be based on the Dirac equation. A rather concise presentation on the Dirac equation structure and its solutions is given in this chapter. We will also look at the hydrogen-like atom problem which is of crucial importance for moving to the many-body problem, it provides also a good way to introduce a part of the Dirac formalism and the various associated quantum numbers. We will finish this first chapter by establishing the Pauli Hamiltonian approximation to show the different one-electron relativistic contributions arising from the Dirac equation. To avoid to the reader a heavy sequence of equation, calculation details are given in the appendix V E and only the main results will be shown.

A. The Dirac equation

1. The Schrödinger-like formulation

The Dirac equation of the electron can be written as follows

$$i\hbar\frac{\partial\psi}{\partial t} = \left[\frac{\hbar c}{i} \left(\hat{\alpha}_1 \frac{\partial}{\partial x^1} + \hat{\alpha}_2 \frac{\partial}{\partial x^2} + \hat{\alpha}_3 \frac{\partial}{\partial x^3} + \hat{\beta} m_0 c^2 \right) \right] \psi \quad (1)$$

Where ψ is a 4-component wave function which depends on time and space coordinates (t, x^1, x^2, x^3) and the $\hat{\alpha}$ Dirac matrices are constructed from the Pauli matrices,

the $\hat{\beta}$ matrix is composed of 2×2 unity matrices (see (217) in the appendix V E). It should be noticed that the Dirac equation (1) contains by construction the spin information in contrast to the Schrödinger equation. One can conclude that the spin has a relativistic origin.

2. The Lorentz covariant formulation

One can wonder if, as desired by special relativity, the whole formalism is Lorentz covariant, *i.e.* invariant when changing from an initial reference frame to an other with a Lorentz transformation. This fact is demonstrated in the appendix (VI A 3) for an electron state measured in two inertial reference frame (without external field) with an other representation of the Dirac equation which should be mentioned, the covariant form

$$\left(i\hbar \hat{\gamma}^\mu \frac{\partial}{\partial x^\mu} - m_0 c \mathbb{1}_4 \right) \psi = 0 \quad (2)$$

Where the space and time coordinates are treated on the same footing within the Lorentz metric, the covariant operator is $p = \{ i\hbar \frac{\partial}{\partial x^\mu} \}$, the 4-component momentum. The matrices $\hat{\gamma}$ are built from the Dirac matrices (see the appendix VI A 3).

In the next part we will turn to the Dirac solutions and discuss some aspects of the 4-component wave function.

B. The Dirac equation solutions

In this part we will focus on the Dirac solution for the free particle directly, however the details of the derivation are given in the appendix VI B.

$$i\hbar \frac{\partial \psi}{\partial t} = \hat{H} \psi = \left(c \hat{\boldsymbol{\alpha}} \cdot \hat{\mathbf{p}} + m_0 c^2 \hat{\beta} \right) \psi \quad \Leftrightarrow \quad \left(i\hbar \hat{\gamma}^\mu \frac{\partial}{\partial x^\mu} - m_0 c \mathbb{1}_4 \right) \psi = 0 \quad (3)$$

1. The electronic and positronic wave functions

The two formulations in (3) are equivalent and lead to two pairs of 4-component solution the free particle

$$\psi_+^{(1)}(x) = \mathcal{N} \begin{pmatrix} 1 \\ 0 \\ \frac{p^3}{p^0+m_0c} \\ \frac{p^1+ip^2}{p^0+m_0c} \end{pmatrix} e^{-\frac{i}{\hbar}p_\mu x^\mu} \quad \text{and} \quad \psi_+^{(2)}(x) = \mathcal{N} \begin{pmatrix} 0 \\ 1 \\ \frac{p^1-ip^2}{p^0+m_0c} \\ \frac{-p^3}{p^0+m_0c} \end{pmatrix} e^{-\frac{i}{\hbar}p_\mu x^\mu} \quad (4)$$

$\psi_+^{(1)}(x)$ and $\psi_+^{(2)}(x)$ are associated to a positive energy $E = \sqrt{\mathbf{p}^2c^2 + m_0^2c^4}$

$$\psi_-^{(1)}(x) = \mathcal{N} \begin{pmatrix} \frac{p^3}{p^0-m_0c} \\ \frac{p^1+ip^2}{p^0-m_0c} \\ 1 \\ 0 \end{pmatrix} e^{-\frac{i}{\hbar}p_\mu x^\mu} \quad \text{and} \quad \psi_-^{(2)}(x) = \mathcal{N} \begin{pmatrix} \frac{p^1-ip^2}{p^0-m_0c} \\ \frac{-p^3}{p^0-m_0c} \\ 0 \\ 1 \end{pmatrix} e^{-\frac{i}{\hbar}p_\mu x^\mu} \quad (5)$$

$\psi_-^{(1)}(x)$ and $\psi_-^{(2)}(x)$ are associated to a negative energy $E = -\sqrt{\mathbf{p}^2c^2 + m_0^2c^4}$

\mathcal{N} is a normalization factor $\mathcal{N} = \sqrt{\frac{|E|+m_0c^2}{2|E|}}$

The presence of negative energies requires a physical interpretation. An initial model, illustrated on the left in the figure 1, was the existence of a continuum of negative energy but this model leads to a matter collapse. For instance, with the hydrogen atom and this model, the 1s electron will be able to emit a photon to fall in a lower energy state an infinite number of times.

To fix this problem Dirac has introduced the hole theory [31]. In this model the negative energy states are occupied with (virtual) electrons. Dirac introduces the vacuum state which is by definition, the absence of real electron (electrons in positive energy states). In the absence of external fields, the vacuum represents the energetically lowest (negative) continuum which every state is occupied with electrons, we call it the electron sea (or the Dirac sea). The radiative catastrophe is avoided by virtue of the Pauli exclusion principle which is naturally applied in negative energy states. It should be noted that this electron sea remains virtual and experimentally undetectable as long as nothing perturbs it.

However an electron in a negative energy state can absorb a photon, if the absorbed photon energy is $\hbar\omega > 2m_0c^2$ then a negative energy electron can be excited into a positive energy state. In this case we get a real electron and a hole. This

hole behaves like a particle with a $+|q_e|$ charge because it can be annihilated by an electron with a $-|q_e|$ charge. The hole is interpreted as the positron first measured by Anderson [32], one of the biggest prediction of the Dirac equation. The electron-hole creation phenomenon is naturally identified to the electron-positron pair creation. The inverse phenomenon, *i.e.* an electron which fills a hole in a negative energy state is also possible. This occurrence is identified as the annihilation of an electron-positron pair (matter-antimatter annihilation). On the right in the figure 1 an illustration of the hole theory is shown.

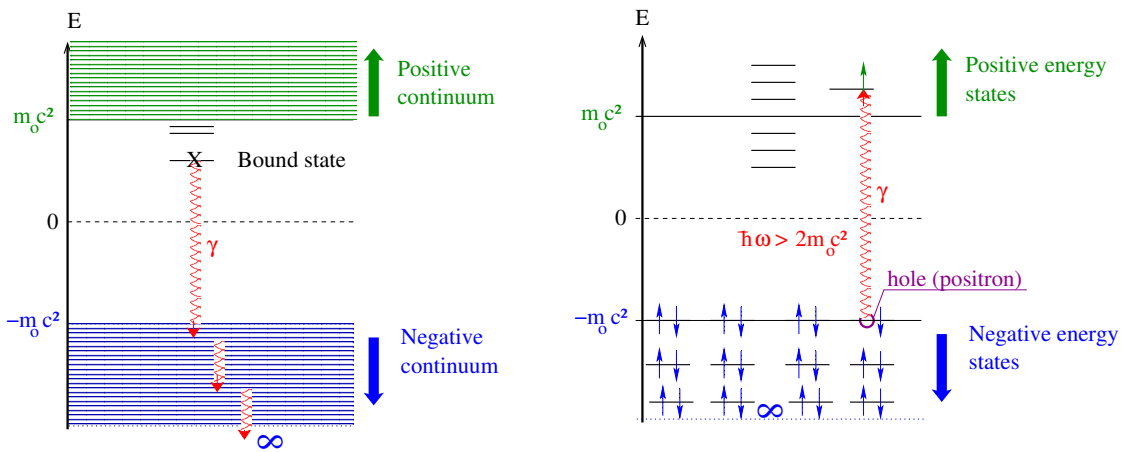


FIGURE 1. On the left the negative energy continuum which leads to the radiative catastrophe illustrated in red, on the right the Dirac sea (in blue) with the creation of a electron-positron pair.

The wave functions $\psi_+^{(1)}$ and $\psi_+^{(2)}$ in (4) both describe an electron of energy $E = \sqrt{\mathbf{p}^2 c^2 + m_0^2 c^4}$ and the wave function $\psi_-^{(1)}$ and $\psi_-^{(2)}$ in (5) both describe a positron associated to a negative energy $E = -\sqrt{\mathbf{p}^2 c^2 + m_0^2 c^4}$.

In the following we will work with the wave function $\psi_+^{(1)}$ and $\psi_+^{(2)}$ in (4) only. However this is a first approximation, if we do so we miss a part of quantum electrodynamic radiative corrections. It is shown in [33] that such corrections added in a perturbative fashion bring hundreds cm^{-1} for differential excited states energies in very heavy atoms (beyond actinide). The difference between these two wave functions can be more easily seen if we look at the free particle in the rest frame, *i.e.*

$p = \{\frac{E}{c}, 0, 0, 0\}$, we get these two electronic solutions

$$\psi_+^{(1)}(\mathbf{p} = 0) = \begin{pmatrix} 1 \\ 0 \\ 0 \\ 0 \end{pmatrix} e^{-\frac{i}{\hbar}Et} \quad \text{and} \quad \psi_+^{(2)}(\mathbf{p} = 0) = \begin{pmatrix} 0 \\ 1 \\ 0 \\ 0 \end{pmatrix} e^{-\frac{i}{\hbar}Et} \quad (6)$$

associated to a positive energy $E = m_0c^2$ (note that in this case $\mathcal{N} = 1$)

Let us introduce the 4-component spin operator $\hat{\mathbf{s}}_{4,z}$ such as

$$\hat{\mathbf{s}}_{4,z} = \hat{\mathbf{s}}_z \otimes \mathbb{1}_2 = \frac{\hbar}{2} \begin{pmatrix} \hat{\sigma}_z & 0 \\ 0 & \hat{\sigma}_z \end{pmatrix} \quad (7)$$

If we apply the operator (7) on the wave functions (6) we get

$$\begin{aligned} \hat{\mathbf{s}}_{4,z} \psi_+^{(1)}(\mathbf{p} = 0) &= \frac{\hbar}{2} \psi_+^{(1)}(\mathbf{p} = 0) \\ \hat{\mathbf{s}}_{4,z} \psi_+^{(2)}(\mathbf{p} = 0) &= -\frac{\hbar}{2} \psi_+^{(2)}(\mathbf{p} = 0) \end{aligned} \quad (8)$$

We recover the spin eigenvalue equations (8) with the eigenfunctions (6), the spin projection quantum number is $m_s = \frac{1}{2}$ for $\psi_+^{(1)}(\mathbf{p} = 0)$ and $m_s = -\frac{1}{2}$ for $\psi_+^{(2)}(\mathbf{p} = 0)$. The two wave functions describe two different spin projections, thus the spin arises naturally in the Dirac equation. One can find that the operator $\hat{\mathbf{s}}_{4,z}$ is included in the $\hat{\alpha}_3$ matrix.

Each solution is a 4-component wave function presented in (4) and (5) can thus describe both electrons and positrons for a given spin. From now on we will write them in the bispinor notation with a large and a small component.

$$\psi(\mathbf{x}, t) = \psi(x) = \begin{pmatrix} \psi_1(x) \\ \psi_2(x) \\ \psi_3(x) \\ \psi_4(x) \end{pmatrix} = \begin{pmatrix} \psi^L(x) \\ \psi^S(x) \end{pmatrix} \quad (9)$$

The reason for this notation is that the large component will be the dominant part of the wave function when describing an electron since $\|\mathbf{p}\| \ll mc$ (however not in the ultra-relativistic case).

2. The spatio-temporal separation of the wave function

Since we are interested in stationary energy states, the time-dependent part of the 4-component wave function ψ is not needed, (except when we use linear response

theory, we will come back to this point later on).

The 4-component relativistic wave function $\psi(x) = \psi(\mathbf{x}, t)$ is a function of a Lorentz 4-vector x but, however its separation into a spatial wave function $\psi(\mathbf{x})$ and a time wave function $\phi(t)$ such as

$$\psi(\mathbf{x}, t) = \psi(\mathbf{x})\phi(t) = \psi(\mathbf{x})e^{-\frac{i}{\hbar}Et} \quad (10)$$

must be applied carefully. The principal reason is that the Lorentz transformation mixes the spatio-temporal components (\mathbf{x}, t) from an inertial reference frame to another. Consequently this separation can be done only if we work in one inertial reference frame. As an example, the stationary-state study of atoms is possible in the inertial reference frame of the nucleus at rest. For molecules we will work in the Born-Oppenheimer inertial reference frame.

This separation allows us to treat the stationary states with a time independent Hamiltonian \hat{h}^D and a time independent wave function. Let us introduce the stationary Dirac equation

$$\hat{h}^D \psi(\mathbf{x}) = E\psi(\mathbf{x}) \quad \Rightarrow \quad \left(c\hat{\boldsymbol{\alpha}} \cdot \hat{\mathbf{p}} + \hat{\beta}m_0c^2 \right) \psi(\mathbf{x}) = E\psi(\mathbf{x}). \quad (11)$$

where $\hat{\boldsymbol{\alpha}}$ is a vector with the three cartesian components $\{\hat{\alpha}_1, \hat{\alpha}_2, \hat{\alpha}_3\}$ and we recover the relativistic energy E

$$E = \pm \sqrt{\mathbf{p}^2 + m_0c^2} \quad (12)$$

We use only the positive value of (12) when working with electronic wave functions. The solution of the energy eigenvalue equation (11) leads to the stationary solutions.

C. The coupling with the electromagnetic field

In order to treat atomic and molecular problems, we need to introduce an external electromagnetic field in the Dirac equation

$$(-i\hbar\hat{\gamma}^\mu\partial_\mu + m_0c\mathbb{1}_4) \psi(x) = 0 \quad (13)$$

To do so we use the minimal coupling principle (with $e = \frac{q_e}{4\pi\epsilon_0} = q_e$ in gaussian units), in other words, we add the electromagnetic potential 4-vector A to the 4-momentum

$\hat{p} :$

$$-i\hbar\partial_\mu \rightarrow -i\hbar\partial_\mu + \frac{e}{c}A_\mu = \begin{pmatrix} \hat{p}^0 + \frac{e}{c}A^0 \\ \hat{\mathbf{p}} - \frac{e}{c}\mathbf{A} \end{pmatrix} \quad \text{with} \quad A_\mu = \begin{pmatrix} A^0 \\ \mathbf{A} \end{pmatrix} \quad (14)$$

With \mathbf{A} the vector potential as $\mathbf{A} = \{A^1, A^2, A^3\}$ and A^0 the scalar electric potential, q_e is the electric charge. For stationary fields, the first component of the 4-vector (14) corresponds to the electric field propagation at the speed of light c , the three other components correspond to the magnetic field propagation at the speed of light c . We establish the Dirac equation including an external electromagnetic field

$$\left[\hat{\gamma}^\mu \left(-i\hbar\partial_\mu + \frac{e}{c}A_\mu \right) + m_0c\mathbb{1}_4 \right] \psi(x) = 0 \quad (15)$$

One can also find the Hamiltonian form in function of the matrix operators $\hat{\alpha}^k = \hat{\gamma}^0\hat{\gamma}^k$ and $\hat{\beta} = \hat{\gamma}^0$ (with $k \in \{1, 2, 3\}$) by multiplying equation (15) from the left with $\hat{\gamma}^0$

$$i\hbar\frac{\partial}{\partial t}\psi(x) = \left[c\hat{\boldsymbol{\alpha}} \cdot \hat{\mathbf{p}} - e\hat{\boldsymbol{\alpha}} \cdot \mathbf{A} + \hat{\beta}m_0c^2 + eV\mathbb{1}_4 \right] \psi(x). \quad (16)$$

In this form we distinguish $-e\hat{\boldsymbol{\alpha}} \cdot \mathbf{A}$ the coupling of an electron with an external stationary magnetic field $\mathbf{B}_{\text{ext.}}$ and eV the coupling of the electron with an external stationary electric field $\mathbf{E}_{\text{ext.}}$. It should be stressed that the equation (15) or (16) represents the interaction of an electron with an external field only if we treat all electromagnetic fields classically. If we use quantum electrodynamics (QED) where the electromagnetic field is quantized, the interaction with a given field is more complex, but it is possible to add a radiative correction term to the Dirac equation [33]. For the implementation presented in this manuscript, the field is treated as presented above without the radiative correction which represents a variable contribution depending on the system as discussed before in IB 1.

D. The Dirac hydrogen atom

The one-electron atom electronic energy states are crucial to approach the multi-electronic system, the electron in a nuclear potential problem can be solved analytically. The analytical results obtained open the way to multi-electronic atoms and molecules treatment. Only the main results will be shown, for more details the reader can consult the appendix VIC or the following books [34, 35].

The formalism established permits us to study the stationary states of the hydrogen-like atom; however several approximations are necessary. The nuclear structure will be neglected, it will be treated like a point charge which generates a coulombic potential. (However the method presented in this manuscript considers a finite-size nuclear model). The hyperfine coupling effect between the electron spin and the nuclear spin will not be taken into account. We will also neglect the nuclear motion by considering it fixed and the electromagnetic interaction between the nucleus and the electron will be considered as instantaneous, thus we neglect the nucleus-electron interaction retardation effects.

We want to establish the Dirac equation solutions for the stationary states of the hydrogen atom. As discussed in IB2 it is possible to separate the space and time variables of the wave function $\psi(x)$ to get a product of functions (10). We use this product with the Hamiltonian form of Dirac with a scalar potential $V = -\frac{Ze}{r}$, r being the electron-nucleus distance and Z the number of protons in the nucleus. Since there is no external stationary magnetic field, $\mathbf{A} = 0$, we get the following

$$\begin{pmatrix} \left[m_0 c^2 - \frac{Ze^2}{r} \right] \mathbb{1}_2 & c \hat{\boldsymbol{\sigma}} \cdot \hat{\mathbf{p}} \\ c \hat{\boldsymbol{\sigma}} \cdot \hat{\mathbf{p}} & \left[-m_0 c^2 - \frac{Ze^2}{r} \right] \mathbb{1}_2 \end{pmatrix} \begin{pmatrix} \psi^L(\mathbf{x}) \\ \psi^S(\mathbf{x}) \end{pmatrix} = E \begin{pmatrix} \psi^L(\mathbf{x}) \\ \psi^S(\mathbf{x}) \end{pmatrix} \quad (17)$$

in bispinor form. It can be seen in the appendix VIC3 that the spin-orbit operator ($\hat{\boldsymbol{\sigma}} \cdot \hat{\mathbf{l}}$) is included in the $\hat{\boldsymbol{\sigma}} \cdot \hat{\mathbf{p}}$ terms. The spin-orbit operator can be expressed as function of the usual quantum operators $\hat{\mathbf{j}}^2$, $\hat{\mathbf{l}}^2$ and $\hat{\mathbf{s}}^2$ related to, respectively, the total angular momentum, the azimuthal quantum number and the spin quantum number. It should be noted that only the total angular momentum quantum number j is a good quantum number for the Dirac equation, *i.e* its associated operator commutes with the Dirac Hamiltonian

$$[\hat{h}^D, \hat{\mathbf{j}}_4^2] = 0 \quad \text{with} \quad \hat{\mathbf{j}}_4^2 = \hat{\mathbf{l}}^2 \cdot \mathbb{1}_4 + \frac{\hbar}{2} \begin{pmatrix} \hat{\boldsymbol{\sigma}} & 0 \\ 0 & \hat{\boldsymbol{\sigma}} \end{pmatrix} \quad (18)$$

the 4-dimension adapted square total angular momentum operator.

If we solve the coupled differential equation system we obtain the energy states of the hydrogen-like atom in function of the principal quantum number n and j

$$E(Z, n, j) = \frac{m_0 c^2}{\sqrt{1 + \frac{Z^2 \alpha^2}{\left(n - j - \frac{1}{2} + \frac{1}{2} \sqrt{4j^2 + 4j + 1 - 4Z^2 \alpha^2} \right)^2}}} \quad (19)$$

Where we introduce Sommerfeld's fine-structure constant $\alpha = \frac{e^2}{\hbar c}$.

The fully solved system (17) gives also all desired wave functions, the reader can find the analytical wave function for the ground state in [34] and for the lowest lying states in [36]. As an example here is the analytical wave function for the ground state of the one electron atom $^1S_{1/2}$ (with $n = 1$, $j = \frac{1}{2}$ and $m_j = \frac{1}{2}$) in spherical coordinates

$$\psi_+^{(1)}(r, \theta, \varphi) = \frac{[2m_0 Z \alpha]^{\frac{3}{2}}}{\sqrt{4\pi}} \sqrt{\frac{1 + \sqrt{1 - Z^2 \alpha^2}}{2\Gamma(1 + 2\sqrt{1 - Z^2 \alpha^2})}} [2m_0 Z \alpha r]^{\sqrt{1 - Z^2 \alpha^2} - 1} e^{-m_0 Z \alpha r} \begin{pmatrix} 1 \\ 0 \\ \frac{i(1 - \sqrt{1 - Z^2 \alpha^2})}{Z \alpha} \cos(\theta) \\ \frac{i(1 - \sqrt{1 - Z^2 \alpha^2})}{Z \alpha} \sin(\theta) e^{i\varphi} \end{pmatrix} \quad (20)$$

Where Γ is a function resulting from the normalization condition.

The bound electronic energy states of the one electron atom depend on the quantum number j , consequently spin-orbit interaction splits $l > 0$ states (*i.e.* np, nd, nf, \dots energy states) into $j + \frac{1}{2}$ and $j - \frac{1}{2}$ states which are each degenerate $2j + 1$ times. In the Schrödinger picture we have an accidental degeneracy of n states regardless of l . The two energy pictures are illustrated in the figure 2, the various quantum number values characterizing the Dirac energy states can be found in table I. However, in the Dirac picture there is a degeneracy between nl_j and $n(l + 1)_j$ which is not the case in experiment, these levels are measured split due to the Lamb shift [37, 38], a QED effect of the order of $\alpha(Z\alpha)^4$.

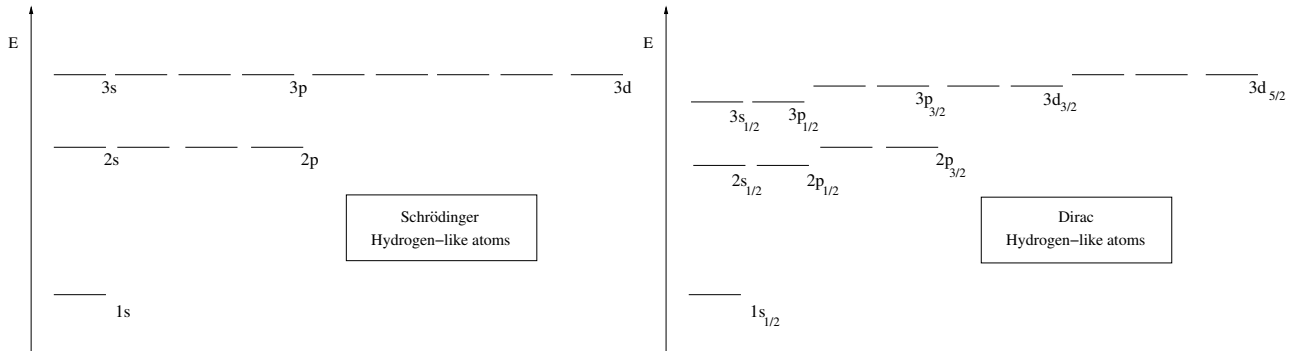


FIGURE 2. Difference between Schrödinger and Dirac energy levels of the one electron atom, the fine structure due to the coupling of spin and orbital momenta lifts the degeneracy between $j + \frac{1}{2}$ and $j - \frac{1}{2}$ states.

TABLE I. Summary table of quantum numbers and symbols used in atomic spectroscopy

Symbols	$s_{1/2}$	$p_{1/2}$	$p_{3/2}$	$d_{3/2}$	$d_{5/2}$	$f_{5/2}$	$f_{7/2}$	$g_{7/2}$	$g_{9/2}$
κ	-1	1	-2	2	-3	3	-4	4	-5
l	0	1	1	2	2	3	3	4	4
$j = \kappa - \frac{1}{2}$	1/2	1/2	3/2	3/2	5/2	5/2	7/2	7/2	9/2
Parity $(-1)^l$	+	-	-	+	+	-	-	+	+
Degeneracy	2	2	4	4	6	6	8	8	10
$(2 \kappa = 2j + 1)$									

E. The Pauli Equation

In this section we will present the Pauli Hamiltonian which results from an approximation of the Dirac Hamiltonian. Our implementation is not based on it, however it provides an elegant way to show the various relativistic contributions where each term will be explicitly associated to an one electron effect. The following Pauli Hamiltonian is obtained without external magnetic field by eliminating the small component ψ^S and renormalizing the large component ψ^L via a transformation, the procedure details are in the appendix VID and can also be found in the K. Dyall's book [39] or in the M. Reiher book [34].

$$\hat{H}^{\text{Pauli}} = \hat{T} + V - \frac{1}{8m_0^3c^2}\hat{\mathbf{p}}^4 + \frac{\hbar^2}{8m_0^2c^2}(\nabla^2V) + \frac{\hbar}{4m_0^2c^2}\hat{\boldsymbol{\sigma}} \cdot (\nabla V) \times \hat{\mathbf{p}} \quad (21)$$

The first term \hat{T} is the nonrelativistic kinetic energy operator, always positive.

The second one V is the nonrelativistic potential energy operator depending on the nucleus, for example this one (23)

The third term $-\frac{\hat{\mathbf{p}}^4}{8m_0^3c^2}$ is the mass-velocity which gives a negative relativistic contribution to the energy. This is a scalar correction and can be seen in the Taylor expansion of the free particle relativistic energy

$$E = \sqrt{\mathbf{p}^2c^2 + m_0^2c^4} = m_0c^2\sqrt{1 + \left(\frac{\hat{\mathbf{p}}}{m_0c}\right)^2} = m_0c^2 + \frac{\hat{\mathbf{p}}^2}{2m_0} - \frac{\hat{\mathbf{p}}^4}{8m_0^3c^2} + \dots \quad (22)$$

where we recover the rest mass energy, the nonrelativistic kinetic energy and the mass-velocity term which comes from the variation of the mass with the velocity,

it is a relativistic correction of the mass. The valence contribution of this effect is important for energy differences as excitation energies and potential curves, the table II gives an order of magnitude of mass-velocity correction.

TABLE II. Contribution of mass-velocity correction compared to the nonrelativistic kinetic energy T in function of the absolute electron velocity $||\mathbf{v}||$

$ \mathbf{v} $	% of T
$0.1c$	-0.25
$0.4c$	-4
$0.6c$	-9

The fourth contribution $\frac{\hbar^2}{8m_0^2c^2}(\nabla^2V)$ is called the Darwin term, we can write this operator in a more explicit manner by considering a point nuclear potential then

$$V = -\frac{Ze^2}{r} \quad , \quad \nabla V = \frac{Ze^2}{r^3}\mathbf{r} \quad , \quad \nabla^2V = 4\pi Ze^2\delta(\mathbf{r}) \quad (23)$$

The Darwin operator can be written

$$\frac{\hbar^2}{8m_0^2c^2}(\nabla^2V) = \frac{\hbar^2\pi Ze^2}{2m_0^2c^2}\delta(\mathbf{r}) \quad (24)$$

This is again a scalar term which have no nonrelativistic analog. It becomes important for the electron closed to the nucleus like for s type functions because of its Dirac delta function centered at the atomic nucleus, it is called a contact term. This scalar relativistic correction does not depend on $\hat{\mathbf{p}}$ but depends on the nuclear charge Z therefore, it becomes important for heavy systems. The Darwin term is also the cause of the zitterbewegung phenomena, *i.e.* the trembling motion of the electron around its classical location $\langle \mathbf{x} \rangle$, the reader can find much more details about this in the W. Greiner book [40].

The last term in the Pauli Hamiltonian (21) can be written as

$$\frac{\hbar}{4m_0^2c^2}\hat{\boldsymbol{\sigma}} \cdot (\nabla V) \times \hat{\mathbf{p}} = \frac{\hbar Ze^2}{4m_0^2c^2r^3}\hat{\boldsymbol{\sigma}} \cdot \hat{\mathbf{l}} = \frac{2Ze^2}{4m_0^2c^2r^3}\hat{\mathbf{s}} \cdot \hat{\mathbf{l}} \quad (25)$$

using the potential in (23) and the relation between the spin vector and the Pauli pseudovector. This fifth contribution is then a one electron spin-orbit coupling which

is important for elements with heavy nucleus (because of Z). It represents the coupling between the electron spin in the nucleus electric field and is responsible for the spin orbit splitting of $l > 0$ orbitals as illustrated in the figure 2. We will see in the following chapter II that the four component many body spin-orbit contains other contributions due to electron-electron interaction.

Chapter II

Relativistic Many Body Theory

II. RELATIVISTIC MANY BODY THEORY

The many-body problem must be understood in atoms and molecules as a many-particle system with an interaction between the particles. So far we avoided the many-particle problem two times by introducing some approximation. First the vacuum itself is a many-particle problem in quantum electrodynamics but we choose the no-pair approximation with the Dirac hole theory since we are rarely in the ultra-relativistic case in molecular science. Second, we treat the nuclei as stationary sources of external electric fields (the electromagnetic field is not quantized) and the nuclear structures are not considered as a complex many-particle system as in nuclear physics but a homogeneous charge distribution in a finite-size volume. Finally the many-body problem arises at our level of theory with electron-electron interaction. In this chapter we will start with the construction of a bielectronic interaction model in first quantization with some acceptable approximations for molecular science. Then we will introduce a multi-electronic molecular Hamiltonian and discuss its different contributions. Next we will enter into the second quantization world which facilitates the formalism of the many-body problem by presenting a new form of the electronic Hamiltonian. We will also briefly discuss some crucial tools of the many-body treatment : basis sets, the self-consistent-field method, integral transformation, the Kramers operator, the double group point symmetry and finally the correlation methods.

A. The electron-electron relativistic interaction

In classical electrodynamics the electron-electron interaction is mediated by a continuous electromagnetic field [41] at the speed of light. In quantum electrodynamics theory (QED), this interaction is mediated by the exchange of virtual photons which are the quanta of the quantized electromagnetic field [42, 43]. These virtual photons mediate the electromagnetic interaction at a finite velocity c . For the two level of theory the electron-electron interaction is not instantaneous and the second electron is affected by a retarded potential from the first electron. The QED also states that the electrons are the quanta of a fermionic field within (as for the electromagnetic field) a varying number of particles. By considering the no-pair ap-

proximation, we want no creation and no annihilation of electron-positron pairs and thus, we need a constant number of electrons (or positrons).

1. The bielectronic interaction potential

There are several ways to construct an electron-electron interaction potential. One can start from the general QED retarded potential and approximate, we can also start from the classical electromagnetic interaction between two point charges, then by applying a Lorentz transformation we get the retarded effect and finally we quantize the resulting operator. Only the main result is presented here but the details about the derivation can be found in the reference [34].

$$\hat{V}_{12} = e^2 \left[\frac{1}{r_{12}} \mathbb{1}_4 - \frac{\hat{\boldsymbol{\alpha}}_1 \cdot \hat{\boldsymbol{\alpha}}_2}{2c^2 r_{12}} - \frac{(\hat{\boldsymbol{\alpha}}_1 \cdot \mathbf{r}_{12})(\hat{\boldsymbol{\alpha}}_2 \cdot \mathbf{r}_{12})}{2c^2 r_{12}^3} \right] \quad (26)$$

Where $\hat{\boldsymbol{\alpha}}_1$ and $\hat{\boldsymbol{\alpha}}_2$ are respectively the vectors containing the Dirac matrices for electron 1 and 2, $r_{12} = \|\mathbf{r}_{12}\| = \|\mathbf{r}_1 - \mathbf{r}_2\|$ is the inter-electronic distance. The Coulomb-Breit potential energy (26) is the low-frequency limit approximation to the order $\frac{1}{c^2}$ of the more general QED potential [44]. The three terms in the brackets can be seen as three other levels of approximation for the bielectronic interaction. The first one is the instantaneous Coulomb interaction

$$\hat{g}^{\text{Coulomb}}(1, 2) = \frac{e^2}{r_{12}} \mathbb{1}_4 \quad (27)$$

The Coulomb term represents the instantaneous Coulomb interaction between two electrons. In analogy with the Pauli Hamiltonian that we introduced in (21), it is possible to expand this term as

$$\frac{e^2}{r_{12}} \quad (28)$$

$$+ \frac{\hbar e^2}{4m_0^2 c^2 r_{12}^3} [\hat{\boldsymbol{\sigma}}_1 \cdot (\mathbf{r}_{12} \times \hat{\mathbf{p}}_1) - \hat{\boldsymbol{\sigma}}_2 \cdot (\mathbf{r}_{12} \times \hat{\mathbf{p}}_2)] \quad (29)$$

$$- \frac{e^2 \hbar^2 \pi}{m_0^2 c^2} \delta(\mathbf{r}_{12}). \quad (30)$$

In this form one can distinguish three contributions, the first one (28) is the classical Coulomb interaction, the second one (29) is called the spin-own-orbit interaction, *i.e.* the spin-orbit interaction of an electron generated by the electric field of another

electron. The last term (30) is a Darwin-type correction to the Coulomb term, a contact term similar to the one-electron analog introduced in (24).

The implementation presented in this manuscript is based on the Coulomb bielectronic interaction. The Breit terms which contain some retardation effects and direct magnetic interaction such as spin-spin coupling are not taken into account. For the sake of brevity, the Breit term is discussed in more detail in T. Saue’s thesis [45] or in M. Reiher’s book [34]. We will now turn to the multi-electronic Hamiltonian based on the Coulomb interaction \hat{g}^{Coulomb} .

2. The multi-electronic Dirac-Coulomb Hamiltonian

As we have seen in the section above, the Coulomb interaction potential contains another contribution to the spin-orbit coupling despite of its classical and instantaneous description. A rigorous Hamiltonian can be constructed within a good description of one-electron relativistic effects as we have seen in the first chapter and a two electron Coulomb interaction

$$\hat{H}^{\text{DC}} = \sum_i^N \left[c\hat{\boldsymbol{\alpha}}_i \cdot \hat{\mathbf{p}}_i + (\hat{\beta} - \mathbb{1}_4)m_0c^2 - \sum_I^A \frac{Z_I e^2}{||\mathbf{r}_i - \mathbf{R}_I||} \mathbb{1}_4 \right] + \sum_{i < j}^N \frac{e^2}{r_{ij}} \mathbb{1}_4 + \sum_I^A \frac{\mathbf{p}_I^2}{2m_I} \mathbb{1}_4 + \sum_{I < J}^A \frac{Z_I Z_J e^2}{R_{IJ}} \mathbb{1}_4 \quad (31)$$

The Dirac-Coulomb Hamiltonian (31) for a molecule with N electrons and A nuclei was first developed in 1935 by Swirles [46], it becomes a Hamiltonian of choice in relativistic quantum physics [47]. Our implementation is based on the Dirac-Coulomb Hamiltonian in its second-quantized form but it is convenient to show the first-quantized form in order to discuss the different contributions. The bracketed one-electron part contains the relativistic kinetic energy of electrons (see equation (22)), the electron-nucleus interaction, the one-electron spin-orbit coupling and m_0c^2 , the rest mass energy. One should notice that the total energy is shifted by $(-\mathbb{1}_4 m_0c^2)$ to have zero for the lowest possible energy value and not m_0c^2 ($E_0 = E - m_0c^2$). The Coulomb bielectronic interaction (27) follows after brackets and finally, the two last terms are nuclear contributions. The second to last term is the classical nuclear kinetic energy of each nucleus, the last one is the classical instantaneous Coulomb interaction between nuclei with $R_{IJ} = ||\mathbf{R}_I - \mathbf{R}_J||$ the internuclear distance.

The 4-component Hamiltonian (31) is composed of one-electron part, a bielectro-

nic part and a nuclear part

$$\hat{H}^{\text{DC}} = \sum_i^N \hat{h}^D(i) + \sum_{i<j}^N \hat{g}^{\text{Coulomb}}(i, j) + \hat{V}^{\text{NUC}} \quad (32)$$

We have now a 4-component relativistic molecular Hamiltonian for multi-electronic systems. However we lost Lorentz invariance by adding a second electron and this is an approximation. Besides, the Born-Oppenheimer approximation is not compatible with special relativity either. Nevertheless, relativistic corrections to the nuclear motion are expected to be small [48]. The no-pair approximation is also there, otherwise even the one-electron problem would have been a many-particle problem due to the possible creation of virtual electron-positron pairs. Consequently we are in the framework of Dirac's hole within the fully filled Dirac sea of negative-energy electrons and we work with classical electromagnetic fields. This implies we neglect QED effect such as self energy (the interaction of the electron with the zero-point fluctuations of the quantized electromagnetic field) and the vacuum polarization (the electron interaction with the zero-point fluctuations of the quantized fermionic field). We can state that the electron-electron interaction will be correct only to the order $(Z\alpha)^2$.

If we turn to the solving of the stationary equation for an N -electron positive energy state Ψ_+

$$\hat{H}^{\text{DC}}\Psi_+(\mathbf{x}_1, \dots, \mathbf{x}_N) = E\Psi_+(\mathbf{x}_1, \dots, \mathbf{x}_N) \quad (33)$$

which is a set of multivariables coupled first order differential equations with a singularity for each particle pair. An analytical solution is not possible, we have to construct approximate solutions. First we will reformulate (31) in second quantization which is a much more adapted framework for many-body problems and we will present some very convenient tools to deal with the relativistic many-body theory. In the next section we will discuss two other many-body Hamiltonians obtained from an approximation of the Dirac-Coulomb Hamiltonian.

3. Spin-free and Lévy-Leblond Hamiltonian

As we have seen in the first chapter in VI D, the relativistic contributions can be classified into scalar and non-scalar effect. It is possible to build a four-component

Hamiltonian which contains only scalar relativistic effects without the spin-orbit contribution : the Spin-Free Hamiltonian [39]. It is also possible to build the non-relativistic limit of the Dirac Hamiltonian : the four-component Lévy-Leblond hamiltonian [49]. This formulation is totally analog to the Schrödinger description, it contains no relativistic effect at all. Both are implemented in our code in second quantization.

B. Tools for relativistic many-body theory

1. Second quantization

In the standard formulation of quantum mechanics the observables are represented by operators and the states by functions. In the second quantization formalism the wave function is also represented by operators : the creation and annihilation operators (\hat{a} and \hat{a}^\dagger) which act on a vacuum state $|0\rangle$. The antisymmetric nature of the electronic wave function relies on these operators' algebra. The electronic molecular Hamiltonians will be built from these creation and annihilation operators such that

$$\hat{a}_p |0\rangle = 0 \quad \text{et} \quad \hat{a}_p^\dagger |0\rangle \neq 0. \quad (34)$$

Electrons are fermions because they have a half-integer spin $s = \frac{1}{2}$. Consequently, the associated creation and annihilation operators of an electron in a given spinor (p, q, \dots) satisfy these anti-commutation laws

$$[\hat{a}_p^\dagger, \hat{a}_q]_+ = \hat{a}_p^\dagger \hat{a}_q + \hat{a}_q \hat{a}_p^\dagger = \delta_{pq} \quad \text{et} \quad [\hat{a}_p, \hat{a}_q]_+ = [\hat{a}_p^\dagger, \hat{a}_q^\dagger]_+ = 0 \quad (35)$$

It should be noticed that these operators (34) are strongly linked to the chosen vacuum $|0\rangle$. The second quantization is a particle-number-independent formalism, it is thus a framework of choice for the many-body problem study.

In the book of T. Helgaker, P. Jørgensen and J. Olsen [50] the reader can find a mapping between first and second quantization operators. The Dirac-Coulomb Hamiltonian electronic part can be expressed in second quantization (see also [34]).

$$\begin{aligned} \hat{H}_{el}^{DC} &= \sum_{pq} h_{pq} \hat{p}^\dagger \hat{q} + \frac{1}{2} \sum_{pqrs} (pq|rs) \hat{p}^\dagger \hat{r}^\dagger \hat{s} \hat{q} \\ &= \sum_{pq} h_{pq} \hat{p}^\dagger \hat{q} + \frac{1}{4} \sum_{pqrs} \langle pq || rs \rangle \hat{p}^\dagger \hat{q}^\dagger \hat{s} \hat{r} \end{aligned} \quad (36)$$

We recover the one-electron part and the bielectronic part as sums over general spinors p, q, r, s . We use from here a simplified notation for the creation and annihilation operators

$$\hat{a}_p^\dagger \hat{a}_q \equiv \hat{p}^\dagger \hat{q} \quad (37)$$

Just in front of the one- and two-electron operators in (36) we find h_{pq} and $(pq|rs)$ which are, respectively, the one- and two-electron integrals

$$h_{pq} = \langle \psi_p(\mathbf{r}_i) | \hat{h}^D(i) | \psi_q(\mathbf{r}_i) \rangle \quad (38)$$

the one-electron integral in Dirac bracket representation for the electron i ,

$$(pq|rs) = \langle pr|qs \rangle = \langle \psi_p(\mathbf{r}_i) \psi_r(\mathbf{r}_j) | \hat{g}^{\text{Coulomb}}(i, j) | \psi_q(\mathbf{r}_i) \psi_s(\mathbf{r}_j) \rangle \quad (39)$$

the bielectronic integral in Mulliken and Dirac representation for the Coulombic interaction between the electrons i and j . The two notations can be useful depending on the context

$$\text{Mulliken} \quad (\text{particle } 1^* \text{ particle } 1 | \text{particle } 2^* \text{ particle } 2)$$

$$\text{Dirac} \quad \langle \text{particle } 1^* \text{ particle } 2^* | \text{particle } 1 \text{ particle } 2 \rangle$$

The second form of the electronic Hamiltonian (36) is expressed with the antisymmetrized integrals such as

$$\langle pq || rs \rangle = \langle pq | rs \rangle - \langle pq | sr \rangle \quad (40)$$

These integrals depend on the knowledge of the one-electron wave function for each given spinors (p, q, r, s) at a known energy level. Accordingly, the integrals (38) and (39) can be calculated after the Dirac-Hartree-Fock solution of (33). We will come back to integrals evaluation later on, in II C 2. We continue our tool presentation by introducing the basis sets concept which is of crucial importance for the calculation of atomic and molecular state energies.

2. LCAO - Basis sets

In quantum mechanics, the molecular system wave function is in theory, represented by a basis expansion of infinite dimension. For the study of isolated molecular

systems, it can be very convenient to use the linear combination of atomic orbitals (LCAO) first introduced by J. Lennard-Jones

$$\phi^{\text{MO}}(\mathbf{r}) = \sum_i^{\text{N}_{\text{atoms}}} b_i \psi_i(\mathbf{r}, \mathbf{R}_A). \quad (41)$$

We then form a number of molecular spinors equal to the number of atomic spinor, each molecular spinor ϕ^{MO} (41) is a linear combination of atomic spinor ψ centered in its own nucleus at the position \mathbf{R}_A .

Atomic spinor components i , $\psi_k^{(i)}$, are expanded in a basis represented by Gaussian functions (42). These functions allow an easy manipulation in particular when integrals are evaluated [50].

$$\psi_k^{(i)}(\mathbf{r}) = \sum_{\mu}^{\text{N}_{\text{function}}} N_{k\mu}^{(i)} (x - x_A)^{\alpha_{\mu}} (y - y_A)^{\beta_{\mu}} (z - z_A)^{\gamma_{\mu}} e^{-\zeta_{\mu}(\mathbf{r} - \mathbf{R}_A)^2} \quad (42)$$

Where (42) is a Cartesian Gaussian function, the sum of the exponents α_{μ} , β_{μ} and γ_{μ} is related to the angular quantum number ($\alpha_{\mu} + \beta_{\mu} + \gamma_{\mu} = l$). A basis-set contains several Gaussian functions for each considered value of the angular momentum l (s, p, d, \dots). Large exponents describe predominantly the core orbitals, close to the nucleus, and the very low-value exponents describe the diffuse orbitals. To construct a basis-set, each Gaussian exponent is optimized separately with a self-consistent-field method [50].

A lot of basis-set types exist, useful for various purposes (see EMSL website [51]). In a general manner, the more basis functions is contained in the basis-set, the better will be the description. The quality and the suitability of the basis is of crucial importance for a given system. Especially if one wants to study excited states, the Q ζ quality basis is always taken as a reference for our calculations and a basis-set error is evaluated.

As discussed in the first chapter, the one-electron problem in a central field can be solved with a separation of angular and radial parts. Since we generate one-electron atomic functions from the basis-set, the Gaussian combination yields to fit better as possible the analytic radial function [50].

The use of four-component wave function requires however an additional condition, to have stable results it has been shown that the expansion for the large and the small component should be performed in a balanced way. The solution for this

problem is called the kinetic-balanced [52], thereby the kinetic energy approaches the non-relativistic limit in a correct fashion [39], we use this feature in our code

$$\psi^S \simeq \frac{\hat{\sigma} \cdot \hat{\mathbf{p}}}{2m_0c} \psi^L. \quad (43)$$

It should be noticed that the number of small component functions is significantly larger compared to the large component. Indeed, because of the derivative operator in (43), every large component Gaussian basis-set spinor ψ_k^L gives rise to two small component basis functions with the same exponent (for example : from a large p -type you get a s - and a d -type basis function for the small component). Consequently, relativistic four-component calculations implies the use of larger basis-set generated from usual basis-set. Besides the use of contracted Gaussian functions to reduced the size of the Fock matrix [53] is problematic due to the small component [54].

We prefer when it is available, to use K. Dyall uncontracted Gaussian basis-set optimized for four-component relativistic calculations [55–58]. Our four-component molecular spinors are consequently a linear combination of four-component atomic spinors expanded into a Gaussian basis [34]

$$\phi_j^{\text{MO}}(\mathbf{r}) = \sum_{\mu} \begin{pmatrix} c_{j\mu}^{(1)} \psi_{\mu}^{(1)}(\mathbf{r}, \mathbf{R}_A) \\ c_{j\mu}^{(2)} \psi_{\mu}^{(2)}(\mathbf{r}, \mathbf{R}_A) \\ c_{j\mu}^{(3)} \psi_{\mu}^{(3)}(\mathbf{r}, \mathbf{R}_A) \\ c_{j\mu}^{(4)} \psi_{\mu}^{(4)}(\mathbf{r}, \mathbf{R}_A) \end{pmatrix} \quad (44)$$

To reduce the number of integral generated from the basis functions, we exploit the group point symmetry in our implementation, this will be briefly presented in the next section.

3. Double group point symmetry

In order to make use of molecular symmetry in a relativistic formalism we use double point group symmetry. The difference with the usual point group symmetry used in non-relativistic code is the generalization to the transformation properties of fermion ($s = \frac{1}{2}$) particles. Two different situations can arise, the number of valence electron can be even or odd. In the even case, the total spin is an integer and consequently, the many-electron wave function transforms as one of the regular

group bosonic irreducible representations. If the number of electron is odd the total spin is a half integer, then the identity operation E implies a rotation of 4π around an arbitrary axis. It follows the addition of the 2π rotation operation \bar{E} to regular groups of order n to give a double groupe of order $2n$. For more details about double group point symmetry the reader can consult [59].

The current implementation is limited to the real double groups (D_{2h}^* , D_2^* and C_{2v}^*) since the systems of interest are atoms or diatomics with high symmetry. Complex (C_{2h}^* , C_2^* and C_s^*) and quaternion double groups (C_1^* and C_i^*) will be implemented later if needed.

4. Kramers time-reversal symmetry

Since we use the spin-dependent Dirac-Coulomb Hamiltonian (31) (without external magnetic fields), spin and spatial symmetry are entangled. Thus spin restriction does not hold contrary to a non-relativistic wave function. However, the energy levels of one-electron spinors will be at least doubly degenerate which for the relativistic formalism allows us to exploit the Kramers time-reversal symmetry [60–64]. Accordingly a Kramers-restricted basis of electronic spinors $\{\psi_p, \psi_{\bar{p}}\}$ (Kramers pairs) is constructed, where each unbarred spinor ψ_p is related to a barred spinor, its energy-degenerate partner (Kramers partner), $\psi_{\bar{p}}$, through time reversal,

$$\hat{K}\psi_p = \psi_{\bar{p}} \quad , \quad \hat{K}\psi_{\bar{p}} = -\psi_p \quad , \quad \hat{K}(a\psi_p) = a^*\hat{K}\psi_p \quad (45)$$

with a being a complex number. The Kramers time-reversal operator reverses the movement, flips the spin and changes the sign of the momentum, leaving only position invariant

$$\hat{K}\phi_p(t) = \phi_{\bar{p}}(-t) \quad , \quad \hat{K}\hat{\sigma}\hat{K}^\dagger = -\hat{\sigma} \quad , \quad \hat{K}\hat{\mathbf{p}}\hat{K}^\dagger = -\hat{\mathbf{p}} \quad , \quad \hat{K}\hat{\mathbf{r}}\hat{K}^\dagger = \hat{\mathbf{r}} \quad (46)$$

In the 4-component relativistic framework this operator can be written as

$$\hat{K} = -i\hat{\Sigma}_2\hat{K}_0 = -i \begin{pmatrix} \hat{\sigma}_2 & 0 \\ 0 & \hat{\sigma}_2 \end{pmatrix} \hat{K}_0 \quad (47)$$

with $\hat{\Sigma}_2 = \mathbb{1}_2 \otimes \hat{\sigma}_2$ the second component of the 4-component spin operator $\hat{\Sigma} = \mathbb{1}_2 \otimes \hat{\sigma}$ introduced in the first appendix (293), and \hat{K}_0 is the complex conjugation operator.

The Kramers operator has no eigenvalue and does not represent an observable because of its antiunitarity, but \hat{K} commutes with the Dirac-Coulomb Hamiltonian (31)

$$\hat{K}\hat{K}^\dagger = \hat{K}^\dagger\hat{K} = \mathbb{1}_4 \quad , \quad \hat{K}^\dagger = \hat{K}^{-1} \quad , \quad [\hat{K}, \hat{H}^{\text{DC}}] = 0. \quad (48)$$

Time-reversal symmetry is considered as a fundamental symmetry that can be exploited to describe many-particles system such as atoms and molecules in a relativistic context.

In the framework of second quantization we can also write these relations as

$$\hat{K}\hat{p}^\dagger = \hat{\bar{p}}^\dagger\hat{K} \quad , \quad \hat{K}\hat{\bar{p}}^\dagger = -\hat{p}^\dagger\hat{K} \quad (49)$$

$$\hat{K}\hat{p} = \hat{\bar{p}}\hat{K} \quad , \quad \hat{K}\hat{\bar{p}} = -\hat{p}\hat{K}. \quad (50)$$

It is convenient to introduce a Kramers number operator \hat{K}_z (z constitutes an arbitrary choice) of an eigenfunction $|\Phi\rangle$ associated with its eigenvalue M_K as

$$\hat{K}_z = \frac{1}{2} \left(\sum_p \hat{p}^\dagger \hat{p} - \sum_{\bar{p}} \hat{\bar{p}}^\dagger \hat{\bar{p}} \right) \quad , \quad \hat{K}_z |\Phi\rangle = M_K |\Phi\rangle \quad , \quad M_K = \frac{N_p - N_{\bar{p}}}{2} \quad (51)$$

with N_p and $N_{\bar{p}}$ the number of unbarred and barred operators respectively.

The second-quantized operators can be classified into several classes depending on the Kramers-flip ΔM_K which is defined as

$$\Delta M_K = \frac{(N^c - \overline{N^c}) + (\overline{N^a} - N^a)}{2} \quad (52)$$

with N^c , $\overline{N^c}$ and N^a , $\overline{N^a}$ the number of unbarred, barred creators and annihilators, respectively, for a given operator. The non-relativistic ones are those with $\Delta M_K = 0$ (no Kramers-flip), $\Delta M_K = \pm 1$ are operators with one Kramers-flip and $\Delta M_K = \pm 2$ with two Kramers-flips. The $+$ sign stands for an unbarred to barred flip and conversely for $-$ sign.

The Kramers time-reversal symmetry is very useful to reduce the number of independent integrals and, consequently, the computational effort. For the one-electron integrals we establish the following relations

$$\begin{aligned} h_{\bar{p}\bar{q}} &= \langle \psi_{\bar{p}} | \hat{h}^D | \psi_{\bar{q}} \rangle = \langle \hat{K} \psi_p | \hat{h}^D | \hat{K} \psi_q \rangle \\ &= \langle \psi_p | \left(\hat{K}^\dagger \hat{h}^D \hat{K} | \psi_q \rangle \right)^* = \langle \psi_p | \hat{h}^D | \psi_q \rangle^* \\ &= \langle \hat{h}^D \psi_q | \psi_p \rangle = \langle \psi_q | \hat{h}^{D\dagger} | \psi_p \rangle \\ &= \langle \psi_q | \hat{h}^D | \psi_p \rangle \\ h_{\bar{p}\bar{q}} &= h_{qp} \end{aligned} \quad (53)$$

by using equations (45) and the Hamiltonian hermiticity twice.

$$\begin{aligned}
h_{\bar{p}q} &= \langle \psi_{\bar{p}} | \hat{h}^D | \psi_q \rangle = \langle \hat{K} \psi_p | \hat{h}^D | \psi_q \rangle \\
&= - \langle \psi_p | \left(\hat{K}^\dagger \hat{h}^D \hat{K} \hat{K} | \psi_q \rangle \right)^* = - \langle \psi_p | \hat{h}^D | \psi_{\bar{q}} \rangle^* \\
h_{\bar{p}q} &= -h_{p\bar{q}}^*
\end{aligned} \tag{54}$$

$$\begin{aligned}
h_{p\bar{q}} &= \langle \psi_p | \hat{h}^D | \psi_{\bar{q}} \rangle = \langle \psi_p | \hat{h}^D | \hat{K} \psi_q \rangle \\
&= \langle \psi_p | \left(\hat{K}^\dagger \hat{h}^D \hat{K} \hat{K} | \psi_q \rangle \right) = - \langle \psi_p | \left(\hat{K}^\dagger \hat{h}^D | \psi_q \rangle \right) \\
&= - \langle \hat{K} \psi_p | \hat{h}^D | \psi_q \rangle^* = - \langle \psi_{\bar{p}} | \hat{h}^D | \psi_q \rangle^* \\
&= - \langle \psi_q | \hat{h}^D | \psi_{\bar{p}} \rangle \\
h_{p\bar{q}} &= -h_{q\bar{p}}
\end{aligned} \tag{55}$$

We obtain the relations above (54) and (55) with the same mechanisms, hence we have shown that the unique types of one-particle integrals in a Kramers basis reduce to

$$h_{pq} \quad \text{and} \quad h_{p\bar{q}} \tag{56}$$

and then thanks to Kramers symmetry and \hat{h}^D hermiticity we reduce to one fourth the number of unique one-electron integrals. Likewise, for two-electron integrals the following relations can be established by using the Hamiltonian hermiticity, Kramers symmetry and, in addition, particle exchange symmetry

$$\begin{aligned}
(pq|rs) &= (pq|\bar{s}\bar{r}) = (\bar{q}\bar{p}|rs) = (\bar{q}\bar{p}|\bar{s}\bar{r}) \\
(\bar{p}q|rs) &= (\bar{p}q|\bar{s}\bar{r}) = -(\bar{q}p|rs) = -(\bar{q}p|\bar{s}\bar{r}) \\
(\bar{p}q|\bar{r}s) &= -(\bar{p}q|\bar{s}r) = -(\bar{q}p|\bar{r}s) = (\bar{q}p|\bar{s}r) \\
(\bar{p}q|r\bar{s}) &= -(\bar{p}q|s\bar{r}) = -(\bar{q}p|r\bar{s}) = (\bar{q}p|s\bar{r}).
\end{aligned} \tag{57}$$

The two-electron integral number reduction is much more important since we use only these four

$$(pq|rs) \quad , \quad (\bar{p}q|rs) \quad , \quad (\bar{p}q|\bar{r}s) \quad , \quad (\bar{p}q|r\bar{s}), \tag{58}$$

strongly reducing the computational effort. According to (52) the Dirac-Coulomb Hamiltonian (36) can be written in terms of unbarred- and barred-Kramers creation and annihilation operators. The different contributions can be classified in terms of

their ΔM_K value,

$$\begin{aligned}
& \hat{H}_{el}^{DC} = \\
\Delta M_K = +2 & \quad \frac{1}{2} \sum_{pqrs} (p\bar{q}|r\bar{s}) \hat{p}^\dagger \hat{r}^\dagger \hat{s} \hat{q} \\
\Delta M_K = +1 & \quad \sum_{pq} h_{p\bar{q}} \hat{p}^\dagger \hat{q} + \sum_{pqrs} \left[(p\bar{q}|rs) \hat{p}^\dagger \hat{r}^\dagger \hat{s} \hat{q} + (p\bar{q}|\bar{r}s) \hat{p}^\dagger \hat{r}^\dagger \hat{s} \hat{q} \right] \\
\Delta M_K = 0 & \quad \sum_{pq} \left(h_{pq} \hat{p}^\dagger \hat{q} + h_{p\bar{q}} \hat{p}^\dagger \hat{q} \right) \\
& \quad + \frac{1}{2} \sum_{pqrs} \left[(pq|rs) \hat{p}^\dagger \hat{r}^\dagger \hat{s} \hat{q} + (\bar{p}\bar{q}|\bar{r}\bar{s}) \hat{p}^\dagger \hat{r}^\dagger \hat{s} \hat{q} + 2\{(pq|\bar{r}\bar{s}) - (p\bar{s}|\bar{r}q)\} \hat{p}^\dagger \hat{r}^\dagger \hat{s} \hat{q} \right] \\
\Delta M_K = -1 & \quad \sum_{pq} h_{p\bar{q}} \hat{p}^\dagger \hat{q} + \sum_{pqrs} \left[(\bar{p}\bar{q}|rs) \hat{p}^\dagger \hat{r}^\dagger \hat{s} \hat{q} + (\bar{p}q|\bar{r}s) \hat{p}^\dagger \hat{r}^\dagger \hat{s} \hat{q} \right] \\
\Delta M_K = -2 & \quad \frac{1}{2} \sum_{pqrs} (\bar{p}q|\bar{r}s) \hat{p}^\dagger \hat{r}^\dagger \hat{s} \hat{q}
\end{aligned} \tag{59}$$

Only the $\Delta M_K = 0$ terms in the electronic Hamiltonian (59) are the non-relativistic operators. The other operators are relativistic Kramers-flip operators, *i.e.* an electron initially in a barred spinors can be excited to an unbarred spinor and reciprocally. Some operators were combined in the Hamiltonian to minimize the number of unique operators to increase efficiency.

5. Spinor strings

A multi-electronic molecular wave function $|\Phi\rangle$ can be represented in terms of a Slater determinant (60)

$$|\Phi\rangle = \frac{1}{\sqrt{N!}} \begin{bmatrix} \phi_p(1) & \phi_q(1) & \cdots & \phi_r(1) \\ \phi_p(2) & \phi_q(2) & \cdots & \phi_r(2) \\ \vdots & \vdots & \ddots & \vdots \\ \phi_p(N) & \phi_q(N) & \cdots & \phi_r(N) \end{bmatrix}. \tag{60}$$

The single reference N -electron wave function $|\Phi\rangle$ with $\phi_p, \phi_q, \dots, \phi_r$ the positive-energy-one-electron-molecular spinors. The latter function is expanded in a basis set as we saw previously in IIB2. By using second quantization, Slater determinants can be expanded in terms of creation operator strings. Many modern methods in quantum chemistry capable of performing large-scale many-body calculations are based on such a representation, the string-based methods [19, 65–69]. The string-based wave function can be generalized to a relativistic description [70–72]. As for

the Hamiltonian, the multi-electronic wave function will be described by second-quantized strings acting on a true vacuum state $|0\rangle$ (the state with no electron)

$$\mathcal{S}^\dagger |0\rangle = \prod_p^{N_p} \hat{p}^\dagger |0\rangle \quad \text{and} \quad \bar{\mathcal{S}}^\dagger |0\rangle = \prod_{\bar{p}}^{N_{\bar{p}}} \hat{\bar{p}}^\dagger |0\rangle \quad (61)$$

with the strings \mathcal{S} and $\bar{\mathcal{S}}$ referring to two sets of unbarred- and barred-Kramers spinors. Then we can write a multi-electronic wave function $|\Phi\rangle$ by using (61)

$$|\Phi\rangle = \mathcal{S}^\dagger \bar{\mathcal{S}}^\dagger |0\rangle \quad (62)$$

C. Methods for the relativistic many-body problem

1. Dirac-Hartree-Fock (DHF)

The Dirac-Hartree-Fock method is based on an independent-particle model. In this picture, each electron 'feels' a mean-field potential which comes from the nuclei and the other electrons. The Coulomb-correlated movement of the electrons is not taken into account, *i.e.* the two-electron term goes into an effective one-particle term and the fluctuation potential of the two-electron interaction is neglected.

The model aims to find in this context the total ground state energy of the system and the spinor energy levels by considering a single-reference ground-state wave function.

This first step is done in the empty dirac framework (consider the right figure 1 with empty negative energy states), the only occupied spinors are those of positive energy. Accordingly, the unfilled negative electronic states are considered as orthogonal complement that is optimized but never filled. The variational principle is employed in a twofold way : the energy is minimized with respect to spinor transformations among positive energy spinors and maximized with respect to spinor transformations involving positive and negative energy spinors. This is the mini-max procedure [73]. After this procedure, the negative-energy states are discarded [74], we call it the no-pair approximation *a posteriori*. However it remains a coupling between the small and the large component and the resulting positive-energy many-body wave function $|\Phi_+\rangle$ is still a 4-component one.

The main principle of DHF method is the following : We start with a set of one-electron spinors from an initial guess and then refine them iteratively. The relativistic

Roothaan equation [34] is solved for each iteration

$$\mathcal{F}C = \epsilon SC \quad \text{with} \quad \mathcal{F} = h^D + \sum_i [J_{ii} - K_{ii}] \quad (63)$$

where C is a Dirac-Fock coefficient matrix, S an overlap matrix, ϵ is the molecular spinor energy vector. The Fock operator $\hat{\mathcal{F}}$ contains the one-electron contributions \hat{h}^D , the coulomb contribution \hat{J} and the exchange contribution \hat{K} , more details can be found in [34]. The improvement of this set is done by diagonalizing the Fock matrix which corresponds to a 'rotation' of the spinors in the entire function space. After several iterations, the unitary transformation process reaches a stage where the spinors remain unchanged under further rotations, the spinors are then self consistent. The reader can find a more complete description of DHF concepts and equations in references [34, 39].

At the end of this first step, the DHF total energy

$$E^{\text{DHF}} = \langle \Phi_+ | \hat{\mathcal{F}} | \Phi_+ \rangle \quad (64)$$

of the system's ground state is obtained as well as a set of optimized molecular spinors ϕ_p associated to an energy ϵ_p .

2. Integral transformation

This second step consists in an integral transformation from the primitive basis (from the basis input (42)) to the atomic or molecular basis (44). Here the Dirac-Fock coefficients are required (63) and then all the needed atomic or molecular integrals are explicitly evaluated and stored to disc. The integral transformation depends on the number of frozen spinors and on the basis cut-off, *i.e.* it depends on the number of active and chosen virtual spinors.

3. Correlation energy - The correlated wave function

In the previous section we neglected the 'correlation energy' and defined the Dirac-Hartree-Fock energy E^{DHF} . The principal purpose of this manuscript focusses on the missing correlation energy E^{corr} defined as

$$E^{\text{corr}} = E - E^{\text{DHF}} \quad (65)$$

where E is the exact energy for a given Hamiltonian in the limit of an infinite basis set. In practice, we use finite basis-sets, thus we should define the basis-set correlation energy

$$E_{\text{basis}}^{\text{corr}} = E_{\text{basis}} - E_{\text{basis}}^{\text{DHF}}. \quad (66)$$

The latter (66) represents the correlation energy in a given finite basis-set.

When the two first steps, *i.e.* the self-consistent field and the integral transformation procedures are realized, one can construct a correlated multi-electronic wave function. Indeed the DCHF multi-electronic wave function does not contain the correlation energy. The correlation energy is typically less than 1% of the total energy. However, for spectroscopic constants as equilibrium bond length r_e or the harmonic vibrational frequency ω_e , correlation errors can reach 10%. Turning to our main concern : the excitation energies T_e or T_v , obtained from the subtraction of the excited-state total energy and the ground-state total energy, correlation errors can reach more than 30%. A high accuracy many-body method must take into account the correlation energy as best as possible. A significant number of correlation methods exist but it will be out of topic to describe all of them. The major routes for addressing dynamic electron correlations are firstly, the treatment of the fluctuation potential as a perturbation based on Hartree-Fock wave function as zero-order approximation, this leads to many-body perturbation theory (MBPT). Secondly, multi-determinantal/excitation manifold theories like Configuration Interaction (CI) and the Coupled Cluster (CC). Thirdly, mono-determinantal theory that takes correlation into account as Density Functional Theory (DFT). We will focus on the coupled cluster method, however, the reader will find a relativistic post-Hartree-Fock method review in references [8, 47, 75] and for CC methods in reference [76].

Correlation can be of different nature, in the bonding region, the **superposition of spatial functions of different configurations** gives rise to **dynamic correlation**. As an example let us consider a configuration interaction of states for H_2 molecule :

$$|\Phi^{\text{CI}}\rangle = c |^1\Sigma_g^+\rangle + c' |^2^1\Sigma_g^+\rangle = \frac{1}{\sqrt{2}} [c\sigma(1)\sigma(2) + c'\sigma^*(1)\sigma^*(2)] \frac{1}{\sqrt{2}} [\alpha(1)\beta(2) - \beta(1)\alpha(2)] \quad (67)$$

However a **superposition** in the bonding region of **spatial functions of the same configuration** gives rise to **Fermi correlation (or exchange correlation)**. As an example

let us consider some open-shell configurations for H_2

$${}^3\Sigma_u^+ : \sigma(1)\sigma^*(2) - \sigma(1)^*\sigma(2) \quad \text{and} \quad {}^1\Sigma_u^+ : \sigma(1)\sigma^*(2) + \sigma(1)^*\sigma(2) \quad (68)$$

The latter is encoded in the determinant and is known to energetically stabilize higher-spin states compared to lower-spin states originating in the same orbital configuration, due to the Fermi hole and therefore reduced Coulomb repulsion. In the dissociation limit, the molecular states correlate with atomic dissociation channels and **the molecular orbitals become atomic**. In this case, there is no two-electron contributions (but there is of course still atomic electron correlation in the separate atoms) due to the large distance between them and functions which correspond to **different molecular configurations are degenerate**. This third kind of correlation is called **static correlation (or near-degeneracy of states correlation or long-range correlation)**. As an example let us consider again H_2

$${}^1\Sigma_g^+ \rightarrow {}^2S \quad \text{and} \quad {}^3\Sigma_u^+ \rightarrow {}^2S \quad , \quad \sigma \rightarrow s_1 \quad \text{and} \quad \sigma^* \rightarrow s_2 \quad (69)$$

Then the atomic wavefunctions for the neutral dissociation channels can be written as

$$\begin{aligned} \text{'' } \uparrow\uparrow \text{''} : & \quad [s_1(1)s_2(2) - s_2(1)s_1(2)] \cdot (\text{symetric spin part}) \quad \text{and} \\ \text{'' } \uparrow\downarrow \text{''} : & \quad [s_1(1)s_2(2) + s_2(1)s_1(2)] \cdot (\text{antisymetric spin part}) \end{aligned} \quad (70)$$

It is only visible in the atomic limit, but it carries over to the molecular region, for example, if an excited state has the same symmetry as the ground state. This case necessitates a multi-determinantal wave function *a priori*.

In figure 3 we display the illustrative quality evolution in terms of accuracy and cost of a calculation with three axes. However the exact solution to the correlation problem is the Full Configuration Interaction (FCI) method, which is almost always infeasible when one increases the number of spinors or active electrons. This model will be discussed later on in III A 5.

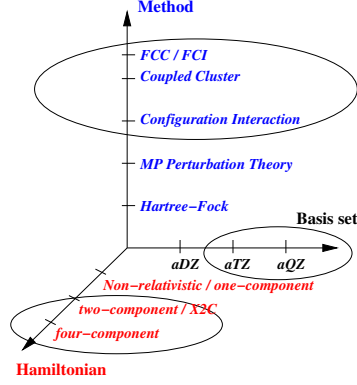


FIGURE 3. Schematic illustration of the accuracy and the cost of a calculation depending on the Hamiltonian, the basis quality and the correlated method.

From the figure 3 we can evaluate the computational scaling depending S

$$S = y(\textcolor{blue}{x})f(\textcolor{blue}{x})N^x \quad (71)$$

with $y(x) \simeq 4\sqrt{\pi\left(\frac{x}{2} - 1\right)}$, ($x \geq 4$) the relativistic prefactor, $f(x)$ a general prefactor both derived in the reference [77], N the basis-set dimension and $\textcolor{blue}{x}$ the method scaling exponent (CCSD $x = 6$, CCSDT $x = 8$, CCSDTQ $x = 10$...). Other less standard schemes are possible with the Generalized Active Spaces (GAS) presented in the next part, the $CC(n_m)$ parametrization. For such schemes the equation (71) should be slightly modified.

4. Generalized Active Spaces

A powerful concept to build the electronic wave function is to introduce an arbitrary number of orbital spaces in accord with physical and chemical arguments. It allows for the possibility to restrict the electronic occupation of the subspaces. Our implementation is based on the Generalized Active Space (GAS) concept first introduced in the context of non-relativistic quantum physics by J. Olsen [78] and is a generalization of the Restricted Active Spaces (RAS) concept [79]. We define three types of spaces, the frozen space, an inactive space where the electrons do not benefit from a correlation treatment but are taken into account for the total energy since we work with an all-electron method. A core Fock matrix is generated for these spinors. The occupied space (or hole space), an active space which can be divided into

an arbitrary number of subspaces (for example a core-space and a valence space). It contains only occupied spinors for single-reference methods, but it can contain a Complete Active Space (CAS) for multi-reference methods which is a complete distribution of an arbitrary number of electrons in an arbitrary number of spinors. The third type is the virtual space (or particle space), an active space with only unoccupied spinors. It can also be divided into an arbitrary number of subspaces (for example a first subspace with the most important virtual spinors to describe a system and a second subspace with the other virtual spinors). In the context of our coupled cluster implementation it provides a way to construct quasi-multi-reference schemes. We will come back to this point later on in III A 6.

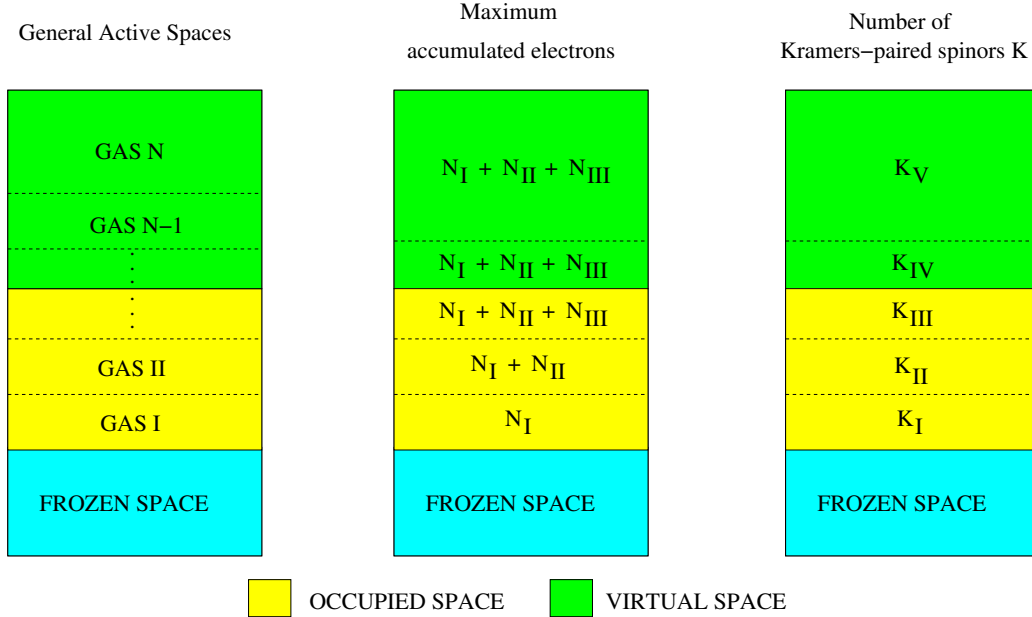


FIGURE 4. Structure of the General Active Spaces, on the left the three main spaces and their possible divisions. In the middle the number of correlated electron per GAS and on the right the number of Kramers-paired spinors per GAS

Figure 4 illustrates the concept. An atomic or a molecular system can be parametrized in this framework. Indeed, after the initial mean-field step (see IIC 1) we have a set of Kramers-paired spinors. Then we can decide to freeze the deepest core-electrons which contribute quite few to the differential core-correlation energy for valence states. From the chosen lowest-energy occupied Kramers-paired spinors we start to fill the arbitrary number of GAS's. The virtual space is filled with unoc-

cupied spinors also obtained in the initial Hartree-Fock step (II C 1) below a chosen cut-off. This virtual space cut-off must be chosen carefully since some virtual spinors can have a crucial contribution for the many-particle system description. We follow a standard procedure where we look for an energy gap between spinors and cut inside the gap. We always try to compare our cut-off calculations to some higher cutoff or to full basis calculations in order to evaluate the cutoff error (see in the applications IV or [80] or in IV A).

We will see later on in III A 6 that some different excitation restrictions can be applied for each GAS which allow us to apply an arbitrary number of minimum and maximum number of electrons in each GAS. This feature permits to construct very elaborate GAS-parametrized wave functions adapted to a given multi-electronic system. In fact, GAS allows to construct any arbitrary correlation expansion.

5. Normal-ordered second-quantized operators

As discussed above in II B 1, II B 4 and II B 5, the electronic Hamiltonian is represented in second quantization with strings of creation and annihilation operators, as well as for the multi-electronic wave function and for the coupled cluster excitation operators. The evaluation of the corresponding matrix elements will consist in evaluating heavy sequences of these second-quantized operators. For convenience and to ease the implementation these operator strings will be written in normal-ordered form, *i.e.* all the creation operators on the left and all the annihilation operators on the right. An arbitrary second-quantized string can always be reordered in a normal ordered form by using the anticommutation relations introduced in (35), as an example

$$\begin{aligned}\hat{p}\hat{q}^\dagger\hat{r}\hat{s}^\dagger &= -\hat{q}^\dagger\hat{p}\hat{r}\hat{s}^\dagger + \delta_{pq}\hat{r}\hat{s}^\dagger = \hat{q}^\dagger\hat{p}\hat{s}^\dagger\hat{r} - \delta_{rs}\hat{q}^\dagger\hat{p} - \delta_{pq}\hat{s}^\dagger\hat{r} + \delta_{pq}\delta_{rs} \\ &= -\hat{q}^\dagger\hat{s}^\dagger\hat{p}\hat{r} + \delta_{sp}\hat{q}^\dagger\hat{r} - \delta_{rs}\hat{q}^\dagger\hat{p} - \delta_{pq}\hat{s}^\dagger\hat{r} + \delta_{pq}\delta_{rs}\end{aligned}\tag{72}$$

This normal-ordering is systematically done in our implementation when such strings arise.

6. The particle-hole formalism

In post-Hartree-Fock many-body theory it is often more convenient to deal with the multi-electronic reference determinant, $|\Phi\rangle$ (see III A 4), rather than the no-electron vacuum state $|0\rangle$. Indeed the Fermi-vacuum will be expressed in terms of creator strings (see (185)). If one wants to work with $|0\rangle$, heavy steps or reordering arise. It is in this context very convenient to change the reference vacuum in order to use the Fermi vacuum as a reference state for our description. This procedure is called the particle-hole formalism [81–83]. All the occupied spinors in $|\Phi\rangle$ are considered as hole spinors and all the unoccupied spinors with respect to $|\Phi\rangle$ are called particle spinors (see figure 5). Accordingly, we define the quasi-operators of creation and annihilation of hole or particle

$$\begin{aligned} \hat{i}|\Phi\rangle &\neq 0 \quad , \quad \hat{a}|\Phi\rangle = 0 \\ \hat{i}^\dagger|\Phi\rangle &= 0 \quad , \quad \hat{a}^\dagger|\Phi\rangle \neq 0 \end{aligned} \tag{73}$$

where the following convention is used : $i, j, k, \dots \in \mathbb{H}$ indices for hole quasi-operators and $a, b, c, \dots \in \mathbb{P}$ indices for particle quasi-operators. \mathbb{H} and \mathbb{P} refer, respectively, to the hole and particle manifold.

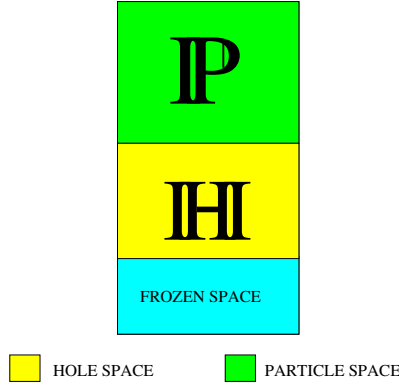


FIGURE 5. Particle and hole spaces, \mathbb{H} and \mathbb{P} can thus be divided into subspaces as illustrated in 4.

For general indices we still use $p, q, r, s, \dots \in \mathbb{H} \oplus \mathbb{P}$. The anticommutation rela-

tions for the quasi-operators are defined as

$$\begin{aligned}
\left[\hat{i}^\dagger, \hat{j} \right]_+ &= \delta_{ij} \quad , \quad \left[\hat{a}^\dagger, \hat{b} \right]_+ = \delta_{ab} \\
\left[\hat{i}, \hat{j} \right]_+ &= \left[\hat{a}, \hat{b} \right]_+ = \left[\hat{i}^\dagger, \hat{j}^\dagger \right]_+ = \left[\hat{a}^\dagger, \hat{b}^\dagger \right]_+ = 0 \\
\left[\hat{i}^\dagger, \hat{a} \right]_+ &= \left[\hat{a}^\dagger, \hat{i} \right]_+ = \left[\hat{i}, \hat{a} \right]_+ = \left[\hat{i}^\dagger, \hat{a}^\dagger \right]_+ = 0.
\end{aligned} \tag{74}$$

Relation (74) is given just for completeness. Indeed, we will see in the following part that the use of quasi-operators contraction is much more powerful.

7. The contraction concept and the Wick theorem

As we saw above in equation (72), that an arbitrary second-quantized string of annihilation and creation operators can be expressed as a linear combination of normal-ordered strings multiplied by a Kronecker delta function. Some of these strings contain a reduced numbers of operators. These reduced terms may be viewed as arising from contractions between operator pairs. Within the particle-hole formalism a contraction between two quasi-operators is

$$\overline{\hat{i}^\dagger \hat{j}} = \hat{i}^\dagger \hat{j} - \left\{ \hat{i}^\dagger \hat{j} \right\} = \hat{i}^\dagger \hat{j} + \hat{j} \hat{i}^\dagger = \delta_{ij} \tag{75}$$

$$\overline{\hat{a} \hat{b}^\dagger} = \hat{a} \hat{b}^\dagger - \left\{ \hat{a} \hat{b}^\dagger \right\} = \hat{a} \hat{b}^\dagger + \hat{b}^\dagger \hat{a} = \delta_{ab} \tag{76}$$

where the brackets $\{ \}$ are the normal-ordered string with respect to the Fermi-vacuum which allow the permutation of operators as

$$\left\{ \hat{a} \hat{b}^\dagger \right\} = - \left\{ \hat{b}^\dagger \hat{a} \right\} = - \hat{b}^\dagger \hat{a} \tag{77}$$

Thus all the other contraction types vanish.

We can now introduce the Wick theorem [84] which states : an arbitrary string of annihilation and creation operators, $ABC \dots XYZ$, may be written as a linear combination of normal-ordered strings as

$$\begin{aligned}
ABC \dots XYZ &= \{ ABC \dots XYZ \} \\
&+ \sum_{\text{singles}} \{ \overline{AB} \dots XYZ \} \\
&+ \sum_{\text{doubles}} \{ \overline{ABC} \dots XYZ \} \\
&+ \dots ,
\end{aligned} \tag{78}$$

where singles and doubles refer to the number of pairwise contractions included in the summation. To make this point perfectly clear some examples are given in the appendix II.

Considering we deal only with normal-ordered strings $\{ABC \dots\}$, $\{XYZ \dots\}$, as in our implementation, it could often occur to have some product between several normal-ordered strings. For this purpose we use the generalized Wick theorem

$$\begin{aligned}
\{ABC \dots\} \{XYZ \dots\} &= \{ABC \dots XYZ \dots\} \\
&+ \sum_{\text{singles}} \overbrace{\{ABC \dots XYZ \dots\}}^{\text{single contraction}} \\
&+ \sum_{\text{doubles}} \overbrace{\{ABC \dots XYZ \dots\}}^{\text{double contraction}} \\
&+ \dots
\end{aligned} \tag{79}$$

The theorem holds for an arbitrary number of string products. We will see in chapter III that the generalized Wick theorem provides a very powerful numerical way to evaluate matrix elements since only fully contracted elements do not vanish.

8. The pure-correlation electronic Hamiltonian

The introduction of normal-ordering, particle-hole formalism induces a slight modification of the electronic Hamiltonian structure (see appendix VII A or [81] for the proof)

$$\hat{H}_{\text{el}} = \sum_{pq}^{\text{H}\oplus\text{P}} f_{pq} \{\hat{p}^\dagger \hat{q}\} + \frac{1}{4} \sum_{pqrs}^{\text{H}\oplus\text{P}} \langle pq || rs \rangle \{\hat{p}^\dagger \hat{q}^\dagger \hat{s} \hat{r}\} + \langle \Phi | \hat{H}_{\text{el}} | \Phi \rangle \tag{80}$$

with

$$\hat{H}_{\text{el}} = \hat{F} + \hat{V} + E^{\text{HF}}. \tag{81}$$

The electronic Hamiltonian is now divided into a one-electron term, a pure correlation operator \hat{V}

$$\hat{H} = \hat{F} + \hat{V} \tag{82}$$

and the Hartree-Fock total energy E^{HF} introduced in II C 1. Since the Hartree-Fock contribution is already known at the correlation step, we can now exclusively work with the pure electronic correlation Hamiltonian \hat{H} . In the latter we distinguish the one-electron term \hat{F} : the Fock operator which contains the Fock integrals f_{pq}

defined as

$$f_{pq} = h_{pq} + \sum_i^{\mathbb{H}} \langle pi || qi \rangle \quad (83)$$

and the fluctuation potential \hat{V} , the bielectronic part, the pure correlation operator.

Now, since the electronic Hamiltonian (82) is well suited for a correlation model as coupled cluster, this method is presented in the next chapter.

Chapter III

Coupled Cluster Theory

III. COUPLED CLUSTER THEORY

Electronically excited states of small molecules play an important role in many modern areas of research. For example the study of molecule formation in the astrophysics context involving the knowledge of molecular excited states [3, 4, 85]. In ultracold science an accurate description of molecular electronically excited states is crucial [86]; it is also the case for fundamental physics [87, 88]. Consequently we need a method capable of calculating very accurate excitation energies for molecules, which implies a correct assessment of the correlation energy.

In the previous chapter we discuss the correlation energy problem, and its various source. The best way to address correlation energy when the FCI is not possible is to include higher excited determinant in the wave function. We will thus focus on a Wave Function Theory (WFT) which can be systematically improved and allows for detailed insight into correlation contributions. The Configuration Interaction (CI) method can be used at a truncated level (CISD, CISDT) but shows a very slow convergence with respect to the expansion towards the FCI limit. Besides, for a high-accurate treatment of dynamic correlation in both ground state and excitation energies or spectroscopic constants, high rank determinants are required (CISDTQ or beyond) and often leads to a computational limit. However Multi-Reference (MR) CI can be employed to handle Fermi and static correlation *a priori* in the reference wavefunction. The Coupled Cluster (CC) theory allows high rank determinants at a lower rank, for example CCSD can generate quadruply excited determinants by coupling excitations. Dynamic correlation can thus be handled in a very accurate way and the use of Generalized Active Space (GAS) allows a treatment *a posteriori* of the Fermi and static correlation; however where these latter effects are very strong a multi-reference model *a priori* is required.

A. Coupled Cluster wave function

CC theory was developed in the 1950s in the context of nuclear [89] and solid-state physics to rigorously address the fermionic many-body problem. It is a modern and encompassing variant of non-linear theories with coupled terms. In the atomic and molecular many-electron problem, CC theory is the most accurate theory to the

day applicable to both ground and electronically excited states, and is widely used for the computation of atomic and molecular properties.

In this third chapter we will discuss mainly the multi-reference single-reference coupled cluster theory. In the first part, we will first give some general aspects of the formalism, then we will show explicitly the hierarchy of excitations in the CC operators. Thirdly, the GAS-CC wave function ansatz will be presented, then we will introduce the Fermi vacuum concept and we will discuss the truncated CC models. Next we will see what new elaborate wave functions the Generalized Active Space (GAS) allow us to construct in order to struggle *a posteriori*, with the multi-reference problem. In the second part we will focus on the ground-state CC energy by presenting the projected CC equations : the energy and the amplitude equation. We will show how we proceed to solve them *via* an iterative algorithm based on a commutator-based expansion and the evaluation of Wick contractions. The last part is the main purpose of my PhD, the CC excitation energies evaluation. Firstly we will introduce the CC Jacobian matrix and the linear response equation, then we will present the commutator-based implementation of this CC Jacobian matrix and finally a comparison with the previous CI-driven CC algorithm.

1. General aspects

After the mean-field evaluation (see II C 1), a correlation model requires the Hartree-Fock energy and the one- and two-electron integrals (38) and (39) evaluated in the transformation process (see II C 2) to go further. Only after these two steps the evaluation to add the correlation energy contribution can be carried out.

Accordingly to the correlation energy definition given in II C 3 one can conclude that any correlation operator working on any state can be written as

$$(1 + t_\mu \hat{\tau}_\mu) \tag{84}$$

The operator (84) will generate the initial electronic configuration and all the desired virtual configurations *via* the excitation operator $\hat{\tau}_\nu$ associated with an amplitude t_μ . But, the operator (84) used in a linear expansion (CI model) leads to size-consistency problems if one wants to truncate the virtual excitation rank before the full expansion of (84). A model is size-consistent if at any level of truncation

for two non-interacting subsystems \mathcal{A} and \mathcal{B} the energy is additive-separable (size consistent)

$$E = E_{\mathcal{A}} + E_{\mathcal{B}} \quad (85)$$

and the wave function $\psi_{\mathcal{AB}}$ has to give rise to a multiplicatively-separable wave operator

$$\psi_{\mathcal{AB}} = \psi_{\mathcal{A}} \cdot \psi_{\mathcal{B}}. \quad (86)$$

The size consistency is therefore needed to describe compounds and fragments with the same accuracy (if they don't interact). A many-body method is called size extensive if and only if for N interacting subsystems \mathcal{A} the correlation energy of $N\mathcal{A}$ scales linearly with N (in the limit of $N \rightarrow \infty$). To overcome this problem the correlation operators (84) must be coupled to construct a pair-correlated operator, in other words the cluster operators $\hat{\tau}_{\mu}$ must be coupled with each others, the coupled cluster operator will be in product form

$$\prod_{\mu}^{N_c} (1 + t_{\mu} \hat{\tau}_{\mu}) = \prod_{\mu}^{N_c} (1 + \hat{T}_{\mu}) \quad (87)$$

where we introduce the general excitation operator \hat{T}_{μ} and N_c is the number of possible excited determinants. This product corresponds to the first terms of the exponential Taylor expansion

$$\prod_{\mu}^{N_c} e^{\hat{T}_{\mu}} = \prod_{\mu}^{N_c} \left(1 + \hat{T}_{\mu} + \frac{1}{2} \hat{T}_{\mu}^2 + \frac{1}{3!} \hat{T}_{\mu}^3 + \dots \right) \quad (88)$$

The non linear terms inside the product in the expression (88) vanish because a specific \hat{T}_{μ} operator can be applied only once on an initial state. Here is a representative example with an excitation operator $\hat{T}_{1s\overline{1}s}^{2s\overline{2}s}$ which excites the initial electronic configuration $|1s\overline{1}s\rangle$ to $|2s\overline{2}s\rangle$, then

$$\left(\hat{T}_{1s\overline{1}s}^{2s\overline{2}s} \right)^2 |1s\overline{1}s\rangle = \hat{T}_{1s\overline{1}s}^{2s\overline{2}s} \cdot \hat{T}_{1s\overline{1}s}^{2s\overline{2}s} |1s\overline{1}s\rangle = \hat{T}_{1s\overline{1}s}^{2s\overline{2}s} |2s\overline{2}s\rangle = 0 \quad (89)$$

Then the cluster operators satisfy the following nilpotent relation

$$\hat{\tau}_{\mu}^2 = 0 \quad (90)$$

and the expressions (88) reduces to

$$\prod_{\mu}^{N_c} e^{\hat{T}_{\mu}} = \prod_{\mu}^{N_c} (1 + \hat{T}_{\mu}) \quad (91)$$

since excitation operators \hat{T}_μ commute with each other in our implementation due to the fact that we work with one occupied space and one virtual space (which can be divided into subspaces).

$$[\hat{T}_\mu, \hat{T}_\nu] = 0 \quad (92)$$

((92) is not fulfilled for every CC ansatz, for examples see [62, 90]) we can rewrite (91)

$$\prod_{\mu}^{N_c} e^{\hat{T}_\mu} = e^{\sum_{\mu}^{N_c} \hat{T}_\mu} = e^{\hat{T}} \quad (93)$$

which is the most common form for the coupled cluster operator. Besides it is also a very convenient formulation to do analytical developments. The present implementation detailed in this manuscript is both formally size-extensive and size-consistent, due to term-wise extensivity. In the following part we will look how the coupled cluster can reach the different excitation levels.

2. Hierarchy of excitation levels

Using the exponential form (93) with the general excitation operator \hat{T}

$$\hat{T} = \sum_{\mu}^{N_c} \hat{T}_\mu = \sum_n^N \sum_i^{I(n)} \hat{T}_{n,i} \quad (94)$$

where n is the excitation rank (single, double, triple,..., N) and i denotes different excitation types among the $I(n)$ types for a given excitation rank n . Let us look at the different excitation rank contributions for the operators $e^{\hat{T}_1}$ ($n = 1$) and $e^{\hat{T}_2}$ ($n = 2$) from equation (87)

$$e^{\hat{T}_1} = \left(1 + \hat{T}_{1,1}\right) \left(1 + \hat{T}_{1,2}\right) \left(1 + \hat{T}_{1,3}\right) \dots \quad (95)$$

$$e^{\hat{T}_2} = \left(1 + \hat{T}_{2,1}\right) \left(1 + \hat{T}_{2,2}\right) \left(1 + \hat{T}_{2,3}\right) \dots \quad (96)$$

Accordingly the general coupled cluster operator expands explicitly as

$$e^{\hat{T}} = \prod_i^{I(1)} \left(1 + \hat{T}_{1,i}\right) \prod_i^{I(2)} \left(1 + \hat{T}_{2,i}\right) \prod_i^{I(3)} \left(1 + \hat{T}_{3,i}\right) \dots \quad (97)$$

By looking at (97) we can extract the different excitation rank contributions and compare with the linear CI method by writing the coupled cluster operator as

$$e^{\hat{T}} = \sum_n \hat{C}_n \quad (98)$$

$$\hat{C}_0 = 1 \quad (99)$$

$$\hat{C}_1 = \hat{T}_1 \quad (100)$$

$$\hat{C}_2 = \hat{T}_2 + \frac{1}{2!}\hat{T}_1^2 \quad (101)$$

$$\hat{C}_3 = \hat{T}_3 + \hat{T}_1\hat{T}_2 + \frac{1}{3!}\hat{T}_1^3 \quad (102)$$

$$\hat{C}_4 = \hat{T}_4 + \hat{T}_1\hat{T}_3 + \frac{1}{2!}\hat{T}_2^2 + \frac{1}{2!}\hat{T}_1^2\hat{T}_2 + \frac{1}{4!}\hat{T}_1^4 \quad (103)$$

The operators \hat{C}_n show which excitation processes contribute at each excitation level n . CI operators are the operators \hat{T}_n , they are also CC operators and are called connected operators. The coupled cluster brings in addition disconnected operators which are a coupling between two connected operators and give higher rank contribution. For instance in CC model there are five distinct mechanisms to contribute to quadruply excited electronic configurations (103) where, \hat{T}_2^2 represents the independent interactions between two distinct pairs of electrons, \hat{T}_4 describes the simultaneous interaction of four electrons.

The maximum excitation rank N introduced in (94) is determined by the number of correlated electrons in the general active spaces (see GAS definition in the previous chapter II C 4). The maximum number of excitation type per rank $n : I(n)$, is deduced from the number of spinors in the active and virtual spaces. In the following we introduce the GAS-CC ansatz to construct the associated GAS-CC wave function.

3. The relativistic GAS-CC wave function ansatz

The Coupled Cluster method presented in this manuscript is based on the general active space concept (GAS) [91] presented in II C 4. The reader could find other works based on the same ansatz [18, 72, 77, 92] and other CC approaches can be found in this review [76]. The excitation operators $\hat{\tau}_n^{\text{GAS}}$ of general n -rank called cluster, are constructed from these spaces. We obtain the Coupled Cluster wave function by acting with the exponential parametrization (93) on a chosen vacuum reference $|\Phi\rangle$. The actual implementation relies on a single-reference vacuum called the Fermi vacuum, which is distinguished from genuinely multi-references implementations called MRCC which rely on a multi-reference vacuum *a priori* [90]. In our case, for the single-reference CC, the additional electronic configurations other than

the Fermi vacuum are treated *via* the GAS's with high rank excitation operators. The relativistic GAS-CC wave function ansatz is the following

$$|\psi^{\text{GAS-CC}}\rangle = e^{\sum_i^n \hat{T}_i^{\text{GAS}}} |\Phi\rangle \quad (104)$$

where the general n -rank excitation operator is constructed from independent Kramers unbarred and barred creation and annihilation operators

$$\hat{T}_n^{\text{GAS}} = \sum_{\substack{\mathbb{P}, \mathbb{H} \\ a < b < \dots; \bar{a} < \bar{b} < \dots, \\ i < j < \dots; \bar{i} < \bar{j} < \dots}} t_{ij\dots\bar{i}\bar{j}\dots}^{ab\dots\bar{a}\bar{b}\dots} \left\{ \hat{a}^\dagger \hat{b}^\dagger \dots \hat{\bar{a}}^\dagger \hat{\bar{b}}^\dagger \dots \hat{j} \hat{i} \dots \hat{j} \hat{i} \right\} \quad (105)$$

The curly braces refer to second-quantized normal-ordered operators as defined in chapter II C 6. The spinor indices $\{a, b, \dots, \bar{a}, \bar{b}, \dots\} \in \mathbb{P}$ refer to Kramers unbarred and barred particle quasi-operators and the spinor indices $\{i, j, \dots, \bar{i}, \bar{j}, \dots\} \in \mathbb{H}$ refer to Kramers unbarred, barred hole quasi-operators. The $t_{ij\dots\bar{i}\bar{j}\dots}^{ab\dots\bar{a}\bar{b}\dots}$ are the coupled cluster amplitudes associated with the cluster excitation operators to the right. The excitation operators can be classified with ΔM_K introduced in (52) for a given excitation rank n .

It can be useful for analytical calculations to deal with an unrestricted-index form of the general excitation operator (105). In this case all the possible permutations are taken into account including those between barred and unbarred indices

$$\hat{T}^{\text{GAS}} = \sum_{n=1}^N \left(\frac{1}{n!} \right)^2 \sum_{\substack{\mathbb{P}, \mathbb{H} \\ ab\dots; \bar{a}\bar{b}\dots, \\ ij\dots; \bar{i}\bar{j}\dots}} t_{ij\dots\bar{i}\bar{j}\dots}^{ab\dots\bar{a}\bar{b}\dots} \left\{ \hat{a}^\dagger \hat{b}^\dagger \dots \hat{\bar{a}}^\dagger \hat{\bar{b}}^\dagger \dots \hat{j} \hat{i} \dots \hat{j} \hat{i} \right\}. \quad (106)$$

Accordingly a prefactor is required to avoid the multiple counting of terms (the operator is still normal-ordered). The coupled cluster amplitudes get a minus sign for each permutation of indices, for example

$$t_{ij\dots\bar{i}\bar{j}\dots}^{ab\dots\bar{a}\bar{b}\dots} = -t_{ji\dots\bar{j}\bar{i}\dots}^{ab\dots\bar{a}\bar{b}\dots} \quad (107)$$

The Kramers symmetry introduced in the previous chapter can also be used to reduce the number of amplitudes. However, this requires that \hat{K} commutes with \hat{T} , which is satisfied in our implementation since it is a single reference model where the spinors are Kramers-paired. For multi-reference models this commutation condition does not hold and the way to proceed is much subtler [62]. Then the following

relations (108) can be established for arbitrary order CC amplitudes depending on N , ΔM_k and $M_{ub} = \frac{N^c + N^a}{2} - \frac{\overline{N}^c + \overline{N}^a}{2}$.

$$t_{N, \Delta M_k, M_{ub}} = (-1)^{|\Delta M_k|} t_{N, -\Delta M_k, -M_{ub}}^* \quad (108)$$

the latter is not yet exploited in the current implementation.

If we turn to the implementation, the general excitation operators are represented by second-quantized strings \mathcal{S} in their respective spaces which depend on the excitation rank and on the GAS parametrization

$$\mathcal{S}_p^\dagger = \prod_{a \in \mathbb{P}} \hat{a}^\dagger, \quad \overline{\mathcal{S}}_p^\dagger = \prod_{\bar{a} \in \mathbb{P}} \hat{\bar{a}}^\dagger, \quad \mathcal{S}_h = \prod_{i \in \mathbb{H}} \hat{i}, \quad \overline{\mathcal{S}}_h = \prod_{\bar{i} \in \mathbb{H}} \hat{\bar{i}} \quad (109)$$

and thus a given n -rank excitation operator is generated as

$$\hat{T}_n^{\text{GAS}} = \sum_{\mathbb{P}, \mathbb{H}} \left\{ \mathcal{S}_p^\dagger \overline{\mathcal{S}}_p^\dagger \overline{\mathcal{S}}_h \mathcal{S}_h \right\} \quad (110)$$

4. The Fermi vacuum $|\Phi\rangle$

The Fermi vacuum is defined by

$$|\Phi\rangle = \left(\prod_i^{\mathbb{H}} \hat{i}^\dagger \right) |0\rangle \quad (111)$$

With $|0\rangle$ the electron vacuum state, considered in this approach as a state without any electron. An illustrative example of Fermi vacuum parametrization through generalized active spaces is given in figure 6.

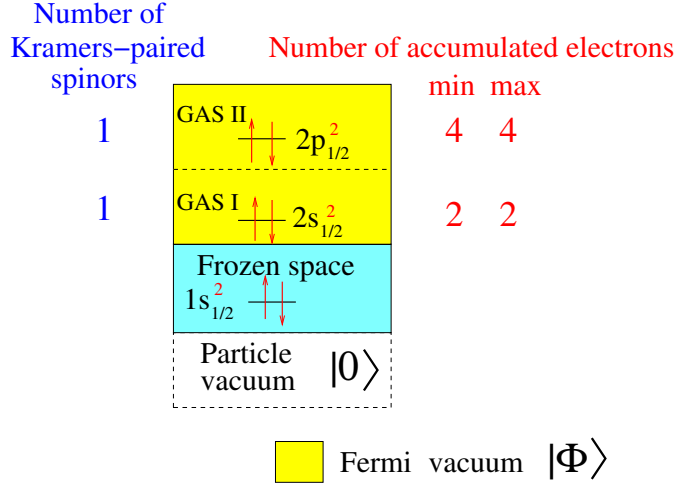


FIGURE 6. An example of Fermi vacuum $|\Phi\rangle$ for the carbon atom, here the Fermi vacuum is $2s_{1/2}$ and $2p_{1/2}$ spin-orbitals both doubly occupied in separate GAS's (the Fermi vacuum can also be set in one GAS).

Using a single determinant as the Fermi vacuum exhibits however some restrictions. Some systems with many open shells can be very difficult to treat like iron with $3d^6$ shells, if the Fermi vacuum is represented by a single determinant, other determinants of the same configuration will miss and they can have a similar weight in the true quantum mechanic ground-state. Then the ground-state CC calculation become just impossible to converge. The figure 7 illustrates how we proceed in such cases

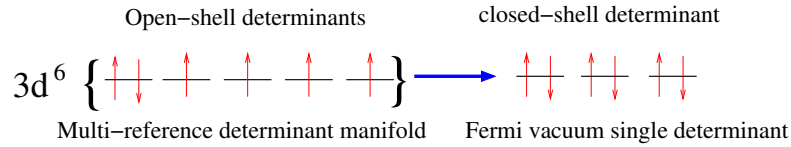


FIGURE 7. For $3d^6$ electronic configurations we must choose only one closed-shell determinant to set the Fermi vacuum.

However we will see in the following that a good choice of Fermi vacuum combined with multi-reference adapted GAS's schemes permits to treat some 'multi-reference' systems.

5. Truncated models and equivalence FCC/FCI

The many-body problem for electrons for a given finite basis-set, a given Hamiltonian and a given active space of N electrons can be solved in an exact manner if $n = N$ in equation (104). This condition is fulfilled if *via* some excitation operators we generate all the possible configurations of the N electrons in all possible spinors belonging to the considered spaces. Such a procedure is called a full configuration interaction (FCI). A totally equivalent wave function can be build in coupled cluster theory for $n = N$ (FCC). However, this parametrization is almost always too expensive in terms of memory, storage and calculation time, it becomes quickly infeasible for larger atomic basis sets.

In the coupled cluster wave function, the general excitation operator $\hat{T} = \sum_i^n t_i \hat{\tau}_i$ can be truncated. The implementation presented here is of general excitation rank because $1 \leq n \leq N$. In other terms we can construct the wave functions CCS, CCSD, CCSDT, CCSDTQ etc... for $n = 1, 2, 3, 4...$, respectively, with S = Single, D = Double, T = Triple, Q = Quadruple excitations and so on up to FCC. This truncation permits to have a balance between accuracy and computational cost. We will see in the following application in IV that CCSDTQ (and some elaborate schemes between CCSDT and CCSDTQ) wave function is extremely close to the FCI (an error of a few cm^{-1} on the excitation energy T_e or T_v and on spectroscopic constants) if an adequate number of electrons is chosen.

6. The GAS parametrization

In the first part of this chapter we introduced the GAS-CC wave function where the general excitation \hat{T}_n^{GAS} depend on the GAS parametrization (see figure 4 in IIC4). The Fermi vacuum is an example of GAS parametrization (see figure 6) where the minimum and maximum number of accumulated electrons in equal; it represents in particular, exactly one electronic determinant. In order to obtain more electronic configurations, as we saw in the wave function ansatz (104), the general excitation operators $\hat{\tau}_n$ can be applied. In accord with the excitation rank n of the cluster operator the minimum number of accumulated electrons can be reduced by n for a given GAS.

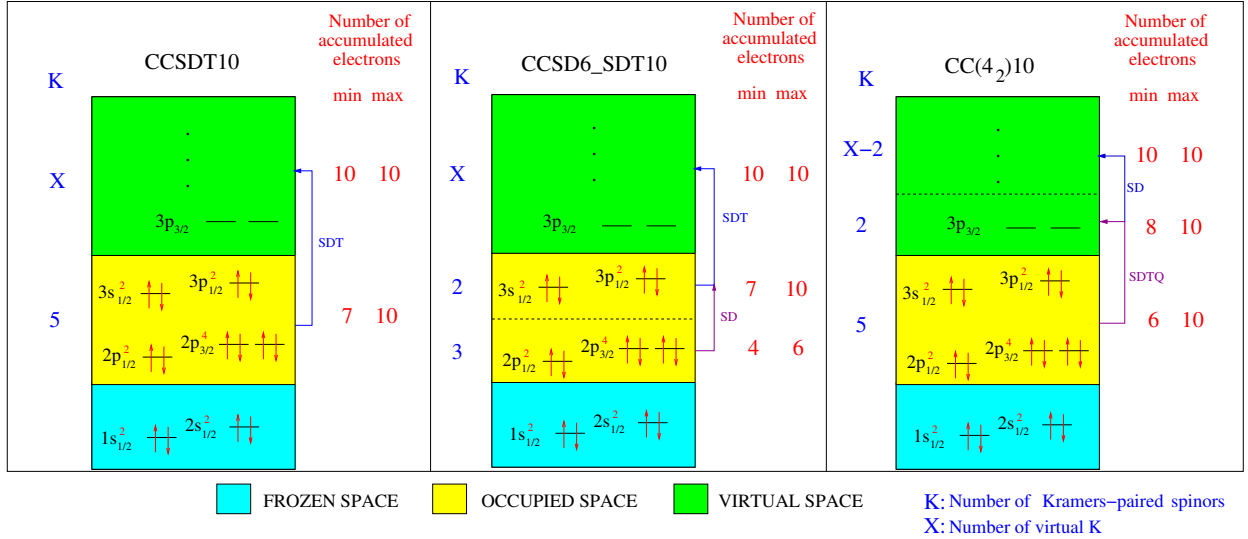


FIGURE 8. Example of three possible GAS parametrizations for the Silicon atom. To the left a standard CCSDT, in the middle a core-correlation model and to the right a $CC(n_m)$ parametrization.

Let us rely on the figure 8 above to illustrate the excitation operators GAS parametrization with three representative schemes. First, to the left we have a standard approach where the first four electrons are inactive for correlation. In the GAS I with the ten electrons in five Kramers-paired spinors, the minimum number of accumulated electrons is reduced by three, in other words, we made three holes in the GAS I which correspond to three electrons excited to the virtual GAS II. Consequently we generate some new electronic configurations occurring from the triple excitation in a spinor set of ten electrons towards virtual spinors; this is the CCSDT10 scheme. The wave function will be a linear combination of all the determinants generated by the connected and disconnected clusters (99, 100, 101, 102) and will be closer to the FCI wave function compared to the single configuration. We turn to the middle GAS parametrization in figure 8. In order to reduce the calculation cost we decide to separate the occupied space in two GAS's and to reduce the excitation rank for the first six electrons. The GAS I with six electrons in three Kramers-paired spinors will be only doubly-excited towards GAS II and GAS III. However electrons from the GAS II still can be triply excited, accordingly the GAS III contains either three electrons from GAS II or two from GAS II and one from GAS I or one from GAS II and two from GAS I. This second scheme permit to include core orbitals with a low-rank

treatment which is useful for any core (in particular for d^{10} or f^{14} cores for heavy atoms). For the scheme name we use the number of electrons per GAS with the appropriate excitation rank (SDT...), the second scheme is thus CCSD6_SDT10. The third scheme on the right in figure 8 is one of the more powerful parametrizations. We consider a GAS I with ten electrons in five Kramers-paired spinors quadruply excited towards a virtual GAS II which contain four important virtual spinors, *i.e.* we allow for configurations with four holes in GAS I, but only double excitations towards the other virtual spinors in GAS III. A important weight is associated for electronic configurations arising from the GAS II virtual spinors. If one wants to describe some excited states arising from known electronic configurations, one can parametrize a CC(n_m) wave function in order to recover all the needed electronic configurations avoiding high-rank excitation towards the whole virtual space. The second and third schemes could also be merged since the concept is generalized.

If we turn to the formalism of excitation operators, for the standard scheme CCSDT we will have these cluster classes

$$\hat{\tau}_I^S, \quad \hat{\tau}_{I,I}^D, \quad \hat{\tau}_{I,I,I}^T. \quad (112)$$

For the second core scheme CCSD_SDT we have

$$\begin{aligned} \hat{\tau}_I^S, \quad \hat{\tau}_{II}^S, \quad \hat{\tau}_{I,I}^D, \quad \hat{\tau}_{I,II}^D, \quad \hat{\tau}_{II,II}^D, \\ \hat{\tau}_{I,I,II}^T, \quad \hat{\tau}_{I,II,II}^T, \quad \hat{\tau}_{II,II,II}^T, \end{aligned} \quad (113)$$

and finally for the third one, the CC(4₂) scheme, we have

$$\begin{aligned} \hat{\tau}_I^S, \quad \hat{\tau}_{II}^S, \quad \hat{\tau}_{I,I}^D, \quad \hat{\tau}_{I,II}^D, \quad \hat{\tau}_{II,II}^D, \\ \hat{\tau}_{I,I,I}^T, \quad \hat{\tau}_{I,I,II}^T, \quad \hat{\tau}_{I,II,II}^T, \\ \hat{\tau}_{I,I,I,I}^Q, \quad \hat{\tau}_{I,I,I,II}^Q, \quad \hat{\tau}_{I,I,II,II}^Q. \end{aligned} \quad (114)$$

We introduced above the operator class concept, excitation operators can be classified in accordance with the GAS which they act on and their excitation rank (Single, Double, Triple, Quadruple, ...).

B. The ground state coupled cluster energy

1. The projected unlinked and linked equations

The solution of coupled cluster of the stationary Schrödinger or Dirac equations with a coupled cluster wave function is done by projection in an iterative way ; there exists some attempts in a variational manner. In this case the problem is tedious due to the fact that even for a truncated CC wave function, all the FCI determinants are required. However some unconventional aspects can be found with an elaborate VCC theory like faster convergence with the excitation rank (see [76]).

The coupled cluster wave function (104) can be used with an Hamiltonian to write the stationary Schrödinger or Dirac equations :

$$\hat{H} |\psi^{\text{GAS-CC}}\rangle = E^{\text{CC}} |\psi^{\text{GAS-CC}}\rangle \quad \Rightarrow \quad \hat{H} e^{\hat{T}} |\Phi\rangle = E^{\text{CC}} e^{\hat{T}} |\Phi\rangle. \quad (115)$$

For clarity, E^{CC} represents CC correlation energy such as

$$E^{\text{CC}} = E^{\text{tot}} - E^{\text{HF}} \quad (116)$$

The projection on the Fermi vacuum bra $\langle\Phi|$ and on the μ excited determinants $\langle\psi_\mu|$ (μ relies to the chosen general active spaces and on the excitation rank n)

$$\langle\psi_\mu| = \langle\Phi| \hat{\tau}_\mu^\dagger \quad (117)$$

gives rise to $\mu + 1$ equations

$$\langle\Phi| \hat{H} e^{\hat{T}} |\Phi\rangle = E^{\text{CC}} \langle\Phi| e^{\hat{T}} |\Phi\rangle \quad (118)$$

$$\langle\Phi| \hat{\tau}_\mu^\dagger \hat{H} e^{\hat{T}} |\Phi\rangle = E^{\text{CC}} \langle\Phi| \hat{\tau}_\mu^\dagger e^{\hat{T}} |\Phi\rangle \quad (119)$$

The coupled cluster operator $e^{\hat{T}}$ on the right- hand side of equation (118) can be written as a Taylor expansion (91). Thus, only the unity operator gives a contribution by virtue of the orthonormality condition

$$\langle\Phi| \Phi\rangle = 1 \quad , \quad \langle\psi_\mu| \Phi\rangle = 0 \quad (120)$$

and then we find the unlinked coupled cluster equations

$$\langle\Phi| \hat{H} e^{\hat{T}} |\Phi\rangle = E^{\text{CC}} \quad , \quad \langle\Phi| \hat{\tau}_\mu^\dagger \hat{H} e^{\hat{T}} |\Phi\rangle = E^{\text{CC}} \langle\Phi| \hat{\tau}_\mu^\dagger e^{\hat{T}} |\Phi\rangle \quad (121)$$

If we multiply the equations (115) at the left by $e^{-\hat{T}}$ before the various projections, we obtain the linked coupled cluster equations (also called the similarity-transformed coupled cluster equations)

$$\langle \Phi | e^{-\hat{T}} \hat{H} e^{\hat{T}} | \Phi \rangle = E^{\text{CC}} \quad (122)$$

$$\langle \Phi | \hat{\tau}_\mu^\dagger e^{-\hat{T}} \hat{H} e^{\hat{T}} | \Phi \rangle = 0 \quad (123)$$

The use of the terminology 'linked' and 'unlinked' refers to the appearance of linked and unlinked diagrams in the perturbation theory. It is shown in [50] that the two representations are equivalent. The algorithm presented in this manuscript is based on the linked form like the CI-driven Coupled Cluster, but it is also possible to construct an algorithm based on the unlinked form. We will discuss the CI-driven algorithm later in (III C 3).

2. The energy equation

The energy equation in (122) can be simplified

$$E^{\text{CC}} = \langle \Phi | e^{-\hat{T}} \hat{H} e^{\hat{T}} | \Phi \rangle = \langle \Phi | \hat{H} e^{\hat{T}} | \Phi \rangle = \langle \Phi | \hat{H} \left(1 + \hat{T} + \frac{1}{2} \hat{T}^2 + \dots \right) | \Phi \rangle \quad (124)$$

since the Hamiltonian \hat{H} is a two particle operator which can deexcite two electrons at most. So if one wants to recover the initial state $|\Phi\rangle$, the excitation rank must be lower or equal to two. Consequently, all connected or disconnected operators which excite at least three electrons vanish. Besides the single excitation operator \hat{T}_1 also vanish due to Brillouin's theorem [93]. Finally, the coupled cluster energy is only determined by double excitations

$$E^{\text{CC}} = \langle \Phi | \hat{H} \left(1 + \hat{T}_2 + \frac{1}{2} \hat{T}_1^2 \right) | \Phi \rangle \quad (125)$$

Notice that we simplified the left term since

$$\langle \Phi | e^{-\hat{T}} = \langle \Phi | \left(1 - \hat{T} + \frac{1}{2} \hat{T}^2 - \dots \right) = \langle \Phi | \quad (126)$$

because when the excitation operators act on the left, on a bra vector, they act as deexcitation operators, since all the hole spinors are already occupied by definition of the Fermi vacuum (185) and under the Pauli principle all the $\langle \Phi | \hat{T}$ bra vectors vanish.

Regarding the energy equation (125), one can notice that the coupled cluster energy depends directly only on connected and disconnected double excitations \hat{T}_2 and \hat{T}_1^2 . However, higher ranks give an indirect contribution since we need to solve the amplitude equations (123) to find the coupled cluster amplitudes t .

If we introduce the normal-ordered Hamiltonian derived in the previous chapter in (82) into (125) we get these four terms to evaluate

$$E^{\text{CC}} = \langle \Phi | \hat{F} \hat{T}_2 | \Phi \rangle + \frac{1}{2} \langle \Phi | \hat{F} \hat{T}_1 \hat{T}_1 | \Phi \rangle + \langle \Phi | \hat{V} \hat{T}_2 | \Phi \rangle + \frac{1}{2} \langle \Phi | \hat{V} \hat{T}_1 \hat{T}_1 | \Phi \rangle \quad (127)$$

since

$$\langle \Phi | \hat{H} | \Phi \rangle = 0 \quad (128)$$

for the pure correlation electronic Hamiltonian. It should be noticed that E^{CC} is correlation energy by definition (116). The four elements (127) can be evaluated with the generalized Wick theorem. As an illustrative example we will explicitly derive these matrix elements and start with

$$\begin{aligned} \langle \Phi | \hat{V} \hat{T}_2 | \Phi \rangle &= \frac{1}{4} \sum_{pqrs}^{\mathbb{H} \oplus \mathbb{P}} \langle pq || rs \rangle \frac{1}{4} \sum_{ij,ab}^{\mathbb{H} \oplus \mathbb{P}} t_{ij}^{ab} \langle \Phi | \{ \hat{p}^\dagger \hat{q}^\dagger \hat{s} \hat{r} \} \{ \hat{a}^\dagger \hat{b}^\dagger \hat{j} \hat{i} \} | \Phi \rangle \\ &= \frac{1}{16} \sum_{pqrs}^{\mathbb{H} \oplus \mathbb{P}} \langle pq || rs \rangle \sum_{ij,ab}^{\mathbb{H} \oplus \mathbb{P}} t_{ij}^{ab} \left(\right. \\ &\quad \langle \Phi | \{ \hat{p}^\dagger \hat{q}^\dagger \hat{s} \hat{r} \hat{a}^\dagger \hat{b}^\dagger \hat{j} \hat{i} \} | \Phi \rangle + \langle \Phi | \{ \hat{p}^\dagger \hat{q}^\dagger \hat{s} \hat{r} \hat{a}^\dagger \hat{b}^\dagger \hat{j} \hat{i} \} | \Phi \rangle \\ &\quad \left. + \langle \Phi | \{ \hat{p}^\dagger \hat{q}^\dagger \hat{s} \hat{r} \hat{a}^\dagger \hat{b}^\dagger \hat{j} \hat{i} \} | \Phi \rangle + \langle \Phi | \{ \hat{p}^\dagger \hat{q}^\dagger \hat{s} \hat{r} \hat{a}^\dagger \hat{b}^\dagger \hat{j} \hat{i} \} | \Phi \rangle \right) \\ &= \frac{1}{16} \sum_{pqrs}^{\mathbb{H} \oplus \mathbb{P}} \langle pq || rs \rangle \sum_{ij,ab}^{\mathbb{H} \oplus \mathbb{P}} t_{ij}^{ab} (\delta_{pj} \delta_{qi} \delta_{rb} \delta_{sa} - \delta_{pj} \delta_{qi} \delta_{ra} \delta_{sb} - \delta_{pi} \delta_{qj} \delta_{rb} \delta_{sa} + \delta_{pi} \delta_{qj} \delta_{ra} \delta_{sb}) \\ &= \frac{1}{16} \sum_{ij,ab}^{\mathbb{H} \oplus \mathbb{P}} t_{ij}^{ab} (\langle ji || ba \rangle - \langle ji || ab \rangle - \langle ij || ba \rangle + \langle ij || ab \rangle) \\ \langle \Phi | \hat{V} \hat{T}_2 | \Phi \rangle &= \frac{1}{4} \sum_{ij,ab}^{\mathbb{H} \oplus \mathbb{P}} t_{ij}^{ab} \langle ij || ab \rangle. \end{aligned} \quad (129)$$

For (129) we applied the Wick rules (79). Only fully contracted terms gives a contribution, consequently the following expressions vanish

$$\begin{aligned} \langle \Phi | \hat{F} \hat{T}_2 | \Phi \rangle &= 0 \\ \langle \Phi | \hat{F} \hat{T}_1^2 | \Phi \rangle &= 0 \end{aligned} \quad (130)$$

because they do not contain any full contraction. The second term which gives a

non-zero contribution can also be evaluated in a very similar manner

$$\begin{aligned}
\langle \Phi | \hat{V} \hat{T}_1 \hat{T}_1 | \Phi \rangle &= \frac{1}{4} \sum_{pqrs}^{\mathbb{H} \oplus \mathbb{P}} \langle pq || rs \rangle \sum_{i,a}^{\mathbb{H} \oplus \mathbb{P}} t_i^a \sum_{j,b}^{\mathbb{H} \oplus \mathbb{P}} t_j^b \langle \Phi | \{ \hat{p}^\dagger \hat{q}^\dagger \hat{s} \hat{r} \} \{ \hat{a}^\dagger \hat{i} \} \{ \hat{b}^\dagger \hat{j} \} | \Phi \rangle \\
&= \frac{1}{4} \sum_{pqrs}^{\mathbb{H} \oplus \mathbb{P}} \sum_{ij,ab}^{\mathbb{H} \oplus \mathbb{P}} t_i^a t_j^b \langle pq || rs \rangle \langle \Phi | \{ \hat{p}^\dagger \hat{q}^\dagger \hat{s} \hat{r} \hat{a}^\dagger \hat{i} \hat{b}^\dagger \hat{j} \} | \Phi \rangle \\
&= \frac{1}{4} \sum_{pqrs}^{\mathbb{H} \oplus \mathbb{P}} \sum_{ij,ab}^{\mathbb{H} \oplus \mathbb{P}} t_i^a t_j^b \langle pq || rs \rangle \left(\langle \Phi | \{ \hat{p}^\dagger \hat{q}^\dagger \hat{s} \hat{r} \hat{a}^\dagger \hat{i} \hat{b}^\dagger \hat{j} \} | \Phi \rangle + \langle \Phi | \{ \hat{p}^\dagger \hat{q}^\dagger \hat{s} \hat{r} \hat{a}^\dagger \hat{i} \hat{b}^\dagger \hat{j} \} | \Phi \rangle \right. \\
&\quad \left. + \langle \Phi | \{ \hat{p}^\dagger \hat{q}^\dagger \hat{s} \hat{r} \hat{a}^\dagger \hat{i} \hat{b}^\dagger \hat{j} \} | \Phi \rangle + \langle \Phi | \{ \hat{p}^\dagger \hat{q}^\dagger \hat{s} \hat{r} \hat{a}^\dagger \hat{i} \hat{b}^\dagger \hat{j} \} | \Phi \rangle \right) \\
&= \frac{1}{4} \sum_{pqrs}^{\mathbb{H} \oplus \mathbb{P}} \sum_{ij,ab}^{\mathbb{H} \oplus \mathbb{P}} t_i^a t_j^b \langle pq || rs \rangle (-\delta_{pj} \delta_{qi} \delta_{sb} \delta_{ra} + \delta_{pi} \delta_{qj} \delta_{sb} \delta_{ra} + \delta_{pj} \delta_{qi} \delta_{sa} \delta_{rb} - \delta_{pi} \delta_{qj} \delta_{sa} \delta_{rb}) \\
&= \frac{1}{4} \sum_{ij,ab}^{\mathbb{H} \oplus \mathbb{P}} t_i^a t_j^b (-\langle ji || ab \rangle + \langle ij || ab \rangle + \langle ji || ba \rangle - \langle ij || ba \rangle) \\
\langle \Phi | \hat{V} \hat{T}_1 \hat{T}_1 | \Phi \rangle &= \sum_{ij,ab}^{\mathbb{H} \oplus \mathbb{P}} t_i^a t_j^b \langle ij || ab \rangle
\end{aligned} \tag{131}$$

Finally, the ground state coupled cluster energy equation is a combination of products of integrals and amplitudes and reduces to

$$E^{\text{CC}} = \frac{1}{4} \sum_{ij,ab}^{\mathbb{H} \oplus \mathbb{P}} (t_{ij}^{ab} + 2t_i^a t_j^b) \langle ij || ab \rangle. \tag{132}$$

In a general spinor form, equation (132) holds for a Kramers-paired expansion with barred and unbarred indices. At this step the integrals are known (from the integral transformation), the t coupled cluster amplitudes will be determined in the following step : the solution of the amplitude equations.

3. The amplitude equations

Turning to the linked amplitude equation (123), the central operator can be expanded by using a Baker-Campbell-Hausdorff (BCH) expansion

$$e^{-\hat{T}} \hat{H} e^{\hat{T}} = \hat{H} + [\hat{H}, \hat{T}] + \frac{1}{2} [[\hat{H}, \hat{T}], \hat{T}] + \frac{1}{6} [[[\hat{H}, \hat{T}], \hat{T}], \hat{T}] + \frac{1}{24} [[[[\hat{H}, \hat{T}], \hat{T}], \hat{T}], \hat{T}]. \tag{133}$$

The expression (133) analytically truncates after the fourfold-nested commutator term due to cluster-commutation conditions and operators ranks. Details and a demonstration can be found in appendix VIII A or in reference [50]. The amplitude

equations can thus be written as

$$\Omega_\mu = \langle \Phi | \hat{\tau}_\mu^\dagger \left(\hat{H} + [\hat{H}, \hat{T}] + \frac{1}{2} [[\hat{H}, \hat{T}], \hat{T}] + \frac{1}{6} [[[\hat{H}, \hat{T}], \hat{T}], \hat{T}] + \frac{1}{24} [[[[\hat{H}, \hat{T}], \hat{T}], \hat{T}], \hat{T}] \right) | \Phi \rangle = 0. \quad (134)$$

The commutator-based algorithm implemented by L.K. Sørensen, J. Olsen and T. Fleig [77] handles this crucial step. A complete documentation exists in L.K. Sørensen PhD manuscript [94]. To avoid too much overlap I will briefly describe the main steps of this procedure.

As we had seen in the previous section IIIB 2, a string composed of Hamiltonian and excitation operators can be reduced by performing contraction. The amplitude equation system will be solved with a similar method based on contraction since the nested commutator can be viewed as string product as well. Firstly, the excited determinant $\langle \psi_\mu |$ can be expressed in terms of the Fermi vacuum $\langle \Phi |$ (see (117)). In other words, the bra-vector gives rise to an additional string

$$\langle \psi_\mu | = \langle \Phi | \hat{\tau}_\mu^\dagger = \langle \Phi | \{ \hat{a}^\dagger \hat{b}^\dagger \dots \hat{j} \hat{i} \}^\dagger = \langle \Phi | \{ \hat{i}^\dagger \hat{j}^\dagger \dots \hat{b} \hat{a} \}. \quad (135)$$

Secondly, due to the use of normal-ordered strings, the generalized Wick theorem allows for significant simplifications of the BCH expansion [81, 83]. Indeed since only fully contracted terms survive, the expression (134) can be cast without commutators as it is demonstrated in the previously-cited references. The Hamiltonian fragment must be connected at least once to every cluster operator on its right

$$\Omega_\mu = \langle \Phi | \hat{\tau}_\mu^\dagger \left(\hat{H} + \hat{H} \hat{T} + \frac{1}{2} \hat{H} \hat{T} \hat{T} + \frac{1}{6} \hat{H} \hat{T} \hat{T} \hat{T} + \frac{1}{24} \hat{H} \hat{T} \hat{T} \hat{T} \hat{T} \right) | \Phi \rangle. \quad (136)$$

and all the other possibilities vanish. To give a representative example, let us take a one-electron fragment of the Hamiltonian \hat{F}_q^p with a singly-excited bra $\langle \Phi | (\hat{\tau}_i^a)^\dagger$ and two single excitation operators \hat{T}_j^b and \hat{T}_k^c

$$\begin{aligned} \langle \Phi | (\hat{\tau}_i^a)^\dagger \left[[\hat{F}_q^p, \hat{T}_j^b], \hat{T}_k^c \right] | \Phi \rangle &= \langle \Phi | \{ \hat{i}^\dagger \hat{a} \} \{ \hat{p}^\dagger \hat{q} \} \{ \hat{b}^\dagger \hat{j} \} \{ \hat{c}^\dagger \hat{k} \} | \Phi \rangle f_{pq} t_j^b t_k^c \\ &= \langle \Phi | \{ \hat{i}^\dagger \hat{a} \hat{p}^\dagger \hat{q} \hat{b}^\dagger \hat{j} \hat{c}^\dagger \hat{k} \} | \Phi \rangle f_{pq} t_j^b t_k^c \\ &\quad + \langle \Phi | \{ \hat{i}^\dagger \hat{a} \hat{p}^\dagger \hat{q} \hat{b}^\dagger \hat{j} \hat{c}^\dagger \hat{k} \} | \Phi \rangle f_{pq} t_j^b t_k^c \\ &= (-\delta_{ij} \delta_{ac} \delta_{pk} \delta_{qb} - \delta_{ik} \delta_{ab} \delta_{pj} \delta_{qc}) f_{pq} t_j^b t_k^c \\ \langle \Phi | (\hat{\tau}_i^a)^\dagger \left[[\hat{F}_q^p, \hat{T}_j^b], \hat{T}_k^c \right] | \Phi \rangle &= -f_{kb} t_i^a t_k^c - f_{jc} t_j^b t_i^a. \end{aligned} \quad (137)$$

Turning to the implementation, the expression (136) is fragmented into five parts :

$$\begin{aligned}
& \langle \Phi | \hat{\tau}_\mu^\dagger \hat{H} | \Phi \rangle \\
& \langle \Phi | \hat{\tau}_\mu^\dagger \hat{H} \hat{T} | \Phi \rangle \\
& \frac{1}{2} \langle \Phi | \hat{\tau}_\mu^\dagger \hat{H} \hat{T} \hat{T} | \Phi \rangle \\
& \frac{1}{6} \langle \Phi | \hat{\tau}_\mu^\dagger \hat{H} \hat{T} \hat{T} \hat{T} | \Phi \rangle \\
& \frac{1}{24} \langle \Phi | \hat{\tau}_\mu^\dagger \hat{H} \hat{T} \hat{T} \hat{T} \hat{T} | \Phi \rangle .
\end{aligned} \tag{138}$$

In the principal loop over the different Hamiltonian operators (sorted by classes), the algorithm determines in advance the vanishing block between these five (138). Then the intermediate contraction routines perform the contractions between the different involved strings. The general contraction routine is based on intermediate steps where operators are contracted one by one

$$\hat{H} \hat{T} \hat{T} \hat{T} \hat{T} = \hat{H}_{\hat{T}} \hat{T} \hat{T} \hat{T} = \hat{H}_{\hat{T}\hat{T}} \hat{T} \hat{T} = \hat{H}_{\hat{T}\hat{T}\hat{T}} \hat{T} = \hat{H}_{\hat{T}\hat{T}\hat{T}\hat{T}} \tag{139}$$

For each term the program will determine all the ways to perform the contractions. Next the different contractions are gathered by performing some permutation. A nice example of this procedure and a good description is given in L.K Sørensen PhD manuscript [94]. At this step it becomes clear that the amplitudes depend on the excitation rank and then will give an indirect contribution in the energy equation (132).

As shown in equation (137), the evaluation of all the possible contributions gives rise to sums of integrals multiplied by amplitudes. Each excited determinant adds an equation of such terms, and finally the system consists of μ non-linear equations since the cluster amplitudes are coupled. The solution of the amplitude equation (134) is then a vector function of amplitudes

$$\mathbf{t}_\mu = \begin{pmatrix} t_i^a \\ \vdots \\ t_{ij}^{ab} \\ \vdots \end{pmatrix} \quad \text{with} \quad \dim(\mathbf{t}_\mu) = \mu. \tag{140}$$

To solve this problem and find the required coupled cluster amplitudes \mathbf{t}_μ a perturbation-based quasi-Newton [50] (with DIIS acceleration [95]) algorithm is employed, which is an iterative procedure.

After several iterations, the set of coupled cluster amplitudes (140) is known and the coupled cluster ground state energy (132) can be calculated.

C. Excited-state coupled cluster energies

General response theory provides a powerful framework for the calculation of atomic and molecular properties [96–99]. The calculation of electronically excited state energies is also possible using a linear version of this formalism which has been demonstrated with GAS-CC functions in reference [100, 101]. In linear response (LR) theory the excited-state energies occur as the poles of the response function.

1. The Coupled Cluster Jacobian matrix

The response theory covers a very large spectrum of applications and the evaluation of excited-state energies represents one aspect of this theory. To avoid the introduction of too much formalism, we invite the reader to consult the afore-mentioned references. The excited-state energies equation require the derivative of the CC vector function Ω_μ (123) with respect to the coupled cluster amplitudes t_ν according to linear response theory :

$$\begin{aligned}\frac{\partial}{\partial t_\nu}\Omega_\mu &= \frac{\partial}{\partial t_\nu} \langle \Phi | \hat{\tau}_\mu^\dagger e^{-\hat{T}} \hat{H} e^{\hat{T}} | \Phi \rangle \\ &= \langle \Phi | \hat{\tau}_\mu^\dagger e^{-\hat{T}} \hat{H} \hat{\tau}_\nu e^{\hat{T}} | \Phi \rangle - \langle \Phi | \hat{\tau}_\mu^\dagger \hat{\tau}_\nu e^{-\hat{T}} \hat{H} e^{\hat{T}} | \Phi \rangle\end{aligned}\quad (141)$$

since

$$\frac{\partial}{\partial t_\nu} \hat{T} = \frac{\partial}{\partial t_\nu} \sum_i^n t_i \hat{\tau}_i = \hat{\tau}_\nu. \quad (142)$$

By considering the commutation between the excitation operators (92),

$$\begin{aligned}\left[\hat{\tau}_\nu, e^{-\hat{T}} \right] &= \hat{\tau}_\nu e^{-\hat{T}} - e^{-\hat{T}} \hat{\tau}_\nu = \hat{\tau}_\nu \left(1 - \hat{T}_1 + \frac{1}{2} \hat{T}_2 - \dots \right) - e^{-\hat{T}} \hat{\tau}_\nu \\ &= \left(1 - \hat{T}_1 + \frac{1}{2} \hat{T}_2 - \dots \right) \hat{\tau}_\nu - e^{-\hat{T}} \hat{\tau}_\nu = e^{-\hat{T}} \hat{\tau}_\nu - e^{-\hat{T}} \hat{\tau}_\nu = 0\end{aligned}\quad (143)$$

equation (141) can be written

$$A_{\mu\nu} = \langle \Phi | \hat{\tau}_\mu^\dagger e^{-\hat{T}} \left[\hat{H}, \hat{\tau}_\nu \right] e^{\hat{T}} | \Phi \rangle \quad (144)$$

According to linear response theory, the diagonalization of the CC Jacobian matrix (144) gives the excitation energies ω_f which are obtained from the eigenvalue equation

$$\mathbf{A}^{\text{CC}} |\psi_f\rangle = \text{diag}(\omega_f) |\psi_f\rangle \quad (145)$$

where \mathbf{A}^{CC} is the corresponding diagonal matrix and $|\psi_f\rangle$ is the right eigenvector that corresponds to the eigenvalue ω_f . The name Jacobian is related to the mathematical structure of $A_{\mu\nu}$: this is a matrix of all first-order partial derivatives of a vector-valued function. Before diagonalization, the CC Jacobian matrix $A_{\mu\nu}$ will have the following structure

$$A_{\mu\nu} = \begin{pmatrix} \langle \psi_{\mu_1} | e^{-\hat{T}} [\hat{H}, \hat{\tau}_{\nu_1}] e^{\hat{T}} | \Phi \rangle & \langle \psi_{\mu_1} | e^{-\hat{T}} [\hat{H}, \hat{\tau}_{\nu_2}] e^{\hat{T}} | \Phi \rangle & \cdots & \langle \psi_{\mu_1} | e^{-\hat{T}} [\hat{H}, \hat{\tau}_{\nu_N}] e^{\hat{T}} | \Phi \rangle \\ \langle \psi_{\mu_2} | e^{-\hat{T}} [\hat{H}, \hat{\tau}_{\nu_1}] e^{\hat{T}} | \Phi \rangle & \langle \psi_{\mu_2} | e^{-\hat{T}} [\hat{H}, \hat{\tau}_{\nu_2}] e^{\hat{T}} | \Phi \rangle & \cdots & \langle \psi_{\mu_2} | e^{-\hat{T}} [\hat{H}, \hat{\tau}_{\nu_N}] e^{\hat{T}} | \Phi \rangle \\ \vdots & \vdots & \ddots & \vdots \\ \langle \psi_{\mu_N} | e^{-\hat{T}} [\hat{H}, \hat{\tau}_{\nu_1}] e^{\hat{T}} | \Phi \rangle & \langle \psi_{\mu_N} | e^{-\hat{T}} [\hat{H}, \hat{\tau}_{\nu_2}] e^{\hat{T}} | \Phi \rangle & \cdots & \langle \psi_{\mu_N} | e^{-\hat{T}} [\hat{H}, \hat{\tau}_{\nu_N}] e^{\hat{T}} | \Phi \rangle \end{pmatrix} \quad (146)$$

2. Commutator-based Coupled Cluster Jacobian implementation

The challenge was not the diagonalization algorithm itself which was already implemented by J. Olsen, but rather to implement the BCH terms in (148). The latter constitutes the central part of my PhD project : an efficient commutator-based implementation of the CC Jacobian matrix in non-relativistic and relativistic formalism.

$$A_{\mu\nu} = \left\langle \Phi \left| \hat{\tau}_{\mu}^{\dagger} \left([\hat{H}, \hat{\tau}_{\nu}] + [[\hat{H}, \hat{\tau}_{\nu}], \hat{T}] + \frac{1}{2} [[[\hat{H}, \hat{\tau}_{\nu}], \hat{T}], \hat{T}] + \frac{1}{6} [[[[\hat{H}, \hat{\tau}_{\nu}], \hat{T}], \hat{T}], \hat{T}] \right) \right| \Phi \right\rangle \quad (147)$$

since the CI-driven formulation did not offer an efficient scaling. I will discuss this approach later on in III C 3.

The CC Jacobian matrix (146) can have a size of $\simeq 50$ millions amplitudes, it is obviously not stored fully, we use an iterative algorithm to diagonalize the non-hermitian matrix (Davidson-Olsen)[102]. The eigenvalue problem is then solved iteratively where in each iteration, the linear transformation is calculated, *i.e.* we evaluate the linear transformation of a trial vector \mathbf{x} with the CC Jacobian matrix

$$\begin{aligned} J_{\mu} &= \sum_{\nu} A_{\mu\nu} x_{\nu} \\ &= \sum_{\nu} \left\langle \Phi \left| \hat{\tau}_{\mu}^{\dagger} \left([\hat{H}, \hat{\tau}_{\nu}] + [[\hat{H}, \hat{\tau}_{\nu}], \hat{T}] + \frac{1}{2} [[[\hat{H}, \hat{\tau}_{\nu}], \hat{T}], \hat{T}] + \frac{1}{6} [[[[\hat{H}, \hat{\tau}_{\nu}], \hat{T}], \hat{T}], \hat{T}] \right) \right| \Phi \right\rangle x_{\nu} \end{aligned} \quad (148)$$

The first attempt was to perform a linear transformation of the central term : $\tilde{H} = [\hat{H}, \hat{\tau}_\nu]$ to benefit from the rank reduction which occurs with the commutation. We spent a year and a half trying to generate a new linear-transformed Hamiltonian for a cluster $\hat{\tau}_\nu$ at an arbitrary excitation rank. The idea was to follow a similar procedure than [103] and perform a one-index transformation of the central commutator. Thereby we generate new operators and new integrals. The principal problem of this approach occurs when the clusters $\hat{\tau}_\nu$ have an excitation rank ≥ 2 we have to deal with ≥ 3 -particle transformed Hamiltonian \tilde{H} . A significant number of routines would have been modified and adapted with some massive changes in the code structure. The first tests were not very convincing so I decided to exploit another way that we had already considered as a possible route but had not foreseen as being the less problematic option.

We succeeded with the second attempt, and we will now focus on this decisive step. Due to the fact that the matrix elements structure in (148) is very similar to the amplitude equation structure (138), I modified the CC amplitude equation routines for our present purpose

$$\begin{array}{cccccccccc}
e^{-\hat{T}} \underbrace{\hat{H}} e^{\hat{T}} = & \hat{H} + [\hat{H}, \hat{T}] + \frac{1}{2}[[\hat{H}, \hat{T}], \hat{T}] + \frac{1}{6}[[[\hat{H}, \hat{T}], \hat{T}], \hat{T}] + \frac{1}{24}[[[[\hat{H}, \hat{T}], \hat{T}], \hat{T}], \hat{T}] \\
\downarrow & \downarrow & \downarrow & \downarrow & \downarrow & \downarrow & \downarrow & \downarrow & \downarrow \\
[\hat{H}, \hat{\tau}_\nu] & 0 & \hat{\tau}_\nu & 1 & \hat{\tau}_\nu & \frac{1}{2} & \hat{\tau}_\nu & \frac{1}{6} & \hat{\tau}_\nu.
\end{array} \tag{149}$$

Above in (149), the apparent minor changes are shown to transform a CC vector element to a CC Jacobian matrix element. The different nested-commutators ranks occur in different loops which have been modified. The rank-zero loop, *i.e.*, the \hat{H} term alone can be simply removed and the higher-rank loops were modified. The different BCH coefficients were shifted by one rank, concretely, J Olsen and I wrote a new routine which handle these new coefficient distribution. One of the general excitation rank : $\hat{T} = \sum_\nu t_\nu \hat{\tau}_\nu$ has been replaced by only one specific cluster $\hat{\tau}_\nu$ associated to the right vector ν -component x_ν instead of an amplitude. Thereby, the right vector \mathbf{x} is then optimized iteratively at the same time as the linear transformation.

In figure 9, the different steps are shown in a diagram, Hamiltonian operators (80) and cluster operators (106) are expanded in four types of second-quantized strings by using the spin-string method introduced by Knowles and Handy [104] : unbarred-

creation-strings, barred-creation-strings, barred-annihilation-strings and unbarred-annihilation-strings. The algorithm performs an initial loop over the different Hamiltonian operator terms, which then allows for transformed integrals to be sorted. The second principal loop is the setup of the different \hat{T}^{GAS} operators where CC amplitudes are sorted. In the third principal loop, each block of nested commutators (148) is treated in an individual loop. The specific equation for a given Hamiltonian operator term, excitation operators, projected term from the excitation manifold $\langle \psi_{\mu}^{\text{GAS}} |$ and cluster operator $\hat{\tau}_{\nu}^{\text{GAS}}$ is set up in accord with equation (148). The algorithm determines the optimum solution among the number of possible Wick contractions and, finally, obtains indices of integrals and CC amplitudes required to calculate the sum of matrix elements. This task is incorporated into an iterative diagonalizer for non-hermitian matrices [102]. The linear response module gives the number of desired low-lying excitation energies for a given symmetry. More details on the basic contraction algorithm can be found in reference [77] which describes commutator-based GAS-CC for electronic ground states.

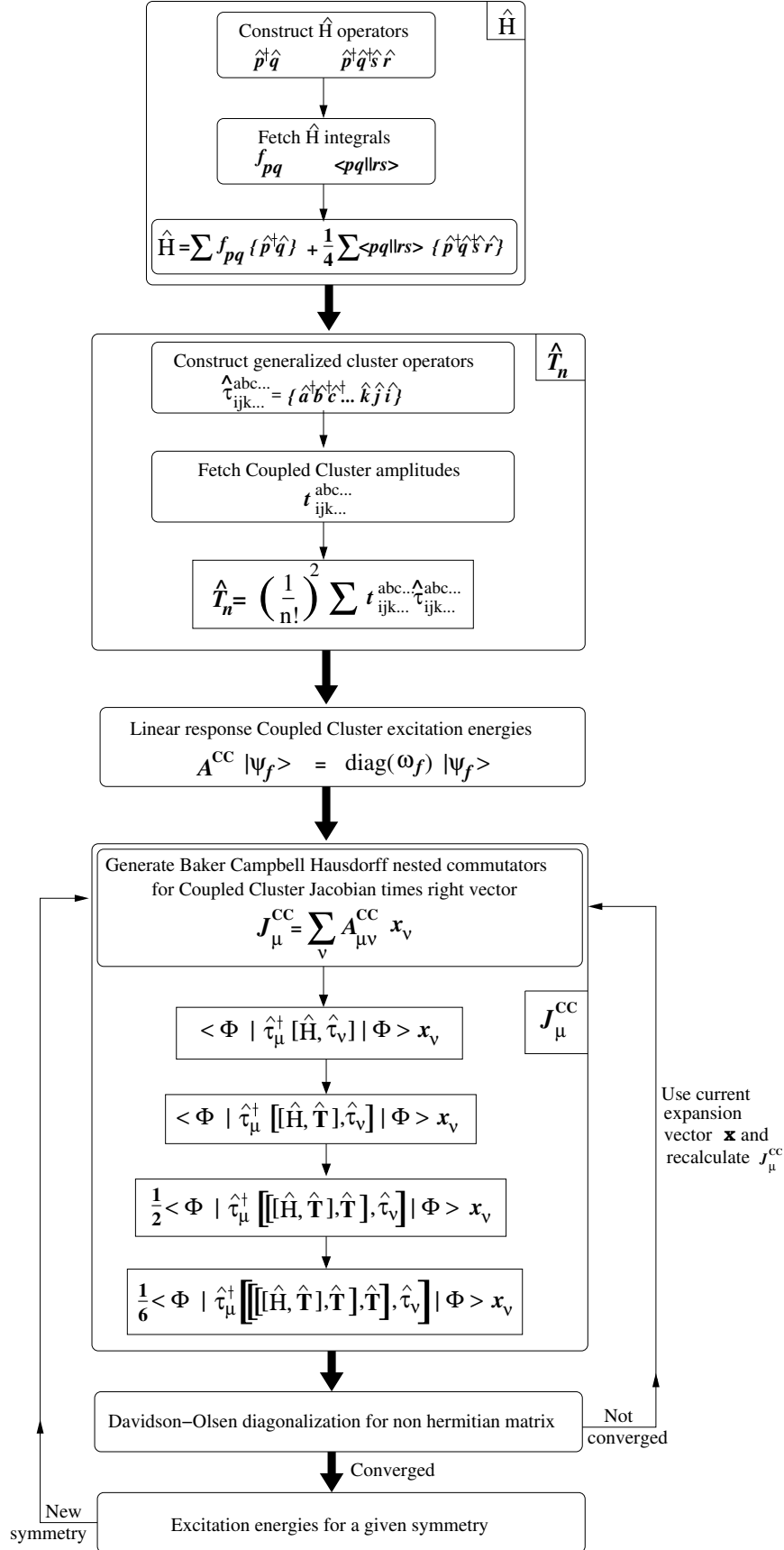


FIGURE 9. Schematic algorithm for the commutator-based coupled cluster CC Jacobian for excited-state energies.

I have verified the correct performance of our newly implemented code by direct comparison with the CI-driven implementation [80] or IV A on various small atomic and molecular test systems. The spin-orbit-free version of the commutator-based CC for excited state is well tested in the second publication IV B. The very-recently implemented Relativistic version of the commutator-based CC Jacobian algorithm can produce CC excitation energies. To check the new implementation I performed several little tests on Carbon atom, they can be found in IV C.

3. Comparison with the ci-driven algorithm

The previous LRCC algorithm was a very useful reference to test the new commutator-based LRCC, it was mainly implemented by L. Sørensen, J.Olsen and T. Fleig [18, 72, 80, 92, 94, 105]. This algorithm is based on the general excitation rank configuration interaction program subroutines, and was adapted to the relativistic formalism by the same authors from an initial spin-orbit-free version [100].

In the CI-driven algorithm, as for the commutator-based algorithm, the CC Jacobian matrix (144) times a right vector \mathbf{x} is evaluated

$$J_\mu = \sum_\nu \langle \Phi | \hat{\tau}_\mu^\dagger e^{-\hat{T}} \left[\hat{H}, \hat{\tau}_\nu \right] e^{\hat{T}} | \Phi \rangle x_\nu. \quad (150)$$

This evaluation is done by separately calculating the two terms of the commutator in (150). The first term

$$J_\mu^{(1)} = \sum_\nu \langle \Phi | \hat{\tau}_\mu^\dagger e^{-\hat{T}} \hat{H} \hat{\tau}_\nu e^{\hat{T}} | \Phi \rangle x_\nu \quad (151)$$

is obtained in the following steps :

$$\begin{aligned} (1) \quad |a\rangle &= e^{\hat{T}} | \Phi \rangle = \left(\sum_{n=0}^{\infty} \frac{1}{n!} \hat{T}^n \right) | \Phi \rangle \\ (2) \quad |b\rangle &= \sum_\nu x_\nu \hat{\tau}_\nu |a\rangle \\ (3) \quad |c\rangle &= \hat{H} |b\rangle \\ (4) \quad |d\rangle &= e^{-\hat{T}} |c\rangle = \left(\sum_{n=0}^{\infty} \frac{(-1)^n}{n!} \hat{T}^n \right) |c\rangle \\ (5) \quad J_\mu^{(1)} &= \langle \Phi | \hat{\tau}_\mu^\dagger |d\rangle \end{aligned} \quad (152)$$

The second term is obtained as

$$J_\mu^{(2)} = \sum_\nu \langle \Phi | \hat{\tau}_\mu^\dagger e^{-\hat{T}} \hat{\tau}_\nu \hat{H} e^{\hat{T}} | \Phi \rangle x_\nu = E^{\text{CC}} x_\nu \quad (153)$$

Finally the subtraction of the two final matrices $\mathbf{J}^{(1)}$ and $\mathbf{J}^{(2)}$ gives the Jacobian times the right vector. More details can be found in the afore-cited references.

The principal problem of the CI-driven approach and as well the principal motivation to implement the commutator-based algorithm is the scaling of the former :

$$S_{\text{CI-driven}}^{(n)} \simeq O^{n+2}V^{n+2} \quad (154)$$

where O is the number of occupied orbitals, V is the number of virtual orbitals and n is the highest excitation rank of the cluster operators. In order to elucidate the scaling of the present algorithm for excited-state calculations, we rewrite the right-hand side of (144) as

$$A_{\mu\nu} = \left\langle \psi_\mu | e^{-\hat{T}} \hat{H} \hat{\tau}_\nu e^{\hat{T}} | \Phi \right\rangle - \left\langle \psi_\mu | e^{-\hat{T}} \hat{\tau}_\nu \hat{H} e^{\hat{T}} | \Phi \right\rangle. \quad (155)$$

Starting with equation (155), we re-express the term

$$e^{-\hat{T}} \hat{\tau}_\nu = \hat{\tau}_\nu - \sum_\mu t_\mu \hat{\tau}_\mu \hat{\tau}_\nu + \frac{1}{2} \left(\sum_\mu t_\mu \hat{\tau}_\mu \right)^2 \hat{\tau}_\nu - \dots \quad (156)$$

which is seen to be a pure de-excitation operator acting on the bra-vector $\langle \psi_\mu |$. Therefore, the highest excitation rank n of the excitation manifold $\langle \psi_\mu |$ is reduced to $n - m$, where m is the excitation rank of an individual term in (156). Since $m \geq 1$, the highest excitation rank in $\langle \psi_\mu | e^{-\hat{T}} \hat{\tau}_\nu$ is $n - 1$. This means that in order for $\hat{H} e^{\hat{T}} | \Phi \rangle$ to be connected to this modified excitation manifold, $e^{\hat{T}} | \Phi \rangle$ has to contain excitations up to rank $n + 1$ since the Hamiltonian has a maximum down rank of two. The second term on the right-hand side of (155) therefore exhibits a computational scaling of $O^{n+1}V^{n+2}$, since in general the highest excitation rank k present in the excitation manifold entails a scaling with the number of occupied orbitals as O^{k+2} .

In contrast to this, the first term on the right-hand side of (155) has no additional cluster operator to the left of the Hamiltonian. This means that for $\hat{H} \hat{\tau}_\nu e^{\hat{T}} | \Phi \rangle$ to be connected to the original excitation manifold with rank n , $\hat{\tau}_\nu e^{\hat{T}} | \Phi \rangle$ has to contain excitations up to rank $n + 2$. Thus, this term is the highest-scaling term of the algorithm and the total algorithm for the CI-based CC Jacobian scales as $O^{n+2}V^{n+2}$, exactly as does the CI-based algorithm for the ground-state vector function [72, 91]. In typical applications, the dimension of the extended space defined by $\hat{H} \hat{\tau}_\nu e^{\hat{T}} | \Phi \rangle$

is one to three orders of magnitude larger than the dimension of the excitation manifold. The fact that the cluster operators \hat{T} , $\hat{\tau}_\nu$, and the Hamiltonian are now relativistic operators has no bearing for the present discussion concerning the orders for the computational scaling. There are, however, increased scaling prefactors in a relativistic algorithm which has been analyzed for commutator-based CC in reference [77].

Turning to the commutator-based algorithm, the scaling has been reduced to

$$S_{\text{cbCC}}^{(n)} \simeq O^n V^{n+2}. \quad (157)$$

We thus establish a principal speedup factor of O^2 . In the following chapter, some applications of the two algorithms will be presented.

Chapter IV

Applications

IV. APPLICATIONS

This last chapter collects all the applications performed during my thesis with the general excitation rank GAS Coupled Cluster. Two papers will be presented within our most important results.

A. Relativistic CI-driven Coupled Cluster applications to the silicon atom and to the molecules AsH, SbH and BiH.

In the following paper we applied the CI-driven algorithm to evaluate some excited state energy at a relativistic level by using Dirac-Coulomb Hamiltonian. We correlate six electrons and reach the limit of the algorithm applicability. However the results presented for Si atom and AsH, SbH and BiH molecules are of high accuracy compared to experimental data. The competition between static and dynamic correlation is discussed among the different compounds as well as the $j - j$ coupling versus LS coupling or the $\omega - \omega$ versus ΛS coupling. The efficiency of the $CC(n_m)$ model is demonstrated by comparing with standard CC and MRCI calculations.

Excitation energies from relativistic coupled-cluster theory of general excitation rank: Initial implementation and application to the silicon atom and to the molecules XH ($X = \text{As}, \text{Sb}, \text{Bi}$)

Mickaël Hubert

Laboratoire de Chimie et Physique Quantiques, IRSAMC, Université Paul Sabatier Toulouse III, 118 Route de Narbonne, F-31062 Toulouse, France

Lasse K. Sørensen and Jeppe Olsen

Theoretical Chemistry, Langelandsgade 140, Aarhus University DK-8000 Århus C, Denmark

Timo Fleig

Laboratoire de Chimie et Physique Quantiques, IRSAMC, Université Paul Sabatier Toulouse III, 118 Route de Narbonne, F-31062 Toulouse, France

(Received 3 February 2012; published 13 July 2012)

We present an implementation of four-component relativistic coupled-cluster theory for the treatment of electronically excited states of molecules containing heavy elements, allowing for a consistent and accurate treatment of relativistic effects such as the spin-orbit interaction and electron correlations as well as their intertwining. Our approach uses general excitation ranks in the cluster operator and, moreover, allows for the definition of active-space selected excitations of variable excitation rank. Initial applications concern the silicon atom and the heavier pnictogen monohydride molecules, where we focus on the first vertical excitation energy to the $\Omega = 1$ electronic state. We discuss the problem of adequately choosing a reference state (Fermi vacuum) and addressing electron correlation in the presence of effects of special relativity of increasing importance. For the heaviest homolog, BiH, where dynamic electron correlation is of major importance, we obtain vertical excitation energies with a deviation of less than 1% from the experimental value.

DOI: [10.1103/PhysRevA.86.012503](https://doi.org/10.1103/PhysRevA.86.012503)

PACS number(s): 31.15.bw, 31.15.am, 31.15.aj

I. INTRODUCTION

Electronically excited states of small molecules containing heavy atoms play an important role in many research areas of modern physics. In the (ultra)cold molecular sciences [1] there is an increasing interest in experimentally generating molecules in their electronic and rovibrational ground state by photoassociation via an electronically excited state [2]. In astrophysics of stars [3], the understanding of collision processes in stellar atmospheres [4] involves the knowledge of molecular excited states, including both main group and transition-metal atoms. As an example from fundamental physics, various extensions to the standard model of elementary-particle physics postulate electric dipole moments (EDM) of leptons [5]. Modern experiments search for the electron EDM in an electronically excited state of diatomic molecules and molecular ions containing a heavy atom [6]. The accurate determination of the electronic structure in excited states of the relevant molecules is of crucial importance in all of these and other research fields.

At present, the most accurate electronic-structure approach to the calculation of electronically excited states in atoms and molecules is the coupled-cluster (CC) method. Recent progress, including developments for excited states [7], has been documented in a monograph [8] covering this highly active field of many-body theory. When turning to the treatment of heavy elements where relativistic generalizations of these methods are required, the general challenge of implementing such methodology becomes manifest in their scarcity (see [9], and references therein). To date, the only relativistic CC methods for the treatment of molecular excited states are the intermediate Hamiltonian Fock-space CC method (IH FSCC) [10,11] by Visscher, Eliav, and co-workers and higher-order

correlation methods [12] by Hirata and co-workers using the equation-of-motion (EOM) CC formalism [13,14]. IH FSCC is limited in that it is not generally applicable and the treatment of excitation ranks higher than doubles in the wave operator is currently not possible. The method of Hirata *et al.* is restricted to the use of two-component valence pseudospinors based on a relativistic effective core potential (RECP) including spin-orbit interaction [15]. Such an approach lacks both the rigor and the flexibility of all-electron four-component methods which use a frozen-core approximation for the electrons of atomic cores.

Our developments aim at a rigorous assessment of the electronically excited states of small molecules including heavy elements, a general challenge in the relativistic electronic many-body problem until today [9]. Central elements of our methodology are (1) a rigorous treatment of special relativity using four-component all-electron Dirac Hamiltonians at all stages of the calculation; (2) methods of general excitation rank in the wave operator; and (3) methods based on developments of the wave function in a basis of strings of particle creation operators in second quantization, so-called string-based methods [16].

In this paper we present a relativistic coupled-cluster implementation based on linear-response theory and four-component relativistic Hamiltonian operators for the calculation of molecular excited states. In the following section on general theory (Sec. II) we review the description of electronically excited states in CC theory (Sec. II A) and our previous relativistic CC approach for electronic ground states (Sec. II B). Section III describes our implementation, in particular, the algorithm for calculating the relativistic CC Jacobian matrix. Here we also present an analysis of the computational scaling of our approach. Section IV is

concerned with initial applications of the method. We have chosen an atomic case (Si) featuring excited states of two different kinds: excited states due to the first-order spin-orbit splitting within a spectroscopic term, and states corresponding to a different spectroscopic term. As a second and molecular example we apply our approach to the second-order spin-orbit splitting of the $^3\Sigma$ ground state of heavier pnictogen hydrides, a notoriously difficult problem [17,18] requiring the treatment of static and dynamic electron correlation as well as spin-dependent magnetic interactions accurately. In the final section (Sec. V) we summarize and draw conclusions from our findings.

II. THEORY

A. Excited states in coupled-cluster theory

Response theory comprises a general and powerful framework for the calculation of atomic and molecular properties [19] as well as excitation energies based, e.g., on CC wave functions [20]. Here, the simple poles of the linear response function correspond to the excitation energies and occur at the eigenvalues of the CC Jacobian matrix.

An alternative way of deriving the CC Jacobian proceeds by an analogy to configuration interaction (CI) theory. Using CC language the CI Schrödinger equation with subtracted ground-state energy E_0 can be rewritten as

$$(\hat{H} - E_0)(t_0 \hat{1} + \hat{T})|\Phi\rangle = 0, \quad (1)$$

where $|\Phi\rangle$ is the reference (or Fermi vacuum) state, $\hat{T} = \sum_{\mu} t_{\mu} \hat{\tau}_{\mu}$ is the cluster excitation operator with $\hat{\tau}_{\mu} \in \{\hat{\tau}_i^a, \hat{\tau}_{ij}^{ab}, \dots\}$, $\hat{\tau}_i^a = \hat{a}_a^\dagger \hat{a}_i$ a single-replacement operator in equal-time second-quantization representation, and t_{μ} the corresponding expansion coefficient.

Projection with the CI excitation manifold $\langle\psi_{\mu}| = \langle\Phi|\hat{\tau}_{\mu}^\dagger$ onto Eq. (1) yields a set of CI coefficient equations for the CI vector function

$$\Omega_{\mu}^{\text{CI}} = \langle\psi_{\mu}|(\hat{H} - E_0)(t_0 \hat{1} + \hat{T})|\Phi\rangle = 0. \quad (2)$$

Taking the derivative with respect to all expansion parameters defines an Hermitian CI Jacobian, the matrix elements of which become

$$\begin{aligned} A_{\mu\nu}^{\text{CI}} &= \frac{\partial}{\partial t_{\nu}} \Omega_{\mu}^{\text{CI}} = \langle\psi_{\mu}|(\hat{H} - E_0)\hat{\tau}_{\nu}|\Phi\rangle \\ &= \langle\psi_{\mu}|\hat{H}|\psi_{\nu}\rangle - E_0 \delta_{\mu\nu}. \end{aligned} \quad (3)$$

Obviously, diagonalization of the matrix A^{CI} yields excitation energies from CI theory. It is straightforward to construct the analogy in CC theory. Here, the amplitude equations corresponding to Eq. (2) are cast (in linked form) as

$$\Omega_{\mu}^{\text{CC}} = \langle\psi_{\mu}|e^{-\hat{T}} \hat{H} e^{\hat{T}}|\Phi\rangle = 0, \quad (4)$$

with the same excitation manifold $\langle\Phi|\hat{\tau}_{\mu}^\dagger$, and the derivative matrix is obtained as

$$A_{\mu\nu}^{\text{CC}} = \frac{\partial}{\partial t_{\nu}} \Omega_{\mu}^{\text{CC}} = \langle\psi_{\mu}|e^{-\hat{T}} [\hat{H}, \hat{\tau}_{\nu}] e^{\hat{T}}|\Phi\rangle. \quad (5)$$

Consequently, diagonalization of the matrix A^{CC} yields excitation energies from CC theory. The difference between Eqs. (3) and (5) can be reduced to the difference in parametrization of

the wave function, linear in CI theory and exponential in CC theory, respectively. The excitation energies ω_A obtained from the eigenvalue equations

$$A^{\text{CC}}|\psi_f\rangle = \omega_A f |\psi_f\rangle \quad (6)$$

are equivalent to those from the EOM CC theory [13,21].

For reasons of computational efficiency, Eq. (6) is solved iteratively by algorithms similar to direct CI techniques, but in the present case for a non-Hermitian matrix A^{CC} . It has been shown earlier [22] how such linear transformations with the CC Jacobian can be evaluated for CC theory with general excitation levels of the cluster operator. This becomes possible by performing subsequent CI expansions using a general CI program.

B. Four-component relativistic approach

We have in the present work generalized the nonrelativistic implementation of Ref. [22] to a relativistic formalism where four-component or two-component relativistic Hamiltonian operators may be used from the outset, and our implementation will be described in Sec. III. Our approach to treating special relativity is identical to the one presented in Refs. [23–25]. In summary, the cluster operators $\hat{T} = \sum_m \hat{T}_m$ are generalized to include the possibility of flipping the Kramers projection of the underlying spinors along with the excitation, e.g., for singles replacements:

$$\hat{T}_1 = \sum_{ia} \{t_i^a \hat{\tau}_i^a + t_i^{\bar{a}} \hat{\tau}_i^{\bar{a}} + t_i^{\bar{a}} \hat{\tau}_i^a + t_i^a \hat{\tau}_i^{\bar{a}}\}. \quad (7)$$

The same generalization of excitation operators also applies to the operators $\hat{\tau}_v$ in the CC Jacobian matrix, Eq. (5). The approach is therefore Kramers restricted, in the sense that the underlying four-component spinors $\{\varphi_i, \varphi_{\bar{i}}\}$ form time-reversal partners (Kramers pairs)

$$\hat{K} \varphi_i = \varphi_{\bar{i}}, \quad \hat{K} \varphi_{\bar{i}} = -\varphi_i, \quad (8)$$

and that this symmetry is exploited for reducing the number of unique Hamiltonian one- and two-particle integrals [16]. An arbitrary number of spinor spaces with arbitrary occupation restraints may be used [generalized active spaces (GAS)] [25,26], which allows for the description of the multireference character of electronic states via active-space selected higher excitations. Double point group symmetry has been implemented for the real-valued [27,28] matrix groups D_{2h}^* , D_{2v}^* , and C_{2v}^* . This ensures for these cases a completely real-valued formalism, also when spin-orbit interaction is included. Our implementation is interfaced to a local version of the DIRAC relativistic electronic-structure package [29]. Currently, this local version limits the present method to the use of the four-component Dirac-Coulomb Hamiltonian (in Born-Oppenheimer approximation)

$$\begin{aligned} \hat{H}^{\text{DC}} &= \sum_A \sum_i [c(\vec{\alpha} \cdot \vec{p})_i + \beta_i m_0 c^2 + V_{iA}] + \sum_{i,j>i} \frac{1}{r_{ij}} \mathbb{1}_4 \\ &+ \sum_{A,B>A} V_{AB}, \end{aligned} \quad (9)$$

where V_{iA} is the potential-energy operator for electron i in the electric field of nucleus A , and V_{AB} represents the potential

energy due to the internuclear electrostatic repulsion of the clamped nuclei.

III. IMPLEMENTATION: ALGORITHM FOR THE RELATIVISTIC COUPLED-CLUSTER JACOBIAN

We now proceed to an outline of our implementation of the eigenvalue equation (6). It may be regarded as a combination of the algorithms described in Refs. [22,23]. Based on the techniques developed for general relativistic CI expansions [30] we evaluate the linear transformation of a coefficient trial vector \mathbf{x} with the CC Jacobian

$$J_{\mu}^{\text{CC}} = \sum_{\nu} A_{\mu\nu}^{\text{CC}} x_{\nu} = \sum_{\nu} \langle \psi_{\mu} | e^{-\hat{T}} [\hat{H}, \hat{\tau}_{\nu}] e^{\hat{T}} | \Phi \rangle x_{\nu}. \quad (10)$$

Following Refs. [22,23] Eq. (10) is solved in four steps:

(1) $|a\rangle = e^{\hat{T}} |\Phi\rangle = (\sum_{n=0}^{\infty} \frac{1}{n!} \hat{T}^n) |\Phi\rangle$. The individual terms in the Taylor expansion comprise repeated transformations of the form $\hat{T} |\psi\rangle$. We here employ the modified relativistic GAS CI implementation of Refs. [23,30] and the final ground-state cluster amplitudes in \hat{T} . The Taylor expansion truncates naturally upon exhausting the possible excitations on a given reference vector.

(2) $|b\rangle = [\hat{H}, \hat{\tau}_{\nu}] |a\rangle = (\hat{H} \hat{\tau}_{\nu} - \hat{\tau}_{\nu} \hat{H}) |a\rangle$. Here, $\hat{H} \hat{\tau}_{\nu} |a\rangle$ corresponds to the calculation of a sigma vector [30] from the reference vector $\hat{\tau}_{\nu} |a\rangle$. In the second term $-\hat{\tau}_{\nu}$ is applied to the sigma vector $\hat{H} |a\rangle$, and the resulting vectors from the two terms are added yielding the commutator.

(3) $|c\rangle = e^{-\hat{T}} |b\rangle = (\sum_{n=0}^{\infty} \frac{(-1)^n}{n!} \hat{T}^n) |b\rangle$. These transformations are evaluated in the same manner as those in step 1.

(4) $J_{\mu}^{\text{CC}} = \langle \psi_{\mu} | c \rangle = \langle \Phi | \hat{\tau}_{\mu}^{\dagger} | c \rangle$. This final step corresponds to the evaluation of a general transition density, which is also possible employing the modified relativistic GAS CI implementation in Refs. [23,30].

Therefore, since the underlying relativistic CI program [30] can treat general excitation levels, we are here immediately able to compute a relativistic CC Jacobian at general excitation rank, both with respect to the cluster operators and the excitation operators.

However, as has been discussed in Refs. [22,23], the present algorithm suffers from an increased operation count compared to conventional (and nonrelativistic) CC implementations for excited states [31]. The increased operation count of CI-based CC has been analyzed earlier [23,32] for ground-state calculations and amounts to a computational scaling of the method as $O^{n+2} V^{n+2}$, where O is the number of occupied orbitals, V is the number of virtual orbitals, and n is the highest excitation rank of the cluster operators. In order to elucidate the scaling of the present algorithm for excited-state calculations, we rewrite the right-hand side of Eq. (5) as

$$A_{\mu\nu}^{\text{CC}} = \langle \psi_{\mu} | e^{-\hat{T}} \hat{H} \hat{\tau}_{\nu} e^{\hat{T}} | \Phi \rangle - \langle \psi_{\mu} | e^{-\hat{T}} \hat{\tau}_{\nu} \hat{H} e^{\hat{T}} | \Phi \rangle. \quad (11)$$

Starting with the second term on the right-hand side of Eq. (11), we reexpress the term

$$e^{-\hat{T}} \hat{\tau}_{\nu} = \hat{\tau}_{\nu} - \sum_{\mu} t_{\mu} \hat{\tau}_{\mu} \hat{\tau}_{\nu} + \frac{1}{2} \left(\sum_{\mu} t_{\mu} \hat{\tau}_{\mu} \right)^2 \hat{\tau}_{\nu} - \dots, \quad (12)$$

which is seen to be a pure deexcitation operator acting on the bra vector $\langle \psi_{\mu} |$. Therefore, the highest excitation rank n of the

excitation manifold $\langle \psi_{\mu} |$ is reduced to $n - m$, where m is the excitation rank of an individual term in Eq. (12). Since $m \geq 1$, the highest excitation rank in $\langle \psi_{\mu} | e^{-\hat{T}} \hat{\tau}_{\nu}$ is $n - 1$. This means that in order for $\hat{H} e^{\hat{T}} | \Phi \rangle$ to be connected to this modified excitation manifold, $e^{\hat{T}} | \Phi \rangle$ has to contain excitations up to rank $n + 1$ since the Hamiltonian has a maximum down rank of 2. The second term on the right-hand side of Eq. (11) therefore exhibits a computational scaling of $O^{n+1} V^{n+2}$, since in general the highest excitation rank k present in the excitation manifold entails a scaling with the number of occupied orbitals as O^{k+2} .

In contrast to this, the first term on the right-hand side of Eq. (11) has no additional cluster operator to the left of the Hamiltonian. This means that for $\hat{H} \hat{\tau}_{\nu} e^{\hat{T}} | \Phi \rangle$ to be connected to the original excitation manifold with rank n , $\hat{\tau}_{\nu} e^{\hat{T}} | \Phi \rangle$ has to contain excitations up to rank $n + 2$. Thus, this term is the highest-scaling term of the algorithm and the total algorithm for the CI-based Jacobian scales as $O^{n+2} V^{n+2}$, exactly as does the CI-based algorithm for the ground-state vector function [23,32]. In typical applications, the dimension of the extended space defined by $\hat{H} \hat{\tau}_{\nu} e^{\hat{T}} | \Phi \rangle$ is one to three orders of magnitude larger than the dimension of the excitation manifold. The fact that the cluster operators \hat{T} , $\hat{\tau}_{\nu}$, and the Hamiltonian are now relativistic operators has no bearing for the present discussion concerning the orders for the computational scaling. There are, however, increased scaling prefactors in a relativistic algorithm which has been analyzed for commutator-based CC in Ref. [25].

IV. APPLICATION AND ANALYSIS

In this section we present applications to the silicon atom and to heavier pnictogen hydrides. The silicon atom has been chosen as an initial test case to verify the applicability of our method. We focus on all Russell-Saunders terms originating from the atomic configuration $3p^2$, i.e., $^3P_{2,1,0}$, 1D_2 , and 1S_0 . Therefore, the problem comprises excited states arising from the same term due to first-order spin-orbit splitting ($^3P_2, ^3P_1, ^3P_0$) and excited states from different terms corresponding to the same electronic configuration. We define the Fermi vacuum determinant as the one where the energetically lowest Kramers pairs are all doubly occupied, i.e., the configuration $1s^2 2s^2 2p^6 3s^2 3p_{1/2}^2$. The purpose here is to show in a simple way the coupled-cluster description of several different excited states by taking into account spin-orbit interaction.

Turning to the molecules, the pnictogen hydrides are characterized by two valence electrons occupying the $(\pi_{1/2}, \pi_{-1/2})$ and $(\pi_{3/2}, \pi_{-3/2})$ Kramers pairs which are here denoted as the spin-orbit split π orbitals assigning λ_{ω} quantum numbers. λ is an approximate quantum number as spin-orbit interaction mixes orbitals of different angular momentum projection m_{ℓ} , e.g., σ character into the π orbitals, $\sigma_{1/2} - \pi_{1/2}$. Their occupation and character therefore differ depending on the pnictogen atom. Since we describe the systems in a spinor basis $\{\varphi_{\omega}\}$ our natural choice of Fermi vacuum is the closed-shell valence occupation $\pi_{1/2}^{\uparrow}, \pi_{-1/2}^{\uparrow}$. Such a reference state is a good approximation to the wave function in the case of BiH where spin-orbit interaction is strong. However, the multireference (MR) character is expected to become more

and more important toward the lighter homologs where the $\pi_{1/2}$ and $\pi_{3/2}$ spinors become quasidegenerate. The first excited state, with $\Omega = 1$, is predominantly described by $\pi_{3/2}^1, \pi_{-1/2}^1$ and the excited state with $\Omega = -1$ is predominantly $\pi_{1/2}^1, \pi_{-3/2}^1$.

Dynamic correlation and relativistic effects are treated on the same footing. The multireference character of states is taken into account via active-space selected higher excitations. Since the GAS-CC method is not strictly invariant to the choice of Fermi vacuum state, we expect a bias of the CC wave function depending on the chosen reference determinant.

A. Computational details

All calculations were performed with the DIRAC relativistic electronic-structure program package, using the latest version [29] for the Hartree-Fock calculations and integral transformations, and a local development version for the CC calculations.

For our initial test calculations on the silicon atom we have tested different basis sets and resorted to using the atomic-natural-orbital (ANO) Relativistic and Core-Correlating (RCC) basis set [33] and to include only the four valence electrons in the correlation treatment. We employed Dyall's triple- ζ and quadruple- ζ basis sets in uncontracted form [34,35] for Bi, Sb, and As. The listed valence and core-correlating functions for the Bi 5*d*, 6*s*, and 6*p* shells, for the Sb 4*d*, 5*s*, and 5*p* shells, and for the As 3*d*, 4*s*, and 4*p* shells have all been included. For H we used Dunning's cc-pVTZ-DK and cc-pVQZ-DK basis sets in uncontracted form [36]. The internuclear distances for AsH, SbH, and BiH are the experimental ones [37,38].

We employed the four-component Dirac-Coulomb Hamiltonian, Eq. (9), throughout. Thus, our models describe one- and two-electron spin-own-orbit coupling and spin-own-orbit-correlation coupling rigorously. We currently do not include spin-spin coupling and spin-other-orbit interactions due to limitations in the implemented Hamiltonian operators. Kramers-paired spinors for the subsequent GAS-CC calculations were obtained from all-electron closed-shell Dirac-Coulomb-Hartree-Fock calculations. In addition, we performed for comparison exemplifying CI and CC calculations based on open-shell average-of-configuration Dirac-Coulomb-Hartree-Fock (DCHF) wave functions. In the open-shell DCHF calculations fractional occupation numbers are introduced in the Fock operator using minimal spaces of Kramers pairs (two electrons in the three 3*p* Kramers pairs in the case of Si, and two electrons in the two π valence Kramers pairs in the molecular cases).

Electron correlations are described in various fashions. On the one hand, we apply the standard CC hierarchy [39] up to full iterative quintuple excitations [CCSDTQP; S = single excitations with respect to the reference state $|\Phi\rangle$, D = double excitations, T = triple, Q = quadruple, and P = pentuple (fivefold) excitations] in the case of SbH. The construction of active spaces is done in an efficient manner by exploiting the GAS concept [26]. In the present case, important subsets of the possible model spaces are denoted as $CC(n_m)$ models [40] (see Fig. 1).

The silicon atom is treated with the standard CC series CCSD to CCSDTQ (the latter of which in this case corresponds to full valence CC), a series of models excluding the correlation

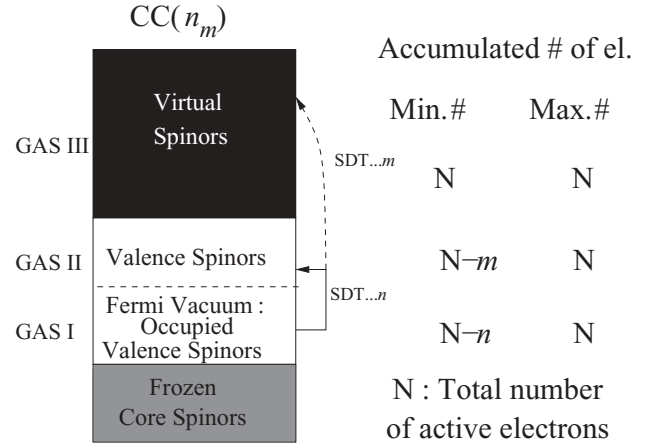


FIG. 1. $CC(n_m)$ ($n > m$) as a subset of GAS excitation manifolds. n is the maximum number of holes in the occupied subspace; m is the maximum number of particles in the virtual subspace.

of the 3*s* electrons among each other (S2CC), and different $CC(n_m)$ schemes. The detailed definitions of these models are to be found in the Appendix.

For all molecular systems we choose to correlate the six valence electrons. The correlation of 3*d* electrons of As, 4*d* electrons of Sb, and 5*d* electrons of Bi does play a role in assessing the ground-state spin-orbit splitting, as studied for the case of BiH by Knecht *et al.* [41], but the effect is only on the order of $+75 \text{ cm}^{-1}$ for this latter molecule. Also here, we use various electron correlation models, the details for the specification of which are to be found in the Appendix.

Comparative four-component generalized-active-space configuration interaction (GAS-CI) calculations were performed with the KR-CI module [18,42] of the DIRAC program package [29]. This approach makes use of the GAS concept in the same way as our presented GAS-CC method [23]. Closed-shell CI calculations have been performed using the newly-implemented linear symmetry double groups [43,44].

B. Results and discussion

We present and discuss in this section our results for Si, AsH, SbH, and BiH. The bulk of the GAS-CC and GAS-CI calculations was carried out with a virtual spinor space size for which the total energy has been converged (see Sec. 3 of the Appendix). The principal purpose here is to show for the case of a few representative model systems the performance of standard CC and $CC(n_m)$ models, and to compare these with a genuine-but linearly parametrized—MR approach, MRCI.

1. Silicon atom

First of all, we performed benchmark CI and MRCI calculations (which are subsets of GAS-CI; see the Appendix) to guide our CC study and to assess the leading effects on excited-state energies. These calculations are presented in Table I. Whereas the os-MRCI calculations consistently yield results close to the FCI values, the truncated closed-shell approaches fail in describing the excited states correctly. Given a balanced starting point for the different electronic states by using average-of-configuration DCHF these are already well

TABLE I. Excitation energies T in cm^{-1} for the 3P_1 , 3P_2 , 1D_2 , and 1S_0 excited states of the Si atom, with different relativistic CC models (defined in Tables V and VI), the Dirac-Coulomb Hamiltonian, and a closed-shell Dirac-Hartree-Fock reference state. MRCI calculations based on an open-shell multireference state (os) and a closed-shell single-reference state (cs). We used a complete active space of two electrons in the three $3p$ orbitals. MRCI models are defined in Table VII. All calculations were performed including single and double excitations of the $3s$ electrons, except where marked otherwise (S2, only singles from the $3s$ shell). The basis sets are of ANO-RCC quality; the cutoff for the virtual spinors is set to 10 a.u. (see text).

State	os-MR			Method				Expt. [52]
	CISD	CISDT	FCI	CISD	CISDT	FCI	cs	
3P_1	79	79	79	5275	1768	89		77.1
3P_2	229	228	228	7368	1519	258		223.2
1D_2	6475	6441	6413	13447	7595	6435		6299.8
1S_0	15606	15691	15551	20917	18821	15574		15394.4

State	Method (all cs)								Expt. [52]
	S2CCSD	S2CC(3 ₂)	S2CCSDT	CCSD	CC(4 ₂)	CCSDT	CC(4 ₃)	FCC ^a	
3P_1	-1225	-86	180	-784	-128	-438	81	89	77.1
3P_2	1318	687	277	1750	666	-222	276	258	223.2
1D_2	10422	6648	6610	10726	6504	5942	6446	6435	6298.8
1S_0	22392	20108	19745	20121	15926	17188	15591	15574	15394.4

^aValues obtained by an equivalent full CI calculation due to an unresolved instability of our FCC calculation at a 10 a.u. cutoff value. We have obtained identical FCC and FCI values for smaller dimensions of the virtual space confirming the proper functionality of the new CC code.

described by MR-CISD, and higher excitations hardly play a role for energy differences.

In the case of a cs reference state we observe that the results at low excitation levels are largely off the mark, and higher excitations gradually lead to improvements, with only the Full (F) CI and Full (F) CC and CC(4₃) models yielding accurate results. We rationalize and explain this behavior first by analyzing the Fermi-vacuum determinant of our reference state. The problem is simplified by considering only the two valence p electrons. Since we use four-component spinors throughout, we write the determinant in terms of good quantum numbers for the two particles $|j(i), m_j(i)\rangle$ and further express this determinant in terms of Russell-Saunders coupled states ML_J , giving

$$\left| \frac{1}{2}, \frac{1}{2}; \frac{1}{2}, -\frac{1}{2} \right| = -\sqrt{\frac{2}{3}} {}^3P_0 - \frac{1}{\sqrt{3}} {}^1S_0, \quad (13)$$

the details of which are to be found in the Appendix, Sec. 4. The reference determinant is therefore biased toward the $J = 0$ state of the 3P_0 term and contains a significant admixture from the 1S_0 term. In order to interpret the excitation energies we expand the singly excited determinants in the same manner, e.g.,

$$\begin{aligned} \left| \frac{3}{2}, \frac{1}{2}; \frac{1}{2}, \frac{1}{2} \right| &= -\frac{1}{2} {}^3P_1 - \frac{1}{2} {}^3P_2 + \frac{1}{\sqrt{2}} {}^1D_2, \\ \left| \frac{3}{2}, \frac{3}{2}; \frac{1}{2}, \frac{1}{2} \right| &= \sqrt{\frac{2}{3}} {}^1D_2 + \frac{1}{\sqrt{3}} {}^3P_2. \end{aligned} \quad (14)$$

Based on a closed-shell model we ensuingly expect a CISD calculation to strongly overestimate the excitation energies of the 3P_1 , 3P_2 , and 1D_2 states, since a single excitation is required for their description, leaving them uncorrelated, in contrast to the ground state. The data clearly confirms this. Furthermore, the overestimation for the 1S_0 state is smaller than, e.g., the

one for the 1D_0 state, since the former is partially represented in the reference state.

Continuing the argument, a CISDT calculation introduces triple excitations, in addition to the already present single and double excitations. Now, Eqs. (14) show that, for example, the 1D_2 state is largely represented by singly excited determinants relative to our reference determinant. Since some of the triple excitations in the CISDT model are double excitations combined with single excitations required to qualitatively describe the 1D_2 excited state, dynamic electron correlation effects are taken into account for the 1D_2 state, in contrast to the CISD model. We therefore expect the 1D_2 excitation energy to be much closer to the experimental value in the CISDT model, which the data confirms.

A similar reasoning applies to explain the obtained results for the 1S_0 state and the 3P_1 and 3P_2 components of the ground-state term. For example, the CISDT model shows the smallest correction for the 1S_0 state which is already partially correlated in the CISD model. A final, but smaller, correction is obtained by adding quadruple excitations, this correction now being largest for the 1S_0 state which appears in doubly excited determinants

$$\begin{aligned} \left| \frac{3}{2}, \frac{3}{2}; \frac{3}{2}, -\frac{3}{2} \right| &= \frac{1}{\sqrt{3}} {}^3P_2 + \frac{1}{\sqrt{6}} {}^1D_2 - \frac{1}{\sqrt{6}} {}^3P_0 + \frac{1}{\sqrt{3}} {}^1S_0, \\ \left| \frac{3}{2}, \frac{1}{2}; \frac{3}{2}, -\frac{1}{2} \right| &= \frac{1}{\sqrt{3}} {}^3P_2 + \frac{1}{\sqrt{6}} {}^1D_2 + \frac{1}{\sqrt{6}} {}^3P_0 - \frac{1}{\sqrt{3}} {}^1S_0, \end{aligned} \quad (15)$$

relative to the reference determinant.

Turning to the CC results in the light of these findings, the CCSD model, containing higher excitations than doubles in disconnected terms (which contribute to the CC energy indirectly due to the coupling of excitations in the CC amplitude equations), yields results of accuracy between CISD and CISDT for the 1D_0 and 1S_0 states, but the correction

overshoots for the 3P_1 and 3P_2 components of the ground-state term. CC(4₂) includes the important higher excitations to give qualitatively correct results except for the first-order spin-orbit splitting, where there is a residual error of several hundred cm⁻¹. Notably, CCSDT does not improve upon the CC(4₂) results. CC(4₃) brings about a significant correction for the two first excited states making all of them qualitatively correct, although the excitation level in the active space is the same as in CC(4₂). FCC (CCSDTQ) yields only a minor correction to this last model.

The slightly different values obtained with closed-shell and open-shell FCC models reflect the differently polarized core and virtual spinors of the atom depending on the DCHF model used.

We conclude that due to the specific choice of coupling picture, here $j - j$, a Fermi vacuum determinant represented in this coupling picture may not comprise a good description of the electronic ground state. As a consequence, CC models based on this vacuum state and truncated at low excitation ranks may yield large errors in calculated excitation energies. Active-space selected higher excitations largely correct for the ensuing errors in atomic excitation energies. High accuracy in the spin-orbit splitting of the Si atomic ground state (excited states $^3P_{1,2}$) is only achieved if in addition dynamic electron correlations are accounted for through at least triple excitations into the virtual spinor space. CCSDT alone, however, is not accurate enough in describing these states which according to Table IV in Ref. [22] means that for the given case of a poor Fermi vacuum state the excitation energy has to be described at least through fifth order in the fluctuation potential. This is approximately the case for the CC(4₃) model which includes important quadruple excitations.

2. The individual pnictogen hydrides

(a) *Arsenic monohydride—AsH*. This system exhibits a small spin-orbit splitting of the π Kramers pairs and, therefore, the $\Omega = 0$ ground state is likely to have strong MR character. Indeed, closed-shell CCSD gives a qualitatively wrong energy estimation and even a state inversion which can be seen in Table II. We rationalize this failure of CCSD by again closely analyzing the Fermi vacuum determinant in the molecular case (see the Appendix, Sec. 5). Based on the analysis, our reference state can be qualitatively described as

$$|(m_j)_1; (m_j)_2|_\Omega = \left| \left(\frac{1}{2} \right); \left(-\frac{1}{2} \right) \right|_0 \approx c_3 |^3\Sigma_0\rangle + c_1 |^1\Sigma_0\rangle, \quad (16)$$

where $c_3 \approx -c_1 = \frac{1}{\sqrt{2}}$ in the case of AsH. This in turn means that the true ground state $|^3\Sigma_0\rangle$ is best represented by a linear combination of the determinants $|(\frac{1}{2}); (-\frac{1}{2})|_0$ and $|(\frac{3}{2}); (-\frac{3}{2})|_0$. It therefore requires higher CC excitations in our single-reference approach to describe the presence of such strongly contributing determinants in the ground state.

A true MR method such as truncated MRCI, as we apply it here for comparison, gives qualitatively correct results but, being a method with a linear wave function parametrization, is limited by its intrinsic properties. CC(4₂) with open-shell spinors describes the MR character qualitatively, but still produces an error of about 80 cm⁻¹ compared with experiment.

TABLE II. Vertical excitation energies (T_v) in cm⁻¹ for the $\Omega = 1$ state of the AsH molecule at the experimental bond length of $R_e^{(0+)} \approx R_e^{(1)} \approx 1.5349$ Å [37] with different relativistic CC models (defined in Tables VIII and IX), the Dirac-Coulomb Hamiltonian, and a closed-shell Dirac-Hartree-Fock reference state. “os” refers to an average-of-configuration reference state with an averaging for two electrons in the two π orbitals. MRCI calculations are based on an open-shell multireference state except if indicated otherwise (cs). We used a formal core space of four electrons in the $4s, \sigma$ orbitals and a complete active space of two electrons in the two π orbitals. The model SD_CISD corresponds to $a = 2, b = 4$ in Table X. The basis sets are of TZ quality (see text), except where marked otherwise. Converged cutoff for virtual spinors is 10 a.u. except if indicated otherwise.

Method	Δ_{SO} (cm ⁻¹)	No. CC amplitudes/CI det.
csCISD	11231	36.015
csCISDT	-2899	1.556.976
csCISDTQ	170	28.650.840
SD_CISD	104	123.472
SD_CISDT	103	2.123.792
SDT_CISDT	102	3.875.024
SDTQ_CISDTQ	106	50.672.784
CCSD	-2661	36.016
CCSD-10000 a.u.	-2666	162.240
CCSD-26 a.u. (QZ)	-2707	147.015
CCSD-59 a.u. (QZ)	-2707	191.535
CC(4 ₂)	-139	123.471
osCC(4 ₂)	39	123.471
CC(4 ₂)-26 a.u. (QZ)	-258	511.771
osCC(4 ₂)-26 a.u. (QZ)	39	511.771
CCSDT	-71	1.556.975
osCCSDT	-79	1.556.975
CC(4 ₃)	68	2.123.791
osCC(4 ₃)	71	2.123.791
CCSDTQ	116	28.650.839
osCCSDTQ	107	28.650.839
Expt. [37] ($T_e = 2\Lambda_0$)	117.7	

(We deduce T_e from the spin-splitting constant Λ_0 given in Ref. [37]: $T_e = 2\Lambda_0$). CCSDT is still not qualitatively correct, but including higher internal excitations, CC(4₃), we observe a positive and qualitatively correct first AsH excitation energy. Comparing osCCSDT, osCC(4₂), and osCC(4₃) we conclude that the quadruple excitations including the double excitations $\pi_{1/2}^2 \rightarrow \pi_{3/2}^2$ combined with double excitations into the virtual spinors are essential to describe the relative energies of the $\Omega = 0$ and $\Omega = 1$ states. This is confirmed by examining the double-excitation cluster amplitude $t_{\pi_{1/2}\pi_{1/2}}^{\pi_{3/2}\pi_{3/2}}$, which is ≈ 0.45 for csCCSD and ≈ 0.79 for csCCSDTQ in the ground state. With higher excitation ranks, open-shell and closed-shell LRCC results become quite the same, as expected. Since the excited state $\Omega = 1$ is essentially obtained by a single excitation $\pi_{1/2}^1 \rightarrow \pi_{3/2}^1$ from our closed-shell Fermi vacuum state, the excitation energy is again correct to the 5th perturbation order for our higher correlated calculation CCSDTQ, according to Table IV in Ref. [22]. CCSDTQ describes both the MR character and dynamic electron correlation accurately. SDTQ-CISDTQ and osCCSDTQ results are almost identical,

as expected, the difference with csCCSDTQ being due to the difference in the molecular orbital basis (see also Sec. IV B3 c). Corresponding closed-shell CI calculations exhibit the same deterioration at lower excitation levels as in the case of the two lowest excited states of the Si atom.

Turning to errors from the employed Dirac-Coulomb Hamiltonian, we estimate the effect of the Gaunt term to be around -4 cm^{-1} and correlation effects from the As $3d$ atomic shell to be $+2 \text{ cm}^{-1}$, according to recent exact two-component MRCISD calculations [45]. Our results indicate that basis-set errors are very small which, however, could be nonzero at CC(4_3) or CCSDTQ levels. The experimental excitation energy is well reproduced in our best calculation (csCCSDTQ) with a deviation of less than 1.5%.

(b) *Stibylene*—*SbH*. SbH is an intermediate case between AsH and BiH in the sense that the spin-orbit splitting of

TABLE III. Vertical excitation energies (T_v) in cm^{-1} for the $\Omega = 1$ state of the SbH molecule at the experimental bond length of $R_e^{(0+)} \approx R_e^{(1)} \approx 1.7226 \text{ \AA}$ [37] with different relativistic CC models (defined in Tables VIII and IX), the Dirac-Coulomb Hamiltonian, and a closed-shell Dirac-Hartree-Fock reference state. “os” refers to an average-of-configuration reference state with an averaging for two electrons in the two π orbitals. MRCI calculations are based on an open-shell multireference state except if indicated otherwise (cs). We used a formal core space of four electrons in the $5s, \sigma$ orbitals and a complete active space of two electrons in the two π orbitals. The model SD_CISD corresponds to $a = 2$, $b = 4$ in Table X. The basis sets are of TZ quality (see text), except where marked otherwise. Converged cutoff for virtual spinors is 4 a.u. except if indicated otherwise.

Method	$\Delta_{\text{SO}} (\text{cm}^{-1})$	No. CC amplitudes/CI det.
csCISD	11474	30.376
csCISDT	− 1347	1.205.176
csCISDTQ	705	20.370.586
SD_CISD	577	103.856
SD_CISDT	572	1.640.160
SDT_CISDT	563	2.987.792
SDTQ_CISDTQ	582	35.857.552
SDTQ_CISDTQP	582	192.560.560
CCSD	− 1070	30.375
CCSD-100 a.u.	− 1071	69.360
CCSD-6 a.u. (QZ)	− 1073	82.140
CCSD-116 a.u. (QZ)	− 1074	226.935
CC(4_2)	476	103.855
osCC(4_2)	555	103.855
CC(4_2)-6 a.u. (QZ)	434	284.496
CCSDT	485	1.205.175
osCCSDT	436	1.205.175
CCSDT-6 a.u. (QZ)	482	5.376.100
CC(4_3)	599	1.640.159
osCC(4_3)	575	1.640.159
CC(4_3)-6 a.u. (QZ)	627	7.397.616
CCSDTQ	641	20.370.585
osCCSDTQ	584	20.370.585
CCSDTQP	645	152.218.389
osCCSDTQP	612	152.218.389
Expt. (T_e) [37]	654.97	

the π spinors becomes appreciable. However, based on our analysis in the Appendix, Sec. 5, we still expect the MR character of the ground state to be large, which is confirmed by the results. These results for stibylene are compiled in Table III. CCSD fails in much the same manner as for AsH, but the error has become smaller. We interpret this behavior by the coefficient c_3 now becoming larger than c_1 [in Eq. (16)] due to increased spin-orbit effects. Ensuingly, CC(4_2) gives a drastic amelioration with a qualitatively correct value and reveals an important contribution of the quadruple excitation including $\pi_{1/2} \rightarrow \pi_{3/2}$. In contrast to AsH, CCSDT no longer improves upon CC(4_2) in this case. A value of acceptable accuracy with an error of less than 10% is already achieved with CC(4_3), which was not the case in AsH. Nevertheless, quadruple excitations still play a significant role and largely correct for this residual error. Our most accurate value at the CCSDTQP level of 645 cm^{-1} deviates by less than 2% from the experimental result (654.97 cm^{-1} [37]). Comparing with the CI results in Table III the SDTQ-CISDTQP value is already leveled by CC(4_3), which is computationally significantly cheaper to perform. Thus, we here encounter a turning point where the advantage of the MRCI method of being a genuine MR approach is surpassed by the CC method due to its superior efficiency in treating higher excitations.

We now turn to residual errors from sources other than the correlation expansion. Considering errors from the truncated Hamiltonian operator, we estimate the effect of the Gaunt term to be -13 cm^{-1} and correlation contributions from the Sb atomic $4d$ shell to be $+5 \text{ cm}^{-1}$ according to recent exact-two-component (X2C)-MRCISD calculations [45]. From our most accurate CC model using different basis sets, CC(4_3), we infer a TZ-QZ basis-set error of $+28 \text{ cm}^{-1}$. Adding these estimated residual errors to our single most accurate result, CCSDTQP, the splitting amounts to 665 cm^{-1} , comprising a deviation of roughly 1.5% from the experimental value.

(c) *Bismuth monohydride*—*BiH*. The heaviest pnictogen homolog, BiH, is a quasi-single-reference case. The spin-orbit splitting of the π spinors is significantly larger compared to AsH and SbH, as relativistic effects are sizable in this system. The weak MR character of the ground state renders the closed-shell Fermi vacuum a much better starting point in this case. The results for bismuth monohydride are compiled in Table IV. Despite the fact that BiH is a quasi-single-reference case in the present description, closed-shell CISD is insufficient, because a single excitation is required for describing the excited state, leaving it uncorrelated relative to the ground state. This interpretation is corroborated by the cs-CISDT model where the triple excitations correlating the excited state are added (doubles on top of singles). As expected, and in accord with the cs-CI results CCSD gives qualitatively good results and CC(4_2) brings about a large amelioration resulting in an error of less than 1%. It should be noted, however, that CCSD still displays an absolute error of nearly 700 cm^{-1} , indicating the remaining bias in our chosen Fermi vacuum state. Again, the importance of the quadruple excitation including $\pi_{1/2} \rightarrow \pi_{3/2}$ contribution is observed. However, a quite accurate value is obtained at this level, in contrast to SbH. Also here, CCSDT does not improve on CC(4_2). Our most accurate value at the CC(4_3) level is 4931 cm^{-1} with a deviation of less than 0.3% from experiment (4917.1 cm^{-1} [37]). In contrast to the CI

TABLE IV. Vertical excitation energies (T_v) in cm^{-1} for the $\Omega = 1$ state of the BiH molecule at an internuclear distance of 1.80 Å (the experimental bond lengths are $R_e^{0^+} = 1.805$ and $R_e^1 = 1.7912$ Å) [37] with different relativistic CC models (defined in Tables VIII and IX), the Dirac-Coulomb Hamiltonian, and a closed-shell Dirac-Hartree-Fock reference state. “os” refers to an average-of-configuration reference state with an averaging for two electrons in the two π orbitals. MRCI calculations are based on an open-shell multireference state except if indicated otherwise (cs). We used a formal core space of four electrons in the $6s, \sigma$ orbitals and a complete active space of two electrons in the two π orbitals. The model SD_CISD corresponds to $a = 2, b = 4$ in Table X. The basis sets are of TZ quality (see text), except where marked otherwise. Converged cutoff for virtual spinors is 10 a.u. except if indicated otherwise.

Method	Δ_{SO} (cm^{-1})	No. CC amplitudes/CI det.
csCISD	16710	61.441
csCISDT	4163	3.475.201
csCISDTQ	4854	83.488.225
SD_CISD	4595	212.137
SD_CISDT	4569	4.769.137
SDT_CISDT	4515	8.738.389
SDTQ_CISDTQ	4596	149.525.014
CCSD	4239	61.440
osCCSD	4103	61.440
CCSD-104 a.u.	4243	168.540
CCSD-11 a.u. (QZ)	4300	144.060
CCSD-86 a.u. (QZ)	4302	277.440
CC(4 ₂)	4867	212.136
osCC(4 ₂)	4763	212.136
CC(4 ₂)-11 a.u. (QZ)	4892	501.408
CCSDT	4855	3.475.200
CC(4 ₃)	4931	4.769.136
Expt. [37] (T_e)	4917.1	

results given in Table IV, the SDTQ-CISDTQ value does not reach the quality of the computationally significantly cheaper CC(4₂). A highly accurate description of both effects due to special relativity and electronic correlation is given here with the CC(4₃) model.

There are still some residual errors from different sources. A TZ-QZ basis-set correction of $+25 \text{ cm}^{-1}$ is obtained by comparing CC(4₂) results. Considering errors from the truncated Hamiltonian operator, we estimate the effect of the Gaunt term to be -60 cm^{-1} and correlation contributions from the Bi atomic $5d$ shell to be $+75 \text{ cm}^{-1}$ according to exact-two-component (X2C) -MRCISD calculations performed by Knecht *et al.* [41]. The remaining deviation may be attributed to the fact that the potential curves for the 0^+ and 1 states are no longer parallel in the case of BiH, thus our vertical excitation energies slightly overshoot the experimental values for T_e . Therefore, residual errors are expected to largely compensate each other, which confirms the accuracy of our highest-level results.

3. Discussion of theoretical aspects across the series

In this section we draw a comparison between the three molecules focusing on selected theoretical issues.

(a) *CC(n_m) models and excitation rank of \hat{T}* . In Fig. 2 we show the convergence evolution of the various CC models

for the vertical excitation energy of the $\Omega = 1$ state of the three molecules. CC(4₂) is set between CCSD and CCSDT and brings some essential quadruple excitations. It roughly equals CCSDT in quality, but at a lower cost. CC(4₃) is a good compromise between CCSDT and CCSDTQ; it provides a high accuracy and avoids full quadruple excitations into the virtual space. For BiH, high accuracy is reached using this model (deviation of 0.3%). These CC models depend on the excitation rank of the operator \hat{T} , which for the standard models CCSD to CCSDTQP is 2 to 5, respectively. For the CC(n_m) model, the rank of \hat{T} depends on the active-space structure. As we elucidate in Table IX, for GAS I (core spinors) we use a maximum rank of 2 to perform double core excitations toward the virtual spinors. In GAS II the maximum rank is 4 ($n = 4$), but those quadruple excitations are restricted to the $\pi_{3/2}$ spinors. Finally, in GAS III the rank is 2 or 3 ($m = 2$ or 3) in order to perform double or triple excitations toward virtual spinors. The CC(n_m) approach enables a flexible adaptation for ground-state and excited-state calculations by taking into account important classes of excitation in the \hat{T} operator for a system-tailored description.

(b) *Multireference problem—Comparison of GAS-CC and MRCI*. The multireference character on these three systems decreases toward the heaviest homolog BiH. This character is linked to the energy difference between the $\pi_{1/2}$ and the $\pi_{3/2}$ spinors. With GAS-CC, which is not a true MR CC approach, we have to impose a single-reference Fermi vacuum $\pi_{1/2}^1 \pi_{-1/2}^1$. For lighter systems than BiH, we ensuingly introduce a certain bias into CC wave function. However, we can compensate for this flawed point of departure with higher excitation ranks. In Fig. 3 we show a comparison between comparable CI and CC models in terms of deviation from experiment for the three molecules. In AsH where MR effects are strong, MR-CI remains superior to GAS-CC up to the level of triple excitations into the virtual spinor space. For SbH, multireference effects are still significant but we obtain a slightly better description at CC(4₃) level surpassing MR-CISDT (see Table III). The single-reference dominated system BiH is significantly better described with CC(4₂) already, improving on MR-CISD by more than 250 cm^{-1} (see Table IV) with the same number of wave function parameters.

(c) *Spinors from closed-shell or open-shell optimization*. In closed-shell optimizations on a system with a near degeneracy of states, the energy gap between the occupied and the unoccupied valence spinors is largely overestimated. This gap becomes much more realistic in the open-shell models. Open-shell spinors could be used in cases of strong near degeneracy and where the excitation level must be kept low. For AsH, it gives a significant amelioration for CC(n_m) models (see Table II). However, as the near degeneracies decrease, closed-shell approaches become the better choice in our molecular series (see Tables III and IV). A systematic difference between cs and os approaches remains even at very high excitation ranks, due to the fact that the different valence models lead to different polarization of the core and virtual spinors. Since the spinor basis is truncated both in the occupied and virtual space, the two models do not yield identical results in the FCI/FCC limit. In the cs case the spinors are optimized for the reference determinant used in the correlated approach. In contrast to this, os spinors

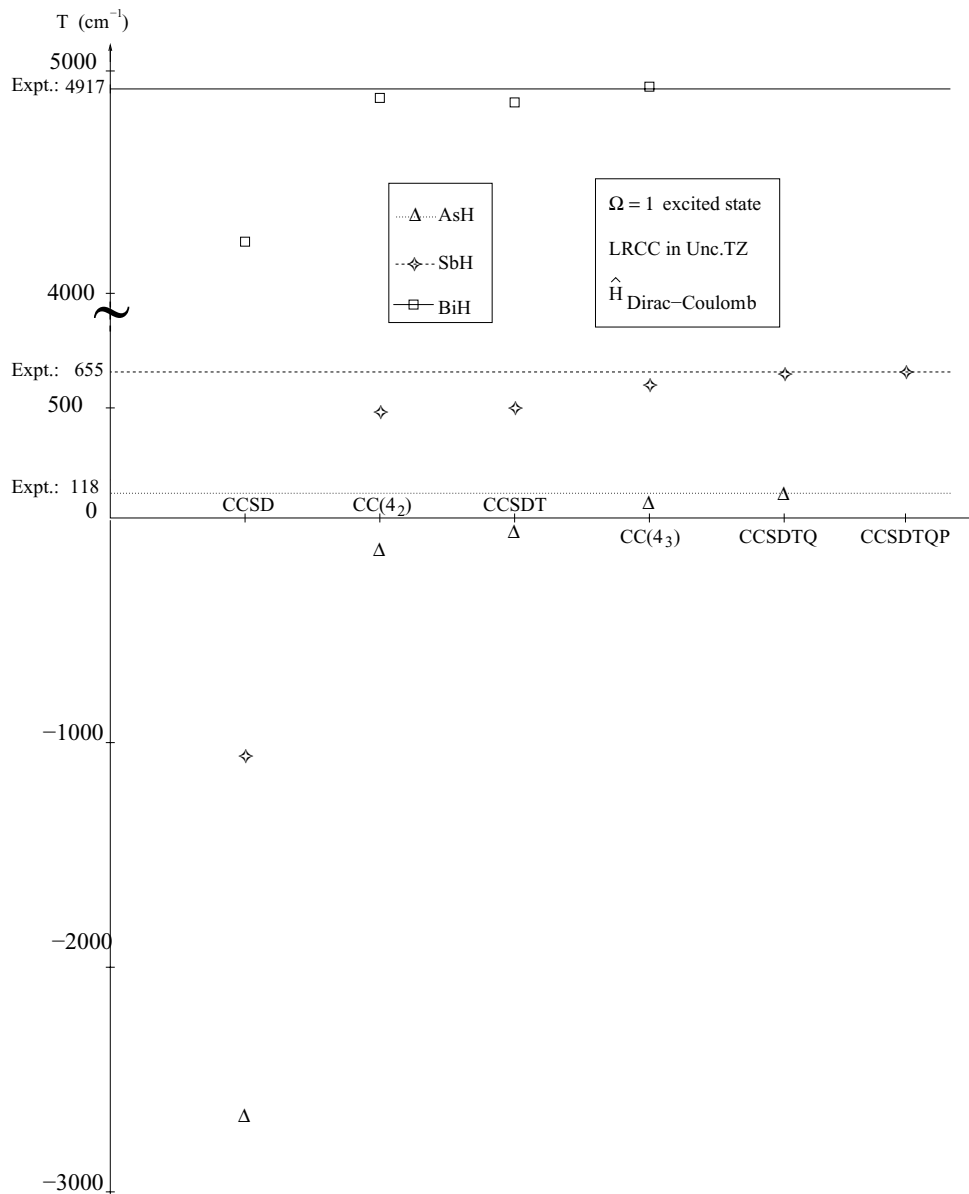


FIG. 2. Convergence of various closed-shell CC models for the three molecules. T values are T_v taken from Tables II, III, and IV; experimental values are $T_e^{\text{expt.}}$ from [37].

comprise an averaging over several states and therefore do not correspond to the reference state used in the correlation approach. Due to this inconsistency, we consider os-CC as a pragmatic approach in certain cases, but csCC results at high excitation ranks our qualitatively best values.

V. CONCLUSION

An implementation of a general excitation rank relativistic coupled cluster is presented with which electronically excited states can be calculated at high accuracy using linear response theory. It has been demonstrated that the relativistic GAS-CC approach is applicable to atomic and molecular electronically excited states, for which we have chosen showcase systems exhibiting strong effects of both relativistic and electron

correlation origin. We regard these findings largely as proof of principle for our method.

We conclude from the present study that within the GAS-CC approach both the multireference character and the importance of dynamic electron correlation on relative energies can be addressed efficiently. The former is achieved by adding active-space selected higher excitations to the standard CC expansion. For BiH (and to some degree also SbH) where the ground state is dominated by a single Slater determinant in the relativistic picture the quality of the GAS-CC results surpasses that of a linear wave-function expansion such as relativistic CI theory, even if the latter is applied as a genuine multireference approach. In cases where our chosen Fermi vacuum determinant is no longer the dominant contributor to the electronic ground state (Si atom, AsH, to some degree SbH) we find that higher CC excitations, at least up to full triples,

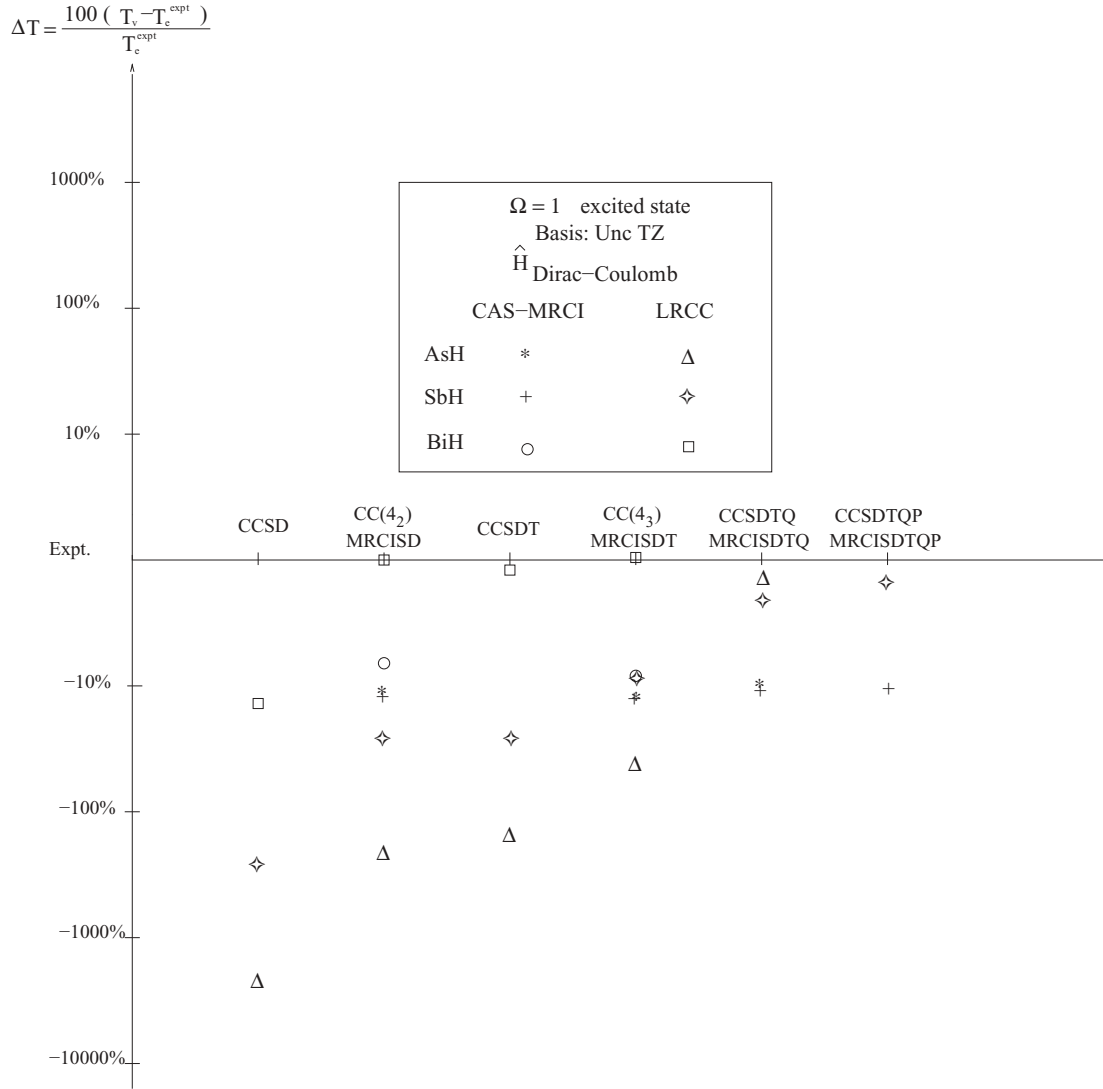


FIG. 3. Deviation from experiment [37] in percent for MRCI and closed-shell CC models for the three molecules. Values are taken from Tables II, III, and IV. ΔT values are calculated from T_v taken from Tables II, III, and IV and experimental values T_e^{expt} from [37]. MRCI models are built according to Table X with $a = 2$, $b = 4$ for SD_CISD, $a = 1$, $b = 3$ for SDT_CISDT, $a = 0$, $b = 2$ for SDTQ_SDTQ, and $a = 0$, $b = 1$ for SDTQ_SDTQP.

have to be included for achieving high accuracy. In such cases true multireference CC (such as Mukherjee's Mk-CC [46]) where a number of reference determinants is treated on equal footing would seem to be the better choice. It is planned to implement such a genuine MR approach into our relativistic methodology.

In ongoing work we are generalizing a computationally more efficient commutator-based evaluation of the CC Jacobian matrix to the four-component relativistic formalism. This improvement will lead to a code with the optimal computational scaling of conventional CC theory also in the calculation of excited states, and will allow us to increase the number of explicitly correlated electrons. On the technical side this is carried out by merging the relativistic commutator-based GAS-CC [25] with the approach described in this paper and including the new and more efficient code for the relativistic CC Jacobian.

ACKNOWLEDGMENTS

This work was granted access to the HPC resources of CALMIP under the allocation 2010-p1050 and 2011-p1050. We furthermore acknowledge technical support by Anthony Scemama with the calculations on the local computing cluster. L.K.S. acknowledges the Villum Fonden for financial support. We thank Radovan Bast for some helpful comments on the calculation of expectation values with DIRAC.

APPENDIX: TECHNICAL DETAILS ON ACTIVE SPINOR SPACES

1. The Si atom

For the silicon atom four different correlation model hierarchies are defined. We use three GAS for the active spinors (see Table V with $3s$ spinors in GAS I, $3p_{1/2}$ spinors in GAS II,

TABLE V. General active space models for Si with three GAS for the standard CC hierarchy. “Min. el.” represents the minimum accumulated number and “Max. el.” the maximum accumulated number of electrons after consideration of a given GAS. $a = 0, 1$ for SD2CC and S2CC, respectively. $b \in \{a, \dots, 2\}$ for CCSDTQ (FCC), CCSDT, and CCSD, respectively. X : Number of virtual Kramers pairs.

GAS	Kramers pairs per irrep. $E_{1/2}$	Min. el.	Max. el.	Shell types
I	1	a	2	$3s$
II	2	b	4	$3p_{1/2}$
III	X	4	4	$3p_{3/2}, 3p_{3/2} +$ virtual Kr. pairs

and virtual spinors in GAS III). This first specification allows for defining the standard CC hierarchy and another hierarchy where only up to one hole in the space of the $3s$ spinors is allowed (S2CC). The third specification allows for the definition of various $CC(n_m)$ correlation models, for which we use four GAS (see Table VI). This particular GAS structure accounts for a selected set of higher excitations, here up to quadruple excitations which decompose, for instance, in the case of $CC(4_2)$ into double excitations from $3s$ to the virtual spinors combined with double excitations from the $3p_{1/2}$ to the $3p_{3/2}$ spinors. Finally, for MRCI calculations, which are genuine MR calculations, we use a specific GAS configuration as shown in Table VII, since here there is no need to define a Fermi vacuum determinant.

2. The pnictogen monohydrides

In the molecular cases we use three different correlation model hierarchies. The standard CC series (CCSD through CCSDTQP) is defined by two GAS for the active spinors (see GAS Table VIII). For the $CC(n_m)$ correlation methods, the minimum number of GAS required is four (see GAS Table IX). Similar to the atomic case, the more pronounced the MR character of the state in question, the more important the amplitude $t_{\pi_{1/2}\pi_{3/2}}^{\pi_{3/2}\pi_{3/2}}$ becomes. The $CC(n_m)$ models partially account for the MR character by introducing such higher excitations which are expected to give large contributions to the states in question. We finally use an extra GAS configuration suited for MRCI calculations (see GAS Table X). These complete-active-space (CAS)-MRCI calculations were performed to provide results from more standard approaches which are compared with CC models.

TABLE VI. Si general active space models with four GAS for the $CC(n_m)$ hierarchy (see Fig. 1). $a = 1$ for S2CC(3_2). if $a = 0$: $b = 1, 2$ for SD2CC(4_3) and SD2CC(4_2), respectively. X : Number of virtual Kramers pairs.

GAS	Kramers pairs per irrep. $E_{1/2}$	Min. el.	Max. el.	Shell types
I	1	a	2	$3s$
II	2	a	4	$3p_{1/2}$
III	4	b	4	$3p_{3/2}, 3p_{3/2}$
IV	X	4	4	Virtual Kr. pairs

TABLE VII. Si general active space models with three GAS for MRCI hierarchy. All are MRCISD2_CAS2in3 type. $a = 0, 1, 2$ for SDTQ-4 (FCI-4), SDT-4, and SD-4, respectively. X : Number of virtual Kramers pairs.

GAS	Kramers pairs per irrep. $E_{1/2}$	Min. el.	Max. el.	Shell types
I	1	0	2	$3s$
II	4	a	4	$3p_{1/2}, 3p_{3/2}, 3p_{3/2}$
III	X	4	4	Virtual Kr. pairs

3. Virtual spinor spaces

GAS-CCSD and CAS-MRCI calculations were performed with increasing sizes of virtual spinor spaces. It is a standard procedure in four-component electronic-structure calculations with uncontracted Gaussian basis sets to use a truncation energy value for the virtual spinors (see, e.g., Ref. [47]) and to perform the correlation calculation in the resulting subspace. We have in all cases converged the excitation energies with respect to this subspace dimension using the CCSD model.

4. Coupling pictures and determinants

a. L - S coupling.

For the sake of simplicity we adopt a two-particle approximation, i.e., we restrict ourselves to the electronic configuration np^2 . All states will be written as $^{(2S+1)}L_J(m_J)$ in accord with the Russell-Saunders convention, and determinants as $|L_{m_L} m_S L_{m_L} m_S\rangle$. In addition, we will use the shorthand notation $|\alpha\rangle = |S = \frac{1}{2}, m_S = \frac{1}{2}\rangle$ and $|\beta\rangle = |S = \frac{1}{2}, m_S = -\frac{1}{2}\rangle$ for spin states, and $|P_+\rangle = |L = 1_{m_L=1}\rangle$, $|P_0\rangle = |L = 1_{m_L=0}\rangle$, and $|P_-\rangle = |L = 1_{m_L=-1}\rangle$.

In order to find the expansion of states $^{(2S+1)}L_J(m_J)$ in terms of determinants $|L_{m_L} m_S L_{m_L} m_S\rangle$ we start out from the state with $\max(m_J)$ for a given $^{(2S+1)}L_J$ and apply shift operators \hat{J}_- to construct the states up to $\min(m_J)$. All m_J states are individually normalized. We obtain

$$^1S_0:$$

$$^1S_0(0) = \frac{1}{\sqrt{3}}(|P_-\alpha P_+\beta| - |P_0\alpha P_0\beta| + |P_+\alpha P_-\beta|). \quad (A1)$$

$$^1D_2:$$

$$^1D_2(2) = |P_+\alpha P_+\beta|, \quad (A2)$$

$$^1D_2(1) = \frac{1}{\sqrt{2}}(|P_0\alpha P_+\beta| + |P_+\alpha P_0\beta|), \quad (A3)$$

$$^1D_2(0) = \frac{1}{\sqrt{6}}(|P_-\alpha P_+\beta| + 2|P_0\alpha P_0\beta| + |P_+\alpha P_-\beta|), \quad (A4)$$

TABLE VIII. AsH, SbH, and BiH general active space models with two GAS for the standard CC hierarchy. $a = 4, 3, 2, 1$ for CCSD-6, CCSDT-6, CCSDTQ-6, and CCSDTQP-6, respectively. $n = 4, 5, 6$ for AsH, SbH, and BiH, respectively. X : Number of virtual Kramers pairs.

GAS	Kramers pairs per irrep. $E_{1/2}$	Min. el.	Max. el.	Shell types
I	3	a	6	$ns, \sigma_{1/2}, \pi_{1/2}$
II	X	6	6	$\pi_{3/2} +$ virtual Kr. pairs

TABLE IX. AsH, SbH, and BiH general active space models with four GAS for the SD4_CC(n_m) hierarchy (see Fig. 1). $a = 3, 4$ for CC(4₃) and CC(4₂), respectively. $n = 4, 5, 6$ for AsH, SbH, and BiH, respectively. X : Number of virtual Kramers pairs.

GAS	Kramers pairs per irrep. $E_{1/2}$	Min. el.	Max. el.	Shell types
I	2	2	4	$ns, \sigma_{1/2}$
II	3	2	6	$\pi_{1/2}$
III	3	a	6	$\pi_{3/2}$
IV	X	6	6	Virtual Kr. pairs

$${}^1D_2(-1) = \frac{1}{\sqrt{2}}(|P_0\alpha P_{-\beta}| + |P_{-\alpha} P_0\beta|), \quad (A5)$$

$${}^3P_0: {}^1D_2(-2) = |P_{-\alpha} P_{-\beta}|. \quad (A6)$$

$${}^3P_0(0) = \frac{1}{\sqrt{3}} \left[|P_0\alpha P_{-\alpha}| + |P_{+\beta} P_0\beta| - \frac{1}{\sqrt{2}}(|P_{+\alpha} P_{-\beta}| + |P_{+\beta} P_{-\alpha}|) \right]. \quad (A7)$$

$${}^3P_1: {}^3P_1(1) = \frac{1}{2}(\sqrt{2}|P_{+\alpha} P_{-\alpha}| - |P_{+\alpha} P_0\beta| - |P_{+\beta} P_0\alpha|), \quad (A8)$$

$${}^3P_1(0) = \frac{1}{\sqrt{2}}(|P_0\alpha P_{-\alpha}| - |P_{+\beta} P_0\beta|), \quad (A9)$$

$${}^3P_1(-1) = \frac{1}{2}(-\sqrt{2}|P_{+\beta} P_{-\beta}| + |P_0\alpha P_{-\beta}| + |P_0\beta P_{-\alpha}|). \quad (A10)$$

$${}^3P_2: {}^3P_2(2) = |P_{+\alpha} P_0\alpha|, \quad (A11)$$

$${}^3P_2(1) = \frac{1}{2}(\sqrt{2}|P_{+\alpha} P_{-\alpha}| + |P_{+\alpha} P_0\beta| + |P_{+\beta} P_0\alpha|), \quad (A12)$$

$${}^3P_2(0) = \frac{1}{\sqrt{6}}[|P_0\alpha P_{-\alpha}| + |P_{+\beta} P_0\beta| + \sqrt{2}(|P_{+\alpha} P_{-\beta}| + |P_{+\beta} P_{-\alpha}|)], \quad (A13)$$

$${}^3P_2(-1) = \frac{1}{2}(\sqrt{2}|P_{+\beta} P_{-\beta}| + |P_0\alpha P_{-\beta}| - |P_0\beta P_{-\alpha}|), \quad (A14)$$

$${}^3P_2(-2) = |P_0\beta P_{-\beta}|. \quad (A15)$$

TABLE X. AsH, SbH, and BiH general active space models with three GAS for MRCI hierarchy. $a = 0, 1, 2$ for SDTQ-4, SDT-4, and SD-4, respectively. $b \geq a, b = 1, 2, 3, 4$ for CISDTQP-6, CISDTQ-6, CISDT-6, and CISD-6, respectively. $n = 4, 5, 6$ for AsH, SbH, and BiH, respectively. X : Number of virtual Kramers pairs.

GAS	Kramers pairs per irrep. $E_{1/2}$	Min. el.	Max. el.	Shell types
I	2	a	4	$ns, \sigma_{1/2}$
II	4	b	6	$\pi_{1/2}, \pi_{3/2}$
III	X	6	6	Virtual Kr. pairs

To find the expansion of a given determinant in terms of ${}^{(2S+1)}L_J$ states we have to invert the matrix \mathbf{X} in

$$\vec{s} = \mathbf{X}\vec{d}, \quad (A16)$$

where \vec{s} is a vector of states and \vec{d} is a vector of determinants. \mathbf{X} is orthonormal, so solving

$$\vec{d} = \mathbf{X}^{-1}\vec{s} \quad (A17)$$

is easy since $\mathbf{X}^{-1} = \mathbf{X}^T$.

We then find that the various determinants for the subspace $m_J = 0$ can be expressed as

$$|P_0\alpha P_{-\alpha}| = \frac{1}{\sqrt{3}}{}^3P_0 + \frac{1}{\sqrt{2}}{}^3P_1 + \frac{1}{\sqrt{6}}{}^3P_2, \quad (A18)$$

$$|P_{+\beta} P_0\beta| = \frac{1}{\sqrt{3}}{}^3P_0 - \frac{1}{\sqrt{2}}{}^3P_1 + \frac{1}{\sqrt{6}}{}^3P_2, \quad (A19)$$

$$|P_{-\alpha} P_{+\beta}| = \frac{1}{\sqrt{3}}{}^1S_0 + \frac{1}{\sqrt{6}}{}^1D_2 + \frac{1}{\sqrt{6}}{}^3P_0 - \frac{1}{\sqrt{3}}{}^3P_2, \quad (A20)$$

$$|P_{+\alpha} P_{-\beta}| = \frac{1}{\sqrt{3}}{}^1S_0 + \frac{1}{\sqrt{6}}{}^1D_2 - \frac{1}{\sqrt{6}}{}^3P_0 + \frac{1}{\sqrt{3}}{}^3P_2, \quad (A21)$$

$$|P_0\alpha P_0\beta| = -\frac{1}{\sqrt{3}}{}^1S_0 + \frac{2}{\sqrt{6}}{}^1D_2. \quad (A22)$$

Notice sign changes for determinants such as $|P_{-\alpha} P_{+\beta}|$. For the other m_J values we find the following expressions:

$m_J = 1$:

$$|P_{+\alpha} P_{-\alpha}| = \frac{1}{\sqrt{2}}{}^3P_1 + \frac{1}{\sqrt{2}}{}^3P_2, \quad (A23)$$

$$|P_{+\alpha} P_0\beta| = \frac{1}{\sqrt{2}}{}^1D_2 - \frac{1}{2}{}^3P_1 + \frac{1}{2}{}^3P_2, \quad (A24)$$

$$|P_{+\beta} P_0\alpha| = -\frac{1}{\sqrt{2}}{}^1D_2 - \frac{1}{2}{}^3P_1 + \frac{1}{2}{}^3P_2. \quad (A25)$$

$m_J = -1$:

$$|P_{+\beta} P_{-\beta}| = -\frac{1}{\sqrt{2}}{}^3P_1 + \frac{1}{\sqrt{2}}{}^3P_2, \quad (A26)$$

$$|P_0\alpha P_{-\beta}| = \frac{1}{\sqrt{2}}{}^1D_2 + \frac{1}{2}{}^3P_1 + \frac{1}{2}{}^3P_2, \quad (A27)$$

$$|P_0\beta P_{-\alpha}| = -\frac{1}{\sqrt{2}}{}^1D_2 + \frac{1}{2}{}^3P_1 + \frac{1}{\sqrt{2}}{}^3P_2. \quad (A28)$$

$m_J = 2$:

$$|P_{+\alpha} P_0\alpha| = {}^3P_2, \quad (A29)$$

$$|P_{+\alpha} P_{+\beta}| = {}^1D_2. \quad (A30)$$

$m_J = -2$:

$$|P_0\beta P_{-\beta}| = {}^3P_2, \quad (A31)$$

$$|P_{-\alpha} P_{-\beta}| = {}^1D_2. \quad (A32)$$

b. J-J coupling

First we want to find the various states $(J_1, J_2)_J$ that arise from J - J coupled spinors. These five states are

$$(3/2, 3/2)_2, (3/2, 3/2)_0, (3/2, 1/2)_2, (3/2, 1/2)_1, (1/2, 1/2)_0. \quad (\text{A33})$$

We expand each spinor (J, m_J) in terms of nonrelativistic spin orbitals using the notation introduced above and the corresponding Clebsch-Gordan coefficients:

$J = 3/2$:

$$(3/2, 3/2) = P_+ \alpha, \quad (\text{A34})$$

$$(3/2, 1/2) = \frac{1}{\sqrt{3}}(\sqrt{2}P_0\alpha + P_+\beta), \quad (\text{A35})$$

$$(3/2, -1/2) = \frac{1}{\sqrt{3}}(\sqrt{2}P_0\beta + P_-\alpha), \quad (\text{A36})$$

$$(3/2, -3/2) = P_-\beta. \quad (\text{A37})$$

$J = 1/2$:

$$(1/2, 1/2) = \frac{1}{\sqrt{3}}(-P_0\alpha + \sqrt{2}P_+\beta), \quad (\text{A38})$$

$$(1/2, -1/2) = \frac{1}{\sqrt{3}}(P_0\beta - \sqrt{2}P_-\alpha). \quad (\text{A39})$$

This allows us to write the m_J components of the various $(J_1, J_2)_J$ states, denoted as $(J_1, J_2)_{J, m_J}$, as

$$(1/2, 1/2)_{0,0} = |(1/2, 1/2), (1/2, -1/2)| = \frac{1}{3}(-|P_0\alpha P_0\beta| + \sqrt{2}|P_+\beta P_0\beta| + \sqrt{2}|P_0\alpha P_-\alpha| + 2|P_-\alpha P_+\beta|), \quad (\text{A40})$$

$$(3/2, 3/2)_{2,2} = |(3/2, 3/2), (3/2, 1/2)| = \frac{1}{\sqrt{3}}(\sqrt{2}|P_+\alpha P_0\alpha| + |P_+\alpha P_+\beta|), \quad (\text{A41})$$

$$(3/2, 3/2)_{2,1} = |(3/2, 3/2), (3/2, -1/2)| = \frac{1}{\sqrt{3}}(\sqrt{2}|P_+\alpha P_0\beta| + |P_+\alpha P_-\alpha|), \quad (\text{A42})$$

$$(3/2, 3/2)_{2,0} = \frac{1}{\sqrt{2}}(|(3/2, 1/2), (3/2, -1/2)| + |(3/2, 3/2), (3/2, -3/2)|) = \frac{1}{\sqrt{2}}\left[\frac{1}{3}(2|P_0\alpha P_0\beta| + \sqrt{2}|P_0\alpha P_-\alpha| + \sqrt{2}|P_+\beta P_0\beta| + |P_-\alpha P_+\beta|) + |P_+\alpha P_-\beta|\right], \quad (\text{A43})$$

$$(3/2, 3/2)_{2,-1} = |(3/2, 1/2), (3/2, -3/2)| = \frac{1}{\sqrt{3}}(-\sqrt{2}|P_-\beta P_0\alpha| - |P_-\beta P_+\beta|), \quad (\text{A44})$$

$$(3/2, 3/2)_{2,-2} = |(3/2, -1/2), (3/2, -3/2)| = \frac{1}{\sqrt{3}}(-\sqrt{2}|P_-\beta P_0\beta| - |P_-\beta P_-\alpha|), \quad (\text{A45})$$

$$(3/2, 3/2)_{0,0} = \frac{1}{\sqrt{2}}(|(3/2, 1/2), (3/2, -1/2)| - |(3/2, 3/2), (3/2, -3/2)|) = \frac{1}{\sqrt{2}}\left[\frac{1}{3}(2|P_0\alpha P_0\beta| + \sqrt{2}|P_0\alpha P_-\alpha| + \sqrt{2}|P_+\beta P_0\beta| + |P_-\alpha P_+\beta|) - |P_+\alpha P_-\beta|\right], \quad (\text{A46})$$

$$(3/2, 1/2)_{2,2} = |(3/2, 3/2), (1/2, 1/2)| = \frac{1}{\sqrt{3}}(-|P_+\alpha P_0\alpha| + \sqrt{2}|P_+\alpha P_+\beta|), \quad (\text{A47})$$

$$(3/2, 1/2)_{2,1} = \frac{1}{2}[\sqrt{3}|(3/2, 1/2), (1/2, 1/2)| + |(3/2, 3/2), (1/2, -1/2)|] = \frac{1}{2}\left(\sqrt{3}|P_0\alpha P_+\beta| + \frac{1}{\sqrt{3}}|P_+\alpha P_0\beta| - \sqrt{\frac{2}{3}}|P_+\alpha P_-\alpha|\right), \quad (\text{A48})$$

$$(3/2, 1/2)_{2,0} = \frac{1}{\sqrt{2}}[|(3/2, 1/2), (1/2, -1/2)| + |(3/2, -1/2), (1/2, 1/2)|] = \frac{1}{3\sqrt{2}}(2\sqrt{2}|P_0\alpha P_0\beta| - |P_0\alpha P_-\alpha| - |P_+\beta P_0\beta| + 2\sqrt{2}|P_-\alpha P_+\beta|), \quad (\text{A49})$$

$$(3/2, 1/2)_{2,-1} = \frac{1}{2}[\sqrt{3}|(3/2, -1/2), (1/2, -1/2)| + |(3/2, -3/2), (1/2, 1/2)|] = \frac{1}{2}\left(-\sqrt{3}|P_0\beta P_-\alpha| - \frac{1}{\sqrt{3}}|P_-\beta P_0\alpha| + \sqrt{\frac{2}{3}}|P_-\beta P_+\beta|\right), \quad (\text{A50})$$

$$(3/2, 1/2)_{2,-2} = |(3/2, -3/2), (1/2, -1/2)| = \frac{1}{\sqrt{3}}(|P_-\beta P_0\beta| - \sqrt{2}|P_-\beta P_-\alpha|), \quad (\text{A51})$$

$$(3/2, 1/2)_{1,1} = \frac{1}{2}[|(3/2, 1/2), (1/2, 1/2)| - \sqrt{3}|(3/2, 3/2), (1/2, -1/2)|] = \frac{1}{2}(|P_0\alpha P_+\beta| - |P_+\alpha P_0\beta| + \sqrt{2}|P_+\alpha P_-\alpha|), \quad (\text{A52})$$

$$(3/2, 1/2)_{1,0} = \frac{1}{\sqrt{2}}[-|(3/2, 1/2), (1/2, -1/2)| + |(3/2, -1/2), (1/2, 1/2)|] = \frac{1}{\sqrt{2}}(|P_0\alpha P_-\alpha| - |P_+\beta P_0\beta|), \quad (\text{A53})$$

$$\begin{aligned}
(3/2, 1/2)_{1,-1} &= \frac{1}{2}[-|(3/2, -1/2), (1/2, -1/2)| + \sqrt{3}|(3/2, -3/2), (1/2, 1/2)|] \\
&= \frac{1}{2}(|P_0\beta P_{-\alpha}| - |P_{-\beta} P_0\alpha| + \sqrt{2}|P_{-\beta} P_{+\beta}|).
\end{aligned} \tag{A54}$$

c. *J-J coupled states in terms of L-S coupled states and back*

Writing the $(1/2, 1/2)_0$ state out in terms of the determinants from Eqs. (A18)–(A32) we find

$$(1/2, 1/2)_0 = \frac{1}{\sqrt{3}} {}^1S_0 + \sqrt{\frac{2}{3}} {}^3P_0. \tag{A55}$$

The remaining states can accordingly be expressed as

$$(3/2, 3/2)_2 = \sqrt{\frac{2}{3}} {}^3P_2 + \frac{1}{\sqrt{3}} {}^1D_2, \tag{A56}$$

$$(3/2, 3/2)_0 = \frac{1}{\sqrt{3}} {}^3P_0 - \sqrt{\frac{2}{3}} {}^1S_0, \tag{A57}$$

$$(3/2, 1/2)_2 = \sqrt{\frac{2}{3}} {}^1D_2 - \frac{1}{\sqrt{3}} {}^3P_2, \tag{A58}$$

$$(3/2, 1/2)_1 = {}^3P_1. \tag{A59}$$

We close this section with the inverse expansion of Russell-Saunders terms in terms of *J-J* coupled states:

$${}^1S_0 = \frac{1}{\sqrt{3}} (1/2, 1/2)_0 - \sqrt{\frac{2}{3}} (3/2, 3/2)_0, \tag{A60}$$

$${}^3P_0 = \sqrt{\frac{2}{3}} (1/2, 1/2)_0 + \frac{1}{\sqrt{3}} (3/2, 3/2)_0, \tag{A61}$$

$${}^3P_1 = (3/2, 1/2)_1, \tag{A62}$$

$${}^3P_2 = \sqrt{\frac{2}{3}} (3/2, 3/2)_2 - \frac{1}{\sqrt{3}} (3/2, 1/2)_2, \tag{A63}$$

$${}^1D_2 = \frac{1}{\sqrt{3}} (3/2, 3/2)_2 + \sqrt{\frac{2}{3}} (3/2, 1/2)_2. \tag{A64}$$

The expansion of determinants over relativistic spinors in terms of Russell-Saunders terms—as referred to in the main body of the paper—can be deduced by combining Eqs. (A40)–(A54) with Eqs. (A60)–(A64).

5. Molecular determinants and states—Choice of Fermi vacuum

a. Wave function of molecular states

For the lightest homolog spin-orbit interaction is a perturbation to electrostatic effects. Furthermore, it is known from similar systems with an approximate valence π^2 configuration that σ – π mixing due to spin-orbit interaction is negligibly small in $4p$ element molecules [48]. We therefore start out from a molecular two-electron valence wave function for the expected electronic ground state which can be written as

$$|{}^3\Sigma_0\rangle = c_0 |{}^3\Sigma_{M_J=0}\rangle + c' |{}^1\Sigma_{M_J=0}\rangle, \tag{A65}$$

the $|{}^1\Sigma\rangle$ state corresponding to the π^2 configuration being the main perturber. We estimate the mixing coefficient c' for a first-order perturbation correction to the wave function with the one-electron spin-orbit Hamiltonian in Pauli approximation:

$$c' = \frac{\langle {}^3\Sigma | \hat{H}^{\text{SO}} | {}^1\Sigma \rangle}{E_{{}^1\Sigma} - E_{{}^3\Sigma}} \approx \frac{151}{7050}. \tag{A66}$$

The value of 151 cm^{-1} has been obtained by using an effective nuclear charge of 7.44 a.u. for a $4p$ electron in As [49] and an expectation value $\langle \frac{1}{r^3} \rangle = 7.0 \text{ a.u.}$ from Ref. [50] for calculating the spin-orbit matrix element. The energy difference of 7050 cm^{-1} has been calculated using the LUCITA module of the DIRAC program package [29] in Dyall's spin-orbit free approximation [51] to the Dirac-Coulomb Hamiltonian.

Normalizing the total wave function thus gives us an estimated contribution of roughly 0.03% of the $|{}^1\Sigma_{M_J=0}\rangle$ to the molecular ground state, which can safely be neglected, even if two-electron spin-orbit contributions were accounted for in addition. This means that the nonrelativistic $|{}^{(2S+1)}\Lambda_{\pm\Omega}\rangle$ wave functions

$$|{}^3\Sigma_0\rangle = \frac{1}{2}[\pi_+(1)\pi_-(2) - \pi_-(1)\pi_+(2)][\alpha(1)\beta(2) + \beta(1)\alpha(2)], \tag{A67}$$

$$|{}^1\Sigma_0\rangle = \frac{1}{2}[\pi_+(1)\pi_-(2) + \pi_-(1)\pi_+(2)][\alpha(1)\beta(2) - \beta(1)\alpha(2)] \tag{A68}$$

are a good approximation to the molecular states in AsH, where we use the notation $[symbol]_{m_\ell}(j)$ denoting $\lambda_{m_\ell}(\vec{r}_j)$ for the spatial wave function of particle j and the spin part in accordance with the definition in Sec. A 4 a.

We finally expand the results in Eqs. (A67) and (A68) into Cartesian components, according to $\pi_+ = -\frac{1}{\sqrt{2}}(\pi_x + i\pi_y)$ and $\pi_- = \frac{1}{\sqrt{2}}(\pi_x - i\pi_y)$, yielding

$$|{}^3\Sigma_0\rangle = \frac{i}{2}[\pi_x(1)\pi_y(2) - \pi_y(1)\pi_x(2)][\alpha(1)\beta(2) + \beta(1)\alpha(2)], \tag{A69}$$

$$|{}^1\Sigma_0\rangle = -\frac{1}{2}[\pi_x(1)\pi_x(2) + \pi_y(1)\pi_y(2)][\alpha(1)\beta(2) - \beta(1)\alpha(2)]. \tag{A70}$$

b. Choice of Fermi vacuum

In order to compare our Fermi vacuum state to the estimated molecular wave functions we have carried out a Mulliken population analysis of the AsH valence spinors as a function of internuclear distance. The results are to be found in Figure 4. The spinors underlying the figure are those energetically highest and still doubly occupied (HOMS). At the equilibrium bond length they are energetically well separated from the bonding spinors by 0.125 a.u. We therefore construct our

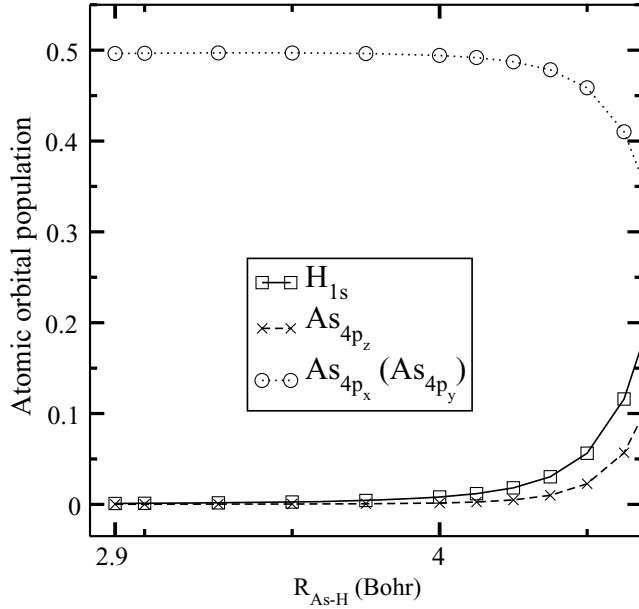


FIG. 4. Mulliken population analysis of the HOMs spinor $m_j = \frac{1}{2}$ as a function of internuclear distance. Since the closed-shell DCHF model does not lead to physically correct dissociation, we exploit the information from close to the equilibrium bond distance only.

two-electron Fermi vacuum state from the HOMs

$$\begin{aligned} \left(m_j = +\frac{1}{2}\right) &= \frac{1}{\sqrt{2}}(-\pi_x - i\pi_y)\beta, \\ \left(m_j = -\frac{1}{2}\right) &= \frac{1}{\sqrt{2}}(+\pi_x - i\pi_y)\alpha, \end{aligned}$$

where we have represented the molecular spinors by their principal character. The form of the spatial part has been obtained from the MO-AO expansion coefficients of the Dirac-Coulomb Hartree-Fock calculation, and the spin function from computing the expectation value $\langle \varphi_{j,m_j} | \hat{S}_z | \varphi_{j,m_j} \rangle$ for the respective spinors φ_{j,m_j} . The Kramers partner has been deduced by applying the time-reversal operator to a given spinor.

Using this information we can rewrite our Fermi vacuum state as

$$\begin{aligned} |(m_j)_1; (m_j)_2| &= \left| \left(m_j = \frac{1}{2}\right); \left(m_j = -\frac{1}{2}\right) \right| \\ &= \frac{1}{2\sqrt{2}} \{ [-\pi_x(1) - i\pi_y(1)]\beta(1)[\pi_x(2) - i\pi_y(2)]\alpha(2) \\ &\quad + [\pi_x(2) + i\pi_y(2)]\beta(2)[\pi_x(1) - i\pi_y(1)]\alpha(1) \} \\ &= \frac{i}{2\sqrt{2}} [\pi_x(1)\pi_y(2) - \pi_y(1)\pi_x(2)][\alpha(1)\beta(2) + \beta(1)\alpha(2)] \\ &\quad + \frac{1}{2\sqrt{2}} [\pi_x(1)\pi_x(2) + \pi_y(1)\pi_y(2)][\alpha(1)\beta(2) \\ &\quad - \beta(1)\alpha(2)]. \end{aligned} \quad (\text{A71})$$

Comparing Eqs. (A67) and (A68) with Eq. (A71) shows that our Fermi vacuum state from a relativistic calculation represents the true ground state only to roughly 50% and contains an equally large contribution from the excited $|^1\Sigma_0\rangle$ state.

- [1] J. Doyle, B. Friedrich, R. V. Krems, and F. Masnou-Seeuws, *Eur. Phys. J. D* **31**, 149 (2004).
- [2] W. C. Stwalley, P. L. Gould, and E. E. Eyler, in *Cold Molecules*, edited by R. V. Krems, W. C. Stwalley, and B. Friedrich (CRC Press, Boca Raton, 2009), Chap. 5.
- [3] M. Asplund, N. Grevesse, A. J. Sauval, and P. Scott, *Annu. Rev. Astron. Astrophys.* **47**, 481 (2009).
- [4] P. S. Barklem, A. K. Belyaev, M. Guitou, N. Feautrier, F. X. Gad  a, and A. Spielfiedel, *Astron. Astrophys.* **530**, A94 (2011).
- [5] E. D. Commins, *Adv. At., Mol., Opt. Phys.* **40**, 1 (1999).
- [6] A. E. Leanhardt, J. L. Bohn, H. Loh, P. Maletinsky, E. R. Meyer, L. C. Sinclair, R. P. Stutz, and E. A. Cornell, *J. Mol. Spectrosc.* **270**, 1 (2011).
- [7] V. V. Ivanov, D. I. Lyakh, and L. Adamowicz, in *Recent Progress in Coupled Cluster Methods*, edited by P.   arsky, J. Paldus, and J. Pittner, Vol. 11, (Springer, Heidelberg, Germany, 2010), Chap. 9.
- [8] *Recent Progress in Coupled Cluster Methods*, edited by P.   arsky, J. Paldus, and J. Pittner (Springer, Heidelberg, 2010).
- [9] T. Fleig, *Chem. Phys.* **395**, 2 (2012).
- [10] L. Visscher, E. Eliav, and U. Kaldor, *J. Chem. Phys.* **115**, 9720 (2001).
- [11] E. Eliav, M. J. Vilkas, Y. Ishikawa, and U. Kaldor, *J. Chem. Phys.* **122**, 224113 (2005).
- [12] S. Hirata, T. Yanai, R. J. Harrison, M. Kamija, and P.-D. Fang, *J. Chem. Phys.* **126**, 024104 (2007).
- [13] J. F. Stanton and R. J. Bartlett, *J. Chem. Phys.* **98**, 7029 (1993).
- [14] M. Musial and R. J. Bartlett, *J. Chem. Phys.* **129**, 134105 (2008).
- [15] P. A. Christiansen and K. S. Pitzer, *J. Chem. Phys.* **73**, 5160 (1980).
- [16] T. Fleig, in *Relativistic Methods for Chemists*, edited by M. Barysz and Y. Ishikawa, Vol. 10, (Springer, Heidelberg, 2010), Chap. 10.
- [17] T. Zeng, D. G. Fedorov, and M. Klobukowski, *J. Chem. Phys.* **131**, 124109 (2009).
- [18] S. Knecht, H. J. Aa Jensen, and T. Fleig, *J. Chem. Phys.* **132**, 014108 (2010).
- [19] J. Olsen and P. J  rgensen, *J. Chem. Phys.* **82**, 3235 (1984).
- [20] H. Koch and P. J  rgensen, *J. Chem. Phys.* **93**, 3333 (1990).
- [21] K. Emrich, *Nucl. Phys. A* **351**, 379 (1981).
- [22] K. Hald, P. J  rgensen, J. Olsen, and M. Jaszu  ski, *J. Chem. Phys.* **115**, 671 (2001).
- [23] T. Fleig, L. K. S  rensen, and J. Olsen, *Theor. Chem. Acc.* **118**, 347 (2007); **118**, 979(E) (2007).
- [24] L. K. S  rensen, T. Fleig, and J. Olsen, *Z. Phys. Chem.* **224**, 671 (2010).
- [25] L. K. S  rensen, J. Olsen, and T. Fleig, *J. Chem. Phys.* **134**, 214102 (2011).

- [26] T. Fleig, J. Olsen, and C. M. Marian, *J. Chem. Phys.* **114**, 4775 (2001).
- [27] T. Saue and H. J. Aa Jensen, *J. Chem. Phys.* **111**, 6211 (1999).
- [28] L. Visscher and T. Saue, *J. Chem. Phys.* **113**, 3996 (2000).
- [29] DIRAC, a relativistic *ab initio* electronic structure program, Release DIRAC10 (2010), written by T. Saue, L. Visscher, and H. J. Aa Jensen, with new contributions from R. Bast, K. G. Dyall, U. Ekstrøm, E. Eliav, T. Enevoldsen, T. Fleig, A. S. P. Gomes, J. Henriksson, M. Iliaš, Ch. R. Jacob, S. Knecht, H. S. Nataraj, P. Norman, J. Olsen, M. Pernpointner, K. Ruud, B. Schimmelpfennig, J. Sikkema, A. Thorvaldsen, J. Thyssen, S. Villaume, and S. Yamamoto.
- [30] T. Fleig, J. Olsen, and L. Visscher, *J. Chem. Phys.* **119**, 2963 (2003).
- [31] O. Christiansen, H. Koch, P. Jørgensen, and J. Olsen, *Chem. Phys. Lett.* **256**, 185 (1996).
- [32] J. Olsen, *J. Chem. Phys.* **113**, 7140 (2000).
- [33] B. O. Roos, R. Lindh, P.-Å. Malmqvist, V. Veryazov, and P. O. Widmark, *J. Phys. Chem. A* **108**, 2851 (2005).
- [34] K. G. Dyall, *Theor. Chim. Acta* **109**, 284 (2003).
- [35] K. G. Dyall, *Theor. Chim. Acta* **115**, 441 (2006).
- [36] Thom. H. Dunning, *J. Chem. Phys.* **90**, 1007 (1989).
- [37] K. P. Huber and G. Herzberg, *Molecular Spectra and Molecular Structure* (Van Nostrand Reinhold, New York, 1979).
- [38] K. P. Huber and G. Herzberg, *Constants of Diatomic Molecules* (data prepared by J. W. Gallagher and R. D. Johnson, III) in *NIST Chemistry WebBook*, edited by P. J. Linstrom and W. G. Mallard, NIST Standard Reference Database Number 69, (National Institute of Standards and Technology, Gaithersburg) <http://webbook.nist.gov> (retrieved December 10, 2008).
- [39] R. J. Bartlett and M. Musial, *Rev. Mod. Phys.* **79**, 291 (2007).
- [40] A. Köhn and J. Olsen, *J. Chem. Phys.* **125**, 174110 (2006).
- [41] S. Knecht, H. J. Aa Jensen, and T. Fleig, *J. Chem. Phys.* **128**, 014108 (2008).
- [42] T. Fleig, H. J. Aa Jensen, J. Olsen, and L. Visscher, *J. Chem. Phys.* **124**, 104106 (2006).
- [43] Stefan Knecht (Odense) (unpublished).
- [44] J. Loras, S. Knecht, and T. Fleig (unpublished).
- [45] Jessica Loras, Master thesis, Laboratory of Quantum Chemistry and Quantum Physics (LCPQ), University Paul Sabatier, Toulouse, 2011.
- [46] U. S. Mahapatra, B. Datta, and D. Mukherjee, *J. Chem. Phys.* **110**, 6171 (1999).
- [47] T. Fleig, *Phys. Rev. A* **72**, 052506 (2005).
- [48] J.-B. Rota, S. Knecht, T. Fleig, D. Ganyushin, T. Saue, F. Neese, and H. Bolvin, *J. Chem. Phys.* **135**, 114106 (2011).
- [49] E. Clementi and D. L. Raimondi, *J. Chem. Phys.* **38**, 2686 (1963).
- [50] J.-P. Desclaux, *At. Data Nucl. Data Tables* **12**, 311 (1973).
- [51] K. G. Dyall, *Introduction to Relativistic Quantum Chemistry* (Chemistry Department, University of Odense, Denmark, 1995).
- [52] W. C. Martin and R. Zalubas, *J. Phys. Chem. Ref. Data* **12**, 323 (1983).

B. Spin-free commutator-based GAS Coupled Cluster applications to ScH spectroscopy.

The following paper was the application of the (spin-free) commutator-based algorithm for excited states which I have presented in the chapter III. We choose to evaluate spectroscopic constants (r_e , ω_e , B_e and D_e) of the ground state $^3\Sigma$, the first excited state $^3\Delta$ and on the low-lying $^1\Delta$ with different CC models, we also evaluate the excitation energies (T_e) for the two excited states. Compared to our previous study we correlated twelve electrons to include core-electron correlation and compare to a four valence electron study. We investigate effect such as basis-set, spin-orbit coupling and core-correlation errors. We compare our results to some existing calculations and some experimental data. We compare the two CC algorithms in terms of required memory and run-time and conclude by stating that we can now increase the number of correlated electrons.

GENERAL ACTIVE SPACE COMMUTATOR-BASED COUPLED
CLUSTER THEORY OF GENERAL EXCITATION RANK FOR
ELECTRONICALLY EXCITED STATES.
IMPLEMENTATION AND APPLICATION TO ScH

Mickaël Hubert[†], Jeppe Olsen[‡], Jessica Loras[†], and Timo Fleig[†]

[†]*Laboratoire de Chimie et Physique Quantiques,
IRSAMC, Université Paul Sabatier Toulouse III,
118 Route de Narbonne, F-31062 Toulouse, France and*
[‡]*Theoretical Chemistry, Langelandsgade 140,
Aarhus University DK-8000 Århus C, Denmark*

Abstract

We present a new implementation of general excitation rank Coupled Cluster theory for electronically excited states based on the Single-Reference Multi-Reference formalism (SRMRCC). The method may include active-space selected and/or general higher excitations by means of the General Active Space (GAS) concept. It may employ molecular integrals over the four-component Lévy-Leblond Hamiltonian or the relativistic spin-orbit-free four-component Hamiltonian of Dyall. In an initial application to ground- and excited states of the scandium monohydride molecule (ScH) we report spectroscopic constants using basis sets of up to quadruple-zeta quality and up to full iterative Triple excitations in the cluster operators. Effects due to spin-orbit interaction are evaluated using two-component Multi-Reference Configuration Interaction for assessing the accuracy of the Coupled Cluster results.

I. INTRODUCTION

Electronically excited states of small molecules play an important role in many modern areas of research. One such field is the study of molecule formation in stellar atmospheres [1] involving the knowledge of molecular excited states [2], including both main group and transition metal atoms. Such molecules are of general interest in astrophysics studies of the gaseous phase in interstellar, circumstellar, and comet matter [3]. In the expanding field of ultracold molecules [4] an accurate description of molecular electronically excited states is of central importance, for instance in the formation process through photoassociation. Spectroscopy tests of fundamental physics, to name another area holding a potential for producing groundbreaking findings, requires accurate information on the electronic structure of molecular systems, very often of electronically excited states. Among the most prominent applications are the search for spacetime-variations of fundamental constants [5] and the search for new physics beyond the Standard Model of elementary particles, for example the electric dipole moment (EDM) of the electron in excited states of diatomic molecules [6].

The Coupled Cluster (CC) method is a well established and powerful approach for addressing molecular electronically excited states [7]. Numerous implementations using truncated wave operators exist, typically at the excitation rank of CC Doubles or sometimes CC Triples and Quadruples excitations for the ground-state cluster amplitudes. Some representative examples are Fock-Space (FS) CC [8], Equation-of-Motion (EOM) CC [9], Complete Active Space (CAS) state-specific CC [10], CC3 response theory [11], or the CC2-R12 model [12]. CC approaches of general excitation rank for molecular excited-state calculations are less abundant. Such implementations have been reported by Kállay et al. [13] and Hirata et al. [14]. CC methods capable of including full iterative Triple (and higher) excitations are of great interest in molecular physics, for example, when complete potential-energy curves of diatomic molecules are sought for which cannot be obtained with the CCSD(T) method [15]. A viable alternative is CC models which allow for active-space selected higher excitations while keeping the number of external particles limited in the cluster operators [16].

We present an efficient general excitation rank CC implementation applicable to

electronic ground and excited states of small molecules which exhibits the conventional computational scaling of the CC method [17]. Our work is based on the CC linear-response approach to excitation energies described in reference [18]. In the latter method Configuration Interaction (CI) expansions were employed for evaluating the CC Jacobian matrix, whereas our present work makes use of a more efficient commutator-based implementation which has earlier been described for relativistic ground-state CC wavefunctions [19]. The novelty of our current implementation as compared to previous work of other groups is twofold: The General Active Space (GAS) concept [20] is used for defining active-space selected higher excitations within the Single-Reference (SR) CC formalism. Second, our method is interfaced to a local version of the **DIRAC** program package [21] and may use the (non-relativistic) Levy-Leblond Hamiltonian operator [22] or the four-component relativistic and spin-orbit-free operator by Dyall [23].

We furthermore apply the extended and improved method to the ground- and lowest-lying electronically excited states of the ScH molecule. Diatomic transition-metal hydrides serve as models for the study of metal-hydrogen bonding in inorganic chemistry [24] and surface science [25] and for the study of the chemisorption of the hydrogen atom on catalytic metal surfaces [26]. Calculations of their spectroscopic properties is challenging because of the need to accurately describe the bonding arising from the mixture of the atomic valence configurations $3d^n 4s^2$ and $3d^{n+1} 4s^1$. In addition, an early theoretical study by Bauschlicher and colleagues [27] on first-row transition metal hydrides showed that the correct description of the lower part of the electronic spectrum of ScH requires the explicit correlation treatment of scandium outer-core electrons and models going beyond Singles and Doubles Configuration Interaction (SDCI). A correlated approach is therefore required which treats higher excitations in an efficient manner, which motivated us to choose the ScH molecule as a showcase application for our present method and its implementation. ScH is also a lighter valence-isoelectronic homologue of the “ $^3\Delta$ ” molecules considered as candidates [28, 29] in search of the electron EDM.

The paper is organized as follows: In the following section (II) we briefly summarize the underlying theory and sketch the commutator-based implementation of the CC Jacobian matrix elements. In section III we present an application to low-lying electronic states of the ScH molecule, including a comparison of Coupled-Cluster and

Configuration Interaction models and an evaluation of spin-dependent relativistic effects. We close this section with a timing analysis of the new algorithm compared to our previous implementation. In the final section (IV) we draw conclusions.

II. THEORY AND IMPLEMENTATION

A. Theory

1. GAS-CC wave function ansatz

Our implementation is based on the General Active Space Coupled Cluster (GAS-CC) wave function *ansatz* first introduced by Olsen [20]. We also refer the reader to other work based on this *ansatz* in references [16, 18, 19, 30].

Denoting an individual excitation rank as k , the highest excitation rank as n and an arbitrary individual excitation as μ the exponential parametrization of the general excitation operator acting on a single reference state (or Fermi vacuum) $|\Phi\rangle$ is written as

$$|\psi^{\text{GAS-CC}}\rangle = e^{\hat{T}^{\text{GAS}}} |\Phi\rangle \quad (1)$$

with

$$\begin{aligned} \hat{T}^{\text{GAS}} &= \sum_{\mu} t_{\mu} \hat{\tau}_{\mu}^{\text{GAS}} = \sum_{k=1}^n \hat{T}_k^{\text{GAS}} \\ &= \sum_{k=1}^n \left(\frac{1}{k!} \right)^2 \sum_{ij\dots ab\dots}^k t_{ij\dots}^{ab\dots} \underbrace{\left\{ \hat{a}^{\dagger} \hat{b}^{\dagger} \dots \hat{j} \hat{i} \right\}}_{\hat{\tau}_{ij\dots}^{ab\dots}} \end{aligned} \quad (2)$$

Curly braces are used for normal-ordered forms of second-quantized operators, and a simplified notation is adopted here: $\hat{a}_b^{\dagger} \equiv \hat{b}^{\dagger}$. Indices $\{a, b, \dots\}$ denote particle quasi-operators and indices $\{i, j, \dots\}$ denote hole quasi-operators referring to the particle hole formalism. The $t_{ij\dots}^{ab\dots}$ and t_{μ} are coupled cluster amplitudes and the $\hat{\tau}_{ij\dots}^{ab\dots}$ are the cluster operators which are pure excitation operators.

The GAS environment provides for the separability of particle space and hole space into an arbitrary number of subspaces, where the general CC excitation operators \hat{T}^{GAS} are constructed with respect to this partitioning and occupation constraints. This genuine feature defines, for instance, CC(n_m) schemes [16] as subsets.

2. Electronic Hamiltonian

The current implementation is a non-relativistic and a scalar relativistic approach using, respectively, the four-component Lévy-Leblond [22] and spin-free Hamiltonians [23] in second quantization

$$\hat{H} = \sum_{p,q} f_{pq} \{\hat{p}^\dagger \hat{q}\} + \frac{1}{4} \sum_{p,q,r,s} \langle pq || rs \rangle \{\hat{p}^\dagger \hat{q}^\dagger \hat{s} \hat{r}\}. \quad (3)$$

Above, a generic purely electronic correlation Hamiltonian is given in terms of the particle-hole formalism with normal ordered quasi-operators. Indices $\{p, q, r, s, \dots\}$ are general (particle or hole), f_{pq} are the one-electron fock integrals. $\langle pq || rs \rangle = \langle pq | rs \rangle - \langle pq | sr \rangle$ are the bi-electronic integrals related to the fluctuation potential.

The use of the Lévy-Leblond and spin-free relativistic Hamiltonians allow us to retain non-relativistic quantum numbers and spatial point-group symmetry.

3. Ground state in CC theory

The Coupled Cluster ground-state energy E_0 is determined by solving the time-independent Schrödinger equation for a given Hamiltonian (3), with a GAS-CC wave function (see Eq. (1)) projected onto the Fermi vacuum and onto the excitation manifold $\langle \psi_\mu^{\text{GAS}} | = \langle \Phi | \hat{\tau}_\mu^{\dagger \text{GAS}}$. We obtain the linked GAS-CC equations

$$E_0 = \left\langle \Phi \left| e^{-\hat{T}^{\text{GAS}}} \hat{H} e^{\hat{T}^{\text{GAS}}} \right| \Phi \right\rangle \quad (4)$$

$$\Omega_\mu^{\text{CC}} = \left\langle \psi_\mu \left| e^{-\hat{T}^{\text{GAS}}} \hat{H} e^{\hat{T}^{\text{GAS}}} \right| \Phi \right\rangle = 0 \quad (5)$$

The CC vector function Ω_μ^{CC} in Eq. (5) can be re-written employing a Baker-Campbell-Hausdorff (BCH) expansion [19]. The ground-state CC amplitudes t_μ from Eq. (5) are employed in the ensuing calculation of electronically excited states.

4. Excited states in CC theory

General response theory provides a powerful framework for the calculation of atomic and molecular properties [31–34]. The calculation of electronically excited energies is also possible using this formalism which has been demonstrated with GAS-CC wave functions (see Eq. (1)) in reference [18].

The derivative of the CC vector function Ω_μ^{CC} in Eq. (5) with respect to CC amplitudes t_ν yields the CC Jacobian matrix, its matrix elements given as

$$A_{\mu\nu}^{\text{CC}} = \frac{\partial}{\partial t_\nu} \Omega_\mu^{\text{CC}} = \left\langle \psi_\mu \left| e^{-\hat{T}} \left[\hat{H}, \hat{\tau}_\nu \right] e^{\hat{T}} \right| \Phi \right\rangle. \quad (6)$$

The Jacobian matrix elements $A_{\mu\nu}^{\text{CC}}$ can be re-written using a BCH expansion in analogy to the CC vector function Ω_μ^{CC} as

$$A_{\mu\nu}^{\text{CC}} = \left\langle \psi_\mu \left| \left(\left[\hat{H}, \hat{\tau}_\nu \right] + \left[\left[\hat{H}, \hat{\tau}_\nu \right], \hat{T} \right] + \frac{1}{2} \left[\left[\left[\hat{H}, \hat{\tau}_\nu \right], \hat{T} \right], \hat{T} \right] + \frac{1}{6} \left[\left[\left[\left[\hat{H}, \hat{\tau}_\nu \right], \hat{T} \right], \hat{T} \right], \hat{T} \right] \right) \right| \Phi \right\rangle. \quad (7)$$

For an Hamiltonian of maximum particle rank 2, this expansion truncates analytically after fourfold commutators, a mathematical proof of which can be found in reference [35].

Diagonalization of the matrix \mathbf{A}^{CC} yields excitation energies from CC theory, see also reference [36]. The excitation energies ω_A obtained from the eigenvalue equations

$$\mathbf{A}^{\text{CC}} |\psi_f\rangle = \omega_{Af} |\psi_f\rangle \quad (8)$$

are equivalent to those from the Equation-of-Motion (EOM) CC theory [37, 38].

B. Implementation of commutator-based algorithm for the CC Jacobian

Previous work on GAS-CC excitation energies [18, 36] exploited Configuration Interaction expansions for the evaluation of Eq. (6), leading to a rather inefficient code. The present implementation of the eigenvalue equations (8) is directly based on the evaluation of nested commutators, yielding the computational scaling of conventional CC theory. We evaluate the linear transformation of a trial vector \mathbf{x} with the CC Jacobian matrix

$$\begin{aligned} J_\mu^{\text{CC}} &= \sum_\nu A_{\mu\nu}^{\text{CC}} x_\nu \\ &= \sum_\nu \left\langle \psi_\mu \left| e^{-\hat{T}} \left[\hat{H}, \hat{\tau}_\nu \right] e^{\hat{T}} \right| \Phi \right\rangle x_\nu. \\ &= \sum_\nu \left\langle \psi_\mu \left| \left(\left[\hat{H}, \hat{\tau}_\nu \right] + \left[\left[\hat{H}, \hat{\tau}_\nu \right], \hat{T} \right] + \frac{1}{2} \left[\left[\left[\hat{H}, \hat{\tau}_\nu \right], \hat{T} \right], \hat{T} \right] + \frac{1}{6} \left[\left[\left[\left[\hat{H}, \hat{\tau}_\nu \right], \hat{T} \right], \hat{T} \right], \hat{T} \right] \right) \right| \Phi \right\rangle x_\nu. \end{aligned} \quad (9)$$

Hamiltonian operators in Eq. (3) and cluster operators in Eq. (1) are expanded in 4 types of second-quantized strings by using the spin-string method introduced

by Knowles and Handy [39]: α -creation-strings, β -creation-strings, β -annihilation-strings and α -annihilation-strings. The algorithm (see figure 1) performs an initial loop over the different Hamiltonian operator terms, which then allows for transformed integrals to be sorted. The second principal loop is the setup of the different \hat{T}^{GAS} operators where CC amplitudes are sorted. In the third principal loop, each block of nested commutators in Eq. (9) is treated in an individual loop. The specific equation for a given Hamiltonian operator term, excitation operators, projected term from the excitation manifold $\langle \psi_{\mu}^{\text{GAS}} |$ and cluster operator $\hat{\tau}_{\nu}^{\text{GAS}}$ is set up in accord with Eq. (9). The algorithm determines the optimum solution among the number of possible Wick contractions and, finally, obtains indices of integrals and CC amplitudes required to calculate the sum of matrix elements. This task is incorporated into an iterative diagonalizer for non-hermitian matrices [40]. The linear response module gives the number of desired low-lying excitation energies for a given symmetry. More details on the basic contraction algorithm can be found in reference [19] which described commutator-based GAS-CC for electronic ground states.

We have verified the correct performance of our newly implemented code by direct comparison with the CI-based implementation [36] on various small atomic and molecular test systems.

III. APPLICATION AND ANALYSIS

In this section we present an initial application to the scandium monohydride molecule with the aim of demonstrating the efficiency of our new implementation and of improving upon earlier studies on this system. We focus on spectroscopic constants of the ground state $^1\Sigma$ and in particular of the low-lying excited states $^3\Delta$ and $^1\Delta$. The closed shell valence occupation $1\sigma^2, 2\sigma^2$ (denoted as $p\lambda^q$ with p a molecular orbital index and q an occupation number) predominantly describes the $^1\Sigma$ ground state, whereas the lowest-lying $^3\Delta$ and $^1\Delta$ states arise mostly from a $1\sigma^2, 2\sigma^1, 1\delta^1$ electronic valence configuration.

Dynamic electron correlation and scalar relativistic effects are treated on the same footing. We do not expect large corrections from spin-orbit interaction (see V). However, since we are interested in making predictions of high accuracy, we

evaluate spin-orbit coupling contributions *via* 2-component MR-CI calculations.

A. Computational details

All calculations were performed with the **DIRAC** relativistic electronic-structure program package, using the latest version [41] for the Hartree-Fock calculations and integral transformations, and a local development version for the CC calculations.

For our exploratory calculations on the ScH molecule we used correlation-consistent polarized valence basis sets in uncontracted form, the cc-pV-T ζ and cc-pV-Q ζ for Sc [42] and H [43]. For obtaining spectroscopic constants, the equilibrium internuclear distance r_e , the harmonic vibrational frequency ω_e , the rotational constant B_e , the dissociation energy D_e and the excitation energy T_e , we performed several Born-Oppenheimer calculations around the minima of the respective potential energy curves. Polynomial fitting and solution of the rovibrational Schrödinger equation were performed with local programs [44]. The dissociation energies were determined by comparing total energies of ScH at the minimum with total energies of Sc + H fragments using the same wavefunction model. In the case of CI we carried out a molecular and a quasi-atomic calculation at a long-range value of 100 a.u.

Throughout this study we use the symmetry point group C_{2v} . In the present case this means that we obtain the Δ states as the lowest eigenvectors in the same symmetry representation (A_1) as that of the reference state ($^1\Sigma, A_1$). We have obtained the components of the Δ states in A_2 representation with degenerate energies, as compared to those in A_1 symmetry.

Spin-orbitals for the subsequent GAS-CC calculations were obtained from all-electron closed-shell and open-shell average-of-configuration spin-free-Hartree-Fock (SFHF) wavefunctions. For the closed-shell SFHF calculations, we set $1\sigma^2 2\sigma^2$ occupation numbers. For the open-shell SFHF calculations, fractional occupation numbers were introduced in the Fock operator using minimal spaces of spin-orbital pairs: 4 electrons in the ten $1\sigma, 2\sigma, 1\pi_x, 1\pi_y, 1\delta_{xy}, 1\delta_{x^2-y^2}, 2\pi_x, 2\pi_y, 3\sigma, 4\sigma$ molecular orbitals (see the Mulliken analysis in figure 2).

We describe electron correlation in ScH states using a series of different models. These are defined in a generic fashion in Figure 3. The principal model groups

include the standard CC hierarchy [45] up to full iterative quadruple excitations (CCSDTQ, S = Single excitations with respect to the reference state $|\Phi\rangle$, D = Double excitations, T = Triple, Q = Quadruple (four-fold) excitations (see Figure 3 with $v_1 = v_2 = 0$ and $n \in \{1, 2, 3, 4\}$), active-space motivated $\text{CC}(n_m)$ models [16, 36] (see Figure 3 with $c_1 = v_1 = 0$ and $v_2 = 8$), and core-core correlation and core-valence correlation (see Figure 3 with $c_2 = v_1 = v_2 = 0$, $c_1 = 4$, $a \in \{1, 2\}$ and $n = 3$). The latter models are of interest since it is known that correlation of the $3s$ and $3p$ core electrons of Sc play an important role in the spectrum of ScH. The construction of the entailing active spaces is done in an efficient manner by exploiting the General Active Space (GAS) concept [20, 46].

We employed the four-component spin-free Hamiltonian, Eq. (3), for CC and CI calculations throughout. For spin-dependent relativistic calculations the eXact 2-component (X2C) and X2C+Gaunt relativistic Hamiltonians [47] with GAS-CI models to estimate the one- and two-electron spin-orbit contributions to correlated excitation energies have been made use of. The X2C Hamiltonian comprises spin-orbit interaction induced by the relative motion of electrons with respect to the nuclei as well as spin-same orbit (SSO) interaction between electrons. The X2C+Gaunt Hamiltonian adds, in the current implementation, spin-other orbit (SOO) interactions between electrons. Two-electron SSO and SOO contributions were included via atomic mean-field integrals (AMFI) [48]. We used the following string-based Hamiltonian-direct CI modules included in the DIRAC11 program package: LUCITA for calculations in the spin-orbit free framework using non-relativistic point group symmetry [49] and KR-CI for calculations in the relativistic 2-component framework using double-point group symmetry [50, 51]. In addition, we used the newly-implemented linear symmetry in the LUCIAREL module [52, 53].

B. Results and discussion: Scandium monohydride - ScH

We present and discuss in this section our results for ScH molecule. We present a comparison of CC and CI/MRCI using the different afore-mentioned models for excitation energies T_e of $^3\Delta$, $^1\Delta$ and molecular spectroscopic constants of the $^1\Sigma$ ground state, $^3\Delta$ and $^1\Delta$ excited states. We discuss the importance of the various effects, evaluate errors and finally predict accurate molecular spectroscopic constants.

1. *Cutoff for the virtual orbital space*

As is common practice in studies using uncontracted atomic basis sets [54, 55] an energy cutoff value is introduced for truncating the space of canonical virtual orbitals. We have found that for the cc-pV-T ζ basis set absolute errors in $^3\Delta$ and $^1\Delta$ vertical excitation energies due to truncation at 9 a.u. (80 virtual orbitals included) are smaller than 20 cm $^{-1}$, correlating both 4 and 12 electrons. The corresponding calculations with the cc-pV-Q ζ basis sets yield absolute errors below 15 cm $^{-1}$ at a cutoff value of 10 a.u. (136 virtual orbitals). We have therefore carried out all further investigations using the afore-mentioned truncated virtual spaces.

2. *Choice of spin-orbital basis - closed-shell or open-shell*

In order to test the dependency of CC excitation energies on the molecular orbital set we have performed a series of exploratory calculations with closed-shell $1\sigma^2 2\sigma^2$ (cs) orbitals and with a set where fractional occupation numbers are introduced in the Fock operator, corresponding to an average of 4 electrons in the 10 molecular orbitals 1σ , 2σ , 1π , 1δ , 2π , 3σ , and 4σ (os4in10).

A Mulliken population analysis of these orbitals can be found in Figure 2. We confirm the findings of Bauschlicher and Walch [56] who discussed the strong participation of d electrons in the ScH bond which is shown by the relatively large d population in our bonding orbital 1σ . Two important further observations are to be made: First, and not surprisingly for the Sc atom, both the energies and the atomic character of the two sets differ significantly. Second, the energies of the outer-core orbital shell $3p$ are noticeably affected, despite the fact that these orbitals have not been included in the Fock operator averaging.

Since we are aiming at a balanced description of several low-lying electronic states of ScH, we investigated the effect of the two orbital sets on CC excitation energies; the results are compiled in Table I. Vertical excitation energies are seen to vary strongly depending on the orbital set, even in Full CI calculations with the four valence electrons. However, as the choice of orbital set also affects the equilibrium bond distance, we investigated in addition the effect on equilibrium excitation energies T_e . The results are conclusive: The (cs) orbitals exhibit a bias

on the $^1\Sigma$ ground state in the CCSD4 model, which however should be removed in the CCSDT4 model. Interestingly, there still remains a large difference between T_e values from (os) and (cs) orbitals for CCSDT4 which we ascribe to different core polarizations in the respective Hartree-Fock calculations which is also visible in the $3p$ orbital energies, figure 2. This difference is seen to strongly affect the ground-state $^1\Sigma$ energy, whereas the excited-state energies remain almost unaffected ($\Delta_{\text{cs-os}}E^{CC}$, CCSDT4). It is noteworthy that the core-polarization effect amounts to more than 2000 cm^{-1} on equilibrium excitation energies in the present case. The CCSD12 calculation again shows too strong a bias on the ground state, which we expect to be rectified when higher excitations (Triples and Quadruples) are included.

Therefore, we have chosen the (os) orbital set as the basis for our further study of ScH which is expected to yield the more balanced description of the states in question. In addition, we have observed (os) CC calculations to converge more rapidly in the present case.

3. Valence, core-valence and core-core correlation

Table II summarizes results from correlating the four valence electrons from 1σ and 2σ spin-orbitals (os) using the T ζ basis. From tests with the Q ζ basis set we infer basis-set errors on excitation energies of less than 40 cm^{-1} .

The results for the 3 states show that by increasing the excitation rank to full Triples (CCSDT) we obtain accurate and quasi-converged results (compared to Full CC). The dissociation energy D_e is already well described by the CC(4₂) model with a residual error of 10^{-3} eV . Turning our attention to the excited states $^3\Delta$ and $^1\Delta$, one can observe that the CC(4₂) model yields much more accurate results than CCSD. It is also remarkable that CC(4₃) improves significantly upon CCSDT for T_e for both excited states, and in this case is very close to FCI. The CC(4₂) model can be compared to the multi-reference (MR)CISD approach, giving values closer to FCI. The same holds for the corresponding models CC(4₃) compared to MRCISDT. The Modified Coupled-Pair Functional (MCPF) results of Chong and co-workers [27] resemble our MRCISD4 results well in case of r_e and ω_e , whereas for the dissociation and excitation energies some larger deviations can be observed.

The earlier study by Chong et al. [27] showed that the inclusion of core-valence

and core-core correlation effects from the scandium outer core $3s^2$, $3p^6$ have a significant effect on the excitation energy of the $^3\Delta$ state. In order to achieve a more accurate description we therefore added these 8 electrons through an additional active space (in case of the models CCS8_SDT12 and CCSD8_SDT12; for further details see Figure 3) and performed the corresponding 12-electron CC and CI calculations. The results given in Table III have been obtained using various different models which allow for direct comparison.

In contrast to the 4-electron calculations CCSD is in general more accurate than the MRCISD approach, which for a larger number of electrons suffers from the incomplete treatment of higher excitations. Exceptions are properties involving relative energies, the excitation energy T_e and dissociation energy of $^3\Delta$ where MRCI yields superior results. This can be explained by the true multi-reference nature of the MRCI approach which favors a balanced description of relative energies of ground- and excited states and those of molecular *vs.* atomic subsystems. Again, the chosen CC(n_m) model CC(4₂) which includes active-space selected higher excitations yields significantly more accurate results than CCSD for the electronic ground state. Not surprisingly, the MCPF results with 12 correlated electrons of Chong et al. are quite close to our CCSD12 results.

A comparison of CCSDT4 (in table II) and CCSDT12 values (in table III) for T_e displays the core correlation contribution to dynamic correlation: 1233 cm⁻¹ for $^3\Delta$ and 1866 cm⁻¹ for $^1\Delta$. Due to the Fermi hole in the triplet state it is reasonable that correlation contributions are more important in the spin singlet state.

In order to check the effect of limiting the core holes in $3s$ and $3p$, we have tested additional models, detailed in Figure 3. Allowing for excitations with only one hole in the ($3s$, $3p$) core (CCS8SDT12) does not lead to very accurate results. Core-valence correlation (comparing CCSDT4 and CCS8SDT12) decreases r_e by ≈ 0.1 a.u., increases ω_e by ≈ 100 cm⁻¹ increases B_e by ≈ 0.3 cm⁻¹ and increases D_e by $0.2 - 0.3$ eV for the three states. The two-hole model CCSD8SDT12 adds core-core correlation to the description and yields results in excellent agreement with CCSDT12. The core-core correlation contribution to T_e amounts to 1511 cm⁻¹ for $^3\Delta$ and 1227 cm⁻¹ for $^1\Delta$, corrections of remarkable importance. The remaining 67 cm⁻¹ for $^3\Delta$ and 58 cm⁻¹ are accounted for by allowing for a third hole in the $3s$ $3p$ core. The CCSD8SDT12 is thus an interesting and accurate alternative to

CC(4₂)12, since it can be defined by merely 3 active orbital spaces, in contrast to the latter where in general 4 active spaces are required[57]. However, the inclusion of cluster operators with 3 virtual indices may become too costly, in particular in systems where the number of valence electrons is larger.

Another interesting finding is the basis set effect. Whereas for all other spectroscopic properties the difference between T ζ and Q ζ sets is almost negligible, the excitation energies exhibit a large correction (CCSDT12) of -651 and -640 cm⁻¹ for the ³ Δ and ¹ Δ states, respectively. A comparison of the change of total energies due to the transition from the smaller to the larger basis set in the CCSDT12 calculations ($\Delta_{T\zeta-Q\zeta}^{E^{CC}}(^1\Sigma)=11143\text{cm}^{-1}$ (1.38 eV), $\Delta_{T\zeta-Q\zeta}^{E^{CC}}(^3\Delta)=11793\text{cm}^{-1}$ (1.46 eV) and $\Delta_{T\zeta-Q\zeta}^{E^{CC}}(^1\Delta)=11783\text{cm}^{-1}$ (1.46 eV)) reveals that ground- and excited states both exhibit large stabilizations with those of the excited states exceeding the ground-state stabilization by 0.08 eV. In summary, our results show that an accurate description of the respective excitation energies in ScH require the use of large atomic basis sets and the inclusion of higher excitations than CC Doubles. Our most accurate result for the ground-state dissociation energy of 2.41 eV (CCSDT12) is 0.16 eV (about 7%) larger than the MCPDF result in reference [27], confirming the conjecture of Chong et al.

4. *Spin-dependent relativistic effects*

To the best of our knowledge there have been no earlier studies of spin-orbit coupling effects on molecular constants or properties of the ScH molecule. In Table V we summarize our results for MRCI calculations using the two-component X2C and X2CG Hamiltonians and correlating 4 electrons.

As expected, effects on equilibrium bond distances r_e and rotational constants B_e are very small. The ground-state dissociation energy is very slightly decreased which can be explained by the atomic Sc spin-orbit splitting in the ground ² D state which amounts to 168.34 cm⁻¹ [58]. First-order spin-orbit splittings in the excited ³ Δ state are on the order of 50 cm⁻¹ and become visible in the equilibrium excitation energies T_e . A significant part of these spin-orbit splittings (about 20%) is due to the Gaunt interaction. We observe a change of -15 cm⁻¹ on the ground-state harmonic frequency. This can be understood by a stretching of the potential-energy curve due

to the lowering of the atomic limit, leading to a smaller vibrational frequency. For the excited-state $^3\Delta_3$, $^3\Delta_2$ and $^3\Delta_1$ terms the frequency is increased. In case of the excited $^1\Delta_2$ state somewhat larger effects on r_e , ω_e and B_e can be observed.

5. *Prediction of molecular spectroscopic constants*

In order to substantiate the accuracy of our present treatment we compare the results from our most accurate model (CCSDT12) with theoretical reference and experimental values, where available. For this purpose we have chosen the most sophisticated previous theoretical studies, which used Multi-Reference CI Singles and Doubles (MRD-CI) and the Modified Coupled Pair Functional (MCPF). For r_e CCSDT and MCPF are of similar quality and clearly outperform MRD-CI. Since we have used (os) orbitals for a balanced description of several electronic states, we may add an orbital correction of -0.004 cm^{-1} (determined as the difference between (T ζ)CCSDT12 (cs) and (os) values) and the spin-orbit correction from Table VI to the present value, yielding a bond length which is very slightly too short, by 0.01 a.u. The Basis-Set Superposition Error (BSSE) is likely to be the major source of this deviation, as similar CC calculations on heavier systems suggest [59, 60]. Applying the same corrections to the harmonic frequency results in 1597 cm^{-1} , in perfect agreement with the experimental value. In this case the BSSE is indeed expected to be negligible ($< 1 \text{ cm}^{-1}$), whereas for the dissociation energy there may be small downward corrections.

As concerns excited-state molecular constants we expect that our predictions are of similar quality as those for the electronic ground state. Of particular importance in the present study are the excitation energies of the low-lying $^3\Delta$ and $^1\Delta$ states which we obtain as $T_e = 0.281 \text{ eV}$ in the former case, significantly larger than the MCPF reference value and strongly affected by basis-set size and higher excitations in the cluster operators. The same is true for the $^1\Delta$ excitation energy. Due to expected error cancellations among relative energies, we do not assume these values to be strongly affected by the BSSE.

C. Computational scaling and timing improvements

The CI-based algorithm [18, 36] for evaluating the CC Jacobian exhibits a principal computational scaling as $O^{n+2}V^{n+2}$, where O is the number of occupied orbitals, V the number of virtual orbitals, and n is the highest excitation rank in the cluster operator. The complete scaling expression of commutator-based CC has been reported in reference [19] as

$$S^{(n)} = O^n V^{n+2} \left(\frac{1}{n!} \right)^2 \frac{1}{4} (n^2 - n) \binom{2n}{n}. \quad (10)$$

In the case of a CCSD calculation the scaling prefactor is close to one, so we consider only the exponential term. The scaling ratio of CI-based to commutator-based CC is given as

$$\frac{S_{\text{CICC}}^{(n)}}{S_{\text{commCC}}^{(n)}} \approx \frac{O^{n+2}V^{n+2}}{O^n V^{n+2}} = O^2 \quad (11)$$

which in the case of a CCSD calculation with 12 active electrons results in an estimated theoretical speedup factor of 144.

Table IV shows run-times for CC excitation energies obtained with the previous (CI-driven) CC algorithm [18] and the new commutator-based algorithm presented in this article (see section II A). The improvement does not become visible with a small number of active electrons (here 4) due to computational overhead. Upon increasing the number of correlated electrons to 12 we observe speedup factors between 65 (single-root calculation) and 101 (four roots), the latter in reasonable agreement with the theoretical value. In addition, the core memory requirements are reduced from 23Gb to 450Mb, which makes a much larger number of simultaneous calculations possible with the current serial code on a typical Linux cluster.

The efficiency of the new algorithm thus allows to include many more electrons in the correlation treatment and to efficiently do excited-state CC calculations on small molecules.

IV. CONCLUSION

A new implementation of a general active space commutator-based coupled cluster of general excitation rank for the calculation of electronically excited states is

presented. It has been demonstrated that the new algorithm based on the explicit evaluation of Baker-Campbell-Hausdorff expansion terms both in the CC vector function and in the CC Jacobian leads to an efficient computational scaling and allows for CC calculations with many active electrons and using excitation ranks higher than CC Doubles excitations and $Q\zeta$ basis sets. For the chosen molecular showcase system (ScH) we have demonstrated how improvements going beyond MRCISD and Coupled-Pair Functional models can be achieved with our GAS-CC approach. We regard these findings both as proof of principle for our present method and its efficiency as well as the results as accurate predictions for low-lying electronic states of the ScH molecule.

In ongoing work we have furthermore completed the implementation of the relativistic generalization of the present commutator-based algorithm, including spin-orbit coupling *via* the 4-component Dirac-Coulomb Hamiltonian. Initial applications of this extended method will be presented in a forthcoming publication.

ACKNOWLEDGMENTS

This work was granted access to the HPC resources of CALMIP under the allocation 2012-p1050 and 2013-p1050.

-
- [1] M. Asplund, N. Grevesse, A. J. Sauval, and P. Scott, *Annu. Rev. Astron. Astrophys.* **47**, 481 (2009).
 - [2] P. S. Barklem, A. K. Belyaev, M. Guitou, N. Feautrier, F. X. Gadéa, and A. Spielfiedel, *Astron. Astrophys.* **530**, A94 (2011).
 - [3] N. G. Bochkarev, *Paleontological Journal* **44**, 778 (2010).
 - [4] J. Ulmanis, J. Deiglmayr, M. Repp, R. Wester, and M. Weidemüller, *Chem. Rev.* **112**, 4890 (2012).
 - [5] C. Chin, M. G. Kozlov, and V. V. Flambaum, *New J. Phys.* **11**, 055048 (2009).
 - [6] E. R. Meyer and J. L. Bohn, *Phys. Rev. A* **78**, 010502 (2008).
 - [7] P. Čársky, J. Paldus, and J. Pittner, eds., *Recent Progress in Coupled Cluster Methods* (Springer, Heidelberg, Germany, 2010) ISBN: 978-90-481-2884-6.
 - [8] M. Musial and R. J. Bartlett, *J. Chem. Phys.* **129**, 044101 (2008).
 - [9] S. Hirata, *J. Chem. Phys.* **121**, 51 (2004).
 - [10] V. V. Ivanov, L. Adamowicz, and D. I. Lyakh, *J. Chem. Phys.* **124**, 184302 (2006).
 - [11] O. Christiansen, H. Koch, and P. Jørgensen, *J. Chem. Phys.* **103**, 7429 (1995).
 - [12] H. Fliegl, C. Hättig, and W. Klopper, *J. Chem. Phys.* **124**, 044112 (2006).
 - [13] M. Kállay and P. Surján, *J. Chem. Phys.* **115**, 2945 (2001).
 - [14] S. H. M. Nooijen and R. J. Bartlett, *Chem. Phys. Lett.* **328**, 459 (2000).
 - [15] Sørensen, L. K., Fleig, T., and Olsen, J., *J. Phys. B* **42**, 165102 (2009).
 - [16] A. Köhn and J. Olsen, *J. Chem. Phys.* **125**, 174110 (2006).
 - [17] T. Helgaker, P. Jørgensen, and J. Olsen, *Molecular Electronic Structure Theory* (John Wiley & Sons, Chichester, 2000).
 - [18] K. Hald, P. Jørgensen, J. Olsen, and M. Jaszuński, *J. Chem. Phys.* **115**, 671 (2001).
 - [19] L. K. Sørensen, J. Olsen, and T. Fleig, *J. Chem. Phys.* **134**, 214102 (2011).
 - [20] J. Olsen, *J. Chem. Phys.* **113**, 7140 (2000).
 - [21] (), DIRAC, a relativistic ab initio electronic structure program, Release DIRAC10 (2010), written by T Saue, L Visscher and H J Aa Jensen, with new contributions from R Bast, K G Dyall, U Ekstrøm, E Eliav, T Enevoldsen, T Fleig, A S P Gomes, J Henriksson, M Iliaš, Ch R Jacob, S Knecht, H S Nataraj, P Norman, J Olsen, M Pernpointner, K Ruud, B Schimmelpfennig, J Sikkema, A Thorvaldsen, J Thyssen,

S Villaume and S Yamamoto.

- [22] J.-M. Lévy-Leblond, Commun. math. Phys. **6**, 286 (1967).
- [23] K. G. Dyall, J. Chem. Phys. **100**, 2118 (1994).
- [24] T. Fehner, “Inorganometallics,” (1992), plenum Press: New York.
- [25] P.B.Armentrout and J. L. Beauchamp, Acc. Chem. Res. **22**, 315 (1989).
- [26] P. Walch, Surf. Sci. **143**, 188 (1984).
- [27] D. P. Chong, S. R. Langhoff, J. C. W. Bauschlicher, S. P. Walch, and H. Partridge, J. Chem. Phys. **85**, 2850 (1986).
- [28] K. C. Cossel, D. N. Gresh, L. C. Sinclair, T. Coffrey, L. V. Skripnikov, A. N. Petrov, N. S. Mosyagin, A. V. Titov, R. W. Field, , E. R. Meyer, E. A. Cornell, and J. Ye, Chem. Phys. Lett. **546**, 1 (2012).
- [29] A. C. Vutha, W. C. Campbell, Y. V. Gurevich, N. R. Hutzler, M. Parsons, D. Patterson, E. Petrik, B. Spaun, J. M. Doyle, G. Gabrielse, and D. DeMille, J. Phys. B **43**, 074007 (2010).
- [30] T. Fleig, L. K. Sørensen, and J. Olsen, Theoret. Chem. Acc. **118**, 347 (2007), erratum: *Theo. Chem. Acc.*, 118:979, 2007.
- [31] J. Olsen and P. Jørgensen, J. Chem. Phys. **82**, 3235 (1984).
- [32] H. Koch and P. Jørgensen, J. Chem. Phys. **93**, 3333 (1990).
- [33] O. Christiansen, P. Jørgensen, and C. Hättig, Int. J. Quantum Chem. **68**, 1 (1998).
- [34] T. Helgaker, S. Coriani, P. Jørgensen, K. Kristensen, J. Olsen, and K. Ruud, Chem. Rev. **112**, 543 (2012).
- [35] T. Helgaker, P. Jørgensen, and J. Olsen, *Molecular Electronic Structure Theory* (John Wiley & Sons, Chichester, 2000).
- [36] M. Hubert, L. K. Sørensen, J. Olsen, and T. Fleig, Phys. Rev. A **86**, 012503 (2012).
- [37] K. Emrich, Nuc. Phys. A **351**, 379 (1981).
- [38] J. F. Stanton and R. J. Bartlett, J. Chem. Phys. **98**, 7029 (1993).
- [39] P. J. Knowles and N. Handy, Chem. Phys. Lett. **111**, 313 (1984).
- [40] J. Olsen, Unpublished.
- [41] (), DIRAC, a relativistic ab initio electronic structure program, Release DIRAC11 (2011), written by R. Bast, H. J. Aa. Jensen, T. Saue, and L. Visscher, with contributions from V. Bakken, K. G. Dyall, S. Dubillard, U. Ekström, E. Eliav, T. Enevoldsen,

- T. Fleig, O. Fossgaard, A. S. P. Gomes, T. Helgaker, J. K. Lærdahl, J. Henriksson, M. Iliaš, Ch. R. Jacob, S. Knecht, C. V. Larsen, H. S. Nataraj, P. Norman, G. Olejniczak, J. Olsen, J. K. Pedersen, M. Pernpointner, K. Ruud, P. Salek, B. Schimmelpfennig, J. Sikkema, A. J. Thorvaldsen, J. Thyssen, J. van Stralen, S. Villaume, O. Visser, T. Winther, and S. Yamamoto (see <http://dirac.chem.vu.nl>).
- [42] N. B. Balabanov and K. A. Peterson, *J. Chem. Phys.* **123**, 064107 (2005).
 - [43] T. H. J. Dunning, *J. Chem. Phys.* **90**, 1007 (1989).
 - [44] “Programs FIT1B and VIB2,” University of Bonn, Germany.
 - [45] R. J. Bartlett and M. Musial, *Rev. Mod. Phys.* **79**, 291 (2007).
 - [46] T. Fleig, J. Olsen, and C. M. Marian, *J. Chem. Phys.* **114**, 4775 (2001).
 - [47] M. Iliaš and T. Saue, *J. Chem. Phys.* **126**, 064102 (2007).
 - [48] “AMFI, an atomic mean-field spin-orbit integral program,” (1996 and 1999), Bernd Schimmelpfennig, University of Stockholm.
 - [49] (1999, 2002), LUCITA is a direct CI program written by J Olsen, *MOLCAS* interface by T Fleig, 1999, *DIRAC* interface by T Fleig, 2002.
 - [50] S. Knecht, H. J. A. Jensen, and T. Fleig, *J. Chem. Phys.* **132**, 014108 (2010).
 - [51] T. Fleig, H. J. Aa. Jensen, J. Olsen, and L. Visscher, *J. Chem. Phys.* **124**, 104106 (2006).
 - [52] S. K. (Odense), Unpublished.
 - [53] J. Loras, S. Knecht, H. J. Aa. Jensen, and T. Fleig, “Effect of the spin-other-orbit interaction on excitation energies in correlated atomic and molecular calculations. The atoms Ti, Zr, Hf, and their monohydrides TiH, ZrH, HfH,” (2013), unpublished.
 - [54] S. Höfener, R. Ahlrichs, S. Knecht, and L. Visscher, *Comp. Phys. Commun.* **13**, 3952 (2012).
 - [55] J.-B. Rota, S. Knecht, T. Fleig, D. Ganyushin, T. Saue, F. Neese, and H. Bolvin, *J. Chem. Phys.* **135**, 114106 (2011).
 - [56] C. W. B. Jr. and S. P. Walch, *J. Chem. Phys.* **76**, 4560 (1982).
 - [57] In the present case, we have allowed for up to 4 holes in a space combining the outer-core and occupied valence orbitals and therefore required only 3 orbital spaces (see Figure 3). When correlating a significantly larger number than 12 electrons it will become advantageous to define a fourth space for core orbitals and to restrict the

number of holes in this space.

- [58] J. Sugar and C. Corliss, J. Phys. Chem. Ref. Data **14**, **Suppl.2**, 1 (1985).
- [59] S. Knecht, L. K. Sørensen, H. J. A. Jensen, T. Fleig, and C. M. Marian, J. Phys. B **43**, 055101 (2010).
- [60] L. K. Sørensen, S. Knecht, T. Fleig, and C. Marian, J. Phys. Chem. A **113**, 12607 (2009).
- [61] J. Anglada, P. J. Bruna, and S. D. Peyerimhoff, Mol. Phys. **66**, 541 (1989).
- [62] R. S. Ram and P. F. Bernath, J. Chem. Phys. **105**, 2668 (1996).

I. TABLES

TABLE I. Comparison of vertical excitation energies T_v (at 3.4 a.u.), of excitation energies T_e and of total energies E^{CC} (in cm^{-1}) for the ground state $^3\Sigma$, and the excited states $^3\Delta$ and $^1\Delta$. $\Delta_{\text{cs-os}}$ defines the difference for a given property using (cs) and (os) orbitals, respectively. We used active spaces of four or twelve electrons where specified (4 or 12). The basis sets are of cc-pV-T ζ quality.

Model/state	$^1\Sigma$	$^3\Delta$	$^1\Delta$	Model/state	$^1\Sigma$	$^3\Delta$	$^1\Delta$	Model/state	$^1\Sigma$	$^3\Delta$	$^1\Delta$
$r_e(\text{cs})$	3.384	3.601	3.624	$r_e(\text{cs})$	3.388	3.609	3.629	$r_e(\text{cs})$	3.330	3.352	3.614
cs CCSD4 T_e	-	3907	6147	cs CCSDT4 T_e	-	3934	5700	cs CCSD12 T_e	-	6343	6516
$r_e(\text{os})$	3.425	3.694	3.715	$r_e(\text{os})$	3.412	3.668	3.692	$r_e(\text{os})$	3.371	3.606	3.621
os CCSD4 T_e	-	855	2798	os CCSDT4 T_e	-	1682	3424	os CCSD12 T_e	-	1516	4997
$\Delta_{\text{cs-os}}T_e$	-	3052	3349	$\Delta_{\text{cs-os}}T_e$	-	2252	2276	$\Delta_{\text{cs-os}}T_e$	-	4827	1519
$\Delta_{\text{cs-os}}E^{\text{CC}}$	-1857	1195	1493	$\Delta_{\text{cs-os}}E^{\text{CC}}$	-2246	6	30	$\Delta_{\text{cs-os}}E^{\text{CC}}$	1040	5866	2559

Model/state	$^1\Sigma$	$^3\Delta$	$^1\Delta$	Model/state	$^1\Sigma$	$^3\Delta$	$^1\Delta$
cs FCC4/FCI4 T_v	-	4374	6207	cs CCSDT12 T_v	-	3154	7277
os FCC4/FCI4 T_v	-	2366	4265	os CCSDT12 T_v	-	3114	5590
$\Delta_{\text{cs-os}}T_v$	-	2008	1942	$\Delta_{\text{cs-os}}T_v$	-	40	1687
$\Delta_{\text{cs-os}}E^{\text{CC}}$	-2283	-274	-341	$\Delta_{\text{cs-os}}E^{\text{CC}}$	82	121	255

TABLE II. Spectroscopic constants for the ground state $^1\Sigma^+$ and for the excited states $^3\Delta$, $^1\Delta$ using the spin-free Hamiltonian, (os) orbitals, and correlating four electrons. The basis sets are of cc-pV-T ζ quality.

$^1\Sigma^+$ ground state								
Model	CCSD4	MRCISD4	CC(4 ₂)4	CCSDT4	MRCISDT4	CC(4 ₃)4	FCC4/FCI4	MCPF [27]
r_e [bohr]	3.425	3.393	3.413	3.412	3.410	3.410	3.411	3.390
ω_e [cm ⁻¹]	1503	1578	1532	1534	1540	1537	1533	1587
B_e [cm ⁻¹]	5.2062	5.3045	5.2431	5.2467	5.2504	5.2502	5.2494	-
D_e [eV]	2.14	2.10	2.12	2.12	2.13	2.12	2.12	2.27
1^{st} excited state: $^3\Delta$								
Model	CCSD4	MRCISD4	CC(4 ₂)4	CCSDT4	MRCISDT4	CC(4 ₃)4	FCC4/FCI4	MCPF [27]
r_e [bohr]	3.694	3.647	3.668	3.668	3.665	3.665	3.665	3.632
ω_e [cm ⁻¹]	1333	1361	1380	1378	1395	1380	1384	1354
B_e [cm ⁻¹]	4.4758	4.5904	4.5382	4.5388	4.5467	4.5458	4.5473	-
D_e [eV]	2.03	1.88	1.91	1.91	1.92	1.91	1.91	2.06
T_e [cm ⁻¹][eV]	855 (0.106)	1775 (0.220)	1695 (0.210)	1682 (0.209)	1726 (0.214)	1725 (0.214)	1727 (0.214)	1734 (0.215)
Excited state: $^1\Delta$								
Model	CCSD4	MRCISD4	CC(4 ₂)4	CCSDT4	MRCISDT4	CC(4 ₃)4	FCC4/FCI4	
r_e [bohr]	3.715	3.669	3.690	3.692	3.686	3.688	3.687	
ω_e [cm ⁻¹]	1326	1398	1374	1373	1390	1383	1380	
B_e [cm ⁻¹]	4.4241	4.5388	4.4844	4.4800	4.4933	4.4904	4.4923	
D_e [eV]	1.79	1.65	1.69	1.70	1.70	1.69	1.69	
T_e [cm ⁻¹][eV]	2798 (0.347)	3644 (0.452)	3478 (0.431)	3424 (0.425)	3516 (0.436)	3505 (0.435)	3505 (0.435)	

TABLE III. Spectroscopic constants for the ground state $^1\Sigma^+$ and for the excited states $^3\Delta$, $^1\Delta$ using the spin-free Hamiltonian, (os) orbitals, and correlating twelve electrons. The basis sets are of cc-pV-T ζ quality.

$^1\Sigma^+$ ground state										
Model	CCSD12	MRCISD12	CCSD12(Q ζ)	CC(4 ₂)12	CCS8SDT12	CCS8SDT12(Q ζ)	CCSD8SDT12	CCSDT12	CCSDT12(Q ζ)	MCPF [27]
r_e [bohr]	3.371	3.253	3.370	3.352	3.288	3.277	3.347	3.349	3.348	3.357
ω_e [cm ⁻¹]	1568	1795	1554	1609	1616	1608	1611	1611	1602	1572
B_e [cm ⁻¹]	5.3735	5.7697	5.3759	5.4337	5.6487	5.6874	5.4510	5.4448	5.4485	-
D_e (eV)	2.43	2.37	2.41	-	2.39	-	2.42	2.41	-	2.25
1^{st} excited state: $^3\Delta$										
Model	CCSD12	MRCISD12	CCSD12(Q ζ)	CC(4 ₂)12	CCS8SDT12	CCS8SDT12(Q ζ)	CCSD8SDT12	CCSDT12	CCSDT12(Q ζ)	MCPF [27]
r_e [bohr]	3.606	3.457	3.605	3.563	3.475	3.457	3.552	3.555	3.550	3.580
ω_e [cm ⁻¹]	1366	1641	1359	1440	1480	1485	1449	1449	1455	1400
B_e [cm ⁻¹]	4.6966	5.1090	4.6979	4.8097	5.0580	5.1096	4.8399	4.8326	4.8442	-
D_e [eV]	2.25	2.01	2.33	-	2.221	-	2.06	2.05	-	2.06
T_e [cm ⁻¹][eV]	1516 (0.188)	2840 (0.352)	645 (0.080)	2987 (0.370)	1337 (0.166)	546 (0.068)	2848 (0.353)	2915 (0.361)	2264 (0.281)	1516 (0.188)
Excited state: $^1\Delta$										
Model	CCSD12	MRCISD12	CCSD12(Q ζ)	CC(4 ₂)12	CCS8SDT12	CCS8SDT12(Q ζ)	CCSD8SDT12	CCSDT12	CCSDT12(Q ζ)	
r_e [bohr]	3.621	-	3.616	3.590	3.514	3.497	3.584	3.586	3.582	
ω_e [cm ⁻¹]	1377	-	1376	1429	1456	1460	1432	1434	1438	
B_e [cm ⁻¹]	4.6564	-	4.7610	4.7387	4.9449	4.9935	4.7542	4.7492	4.7587	
D_e [eV]	1.81	-	1.88	-	1.89	-	1.77	1.76	-	
T_e [cm ⁻¹][eV]	4997 (0.620)	-	4250 (0.527)	5405 (0.670)	4005 (0.497)	3275 (0.406)	5232 (0.649)	5290 (0.656)	4647 (0.576)	

TABLE IV. Speed and memory comparison between commutator-based Coupled Cluster (**cbCC**) and the CI-driven Coupled Cluster (ciCC) algorithms for the calculation (50 iterations) of one or two excited states in the first symmetry A_1 of the C_{2v} point group of ScH. Different CC models were used (CCSD4, CCSD12, defined in Figure 3) with the spin-free Hamiltonian and the open-shell (os4in10) Hartree-Fock reference state. The basis sets are of cc-pV-T ζ quality, r_e is taken to 3.4 a.u.

Speed/memory comparison between cbCC and ciCC						
roots	#iter.	memory	CCSD4	#iter.	memory	CCSD12
1	50	450Mb 450Mb	3min44s 4min27s	50	450Mb 23Gb	23min 1d1h12min
2	46	450Mb 450Mb	6min38s 10min	34	450Mb 23Gb	27min 1d14h48min
3	46	450Mb 450Mb	10min 18min	47	450Mb 23Gb	45min 2d20h2min
4	50	450Mb 450Mb	13min56s 18min27s	37	450Mb 23Gb	48min 3d8h38min

TABLE V. Spectroscopic constants for the ground state $^1\Sigma_0^+$ and the excited states $^3\Delta_{3,2,1}$ and $^1\Delta_2$. We use an average of configuration reference state with an averaging of four electrons in ten Kramers pairs (os4in10). Accordingly we use a complete active space of four electrons in ten Kramers pairs (CAS4in10). The relativistic X2CGaunt Hamiltonian is used with the MRCISD4 model (defined in figure 3). Δ^{SO} gives the spin-orbit correction by comparing the X2CG result with the spin-free calculation MRCISD4 (see table II).

X2CG-MRCISD4	$r_e[\text{bohr}]$	$\omega_e[\text{cm}^{-1}]$	$B_e[\text{cm}^{-1}]$	$D_e[\text{eV}]$	$T_e[\text{cm}^{-1}]$
$^1\Sigma_0^+$	3.393	1563	5.3044	2.09	-
$^3\Delta_1$	3.645	1401	4.5950	1.88	1711
$^3\Delta_2$	3.645	1401	4.5959	1.88	1760
$^3\Delta_3$	3.645	1401	4.5971	1.88	1813
$^1\Delta_2$	3.651	1321	4.5820	1.66	3597
Δ^{SO}	$r_e[\text{bohr}]$	$\omega_e[\text{cm}^{-1}]$	$B_e[\text{cm}^{-1}]$	$D_e[\text{eV}]$	$T_e[\text{cm}^{-1}]$
$^1\Sigma_0^+$	0.000	-15	-0.0001	-0.01	0
$^3\Delta_1$	-0.002	+40	+0.0046	0.00	-64
$^3\Delta_2$	-0.002	+40	+0.0055	0.00	-15
$^3\Delta_3$	-0.002	+40	+0.0067	0.00	+38
$^1\Delta_2$	-0.018	-77	-0.0432	+0.01	-47

TABLE VI. Comparative table with our best predictive model: CCSDT12(Q ζ) (see table III and figure 3) with two other theoretical models and the experimental values for spectroscopic constants of the $^1\Sigma^+$ ground state.

$^1\Sigma^+$	$r_e[\text{bohr}]$	$\omega_e[\text{cm}^{-1}]$	$B_e[\text{cm}^{-1}]$	$D_e[eV]$
MRD-CI[61]	3.41	1621	5.3	2.24
MCPF[27]	3.357	1572	—	2.25
Present work, CCSDT12(Q ζ)	3.348	1602	5.4485	2.41(T ζ)
Experiment[62]	3.35507	1596.9966	5.425432	—

II. FIGURES

FIG. 1. Commutator-based Coupled Cluster for excited states algorithm.

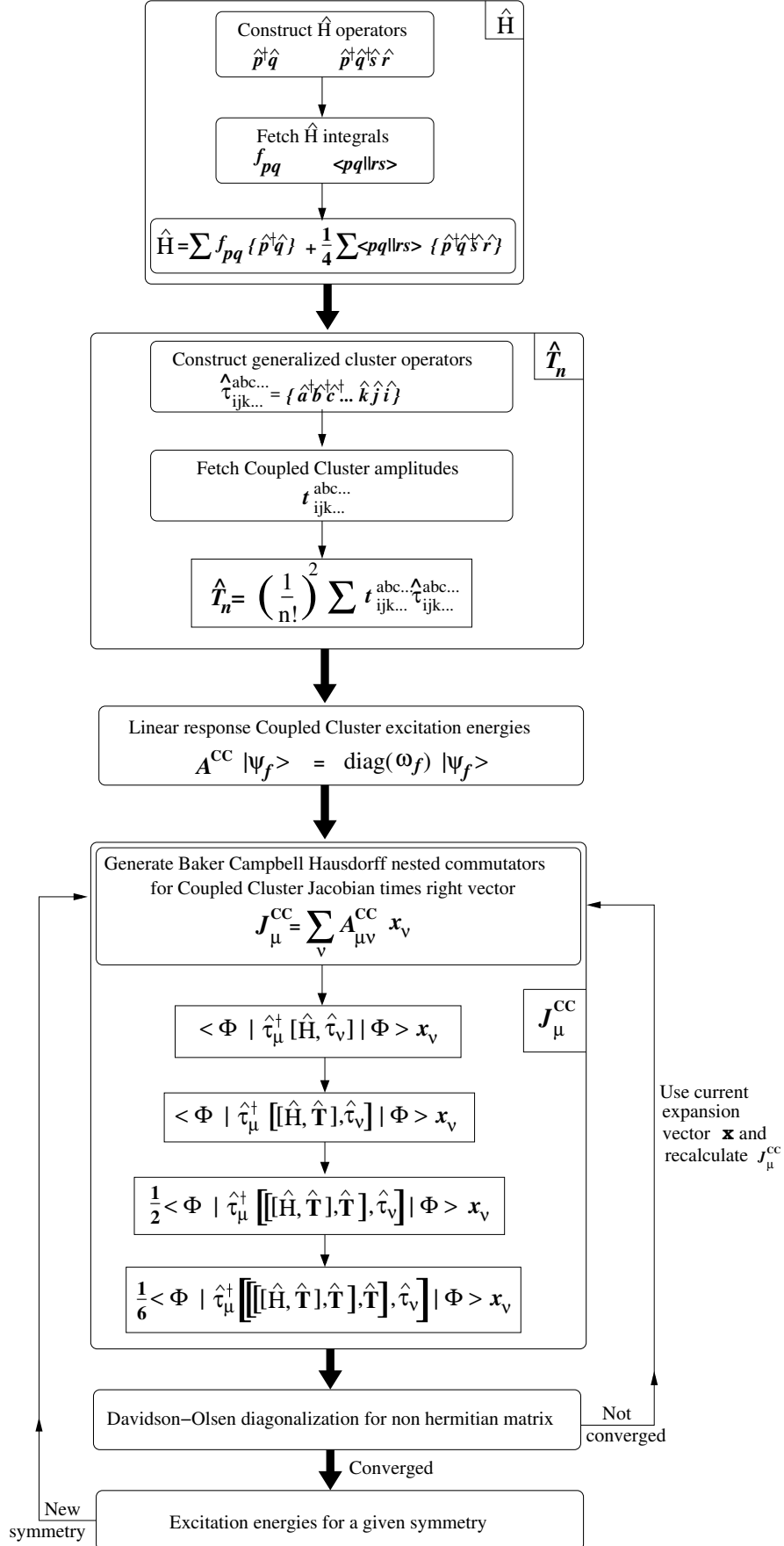


FIG. 2. Molecular orbital energies and atomic character of molecular orbitals based on a Mulliken population analysis for closed-shell and open-shell Hartree-Fock orbitals

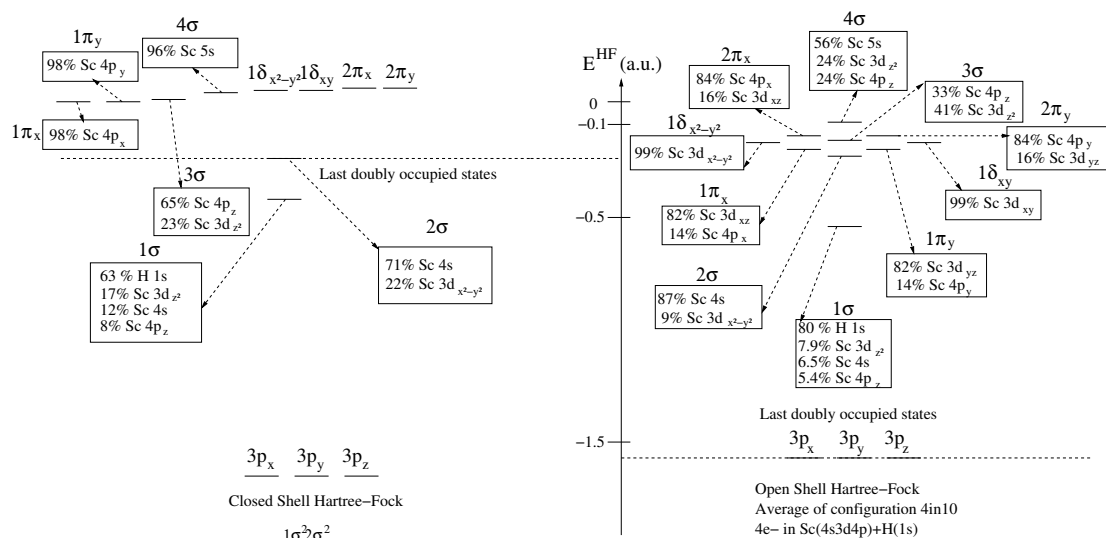


FIG. 3. GAS partitioning for CC and MRCI models with the number of orbitals (spin-free models) or Kramers pairs (X2C(Gaunt) model) in each GAS. A GAS with $c_1 = c_2 = 0$ or $v_1 = v_2 = 0$ does not exist, a GAS with $c_1 = 0$ and $c_2 = 4$ or $v_1 = 8$ and $v_2 = 0$ is merged with the valence GAS. min. el. represents the minimum accumulated number and max. el. the maximum accumulated number of electrons after consideration of a given GAS. The number of GAS varies from two ($c_1 = c_2 = v_2 = 0$) to three ($c_1 = 4$, $c_2 = v_2 = 0$ or $v_2 = 8$, $c_1 = v_1 = 0$) depending on the configuration. The dotted lines attest that the two separate orbital spaces could be merged into one space depending on the parameters c_1 , c_2 , v_1 and v_2 . For valence models with four correlated electrons $c_1 = c_2 = 0$, for core models with twelve correlated electrons $c_1 = 4$ and $c_2 = 0$ or $c_1 = 0$ and $c_2 = 4$. n is the valence excitation rank, a the core excitation rank (if $c_1 = 4$) and m is the virtual excitation rank for CC(n_m) models (if $v_2 = 8$ and $v_1 = c_1 = 0$). For MRCI models, the CAS4in10 is obtained for $v_1 = 8$ and $v_2 = 0$. Electrons which belong to the frozen core are not correlated. For cc-pV-T ζ basis: $b = 80$ for 9a.u. cut-off and $b = 136$ for the full basis. For cc-pV-Q ζ basis: $b = 136$ for 10a.u cut-off and $b = 202$ for the full basis.

<i>GAS partitioning</i>		<i>#of Orbitals</i> <i>(Kr. pairs)</i>	<i>Accumulated # of el.</i>	
	Virtual Orbitals (Kr. pairs)	$b - (v_1 + v_2)$	<i>min.</i> $4+2(c_1+c_2)$	<i>max.</i> $4+2(c_1+c_2)$
$GAS(2 + \frac{v_2}{8} + \frac{c_1}{4})$	$1\pi^{(2)} 1\delta^{(2)} 2\pi^{(2)}$ $3\sigma 4\sigma$	v_2	$4+2(c_1+c_2)-m$	$4+2(c_1+c_2)$
$GAS(\frac{v_2}{4})$				
$GAS(1 + \frac{c_1}{4})$	$1\sigma 2\sigma$	$2 + c_2 + v_1$	$4+2(c_1+c_2)-n$	$4+2(c_1+c_2)$
$GAS(\frac{c_1}{4})$	Sc: $3s 3p^{(3)}$	c_1	$2c_1 - a$	$2c_1$
	Frozen core	$36 - (c_1 + c_2)$		

CCSD4, CCSDT4 and FCC4: $c_1 = c_2 = v_1 = v_2 = 0$ and $n \in \{2, 3, 4\}$
CC(4₂)4 and CC(4₃): $c_1 = c_2 = v_1 = 0$, $v_2 = 8$, $n = 4$ and $m \in \{2, 3\}$
MRCISD4, MRCISDT4 and FCI4: $c_1 = c_2 = v_2 = 0$, $v_1 = 8$ and $n \in \{2, 3, 4\}$
CCSD12 and CCSDT12: $c_1 = v_1 = v_2 = 0$, $c_2 = 4$ and $n \in \{2, 3\}$
CC(4₂)12: $c_1 = v_1 = 0$, $c_2 = 4$, $v_2 = 8$, $n = 4$ and $m = 2$
CCS8SDT12 and CCSD8SDT12: $c_2 = v_1 = v_2 = 0$, $c_1 = 4$, $a \in \{1, 2\}$ and $n = 3$
MRCISD12: $c_2 = v_2 = 0$, $c_1 = 4$, $v_1 = 8$ and $n = 2$

C. Relativistic commutator-based GAS-CC for excited states

I have implemented the relativistic generalization of the commutator-based algorithm for excited states at the end of my PhD, which was my main objective to defend my thesis. This work is based on former developments realized by Lasse Sørensen as presented in III B. The new code is in a period of testing, debugging, and cleaning. However we have started a new application on KRb diatomic molecule of importance in the ultracold sciences. However, some tests on the carbon atom are available to demonstrate the proper workings of the code, they are presented in this section.

1. Carbon tests

Let us consider the carbon atom with four correlated electrons, the $1s_{1/2}$ Kramers pair remains frozen. The purpose here is to show the spin-orbit splitting of 3P state into three states : 3P_0 , 3P_1 , 3P_2 . We take a small basis-set '21G' [51] and apply different CC models. Let us consider the closed-shell Fermi vacuum $2s_{1/2}^2 2p_{1/2}^2$. Closed-shell Dirac-Hartree-Fock spinors are generated and we construct the various CC wave functions based on these spinors. We then confront this little test with experimental data from the NIST [106]. Of course the low quality of the basis will induce errors of several hundred of cm^{-1} . The results are reported in the following table III.

TABLE III. Excitation energies T in cm^{-1} for the four first excited states 3P_1 , 3P_2 , 1D_2 and 1S_0 (the ground state is 3P_0). Various CC models were used with the Dirac-Coulomb Hamiltonian with closed-shell DCHF spinors. I used an active space of four electrons. The basis sets is a 21G. The cut-off for the virtual spinors is set at 5 a.u. (6 virtual Kramers-pairs). I used C_{2v}^* double point group symmetry for convenience.

	Closed-shell DHF spinors					expt.
	CCSD4	CC(4 ₂)4	CCSDT4	CC(4 ₃)4	FCC4/FCI4	
3P_1	-180	-12	-1029	31	32	16
3P_2	713	144	-946	96	96	43
1D_2	12869	12671	11648	12681	12680	10193
1S_0	24989	20645	23932	-	20585	21648

The following tests in table IV are only different in the number of correlated electrons which is six here, the basis is of a better quality : cc-pV-D ζ and 14 virtual Kramers-pairs are considered.

TABLE IV. Excitation energies T in cm^{-1} for the three first excited states 3P_1 , 3P_2 and 1D_2 (the ground state is 3P_0). Various CC models were used with the Dirac-Coulomb Hamiltonian, an closed-shell Hartree-Fock reference state. I used an active space of six electrons. The basis sets are of cc-pV-D ζ quality. The cut-off for the virtual spinors is set at 7 a.u. (14 virtual Kramers-pairs). I used C_{2v}^* double point group symmetry for convenience.

	Closed-shell DHF spinors								expt.
	CCSD6	CC(4 ₂)6	CC(6 ₂)6	CCSDT6	CC(4 ₃)	CCSDTQ6	CCSDTQP6	FCC6/FCI6	
3P_1	-971	-61	-58	-958	12	14	17	17	16.40
3P_2	2589	170	173	-906	52	49	52	52	43.40
1D_2	14106	11910	11913	10986	11928	11926	11929	11929	10193.63
1S_0	28288	23396	23385	26514	23349	23348	23336	23336	21648.01

The GAS-CC tests presented above in tables III and IV gives a qualitatively correct spectrum for excitation energies for the $1s_{1/2}^2 2s_{1.2}^2 2p_{1/2}^2$ configuration of the Carbon atom. The right spin-orbit splitting of the 3P state is observed close to the FCI limit. It is analog to our study on the Silicon atom analysis to explain the bad first-order SO splittings with truncated wave operators (see IV A). The total CC energies were verified by comparing a FCC4 and a FCI4 calculation from a well tested CI code [107]. (the previous CI-driven algorithm gives the same numbers). The use of open-shell spinors obtained from an average of configuration is also possible but the Fermi vacuum remains closed-shell.

D. Technical aspects - input

In this part, some standard inputs are given to perform Coupled Cluster calculation for excited states with the new commutator-based algorithm with our local development version of the DIRAC package. First the code can be obtain for free on the official DIRAC website. The user have to use git version control to access to our version branch or to clone it directly with the command (you need an access) :

git clone -b arducca_cmacke git@repo.ctcc.no :dirac.git

To install it, refer to

<http://www.diracprogram.org/doc/release-12/installation/installation.html>

for detailed informations.

In the following I will give firstly a spin-orbit-free or Lévy-Leblond input for GAS-LRCC calculation (commutator-based) and secondly a Dirac-Coulomb one.

1. Spin-orbit-free or Lévy-Leblond commutator-based GAS-LRCC

Spin-orbit-free and Lévy-Leblond Hamiltonian are respectively for a scalar-relativistic and a non-relativistic calculation as presented in II A 3. A documentation for input can be found in [94], for basis-set it can be found in **DIRAC** website. The following is an input example for a spin-orbit-free CC(4₂)12 calculation used in IV B.

```

**DIRAC                Main call for Dirac program.
.TITLE                 You can specify a title.
ScH os4in10 CC(42)12
.WAVE FUNCTION         Activation of Wave function module.
.4INDEX                Integral transformation. To disable : NO4INDEX, and load your MDCINT and MRCONNNEE files.
**HAMILTONIAN           $\hat{H}$ 
.SPINFREE              Specify SPINFREE or LEVYLEBLOND for the Hamiltonian.
**WAVE FUNCTION        Specification of the wave function you want to use.
.DHF                   Hartree-Fock activated. Comment # to disable and load your DFCOEF file.
.ARDUCCA               GAS-CC Wave function activated.
*DHFCAI                Specifications for the HF procedure.
.CLOSED SHELL          Number of electron in closed-shell spin-orbitals per symmetry.
18                     Here 18 electrons in the first symmetry.
.OPEN SHELL            Number and type of open-shells.
1                      Number of open shell.
4/20                   4 electrons among 20 spin-orbitals of the first symmetry.
.ERGCNV                DHF convergence threshold.
5.D-11
*ARDUCCA               GAS-CC specifications.
.INIWFC
OSHSCF                OSHSCF if you use open-shell spin-orbitals, DHFSCF if you use closed-shell spin-orbitals.
.NEWCCV                Required to activate commutator-based algorithm.
.CITYPE
GASCI
.MULTIP                Multiplicity  $2S + 1$  of the ground state
1                      Here it is a singlet.
.NACTEL                Number of active electron.
12                     12 correlated electrons.
.GASSHE                Number of GAS and their structure among the various symmetries.
3                      Number of GAS.
    4,1,1,0            GAS I (occupied space) :  $3s\ 3p_z\ 1\sigma\ 2\sigma$  in  $A_1$ ,  $3p_x$  in  $B_1$ ,  $3p_y$  in  $B_2$ , nothing in  $A_2$ 
    3,2,2,1            GAS II (1st virtual space) :  $1\delta_{xx-yy}\ 3\sigma_z\ 4\sigma_z$  in  $A_1$ ,  $1\pi_x\ 2\pi_x$  in  $B_1$ ,  $1\pi_y\ 2\pi_y$  in  $B_2$ ,  $1\delta_{xy}$  in  $A_2$ 
    29,17,17,9         GAS III (2nd virtual space) : virtual orbitals before 9au cutoff
.GASSPC                Min. and max. electronic occupation per GAS. The first block is the Fermi vacuum, the second is the CC operators.
2                      Type 2 for Commutator-based GAS-CC.
12 12                  Number of accumulated electrons in GAS I. (see figure 4)
12 12                  Number of accumulated electrons in GAS II. For the Fermi vacuum Minimum = Maximum, no hole.
12 12                  Number of accumulated electrons in GAS III
    8 12               4 holes in the GAS I  $\Rightarrow$  quadruple excitation toward GAS II.
    10 12              2 holes in the GAS II  $\Rightarrow$  double excitation toward
    12 12              Last virtual GAS always closed.
.SEQUEN
1
CI,5
1
GEN_CC,100,2           Generate CC wave function for the ground state or excited states with 100 iterations, the CC amplitudes CCAMP can be stored.
.SYMMETRY              Symmetry of T operator,  $\hat{T}$  always fully symmetric.
1
.RSCCLR                For restarted excited state calculation only, comment it otherwise.
.CCLR                 Activation of Linear Response CC module for excited states. fort.94 can be stored to restart LRCC.
2,0,0,0               2 roots in symmetry  $A_1$ , none in  $B_1$ ,  $B_2$ ,  $A_2$ .
**MOLTRA              Specification for integral transformation.
.ACTIVE
energy -5.00 9.0 0.0001 Energy threshold for the first occupied orbital, the last virtual orbital,  $\pm 0.0001$  a.u.
*END OF                End of the input

```

2. Relativistic 4-component Dirac-Coulomb commutator-based GAS-LRCC

If one wants to employ the 4-component Dirac-Coulomb Hamiltonian described in II A 2, the following gives an input example for KRb molecule with a CCSD18 model.

```

**DIRAC           Main call for Dirac program.
.TITLE           You can specify a title.
KRb os2in8 CCSD18
.WAVE FUNCTION   Activation of Wave function module.
**HAMILTONIAN     $\hat{H}^{\text{DC}}$  by default.
**WAVE FUNCTION  Specification of the wave function you want to use.
.DHF            Dirac-Hartree-Fock activated. Comment # to disable and load your DFCEOF file.
.KRMCSCF        Activation of Kramers module.
.DHFCAL         Specifications for the DHF procedure.
.CLOSED SHELL   Number of electron in closed-shell Kramers-pairs per symmetry.
54             Here 54 electrons in the first symmetry.
.OPEN SHELL     Number and type of open-shells.
1             Number of open shell.
2/16           2 electrons among 16 Kramers spinors of the first symmetry.
.ERGCNV        DHF convergence threshold.
5.D-11
*KRMCSCF        KR-GAS-CC specifications.
.CI PROGRAM
LUCIAREL
.INACTIVE       Number of inactive Kramers pairs.
14            14 frozen Kramers pairs.
.GASSH         Number of GAS and their structure among the various symmetries.
2            Number of GAS.
9            GAS I (occupied space) :  $3s_{1/2}$   $3p_{1/2}$   $3p_{3/2}^{(2)}$  of K,  $4s_{1/2}$   $4p_{1/2}$   $4p_{3/2}^{(2)}$  of Rb, and  $1\sigma_{1/2}$ 
51           GAS II (virtual space) : virtual Kramers pairs before 4 a.u.
.GASSPC        Min. and max. electronic occupation per GAS. The first block is the Fermi vacuum, the second is the CC operators.
2            Type 2 for Commutator-based GAS-CC.
18 18         Number of accumulated electrons in GAS I. (see figure 4)
18 18         Number of accumulated electrons in GAS II. For the Fermi vacuum Minimum = Maximum, no hole.
16 18         2 holes in the GAS I  $\Rightarrow$  double excitation toward GAS II.
18 18         Virtual space closed.
.SEQUEN
1
CI,1
1
GEN_CC,100,2   Generate CC wave function for the ground state with 100 iterations, the CC amplitudes CCAMP can be stored.
.MK2REF        Number of correlated electrons which define  $\Delta M_K$  manifold, introduced in II B 4.
18            18 correlated electrons.
.SYMMETRY      Symmetry of T operator,  $\hat{T}$  always fully symmetric.
1
.CCEX_E       Activation of Linear Response CC module for excited states. fort.98 and fort.68 can be stored to restart LRCC.
2,0,0,0       2 roots in symmetry the first symmetry (bosonic).
.RSCCLR        Flag for restarted calculation; default : off.
.CCLRIT        Number of CCLR iterations in next line.
5            This also works if .RSCCLR is not used.
*END OF        End of the input

```

Conclusion and prospects

A new implementation of a general excitation rank relativistic Coupled Cluster is presented with which electronically excited states can be calculated at high accuracy using linear response theory. In the first paper [80] or in IV A, it has been demonstrated that the relativistic GAS-CC approach is applicable to atomic and molecular electronically excited states, for which we have chosen showcase systems exhibiting strong effects of both relativistic and electron correlation origin. We regard these findings largely as proof of principle for a new method. We can conclude that within the GAS-CC approach both the multi-reference character and the importance of dynamic electron correlation on relative energies can be addressed efficiently. The former is achieved by adding active-space selected higher excitations to the standard CC expansion. For BiH (and to some degree also SbH) where the ground state is dominated by a single Slater determinant in the relativistic picture the quality of the GAS-CC results surpasses that of a linear wavefunction expansion such as relativistic CI theory, even if the latter is applied as a genuine multi-reference approach. In cases where our chosen Fermi vacuum determinant is no longer the dominant contributor to the electronic ground state (Si atom, AsH, to some degree SbH) we find that higher CC excitations, at least up to full Triples, have to be included for achieving high accuracy. In such cases true Multi-Reference CC (such as Mukherjee’s Mk-CC [90]) where a number of reference determinants is treated on equal footing would seem to be the better choice.

We improve significantly the method compared to the previous CI-Driven algorithm used for the afore-discussed applications. The new algorithm implementation presented in the third chapter III C 2, is now based explicitly on the Baker-Campbell-Hausdorff commutator expansion evaluation via Wick contractions. It has been demonstrated using a spin-free Hamiltonian in the second paper in IV B, that the new commutator-based algorithm for both the CC vector function and the CC Jacobian leads to an efficient computational scaling and allows for CC calculations with many active electrons and using excitation ranks higher than CC Doubles excitations and $Q\zeta$ basis sets. For the chosen molecular showcase system (ScH) we have demonstrated how improvements going beyond MRCISD and Coupled-Pair Functional models can be achieved with our GAS-CC approach. We regard these findings both as proof of principle for our present method and its efficiency as well as the results as accurate predictions for low-lying electronic states of the ScH molecule.

Very recently, we have adapted the afore-mentioned commutator-based algorithm to a relativistic formalism which can thus be used with the four-component Dirac-Coulomb Hamiltonian including spin-orbit coupling. A fundamental problem remains when we employ more than two GAS : this slows down significantly the calculation especially for the relativistic algorithm. Initial applications of this extended method will be presented in a forthcoming publication.

These new developments are very promising and the new relativistic commutator-based CC for excited states code is in a cleaning, debugging, testing period. We have just started a new project on KRb molecule to put to the proof the new implementation. Several improvements will be brought about, such as parallelization using openMP/MPI, optimization of memory handling, and Kramers time reversal symmetry should be implemented for excitation operators to reduce the number of amplitudes. Some co-workers (Sørensen and Olsen) are investigating the intermediates contraction algorithm which have to be improved if one wants to use four or more GAS efficiently (they succeed when I wrote these lines). We plan also to implement linear symmetry to treat a maximum of states with a minimum number of roots and thus to reduce the calculation effort.

We want to use the code for molecules of fundamental interests. We plan to implement a Hamiltonian to evaluate the electron electric dipole moment interaction constant as it was done for KR-MRCI in the reference [108]. The code could also be extended for molecular properties.

Résumé en Français de la thèse

V. RÉSUMÉ EN FRANÇAIS

Cette partie entièrement en Français apporte un résumé complet d'une vingtaine de page au lecteur francophone.

A. Introduction

Les états électroniquement excités de petites molécules contenant des atomes lourds jouent un rôle important dans nombre de domaine de recherche en physique moderne. Les sciences ultra-froides [1] se tournent avec un intérêt grandissant vers les molécules générées expérimentalement dans leur état fondamental (électronique ou rovibrationnel) *via* un état électroniquement excité [2]. Concernant l'étude des étoiles en astrophysique [3], la compréhension des processus de collision dans les atmosphères stellaires [4] implique la connaissance des états moléculaires excités incluant des métaux ou des métaux de transition. À titre d'exemple en physique fondamentale, plusieurs extensions au modèle standard en physique des particules élémentaires supputent l'existence d'un moment dipolaire électrique (EDM) pour les leptons [5]. Des expériences modernes concentrent leurs investigations sur la recherche du moment dipolaire électrique de l'électron dans un état électroniquement excité de molécules diatomiques ou d'ions moléculaires contenant un atome lourd [6]. La détermination précise de la structure électronique des états électroniquement excités de ces molécules est donc d'une importance cruciale dans tous ces domaines de recherche et dans bien d'autre.

À ce jour, il existe un nombre important de théorie pour traiter les états électroniquement excités, avec toujours un compromis entre la précision et l'applicabilité. Pour les calculs à grande échelle tels que les complexes organo-metalliques ou les molécules biologiques, la théorie de la fonctionnelle densité dépendante du temps (TD-DFT) est capable de calculer des énergies d'excitation [7], cependant pour un traitement de haute précision les théories basées sur la fonction d'onde (WFT) sont plus adaptées. Parmi ces théories, on distingue principalement les méthodes d'interaction de configuration (CI), le champs auto-cohérent multi-configurationnel (MCSCF), le "Coupled Cluster" (CC), la théorie des perturbations (PT) [8]. La méthode de structure électronique la plus précise pour calculer les énergies d'états

excités électroniquement d'atomes ou de molécules est à ce jour le "Coupled Cluster". Des progrès récents incluant des développements pour les énergies d'excitation [9] ont été reportés dans ce monographe [10] qui couvre ce champs de recherche très actif sous-jacent de la théorie à N -corps.

Nombre d'implémentations utilisant des opérateurs d'onde tronqués existent, typiquement au rang d'excitation CC double (CCSD) ou parfois Triple et Quadruple (CCSDT et CCSDTQ) pour l'état fondamental. Pour en donner quelques exemples représentatifs : "Fock-Space CC" (FSCC) [11], "Equation-Of-Motion" (EOM) CC [12], "Complete-Active-Space" (CAS) "state-specific" (SS) CC [13], théorie de la réponse linéaire (LR) CC3 [14] ou encore le modèle CC2-R12 [15]. Les approches CC au rang d'excitation général pour le calcul des états excités moléculaires sont moins abondantes. Quelques implémentations de ce type ont été publiées par Kállay *et al.* [16] et Hirata *et al.* [17]. Les méthodes CC possédant la capacité d'inclure itérativement les excitations Triple complètes ou au-delà représentent un intérêt grandissant en physique moléculaire. Par exemple, lorsque les courbes de potentiel complètes pour les molécules diatomiques sont telles qu'elles ne peuvent pas être obtenue avec la méthode CCSD(T) [18]. Une alternative viable est un modèle CC qui permet d'effectuer des excitations de haut rang sélectionnées à travers des espaces actifs, on maintient en même temps un nombre limité d'électrons dans l'espace virtuel externe [19].

Lorsque l'on se tourne vers le traitement des éléments lourds où une généralisation relativiste de ces méthodes est requise, le challenge que constitue l'implémentation de telles méthodologies devient flagrant au regard de leur rareté (voir [8] et ses références). À l'heure actuelle, les seules méthodes CC relativistes pour le traitement des énergies d'excitation sont : le "Intermediate Fock-Space CC" (IH-FSCC) [20, 21] de Visscher, Eliav, *et al.* et pour les méthodes de corrélation au rang d'excitation supérieur [22] de Hirata *et al.* utilisant le formalisme EOM-CC [23, 24]. IH-FSCC est limité car il n'est pas généralement applicable et le traitement des excitations de rang supérieur à Doubles dans l'opérateur d'onde est actuellement impossible. La méthode de Hirata *et al.* est limitée à l'utilisation de pseudo-spineurs de valence à deux composantes basés sur des pseudo-potentiels relativistes (RECP) incluant l'interaction spin-orbite [25]. Une telle approche ne possède pas la rigueur et la flexibilité des méthodes "All-electrons" à quatre composantes utilisant l'approximation

du cœur gelé pour les électrons de cœur des atomes.

Les développements méthodologiques présentés dans cette thèse visent un traitement rigoureux pour le calcul des énergies d'excitation électroniques pour les petites molécules incluant des éléments lourds. C'est un véritable challenge pour la théorie quantique relativiste à N -corps à ce jour [8]. Les développements s'articulent autour d'un traitement rigoureux de la relativité restreinte en utilisant des Hamiltoniens de Dirac à quatre composantes prenant en compte tous les électrons à chaque étape du calcul. Les méthodes développées possèdent des opérateurs d'onde de rang d'excitation général et les fonctions d'ondes sont développées en chaînes d'opérateur création et annihilation en seconde quantification [26–28]. L'utilisation de la théorie de la réponse linéaire combinée aux espaces actifs généralisés (GAS) apporte une grande flexibilité pour le traitement des énergies d'excitation. Des fonctions d'onde élaborées peuvent être paramétrées permettant une approche quasi multi-référence avec seulement un déterminant de référence. Ce type de méthode est appelé "Simple Référence Multi Référence Coupled Cluster" (SR-MRCC) [13, 29]. Ainsi les nombreux problèmes surgissant d'une méthode purement MRCC sont contournés, comme par exemple le problème de redondance qui se manifeste en MRCC par un nombre d'amplitude CC bien supérieur au nombre d'équation d'amplitude. L'implémentation actuelle bénéficie des avantages des formalismes simple-références : un nombre d'équation égal au nombre d'amplitude et la commutation des opérateurs d'excitation. Finalement, des applications à divers systèmes atomiques et diatomiques sont exposées dans les références relatives à ce projet (IV A, IV B et IV C).

B. Théorie relativiste de l'électron

La méthode à N -corps présentée dans cette thèse, le Coupled Cluster, a pour but de décrire l'énergie des états électroniquement excités d'atome ou de molécule. Une description précise de ces états nécessite la prise en compte des effets relativistes. Ces effets sont responsables de la levée de dégénérescence des états atomiques Russell-Saunders ^{2S+1}L dû au couplage spin-orbite, c'est à dire l'émergence de la structure fine d'autant plus importante que les noyaux sont lourds. L'origine des effets relativistes vient principalement du fait que certains électrons proche d'un noyau lourd peuvent atteindre des vitesses proche de la vitesse de la lumière. Ces effets peuvent

être traités de façon additive en utilisant la théorie des perturbations avec l'équation de Schrödinger, cependant la description du couplage entre les effets relativistes et la corrélation électronique manquera. Ce couplage peut représenter plusieurs centaines de cm^{-1} pour les différences d'énergies des états excités de système lourd. La théorie de Dirac de l'électron [30] apporte un cadre théorique parfait alliant le traitement quantique de l'électron au principe de relativité restreinte. Les développements méthodologiques présentés dans cette thèse s'appuient ainsi fortement sur l'équation de Dirac.

1. L'équation de Dirac

L'équation de Dirac peut être représentée sous ces deux principales formes (158)

$$i\hbar \frac{\partial \psi}{\partial t} = \hat{H} \psi = \left(c \hat{\alpha} \cdot \hat{\mathbf{p}} + m_0 c^2 \hat{\beta} \right) \psi \quad \Leftrightarrow \quad \left(i\hbar \hat{\gamma}^\mu \frac{\partial}{\partial x^\mu} - m_0 c \mathbb{1}_4 \right) \psi = 0. \quad (158)$$

La première représentation dite hamiltonienne de façon analogue à l'équation de Schrödinger avec un hamiltonien \hat{H} représenté par des matrices 4×4 . Le vecteur $\hat{\alpha}$ contient trois matrices de spin de dimension 4×4 construites à partir des matrices de Pauli et la matrice $\hat{\beta}$ est une matrice de même dimension imposant la métrique de Minkowski. L'équation de droite (158) est la forme covariante tout à fait équivalente à la forme hamiltonienne où les dimensions d'espace et de temps sont représentées par une quadri-impulsion. Les quatre matrices $\hat{\gamma}$ sont contruites à partir des matrices $\hat{\alpha}$ et $\hat{\beta}$ et l'opérateur covariant est sommé sur la dimension de temps et sur les trois dimensions d'espace. L'équation de Dirac contient par construction le spin de l'électron, on peut en conclure que le spin a une origine relativiste.

2. Les solutions de l'équation de Dirac

L'équation (158) peut être résolue pour l'électron libre et mène à deux paires de solution à quatre composantes

$$\psi_+^{(1)}(\mathbf{X}) = \mathcal{N} \begin{pmatrix} 1 \\ 0 \\ \frac{\hat{p}^3}{\hat{p}^0 + m_0 c} \\ \frac{\hat{p}^1 + i\hat{p}^2}{\hat{p}^0 + m_0 c} \end{pmatrix} e^{-\frac{i}{\hbar} \hat{p}_\mu x^\mu} \quad \text{et} \quad \psi_+^{(2)}(\mathbf{X}) = \mathcal{N} \begin{pmatrix} 0 \\ 1 \\ \frac{\hat{p}^1 - i\hat{p}^2}{\hat{p}^0 + m_0 c} \\ -\frac{\hat{p}^3}{\hat{p}^0 + m_0 c} \end{pmatrix} e^{-\frac{i}{\hbar} \hat{p}_\mu x^\mu} \quad (159)$$

$\psi_+^{(1)}(\mathbf{X})$ et $\psi_+^{(2)}(\mathbf{X})$ sont associées à une énergie positive $E = \sqrt{\hat{\mathbf{p}}^2 c^2 + m_0^2 c^4}$

$$\psi_-^{(1)}(\mathbf{X}) = \mathcal{N} \begin{pmatrix} \frac{\hat{p}^3}{\hat{p}^0 - m_0 c} \\ \frac{\hat{p}^1 + i\hat{p}^2}{\hat{p}^0 - m_0 c} \\ 1 \\ 0 \end{pmatrix} e^{-\frac{i}{\hbar} \hat{p}_\mu x^\mu} \quad \text{et} \quad \psi_-^{(2)}(\mathbf{X}) = \mathcal{N} \begin{pmatrix} \frac{\hat{p}^1 - i\hat{p}^2}{\hat{p}^0 - m_0 c} \\ \frac{-\hat{p}^3}{\hat{p}^0 - m_0 c} \\ 0 \\ 1 \end{pmatrix} e^{-\frac{i}{\hbar} \hat{p}_\mu x^\mu} \quad (160)$$

$\psi_-^{(1)}(\mathbf{X})$ et $\psi_-^{(2)}(\mathbf{X})$ sont associées à une énergie négative $E = -\sqrt{\hat{\mathbf{p}}^2 c^2 + m_0^2 c^4}$

La présence d'énergie négative requiert une interprétation physique. Un modèle initial, illustré à gauche sur le figure 10, considère l'existence d'un continuum d'énergie négative mais entraîne un effondrement de la matière. À titre d'exemple prenons ce modèle appliqué à l'atome d'hydrogène : l'électron 1s va pouvoir émettre un photon pour retomber dans un état de moindre énergie un nombre infini de fois.

Pour régler ce problème Dirac a introduit la théorie des trous [31]. Avec ce modèle, les états d'énergie négative sont occupés par des électrons dit virtuels. Dirac s'intéresse alors à la définition de l'état du vide qu'il définit comme l'absence d'électrons réels (les électrons dans des états d'énergie positive). En l'absence de champs électromagnétique externes, le vide représente le continuum d'énergie négative le plus bas dans lequel tous les états sont occupés d'électrons, on l'appelle l'océan électronique (ou océan de Dirac). La catastrophe radiative est évitée en vertu du principe d'exclusion de Pauli qui s'applique naturellement aux états d'énergie négative. Il convient de souligner que cet océan électronique demeure expérimentalement indétectable tant que rien ne le perturbe.

Toutefois, un électron dans un état d'énergie négative peut absorber un photon, si ce photon possède une énergie $\hbar\omega > 2m_0 c^2$ alors un électron d'énergie négative peut être excité vers un état d'énergie positive. Dans ce cas il s'agit d'un électron réel et d'un trou dans le continuum négatif. Ce trou se comporte comme une particule de charge $+|q_e|$ car il peut être annihilé par un électron de charge $-|q_e|$. Le trou est interprété comme un positron mesuré la première fois par Anderson [32], une des plus grandes prédictions de l'équation de Dirac. Le phénomène de création électron-trou est naturellement identifié à la création de paire électron-positron. Le phénomène inverse, c'est à dire un électron qui comble un trou dans un état d'énergie négative est également possible. Ce dernier est interprété comme l'annihilation d'une paire électron-positron (annihilation matière-antimatière). Sur la droite de la figure 10,

une illustration de la théorie des trous est présentée.

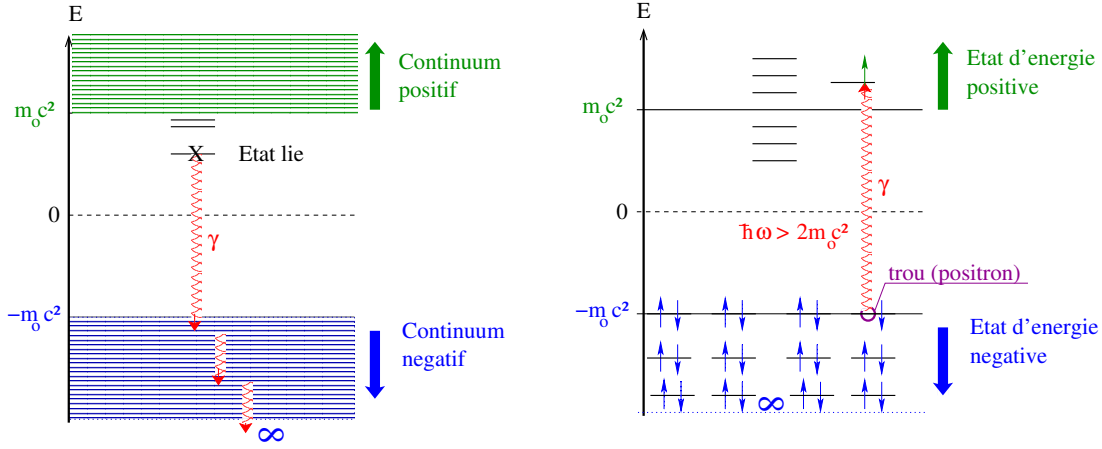


FIGURE 10. Sur la gauche, le continuum d'énergie négative qui entraîne la catastrophe radiative illustrée en rouge. Sur le droite l'océan de Dirac en bleu avec une représentation d'une création d'une paire électron-positron.

Une première approximation de notre approche est de retenir uniquement les solutions d'énergie positive $\psi_+^{(1)}$ et $\psi_+^{(2)}$ (159). Ainsi une partie des corrections radiatives de l'électrodynamique quantique manquera. Cependant, il est montré dans [33] que de telles corrections ajoutées de façon perturbative peut apporter plusieurs centaines de cm^{-1} pour les énergies d'excitation (énergies différentielles) d'atomes ultra-lourds.

3. La séparation spatio-temporelle et le champ électromagnétique externe

L'énergie des états stationnaires est la principale motivation de l'implémentation présentée, il est donc plus aisé de séparer la partie spatiale de la partie temporelle de la fonction d'onde

$$\psi(\mathbf{x}, t) = \psi(\mathbf{x})\phi(t) = \psi(\mathbf{x})e^{-\frac{i}{\hbar}Et}. \quad (161)$$

Cette séparation peut être réalisée à condition de travailler dans un seul référentiel inertiel vu que la transformation de Lorentz couple les composantes spatio-temporelle (\mathbf{x}, t) d'un repère inertiel à un autre. Pour les systèmes atomiques le choix du référentiel se porte sur le noyau au repos et pour les molécules on prendra le référentiel inertiel de Born-Oppenheimer. Ainsi on peut s'intéresser aux états

stationnaires avec une fonction d'onde et un Hamiltonien indépendant du temps

$$\hat{h}^D \psi(\mathbf{x}) = E \psi(\mathbf{x}) \quad \Rightarrow \quad \left(c \hat{\boldsymbol{\alpha}} \cdot \hat{\mathbf{p}} + \hat{\beta} m_0 c^2 \right) \psi(\mathbf{x}) = E \psi(\mathbf{x}) \quad (162)$$

Pour traiter les systèmes atomiques et moléculaires il peut être utile de considérer un champs électromagnétique externe, par exemple pour ajouter un noyau chargé générant un champs électrique. Un champs externe peut être inclu à l'équation de Dirac avec le couplage minimal

$$-i\hbar\partial_\mu \quad \rightarrow \quad -i\hbar\partial_\mu + \frac{e}{c}A_\mu = \begin{pmatrix} \hat{p}^0 + \frac{e}{c}A^0 \\ \hat{\mathbf{p}} - \frac{e}{c}\mathbf{A} \end{pmatrix} \quad \text{avec} \quad \mathcal{A} = \begin{pmatrix} A^0 \\ \mathbf{A} \end{pmatrix} \quad (163)$$

\mathbf{A} étant le potentiel vecteur aux composantes spatiales et A^0 le potentiel électrique scalaire. La première composante du quadri-vecteur (163) correspond à la propagation du champs électrique et les trois autre composantes sont liées à la propagation du champs magnétique toute deux à la vitesse de la lumière c . L'équation de Dirac en champs externe prend alors la forme suivante

$$\left[\hat{\gamma}^\mu \left(-i\hbar\partial_\mu + \frac{e}{c}A_\mu \right) + m_0 c \mathbb{1}_4 \right] \psi(\mathbf{X}) = 0 \quad \Leftrightarrow \quad i\hbar \frac{\partial}{\partial t} \psi(\mathbf{X}) = \left[c \hat{\boldsymbol{\alpha}} \cdot \hat{\mathbf{p}} - e \hat{\boldsymbol{\alpha}} \cdot \mathbf{A} + \hat{\beta} m_0 c^2 + eV \mathbb{1}_4 \right] \psi(\mathbf{X}) \quad (164)$$

Précisons que les équations (164) représentent l'interaction d'un électron avec un champs classique, en électrodynamique quantique un tel champs est quantifié et l'interaction est légèrement modifiée. Il est possible d'ajouter des corrections radiatives de façon perturbative à l'équation de Dirac [33], dans l'implémentation présentée dans ce manuscrit ces corrections ne sont pas ajoutées.

C. La théorie à N-corps relativiste

Le problème à N -corps doit être entendu dans ce contexte comme un système à plusieurs particules en interaction. Ce type de problème est présent à plusieurs niveaux lorsque l'on s'intéresse aux atomes et molécules. Le vide en électrodynamique quantique est un problème à N -corps, nous contournons ce problème avec l'approximation "no-pair" avec la théorie des trous de Dirac. Le problème à N -corps ce manifesterait également pour le noyau mais nous invoquons une approximation le considérant comme une distribution de charge volumique. L'interaction des électrons entre eux est l'objectif de la méthode présentée.

1. L'Hamiltonien multi-électronique de Dirac-Coulomb

$$\hat{H}^{\text{DC}} = \sum_i^N \left[c\hat{\alpha}_i \cdot \hat{\mathbf{p}}_i + (\hat{\beta} - \mathbb{1}_4)m_0c^2 - \sum_I^A \frac{Z_I e^2}{\|\mathbf{r}_i - \mathbf{R}_I\|} \mathbb{1}_4 \right] + \sum_{i < j}^N \frac{e^2}{r_{ij}} \mathbb{1}_4 + \sum_I^A \frac{\mathbf{p}_I^2}{2m_I} \mathbb{1}_4 + \sum_{I < J}^A \frac{Z_I Z_J e^2}{R_{IJ}} \mathbb{1}_4 \quad (165)$$

La physique contenue dans notre approche est bien résumée par l'Hamiltonien de Dirac-Coulomb (165) pour une molécule contenant N électrons et A noyaux. La forme en première quantification permet de distinguer les différentes contributions comme l'énergie cinétique des électrons, le couplage spin-orbite à un électron et l'énergie de masse au repos (cette dernière représente juste un déplacement de l'origine énergétique). Seule l'interaction biélectronique de Coulomb juste après le crochet de droite peut être décomposée en trois parties avec une transformation appropriée

$$\hat{g}^{\text{Coulomb}}(1, 2) = \frac{e^2}{r_{12}} \mathbb{1}_4 \simeq \quad (166)$$

$$\frac{e^2}{r_{12}} \quad (167)$$

$$+ \frac{e^2}{4m_0^2 c^2 r_{12}^3} [\hat{\boldsymbol{\sigma}}_1 \cdot (\mathbf{r}_{12} \times \hat{\mathbf{p}}_1) - \hat{\boldsymbol{\sigma}}_2 \cdot (\mathbf{r}_{12} \times \hat{\mathbf{p}}_2)] \quad (168)$$

$$- \frac{e^2 \pi}{m_0^2 c^2} \delta(\mathbf{r}_{12}). \quad (169)$$

Sous cette forme on distingue respectivement, l'interaction classique et instantanée de Coulomb (166), le couplage d'un électron avec le champs électrique généré par un deuxième électron que l'on nomme le "spin-own-orbit" (168) et enfin, une correction de Darwin au terme de Coulomb de type contact (169).

L'Hamiltonien est implémenté en seconde quantification, un formalisme bien plus adapté pour traiter le problème à N -corps.

$$\begin{aligned} \hat{H}_{el}^{\text{DC}} &= \sum_{pq} h_{pq} \hat{p}^\dagger \hat{q} + \frac{1}{2} \sum_{pqrs} (pq|rs) \hat{p}^\dagger \hat{r}^\dagger \hat{s} \hat{q} \\ &= \sum_{pq} h_{pq} \hat{p}^\dagger \hat{q} + \frac{1}{4} \sum_{pqrs} \langle pq || rs \rangle \hat{p}^\dagger \hat{q}^\dagger \hat{s} \hat{r} \end{aligned} \quad (170)$$

On peut également utiliser des approximations à l'Hamiltonien de Dirac-Coulomb pour désactiver l'interaction spin-orbite, c'est l'Hamiltonien Spin-Free qui ne contient que les contributions relativistes scalaires ; ou encore un analogue non relativiste, l'Hamiltonien de Lévy-Leblond.

2. Outils méthodologiques

Outre la seconde quantification pour modéliser les opérateurs et les intégrales, les fonctions d'ondes sont développées comme une combinaison linéaire d'orbitales atomiques (LCAO) représentées par des combinaisons linéaires de fonctions gaussiennes. Pour limiter le nombre d'intégrale à évaluer on emploie les groupes ponctuels doubles de symétrie permettant d'exploiter la symétrie du système. La symétrie de renversement du temps de Kramers, typique au traitement relativiste, est également utilisée pour réduire le nombre d'intégrale. Les spineurs de Kramers (et donc les déterminants) sont développés en chaîne d'opérateur création et annihilation. Ils sont déterminés *via* la théorie Dirac-Hartree-Fock, une méthode basée sur un traitement de champs moyen où le potentiel de fluctuation est négligé. La corrélation électronique est par définition, l'énergie manquante au traitement Dirac-Hartree-Fock, son évaluation est le principal objectif de la méthode "Coupled Cluster" présentée dans ce manuscrit.

D. Le modèle "Coupled Cluster"

Les développements méthodologiques réalisés pendant mes quatre années de thèse sont résumés dans cette section, ils s'articulent autour de la méthode "Coupled Cluster" pour les états électroniquement excités.

Les états électroniquement excités de petites molécules jouent un rôle très important dans plusieurs secteurs de recherche moderne. À titre d'exemple, l'étude de la formation moléculaire dans le contexte astrophysique requiert la connaissance des états moléculaires excités [3, 4, 85]. Un autre exemple serait la physique ultra-froide où la photo-association de molécules diatomiques nécessite des courbes de potentiels pour divers états excités calculées *ab initio* [86]. La précision des états excités calculés est de rigueur lorsqu'il s'agit de physique fondamentale, pour citer quelques exemples : la recherche du moment dipolaire électrique de l'électron est réalisée expérimentalement impliquant en particulier des molécules diatomiques avec un état excité bien spécifique [6, 88, 108] ; également la recherche sur les variations de constante fondamentale demande une évaluation précise de certains états excités [87]. Une méthode capable de calculer des énergies d'excitation avec précision incluant des effets relati-

vistes important comme le couplage spin-orbite pour des système à N -corps comme les molécules diatomiques est requise.

En outre des effets relativistes, l'énergie de corrélation est d'une importance cruciale pour l'étude de systèmes à N -électrons. La meilleur façon de prendre en compte la corrélation électronique est l'inclusion de déterminants excités dans la fonction d'onde, ces méthodes font partie des théories basées sur la fonction d'onde (WFT). Lorsque tous les déterminants possibles sont présent, on réalise une interaction de configuration complète (FCI). En considérant les limitations computationnelles actuelles, la prise en compte complète de tous les déterminants excités est souvent chose impossible, on emploie alors des méthodes dites tronquées, comme la configuration d'interaction tronquée (CISD, CISDT,...) ou le "coupled cluster" (CC). L'inconvénient du CI tronqué est principalement sa lente convergence par rapport au rang d'excitation (D,T ...) pour atteindre la précision FCI. De plus, un traitement précis de la corrélation dynamique de l'état fondamental et des états excités est requis pour le calcul des constantes spectroscopiques, des déterminants excités de haut rang sont parfois nécessaires (CISDTQ ou plus) menant à une limite computationnelle pour le CI. Le "Coupled Cluster" couple les opérateurs d'excitation par définition, il peut ainsi générer des déterminants de rang plus élevés que son rang d'excitation, par exemple un CCSD (simple et double excitation) va créer des déterminants simplement, doublement, triplement et quadruplement excités.

D'autre type de corrélation peuvent devenir problématique : la corrélation statique et la corrélation de Fermi. Ces effets sont très prononcés pour les systèmes multi-références (MR), c'est à dire dont la fonction d'onde de l'état fondamental doit être représentée par plusieurs déterminants de poids proches. On distingue alors deux types d'approche, les méthodes MR *a priori* qui s'appuient sur plusieurs déterminants de référence (MRCI, MRCC) et les méthodes MR *a posteriori* qui s'appuient sur un seul déterminant Hartree-Fock de référence (SR-MRCC). La méthode CC présentée dans cette thèse appartient à la deuxième catégorie, elle est implémentée dans un environnement d'espaces actifs généralisés (GAS) qui permet de paramétrer des fonctions d'ondes subtiles avec un traitement particulier des déterminants de grande importance.

1. L'opérateur CC - Hiérarchie d'excitation

L'opérateur d'onde "Coupled Cluster" couple les opérateurs d'excitation (clusters) $\hat{\tau}_\mu$ à travers un produit qui peut également être représenté par la fonction exponentielle

$$\prod_{\mu}^{N_c} (1 + t_\mu \hat{\tau}_\mu) = \prod_{\mu}^{N_c} (1 + \hat{T}_\mu) = \prod_{\mu}^{N_c} e^{\hat{T}_\mu} = e^{\sum_{\mu}^{N_c} \hat{T}_\mu} = e^{\hat{T}} \quad (171)$$

avec \hat{T}_μ l'opérateur d'excitation général et N_c est le nombre de déterminant possible, les t_μ sont les amplitudes CC. Les termes non linéaire du développement de Taylor de l'exponentielle sont nuls car un opérateur spécifique \hat{T}_μ ne peut être appliqué qu'une fois sur un déterminant de référence. Le produit d'exponentielles peut s'écrire comme l'exponentielle de la somme des opérateurs d'excitation à condition que qu'ils commutent.

$$[\hat{T}_\mu, \hat{T}_\nu] = 0, \quad (172)$$

c'est le cas dans notre implémentation vu que nous utilisons un seul espace occupé et un seul espace virtuel (ils peuvent être subdivisés en sous-espaces). L'implémentation présentée dans cette thèse est formellement extensive et cohérente en taille.

Ce qui suit démontre comment sont associés les différents rangs d'excitation.

$$\hat{T} = \sum_{\mu}^{N_c} \hat{T}_\mu = \sum_n^N \sum_i^{I(n)} \hat{T}_{n,i} \quad (173)$$

où n est le rang d'excitation (simple, double, triple,..., N) et i dénote les différents types d'excitation parmi les $I(n)$ possibilités pour un rang donné n . Regardons à présent les différentes contributions à chaque rang d'excitation pour les opérateurs Simple et Double $e^{\hat{T}_1}$ ($n = 1$) et $e^{\hat{T}_2}$ ($n = 2$)

$$e^{\hat{T}_1} = (1 + \hat{T}_{1,1}) (1 + \hat{T}_{1,2}) (1 + \hat{T}_{1,3}) \dots \quad (174)$$

$$e^{\hat{T}_2} = (1 + \hat{T}_{2,1}) (1 + \hat{T}_{2,2}) (1 + \hat{T}_{2,3}) \dots \quad (175)$$

L'opérateur CC peut se développer ainsi

$$e^{\hat{T}} = \prod_i^{I(1)} (1 + \hat{T}_{1,i}) \prod_i^{I(2)} (1 + \hat{T}_{2,i}) \prod_i^{I(3)} (1 + \hat{T}_{3,i}) \dots \quad (176)$$

De (176) on peut extraire les contributions des différents rangs d'excitation et comparer avec le développement linéaire de la méthode CI

$$e^{\hat{T}} = \sum_n \hat{C}_n \quad (177)$$

$$\hat{C}_0 = 1 \quad (178)$$

$$\hat{C}_1 = \hat{T}_1 \quad (179)$$

$$\hat{C}_2 = \hat{T}_2 + \frac{1}{2!} \hat{T}_1^2 \quad (180)$$

$$\hat{C}_3 = \hat{T}_3 + \hat{T}_1 \hat{T}_2 + \frac{1}{3!} \hat{T}_1^3 \quad (181)$$

$$\hat{C}_4 = \hat{T}_4 + \hat{T}_1 \hat{T}_3 + \frac{1}{2!} \hat{T}_2^2 + \frac{1}{2!} \hat{T}_1^2 \hat{T}_2 + \frac{1}{4!} \hat{T}_1^4 \quad (182)$$

Les opérateurs \hat{C}_n démontrent quels types de processus d'excitation contribuent à chaque rang d'excitation n . Les opérateurs CI sont les \hat{T}_n , ils sont aussi des opérateurs CC appelés opérateurs connectés. Le CC apporte en plus des opérateurs déconnectés qui sont des couplages entre les connectés et donnent des contributions de rang supérieur. Par exemple avec le modèle CC il y a cinq mécanismes distincts pour générer des quadruples excitations (182) où, \hat{T}_2^2 représente l'interaction indépendante entre deux paires d'électron, \hat{T}_4 décrit l'interaction simultanée de quatre électrons.

Le rang d'excitation maximal N introduit en (173) est déterminé par le nombre d'électron corrélé dans les espaces actifs généralisés. Le nombre maximal de type d'excitation par rang $n : I(n)$, est déduit du nombre de spineur dans les espaces actifs et virtuels.

2. La fonction d'onde CC - Le vide de Fermi

La méthode CC présentée dans ce manuscrit est basée sur des espaces actifs généralisés [91]. Le lecteur pourra trouver d'autre travaux basés sur le même *ansatz* [18, 72, 77, 92] et d'autre approches CC dans ce livre [76]. Les opérateurs d'excitation $\hat{\tau}_n^{\text{GAS}}$ de rang général n appelés "cluster", sont construits à partir de ces espaces. On obtient alors la fonction d'onde CC en faisant agir la paramétrisation exponentielle (171) sur un vide de référence choisi au préalable $|\Phi\rangle$. L'implémentation actuelle est liée au choix d'un vide simple-référence, un simple déterminant appelé le vide de

Fermi. On distingue d'autre type d'approche dites purement multi-référence comme le MRCC qui est lié à un vide constitué d'une combinaison linéaire de plusieurs déterminants *a priori* [90]. Dans notre cas, pour le CC simple-référence, les configurations électroniques autre que le vide de Fermi sont ajoutées *via* les espaces actifs généralisés avec des opérateurs de haut rang d'excitation. La fonction d'onde CC que nous utilisons suit ce type d'*ansatz*

$$|\psi^{\text{GAS-CC}}\rangle = e^{\sum_i^n \hat{T}_i^{\text{GAS}}} |\Phi\rangle \quad (183)$$

où l'opérateur de rang d'excitation général n est construit à partir des opérateurs de Kramers barrés et non-barrés de création et d'annihilation.

$$\hat{T}_n^{\text{GAS}} = \sum_{\substack{\mathbb{P}, \bar{\mathbb{P}}, \mathbb{H}, \bar{\mathbb{H}} \\ a < b < \dots, \bar{a} < \bar{b} < \dots \\ i < j < \dots, \bar{i} < \bar{j} < \dots}} t_{ij \dots \bar{i} \bar{j} \dots}^{ab \dots \bar{a} \bar{b} \dots} \left\{ \hat{a}^\dagger \hat{b}^\dagger \dots \hat{\bar{a}}^\dagger \hat{\bar{b}}^\dagger \dots \hat{j} \hat{i} \dots \hat{\bar{j}} \hat{\bar{i}} \dots \right\} \quad (184)$$

Les accolades dénote que les opérateurs de seconde quantification sont ordonnés. Les indices des spineurs $\{a, b, \dots\} \in \mathbb{P}$, $\{\bar{a}, \bar{b}, \dots\} \in \bar{\mathbb{P}}$ sont associés aux quasi-opérateurs de Kramers de type particule et les indices de spineurs $\{i, j, \dots\} \in \mathbb{H}$, $\{\bar{i}, \bar{j}, \dots\} \in \bar{\mathbb{H}}$ sont associés aux quasi-opérateurs de Kramers de type trou. Les $t_{ij \dots \bar{i} \bar{j} \dots}^{ab \dots \bar{a} \bar{b} \dots}$ sont les amplitudes CC associées au cluster d'excitation à leur droite.

Le vide de Fermi est défini de la sorte

$$|\Phi\rangle = \left(\prod_i^{\mathbb{H}} \hat{i}^\dagger \right) |0\rangle \quad (185)$$

Avec $|0\rangle$ l'état de vide électronique, considéré dans cette approche comme un état sans aucun électron. Une illustration de paramétrisation de vide de Fermi à l'aide des espaces actifs généralisés est donné en figure 11.

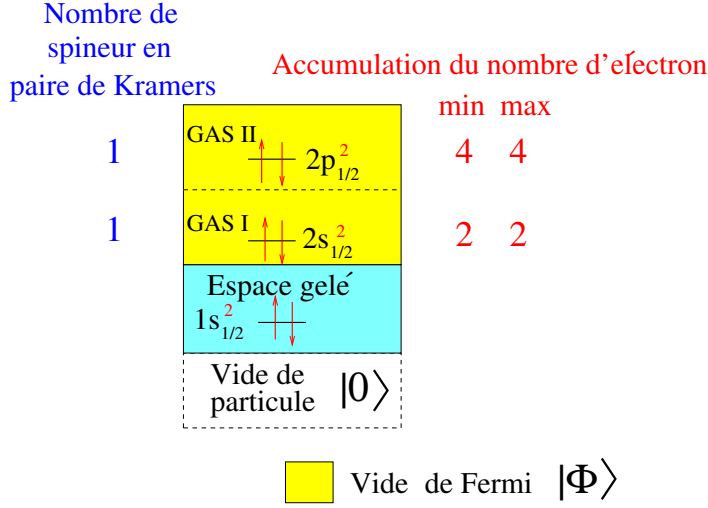


FIGURE 11. Un exemple de vide de Fermi $|\Phi\rangle$ pour l'atome de carbone, ici le vide de Fermi est représenté par les spineurs $2s_{1/2}$ et $2p_{1/2}$ doublement occupés dans des GAS différents (le vide de Fermi peut également être défini dans un seul GAS).

L'utilisation d'un seul déterminant pour représenter le vide de Fermi impose cependant quelques restrictions. Certains systèmes possédant de nombreuses couches ouvertes peuvent être très difficiles à traiter (par exemple le fer avec $3d^6$), si le vide de Fermi est représenté par un seul déterminant, d'autres déterminants de la même configuration vont manquer et ils auraient certainement un poids comparable pour l'état quantique du fondamental.

3. La paramétrisation des espaces actifs généralisés (GAS)

Dans le but de générer plus de déterminants et donc pour modéliser davantage de configurations électroniques, on peut diminuer la valeur du nombre minimal d'électrons accumulés dans un espace. Cela revient à faire un trou dans un espace, les opérateurs d'excitation \hat{T}_n^{GAS} sont alors générés en accord avec la paramétrisation.

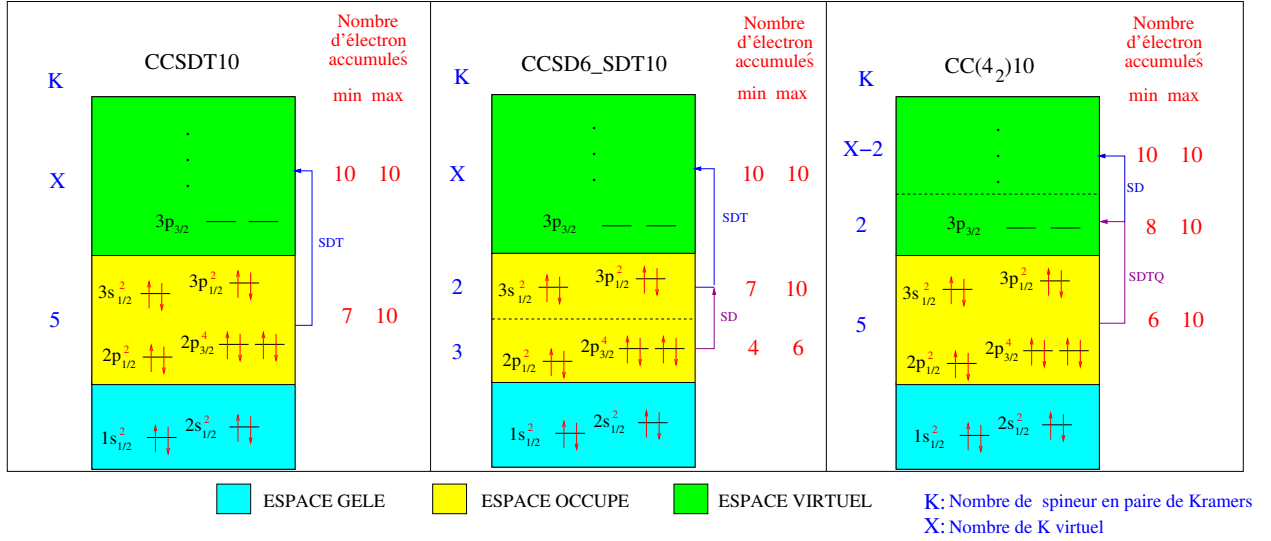


FIGURE 12. Exemple de trois possibles paramétrisations de GAS pour l'atome de Silicium. À gauche un CCSDT standard, au milieu un modèle de corrélation de cœur et à droite un modèle $CC(n_m)$.

La figure 12 ci-dessus illustre trois types de paramétrisation. Sur la gauche, une approche standard où les quatre premiers électrons ne sont pas corrélés. Dans le GAS I constitué de dix électrons dans cinq paires de Kramers, le nombre minimal d'électron accumulé est réduit de trois, en d'autre termes, nous faisons trois trous dans le GAS I qui correspondent à trois électrons excités dans l'espace virtuel GAS II. On génère en conséquence de nouvelles configurations électroniques provenant des triples excitations à partir d'un ensemble de spineur contenant dix électrons vers les spineurs virtuels ; c'est le modèle CCSDT10. La fonction d'onde sera une combinaison linéaire de tous ces déterminants et se rapprochera de la fonction d'onde FCI comparée à celle s'appuyant sur un seul déterminant. La paramétrisation du milieu en figure 12 représente un moyen de réduire le coût computationnel en limitant les excitations du cœur. On sépare l'espace occupé en deux GAS et on réduit ainsi le rang d'excitation pour les six premiers électrons. Le GAS I contient alors six électrons occupant trois paire de Kramers qui seront seulement doublement excités vers les GAS II et III. Cependant les électrons occupant le GAS II peuvent être triplement excités du GAS II vers le GAS III. Ainsi le GAS III contiendra soit trois électrons provenant du GAS II, soit deux provenant du GAS II et un provenant du GAS I ou bien un seul du GAS II et deux provenant du GAS I. Ce second modèle

(CCSD6_SDT10) permet d'inclure des paires de Kramers de cœur avec des excitations de rang faible (typiquement double), il s'avère très utile pour corrélérer un cœur sans exciter tous ses électrons (par exemple d^{10} ou f^{14}). Le troisième modèle à droite sur la figure 12 est la paramétrisation la plus prometteuse. On considère un premier GAS contenant dix électrons dans cinq paire de Kramers quadruplement excités vers un espace virtuel restreint (GAS II) qui est composé de quatre paires de Kramers virtuelles jugées importantes. Nous autorisons quatre trous dans le GAS I mais seulement deux dans le GAS II, c'est à dire uniquement des doubles excitations vers l'espace virtuel le plus étendu (GAS III). Un poids important est associé en conséquence pour les déterminants survenant du GAS II. L'avantage de cette procédure réside dans le choix des états excités à décrire, si on veut modéliser des états excités survenant d'une configuration électronique bien précise, on peut paramétrer le CC(n_m) en accord avec leur structure. Ainsi on peut prendre en compte tous les déterminants importants en évitant les haute excitation (quadruple ou plus) vers l'espace virtuel étendu. Le second et le troisième modèle peuvent être combiné, les espaces actifs généralisés offrent une très grande flexibilité.

4. Les équations CC de l'état fondamental

Pour déterminer l'énergie CC de l'état fondamental, on applique un Hamiltonien de Dirac (ou de Schrödinger) avec une fonction d'onde CC

$$\hat{H} |\psi^{\text{GAS-CC}}\rangle = E^{\text{CC}} |\psi^{\text{GAS-CC}}\rangle \quad \Rightarrow \quad \hat{H} e^{\hat{T}} |\Phi\rangle = E^{\text{CC}} e^{\hat{T}} |\Phi\rangle \quad (186)$$

On projette ensuite cette équation sur les $\mu + 1$ états possibles et on obtient les équations de l'énergie CC et les équations d'amplitude CC

$$\langle \Phi | e^{-\hat{T}} \hat{H} e^{\hat{T}} | \Phi \rangle = E^{\text{CC}} \quad (187)$$

$$\langle \Phi | \hat{\tau}_\mu^\dagger e^{-\hat{T}} \hat{H} e^{\hat{T}} | \Phi \rangle = 0 \quad (188)$$

avec $\langle \psi_\mu | = \langle \Phi | \hat{\tau}_\mu^\dagger$. Les résoudre revient à déterminer itérativement les amplitudes CC t_μ et ainsi l'énergie E^{CC} .

5. Les équations CC pour les états excités

Après cette première étape présentée précédemment, les énergies d'excitation peuvent être déterminées en utilisant la théorie de la réponse linéaire [96–99]. Dans cette théorie les énergies d'excitation sont les pôles de la fonction de réponse : la dérivé de l'équation d'amplitude CC par rapport aux amplitudes

$$A_{\mu\nu} = \frac{\partial}{\partial t_\nu} \langle \Phi | \hat{\tau}_\mu^\dagger e^{-\hat{T}} \hat{H} e^{\hat{T}} | \Phi \rangle = \langle \Phi | \hat{\tau}_\mu^\dagger e^{-\hat{T}} [\hat{H}, \hat{\tau}_\nu] e^{\hat{T}} | \Phi \rangle. \quad (189)$$

Ce qui en résulte est une matrice Jacobienne possédant cette structure

$$A_{\mu\nu} = \begin{pmatrix} \langle \psi_{\mu_1} | e^{-\hat{T}} [\hat{H}, \hat{\tau}_{\nu_1}] e^{\hat{T}} | \Phi \rangle & \langle \psi_{\mu_1} | e^{-\hat{T}} [\hat{H}, \hat{\tau}_{\nu_2}] e^{\hat{T}} | \Phi \rangle & \cdots & \langle \psi_{\mu_1} | e^{-\hat{T}} [\hat{H}, \hat{\tau}_{\nu_N}] e^{\hat{T}} | \Phi \rangle \\ \langle \psi_{\mu_2} | e^{-\hat{T}} [\hat{H}, \hat{\tau}_{\nu_1}] e^{\hat{T}} | \Phi \rangle & \langle \psi_{\mu_2} | e^{-\hat{T}} [\hat{H}, \hat{\tau}_{\nu_2}] e^{\hat{T}} | \Phi \rangle & \cdots & \langle \psi_{\mu_2} | e^{-\hat{T}} [\hat{H}, \hat{\tau}_{\nu_N}] e^{\hat{T}} | \Phi \rangle \\ \vdots & \vdots & \ddots & \vdots \\ \langle \psi_{\mu_N} | e^{-\hat{T}} [\hat{H}, \hat{\tau}_{\nu_1}] e^{\hat{T}} | \Phi \rangle & \langle \psi_{\mu_N} | e^{-\hat{T}} [\hat{H}, \hat{\tau}_{\nu_2}] e^{\hat{T}} | \Phi \rangle & \cdots & \langle \psi_{\mu_N} | e^{-\hat{T}} [\hat{H}, \hat{\tau}_{\nu_N}] e^{\hat{T}} | \Phi \rangle \end{pmatrix} \quad (190)$$

La diagonalisation de cette matrice permet d'obtenir les valeurs propres correspondantes aux énergies d'excitation souhaitées

$$\mathbf{A}^{\text{CC}} |\psi_f\rangle = \text{diag}(\omega_f) |\psi_f\rangle \quad (191)$$

Le challenge ici n'est pas l'implémentation de l'algorithme de diagonalisation mais le traitement des éléments de matrice développés avec la formule de Baker-Campbell-Hausdorff

$$A_{\mu\nu} = \left\langle \Phi \left| \hat{\tau}_\mu^\dagger \left([\hat{H}, \hat{\tau}_\nu] + [[\hat{H}, \hat{\tau}_\nu], \hat{T}] + \frac{1}{2} [[[\hat{H}, \hat{\tau}_\nu], \hat{T}], \hat{T}] + \frac{1}{6} [[[[\hat{H}, \hat{\tau}_\nu], \hat{T}], \hat{T}], \hat{T}] \right) \right| \Phi \right\rangle \quad (192)$$

Le cœur du problème se situe dans l'implémentation de (192). L'équation aux valeurs propres est ensuite résolue itérativement où à chaque itération, une transformation linéaire est réalisée, on évalue la transformation linéaire d'un vecteur d'essai \mathbf{x} avec la matrice Jacobienne CC

$$\begin{aligned} J_\mu &= \sum_\nu A_{\mu\nu} x_\nu \\ &= \sum_\nu \left\langle \Phi \left| \hat{\tau}_\mu^\dagger \left([\hat{H}, \hat{\tau}_\nu] + [[\hat{H}, \hat{\tau}_\nu], \hat{T}] + \frac{1}{2} [[[\hat{H}, \hat{\tau}_\nu], \hat{T}], \hat{T}] + \frac{1}{6} [[[[\hat{H}, \hat{\tau}_\nu], \hat{T}], \hat{T}], \hat{T}] \right) \right| \Phi \right\rangle x_\nu \end{aligned} \quad (193)$$

La clé de la réussite pour accomplir ce processus réside dans la modification des routines pour traiter l'état fondamental. J'ai donc modifié les routines qui gèrent le

traitement des commutateurs pour les équations d'amplitude (188) sous forme BCH

$$\begin{array}{ccccccccccc}
e^{-\hat{T}} \underbrace{\hat{H}} e^{\hat{T}} & = & \hat{H} & + & [\hat{H}, \hat{T}] & + & \frac{1}{2} [[\hat{H}, \hat{T}], \hat{T}] & + & \frac{1}{6} [[[\hat{H}, \hat{T}], \hat{T}], \hat{T}] & + & \frac{1}{24} [[[[\hat{H}, \hat{T}], \hat{T}], \hat{T}], \hat{T}] \\
\downarrow & & \downarrow & & \downarrow & & \downarrow & & \downarrow & & \downarrow \\
[\hat{H}, \hat{\tau}_\nu] & & 0 & & \hat{\tau}_\nu & & 1 & & \hat{\tau}_\nu & & \frac{1}{2} & & \hat{\tau}_\nu & & \frac{1}{6} & & \hat{\tau}_\nu.
\end{array} \tag{194}$$

Ci-dessus(194) une représentation schématique de ce qui a due être modifié pour traiter les éléments de la matrice Jacobienne. Les différents ordres d'imbrication de commutateur sont dans différentes boucles et ont été modifiés. L'ordre zero, c'est à dire l'Hamiltonien seul à été supprimé et les coefficients BCH ont été associés avec un rang de décalage. Un des termes d'excitation général $\hat{T} = \sum_{\nu} t_{\nu} \hat{\tau}_{\nu}$ a due être remplacé par un cluster spécifique $\hat{\tau}_{\nu}$ associé à la composante x_{μ} du vecteur d'essai \mathbf{x} à droite plutôt qu'à une amplitude. Ainsi le vecteur d'essai est optimisé itérativement en même temps que la transformation linéaire.

E. Conclusion

Une nouvelle implémentation de méthode "Coupled Cluster" au rang d'excitation général est présentée, elle permet en particulier le calcul des énergies d'excitation avec une grande précision en utilisant la théorie de la réponse linéaire. Dans la première référence IV A il a été démontré que l'approche GAS-CC relativiste est applicable aux énergies des états électroniquement excités pour des atomes et des molécules. Nous avons choisi des systèmes présentant à la fois des effets relativistes intenses et de fort effets de corrélation dynamique et statique (et de Fermi). Les résultats exposés fournissent une preuve de principe quant à notre nouvelle méthode. On peut conclure qu'avec l'approche GAS-CC, le caractère multi-référence ainsi qu'une corrélation dynamique importante pour les énergies relatives peuvent être traités efficacement. Le premier effet est traité en ajoutant des excitations de haut rang sélectionnées au développement CC standard (CC(n_m)). Pour BiH (et à certain degré pour SbH) où pour le traitement relativiste, l'état fondamental est principalement représenté par un simple déterminant de Slater, la qualité des résultats GAS-CC surpasse ceux de la méthode MRCI malgré son approche purement multi-référence. Dans les cas où le vide de Fermi choisi n'est plus le déterminant dominant pour

l'état fondamental (l'atome de Silicium, AsH et à certain degré SbH) nous trouvons que de hautes excitations sont requises (au moins Triples) pour atteindre une haute précision. Dans de tels cas, un vrai MRCC (comme celui de Mukherjee [90]) où un certain nombre de déterminant de référence est traité sur le même plan semble être le meilleur choix.

Nous avons également amélioré considérablement la méthode, initialement basée sur l'algorithme "CI-driven" utilisé pour les applications citées précédemment. Le nouvel algorithme présenté en V D est à présent basé explicitement sur le développement de Baker-Campbell-Hausdorff des commutateurs évalués *via* des contractions de Wick. Il a été démontré en utilisant un Hamiltonien "spin-orbit-free" en IV B que le nouvel algorithme pour la fonction vecteur CC et pour la matrice jacobienne CC entraîne un gain d'efficacité important, notamment lorsqu'on augmente le nombre d'électron actifs et en utilisant des rangs d'excitation supérieurs à Double avec une grande base de type Q ζ . Le système moléculaire choisi (Sch) nous a permis de démontrer une amélioration systématique au delà des méthodes MRCISD et "Coupled-Pair Functional" avec notre approche GAS-CC. Nous considérons ces résultats comme une preuve de principe quant à l'efficacité du nouveau code, ce sont également de précises prédictions pour les premières énergies d'excitation de la molécule Sch.

Très récemment, nous avons généralisé le nouvel algorithme discuté précédemment au formalisme relativiste qui peut maintenant être utilisé avec l'Hamiltonien à quatre composantes Dirac-Coulomb incluant le couplage spin-orbite. Il demeure cependant un problème lorsque l'on emploie plus de deux GAS, les calculs ralentissent considérablement, en particulier pour les calculs relativistes. De premières applications de ce nouvel algorithme relativiste seront publiées prochainement.

Ces nouveaux développements méthodologiques sont très prometteurs, le nouvel algorithme relativiste basé sur les commutateurs est en période de test, nettoyage, débogage. Nous avons commencé un nouveau projet sur la molécule KRb pour assurer son applicabilité. De nombreuses améliorations sont prévues comme la parallélisation du code en utilisant openMP/MPI, l'optimisation de la gestion de la mémoire, la symétrie de renversement du temps de Kramers doit être implémentée pour les opérateurs d'excitation pour réduire le nombre d'amplitude. Des collaborateurs travaillent actuellement sur l'algorithme de contraction intermédiaire responsable des ralentissements avec l'augmentation du nombre de GAS. Nous projetons également

d'implémenter la symétrie linéaire pour traiter un maximum d'état avec un minimum de racine et réduisant ainsi le coût computationnel.

Nous voulons principalement utiliser ce code pour traiter les molécules d'intérêt fondamental. Nous envisageons également d'implémenter un Hamiltonien pour évaluer les constantes d'interaction pour le moment dipolaire électrique de l'électron de façon similaire au KR-MRCI de la référence [108]. Le code peut également être étendu au calcul des propriétés moléculaires.

Appendix I

VI. APPENDIX FOR RELATIVISTIC QUANTUM THEORY OF THE ELECTRON

In this first appendix, the reader can find key steps to construct the Dirac equation and its solution from physical principles and mathematical tools.

A. The Dirac equation construction

The appendix gives some details about the construction of the Dirac equation introduced in the section I

P.A.M. Dirac in 1928 [30] attempts to find a covariant form of the free particle Schrödinger equation

$$i\hbar\frac{\partial\psi}{\partial t} = \hat{H}\psi \quad (195)$$

with positive and well defined probability density.

The equation (195) is linear with respect to the partial time derivative. It is therefore more natural to build a Hamiltonian which is also linear with respect to spacial derivatives to treat temporal and spacial coordinates on the same footing, as desired in special relativity. (195) becomes

$$i\hbar\frac{\partial\psi}{\partial t} = \left[\frac{\hbar c}{i} \left(\hat{\alpha}_1 \frac{\partial}{\partial x^1} + \hat{\alpha}_2 \frac{\partial}{\partial x^2} + \hat{\alpha}_3 \frac{\partial}{\partial x^3} + \hat{\beta} m_0 c^2 \right) \right] \psi \equiv \hat{H}\psi \quad (196)$$

The $\hat{\alpha}_i$ cannot be scalar to ensure the spacial rotation invariance of (196). As often in quantum mechanics we will see the $\hat{\alpha}_i$ are matrix operators, the $\hat{}$ on top will denote this fact. Consequently the wave function ψ cannot be either scalar and must be represented by a column vector

$$\psi = \begin{pmatrix} \psi_1(\mathbf{x}, t) \\ \psi_2(\mathbf{x}, t) \\ \vdots \\ \psi_N(\mathbf{x}, t) \end{pmatrix} \quad (197)$$

which exhibits a density probability

$$\rho(\mathbf{x}) = \boldsymbol{\psi}^\dagger \boldsymbol{\psi}(\mathbf{x}) = (\psi_1^*, \psi_2^*, \dots, \psi_N^*) \cdot \begin{pmatrix} \psi_1 \\ \psi_2 \\ \vdots \\ \psi_N \end{pmatrix} = \sum_{i=1}^N \psi_i^* \psi_i(\mathbf{x}) \quad (198)$$

directly built. $\rho(\mathbf{x})$ is density probability to find an electron in \mathbf{x} .

The wave function $\boldsymbol{\psi}$ (197) is a column vector analogous to Pauli spin wave function also called the Pauli spinors. Let's focus on the N dimensions of the spinors, *i.e.* on the equation (196) for N dimension spinors and thus squared matrices $\hat{\alpha}_i$ and $\hat{\beta}$ with $N \times N$ dimension. (196) is then a first order of N coupled differential equations for the spinor components ψ_i , $i = 1, 2, \dots, N$:

$$i\hbar \begin{pmatrix} \frac{\partial \psi_1(\mathbf{x},t)}{\partial t} \\ \frac{\partial \psi_2(\mathbf{x},t)}{\partial t} \\ \vdots \\ \frac{\partial \psi_N(\mathbf{x},t)}{\partial t} \end{pmatrix}_N = \frac{\hbar c}{i} \left[\sum_{i=1}^3 \begin{pmatrix} & & & \\ & \hat{\alpha}_i & & \\ & & & \\ & & & \end{pmatrix}_{N \times N} \cdot \begin{pmatrix} \frac{\partial \psi_1(\mathbf{x},t)}{\partial x^i} \\ \frac{\partial \psi_2(\mathbf{x},t)}{\partial x^i} \\ \vdots \\ \frac{\partial \psi_N(\mathbf{x},t)}{\partial x^i} \end{pmatrix}_N + m_0 c^2 \begin{pmatrix} & & & \\ & \hat{\beta} & & \\ & & & \\ & & & \end{pmatrix}_{N \times N} \cdot \begin{pmatrix} \frac{\partial \psi_1(\mathbf{x},t)}{\partial x^i} \\ \frac{\partial \psi_2(\mathbf{x},t)}{\partial x^i} \\ \vdots \\ \frac{\partial \psi_N(\mathbf{x},t)}{\partial x^i} \end{pmatrix}_N \right] \quad (199)$$

If we expand the matrix product $\hat{\alpha}_i$ and $\hat{\beta}$ with the column vector $\boldsymbol{\psi}$ in equation (199), we can establish in a more compact way

$$i\hbar \frac{\partial \psi_\sigma}{\partial t} = \frac{\hbar c}{i} \sum_{\tau=1}^N \left(\hat{\alpha}_1 \frac{\partial}{\partial x^1} + \hat{\alpha}_2 \frac{\partial}{\partial x^2} + \hat{\alpha}_3 \frac{\partial}{\partial x^3} \right)_{\sigma\tau} \psi_\tau + m_0 c^2 \sum_{\tau=1}^N \hat{\beta}_{\sigma\tau} \psi_\tau \equiv \sum_{\tau=1}^N \hat{H}_{\sigma\tau} \psi_\tau \quad (200)$$

This equation must hold with these three natural properties :

1. The relativistic relation between energy and momentum for the free particle

$$E^2 = \mathbf{p}^2 c^2 + m_0^2 c^4 \quad (201)$$

2. The continuity equation for the probability density ρ (198)
3. The equation (200) must be Lorentz covariant.

1. The momentum-energy equation - The Klein-Gordon equation

In order to satisfy the condition 1, each component ψ_σ of the spinor $\boldsymbol{\psi}$ must satisfy a Klein-Gordon equation. (This equation is the result of the direct quanti-

zation of Einstein momentum-energy relation (201) but leads to negative probability densities ($\rho < 0$)).

$$-\hbar^2 \frac{\partial^2 \psi_\sigma}{\partial t^2} = (-\hbar^2 c^2 \nabla^2 + m_0^2 c^4) \psi_\sigma \quad (202)$$

From the equation (196) one can establish

$$-\hbar^2 \frac{\partial^2 \psi}{\partial t^2} = -\hbar^2 c^2 \sum_{i,j=1}^3 \frac{\hat{\alpha}_i \hat{\alpha}_j + \hat{\alpha}_j \hat{\alpha}_i}{2} \frac{\partial^2 \psi}{\partial x^i \partial x^j} + \frac{\hbar m_0 c^3}{i} \sum_{i=1}^3 (\hat{\alpha}_i \hat{\beta} + \hat{\beta} \hat{\alpha}_i) \frac{\partial \psi}{\partial x^i} + \hat{\beta}^2 m_0^2 c^4 \psi \quad (203)$$

If we identify equation (203) with the Klein-Gordon equation (202) it exhibits some restrictions for matrices $\hat{\alpha}_i$ and $\hat{\beta}$:

$$[\hat{\alpha}_i, \hat{\alpha}_j]_+ = \hat{\alpha}_i \hat{\alpha}_j + \hat{\alpha}_j \hat{\alpha}_i = 2\delta_{ij} \mathbb{1}_N, \quad [\hat{\alpha}_i, \hat{\beta}]_+ = \hat{\alpha}_i \hat{\beta} + \hat{\beta} \hat{\alpha}_i = 0, \quad \hat{\alpha}_i^2 = \hat{\beta}^2 = \mathbb{1}_N \quad (204)$$

These latter equations (204) form anticommutation relations which definite an algebra for the spinors ψ . The desired Hamiltonian \hat{H} must be hermitian to get a real associated total energy , consequently the matrices $\hat{\alpha}_i$ and $\hat{\beta}$ must be also hermitian thus

$$\hat{\alpha}_i^\dagger = \hat{\alpha}_i \quad \text{et} \quad \hat{\beta}^\dagger = \hat{\beta} \quad (205)$$

The eigenvalues of these matrices are real. We can show that their are equal to ± 1 by working in the diagonal representations of $\hat{\alpha}_i$ and $\hat{\beta}$. Indeed the eigenvalues v of a matrix \hat{A} are in general, independant of the basis representation

$$\hat{A} \psi_v = v \psi_v \Rightarrow \hat{U} \hat{A} \hat{U}^{-1} \hat{U} \psi_v = v \hat{U} \psi_v \Rightarrow \hat{A}' (\hat{U} \psi_v) = v (\hat{U} \psi_v) \quad (206)$$

(With ψ_v the eigenstate, \hat{U} The transformation matrix and $\hat{A}' = \hat{U} \hat{A} \hat{U}^{-1}$ the diagonal matrix)

Let $\hat{\alpha}'_i$ be the diagonal representation of $\hat{\alpha}_i$ with its eigenvalues $a_1, a_2, a_3, \dots, a_N$.

$$\hat{\alpha}'_i = \begin{pmatrix} a_1 & 0 & 0 & \cdots & 0 \\ 0 & a_2 & 0 & \cdots & 0 \\ 0 & 0 & a_3 & \cdots & 0 \\ \vdots & \vdots & \vdots & \ddots & \vdots \\ 0 & 0 & 0 & \cdots & a_N \end{pmatrix}_{N \times N} \quad (207)$$

From (204) and (206) we get $(\hat{\alpha}'_i)^2 = \hat{U}\hat{\alpha}_i\hat{U}^{-1}\hat{U}\hat{\alpha}_i\hat{U}^{-1} = \hat{U}\hat{\alpha}_i^2\hat{U}^{-1} = \mathbb{1}_N$ thus

$$(\hat{\alpha}'_i)^2 = \mathbb{1}_N = \begin{pmatrix} 1 & 0 & 0 & \cdots & 0 \\ 0 & 1 & 0 & \cdots & 0 \\ 0 & 0 & 1 & \cdots & 0 \\ \vdots & \vdots & \vdots & \ddots & \vdots \\ 0 & 0 & 0 & \cdots & 1 \end{pmatrix}_{N \times N} = \begin{pmatrix} a_1^2 & 0 & 0 & \cdots & 0 \\ 0 & a_2^2 & 0 & \cdots & 0 \\ 0 & 0 & a_3^2 & \cdots & 0 \\ \vdots & \vdots & \vdots & \ddots & \vdots \\ 0 & 0 & 0 & \cdots & a_N^2 \end{pmatrix}_{N \times N} \quad (208)$$

By identification of these two latter matrices (208) one can deduce that

$$a_\tau^2 = 1 \Rightarrow a_\tau = \pm 1 \quad (209)$$

With the same mechanism one can demonstrate that the matrix $\hat{\beta}$ get ± 1 as eigenvalues.

We can also demonstrate the trace of the matrices $\hat{\alpha}_i$ and $\hat{\beta}$ is zero. We use the fact that $\text{tr}(\hat{A}\hat{B}) = \text{tr}(\hat{B}\hat{A})$ and that the trace of a matrix is in general equal to the trace of its diagonal matrix :

$$\text{tr}(\hat{A}') = \text{tr}(\hat{U}\hat{A}\hat{U}^{-1}) = \text{tr}(\hat{A}\hat{U}^{-1}\hat{U}) = \text{tr}(\hat{A}) \quad (210)$$

By multiplying to the right by $\hat{\beta}$ the anticommutation relation (204) we get from (210)

$$\left[\hat{\alpha}_i, \hat{\beta} \right]_+ \cdot \hat{\beta} = 0 \Rightarrow \hat{\alpha}_i \hat{\beta}^2 = -\hat{\beta} \hat{\alpha}_i \hat{\beta} \Rightarrow \hat{\alpha}_i = -\hat{\beta} \hat{\alpha}_i \hat{\beta} \quad (211)$$

One can write from (211) and (210) that

$$\text{tr}(\hat{\alpha}_i) = \text{tr}(-\hat{\beta} \hat{\alpha}_i \hat{\beta}) = -\text{tr}(\hat{\beta} \hat{\alpha}_i \hat{\beta}) = -\text{tr}(\hat{\alpha}_i \hat{\beta}^2) \quad (212)$$

therefore from (204)

$$\text{tr}(\hat{\alpha}_i) = -\text{tr}(\hat{\alpha}_i) \Rightarrow \text{tr}(\hat{\alpha}_i) = 0 \quad (213)$$

With the similar mechanism we also get :

$$\text{tr}(\hat{\beta}) = 0 \quad (214)$$

The trace nullity of the matrices $\hat{\alpha}_i$ and $\hat{\beta}$ conjugate to their ± 1 eigenvalues imply an even dimension. However the even dimension $N = 2$ does not satisfy the relations

(204) because we can only construct three anticommuting matrices, these are the Pauli matrices

$$\hat{\sigma}_1 = \begin{pmatrix} 0 & 1 \\ 1 & 0 \end{pmatrix}, \quad \hat{\sigma}_2 = \begin{pmatrix} 0 & -i \\ i & 0 \end{pmatrix}, \quad \hat{\sigma}_3 = \begin{pmatrix} 1 & 0 \\ 0 & -1 \end{pmatrix} \quad (215)$$

The smaller dimension from which the conditions (204) hold is $N = 4$. We are now going to construct the Dirac equation for $N = 4$ and verify these conditions one by one.

Let us study in details the four matrices 4×4 built from the Pauli matrices and the identity matrix $\mathbb{1}_2$

$$\hat{\alpha}_i = \begin{pmatrix} 0 & \hat{\sigma}_i \\ \hat{\sigma}_i & 0 \end{pmatrix}, \quad \hat{\beta} = \begin{pmatrix} \mathbb{1}_2 & 0 \\ 0 & -\mathbb{1}_2 \end{pmatrix} \quad (216)$$

We get the Dirac matrices :

$$\hat{\alpha}_1 = \begin{pmatrix} 0 & 0 & 0 & 1 \\ 0 & 0 & 1 & 0 \\ 0 & 1 & 0 & 0 \\ 1 & 0 & 0 & 0 \end{pmatrix}, \quad \hat{\alpha}_2 = \begin{pmatrix} 0 & 0 & 0 & -i \\ 0 & 0 & i & 0 \\ 0 & -i & 0 & 0 \\ i & 0 & 0 & 0 \end{pmatrix}, \quad \hat{\alpha}_3 = \begin{pmatrix} 0 & 0 & 1 & 0 \\ 0 & 0 & 0 & -1 \\ 1 & 0 & 0 & 0 \\ 0 & -1 & 0 & 0 \end{pmatrix}, \quad \hat{\beta} = \begin{pmatrix} 1 & 0 & 0 & 0 \\ 0 & 1 & 0 & 0 \\ 0 & 0 & -1 & 0 \\ 0 & 0 & 0 & -1 \end{pmatrix} \quad (217)$$

let us check the conditions (204) by using the anticommutation relations of the Pauli matrices : $[\hat{\sigma}_i, \hat{\sigma}_j]_+ = 2\delta_{ij}\mathbb{1}_2$

$$\begin{aligned} [\hat{\alpha}_i, \hat{\alpha}_j]_+ &= \hat{\alpha}_i \hat{\alpha}_j + \hat{\alpha}_j \hat{\alpha}_i = \begin{pmatrix} 0 & \hat{\sigma}_i \\ \hat{\sigma}_i & 0 \end{pmatrix} \cdot \begin{pmatrix} 0 & \hat{\sigma}_j \\ \hat{\sigma}_j & 0 \end{pmatrix} + \begin{pmatrix} 0 & \hat{\sigma}_j \\ \hat{\sigma}_j & 0 \end{pmatrix} \cdot \begin{pmatrix} 0 & \hat{\sigma}_i \\ \hat{\sigma}_i & 0 \end{pmatrix} \\ &= \begin{pmatrix} \hat{\sigma}_i \hat{\sigma}_j & 0 \\ 0 & \hat{\sigma}_i \hat{\sigma}_j \end{pmatrix} + \begin{pmatrix} \hat{\sigma}_j \hat{\sigma}_i & 0 \\ 0 & \hat{\sigma}_j \hat{\sigma}_i \end{pmatrix} = \begin{pmatrix} \hat{\sigma}_i \hat{\sigma}_j + \hat{\sigma}_j \hat{\sigma}_i & 0 \\ 0 & \hat{\sigma}_i \hat{\sigma}_j + \hat{\sigma}_j \hat{\sigma}_i \end{pmatrix} \\ &= \begin{pmatrix} 2\delta_{ij}\mathbb{1}_2 & 0 \\ 0 & 2\delta_{ij}\mathbb{1}_2 \end{pmatrix} = 2\delta_{ij} \begin{pmatrix} \mathbb{1}_2 & 0 \\ 0 & \mathbb{1}_2 \end{pmatrix} = 2\delta_{ij}\mathbb{1}_4 \end{aligned} \quad (218)$$

$$\begin{aligned} [\hat{\alpha}_i, \hat{\beta}]_+ &= \hat{\alpha}_i \hat{\beta} + \hat{\beta} \hat{\alpha}_i = \begin{pmatrix} 0 & \hat{\sigma}_i \\ \hat{\sigma}_i & 0 \end{pmatrix} \cdot \begin{pmatrix} \mathbb{1}_2 & 0 \\ 0 & -\mathbb{1}_2 \end{pmatrix} + \begin{pmatrix} \mathbb{1}_2 & 0 \\ 0 & -\mathbb{1}_2 \end{pmatrix} \cdot \begin{pmatrix} 0 & \hat{\sigma}_i \\ \hat{\sigma}_i & 0 \end{pmatrix} = \begin{pmatrix} 0 & -\hat{\sigma}_i \\ \hat{\sigma}_i & 0 \end{pmatrix} + \begin{pmatrix} 0 & \hat{\sigma}_i \\ -\hat{\sigma}_i & 0 \end{pmatrix} \\ &= 0 \end{aligned}$$

$$\hat{\beta}^2 = \begin{pmatrix} \mathbb{1}_2 & 0 \\ 0 & -\mathbb{1}_2 \end{pmatrix} \cdot \begin{pmatrix} \mathbb{1}_2 & 0 \\ 0 & -\mathbb{1}_2 \end{pmatrix} = \mathbb{1}_4 \quad (219)$$

It comes directly from the demonstration (218) that $\hat{\alpha}_i^2 = \mathbb{1}_4$. The conditions (204) are valid.

2. The continuity equation

We have to show that the spacial integral $\int \rho d^3\mathbf{x}$ is constant with respect to the time. If this condition is satisfied the probability interprétation of ρ is assured.

It is possible to find a 3-dimension vector \mathbf{j} which represents a current probability in order to satisfy the continuity equation

$$\frac{\partial}{\partial t}\rho + \text{div } \mathbf{j} = 0 \quad (220)$$

If the latter (220) is valid then we get local conservation of the probability. For this purpose, one can take the Dirac equation (196) and multiply it to the left by ψ^\dagger

$$i\hbar\psi^\dagger\frac{\partial\psi}{\partial t} = \frac{\hbar c}{i}\sum_{k=1}^3\psi^\dagger\hat{\alpha}_k\frac{\partial\psi}{\partial x^k} + m_0c^2\psi^\dagger\hat{\beta}\psi \quad (221)$$

We take the hermitian conjugate of the Dirac equation and we multiply it to the right with ψ by using the hermiticity of the matrices $\hat{\alpha}_k$ and $\hat{\beta}$ (205)

$$-i\hbar\frac{\partial\psi^\dagger}{\partial t}\psi = -\frac{\hbar c}{i}\sum_{k=1}^3\frac{\partial\psi^\dagger}{\partial x^k}\hat{\alpha}_k\psi + m_0c^2\psi^\dagger\hat{\beta}\psi \quad (222)$$

If we substract the equation (223) to the equation (221) we get

$$i\hbar\frac{\partial}{\partial t}(\psi^\dagger\psi) = \frac{\hbar c}{i}\sum_{k=1}^3\frac{\partial}{\partial x^k}(\psi^\dagger\hat{\alpha}_k\psi) \quad (223)$$

in other words

$$\frac{\partial\rho}{\partial t} + c\sum_{k=1}^3\frac{\partial}{\partial x^k}(\psi^\dagger\hat{\alpha}_k\psi) = 0 \quad (224)$$

If one identify the latter equation (224) to the continuity equation (220) it is possible to get the current of density probability \mathbf{j}

$$\mathbf{j} = c\psi^\dagger\hat{\boldsymbol{\alpha}}\psi \quad (225)$$

with $\hat{\boldsymbol{\alpha}} = \{\hat{\alpha}^1, \hat{\alpha}^2, \hat{\alpha}^3\}$ a 3-dimension vector. Let us check that the probability is preserved over time

$$\frac{\partial}{\partial t}\int_{\mathcal{V}}d^3\mathbf{x}\rho = \frac{\partial}{\partial t}\int_{\mathcal{V}}d^3\mathbf{x}\psi^\dagger\psi = -\int_{\mathcal{V}}d^3\mathbf{x}\text{div } \mathbf{j} \quad (226)$$

Where \mathcal{V} represents a volume bounded by a surface \mathcal{S} . If we use the divergence theorem (Green-Ostrogradsky) we get

$$\frac{\partial}{\partial t} \int_{\mathcal{V}} d^3\mathbf{x} \rho = - \oint_{\mathcal{S}} \mathbf{j} \cdot d\mathbf{s} = 0 \quad (227)$$

The probability is then well preserved over time form (227).

3. Lorentz covariance

A relativistic theory must be Lorentz covariant, *i.e.* be invariant when we change from an inertial reference frame (or Galilean reference frame) to an other. Let us introduce an event measured by an observer A in an inertial reference frame \mathcal{R}_A and measured by a second observer B in an inertial reference frame \mathcal{R}_B . Let x be the 4-position coordinates of the event \mathcal{R}_A and x' in \mathcal{R}_B . Let say that this event is the measurement of the electron wave function, A measures $\psi(x)$ and B measures $\psi'(x')$. If the Dirac equation is Lorentz covariant then these two fundamental criteria must hold

1. If the observer A measures $\psi(x)$ in \mathcal{R}_A then the observer B could find $\psi'(x')$ in \mathcal{R}_B if he knows $\psi(x)$.

2. The Einstein's principle of relativity states that the laws of physics are the same in every inertial reference frame, including the physic equations. $\psi'(x')$ must be also a solution of the Dirac equation.

To start this demonstration we write the Dirac equation in function of the four dimensions $\{x^0 = ct, x^1, x^2, x^3\}$ to highlight the symmetry between the space and time coordinates.

$$\frac{\hat{\beta}}{c} \left(i\hbar \frac{\partial}{\partial t} + i\hbar c \sum_{k=1}^3 \hat{\alpha}_k \frac{\partial}{\partial x^k} - \hat{\beta} m_0 c^2 \right) \psi = 0 \Rightarrow \left(\hat{\beta} i\hbar \frac{\partial}{\partial ct} + \sum_{k=1}^3 \hat{\beta} \hat{\alpha}_k i\hbar c \frac{\partial}{\partial x^k} - m_0 c \mathbb{1}_4 \right) \psi = 0 \quad (228)$$

Let us define the new matrices

$$\hat{\gamma}^0 = \hat{\beta} \quad , \quad \hat{\gamma}^i = \hat{\beta} \hat{\alpha}_i \quad , \quad i = \{1, 2, 3\} \quad (229)$$

The Dirac equation can be written

$$i\hbar \left(\hat{\gamma}^0 \frac{\partial}{\partial x^0} + \hat{\gamma}^1 \frac{\partial}{\partial x^1} + \hat{\gamma}^2 \frac{\partial}{\partial x^2} + \hat{\gamma}^3 \frac{\partial}{\partial x^3} \right) \psi - m_0 c \mathbb{1}_4 \psi = 0 \quad (230)$$

Let us establish new anticommutation relations for the matrices $\hat{\gamma}$. We know from (204)

$$[\hat{\gamma}^0, \hat{\gamma}^0]_+ = 2\mathbb{1}_4$$

The other are evaluated by using once again the anticommutation relations from (204)

$$[\hat{\gamma}^i, \hat{\gamma}^i]_+ = 2\hat{\beta}\hat{\alpha}_i\hat{\beta}\hat{\alpha}_i = 2(-\hat{\alpha}_i\hat{\beta})\hat{\beta}\hat{\alpha}_i = -2\hat{\alpha}_i\mathbb{1}_4\hat{\alpha}_i = -2\hat{\alpha}_i^2 = -2\mathbb{1}_4 \quad (231)$$

$$[\hat{\gamma}^i, \hat{\gamma}^0]_+ = \hat{\beta}\hat{\alpha}_i\hat{\beta} + \hat{\beta}\hat{\beta}\hat{\alpha}_i = -\hat{\alpha}_i\hat{\beta}^2 + \hat{\beta}^2\hat{\alpha}_i = -\hat{\alpha}_i + \hat{\alpha}_i = 0 \quad (232)$$

We can use Lorentz metric tensor $g^{\mu\nu}$ to write a more general form for the matrices $\hat{\gamma}$ anticommutation

$$g^{\mu\nu} = g_{\mu\nu} = \begin{pmatrix} g^{00} & g^{01} & g^{02} & g^{03} \\ g^{10} & g^{11} & g^{12} & g^{13} \\ g^{20} & g^{21} & g^{22} & g^{23} \\ g^{30} & g^{31} & g^{32} & g^{33} \end{pmatrix} = \begin{pmatrix} 1 & 0 & 0 & 0 \\ 0 & -1 & 0 & 0 \\ 0 & 0 & -1 & 0 \\ 0 & 0 & 0 & -1 \end{pmatrix} \quad (233)$$

$$[\hat{\gamma}^\mu, \hat{\gamma}^\nu]_+ = \hat{\gamma}^\mu\hat{\gamma}^\nu + \hat{\gamma}^\nu\hat{\gamma}^\mu = 2g^{\mu\nu}\mathbb{1}_4 \quad (234)$$

(The $\hat{\gamma}$ define a Clifford algebra) One can demonstrate that $\hat{\gamma}^1, \hat{\gamma}^2, \hat{\gamma}^3$ are unitary and anti-hermitian ($\hat{\gamma}^0$ is hermitian from (205) and (229)).

$$(\hat{\gamma}^i)^2 = \hat{\beta}\hat{\alpha}_i\hat{\beta}\hat{\alpha}_i = -(\hat{\alpha}_i)^2 = -\mathbb{1}_4 \quad (235)$$

from (211), (204) and $(\hat{\gamma}^i)^\dagger = \hat{\alpha}_i\hat{\beta}$ we get

$$(\hat{\gamma}^i)^2 = -\mathbb{1}_4 \Rightarrow \hat{\gamma}^i\hat{\gamma}^{i\dagger} = -\mathbb{1}_4 \Rightarrow (\hat{\gamma}^i)^{-1} = \hat{\gamma}^{i\dagger} \quad (236)$$

The latter proves that $\hat{\gamma}^1, \hat{\gamma}^2, \hat{\gamma}^3$ are unitary. ($\hat{\gamma}^{0\dagger}\hat{\gamma}^0 = \mathbb{1}_4 \Rightarrow (\hat{\gamma}^0)^{-1} = \hat{\gamma}^{0\dagger}$ so also $\hat{\gamma}^0$)

We deduce directly from (204) and (229) the anti-hermicity

$$\hat{\gamma}^{i\dagger} = (\hat{\beta}\hat{\alpha}_i)^\dagger = \hat{\alpha}_i^\dagger\hat{\beta}^\dagger = \hat{\alpha}_i\hat{\beta} = -\hat{\beta}\hat{\alpha}_i = -\hat{\gamma}^i \quad (237)$$

The matrices $\hat{\gamma}$ can be written

$$\hat{\gamma}^0 = \begin{pmatrix} \mathbb{1}_2 & 0 \\ 0 & -\mathbb{1}_2 \end{pmatrix}, \quad \hat{\gamma}^i = \begin{pmatrix} \hat{\sigma}_i & 0 \\ 0 & -\hat{\sigma}_i \end{pmatrix} \quad (238)$$

Let us come back on our two observer, A observes an electronic state in \mathcal{R}_A whose the wave function $\psi(x)$ is solution of the Dirac equation.

$$\left(i\hbar\hat{\gamma}^\mu \frac{\partial}{\partial x^\mu} - m_0 c \mathbb{1}_4 \right) \psi(x) = 0 \quad (239)$$

The Einstein convention is used here for the summation : $\hat{\gamma}^\mu \frac{\partial}{\partial x^\mu} = \sum_{\mu=0}^3 \hat{\gamma}^\mu \frac{\partial}{\partial x^\mu}$

The observer B should observe the same electronic state in \mathcal{R}_B whose the wave function $\psi'(x')$ is solution of the Dirac equation

$$\left(i\hbar\hat{\gamma}'^\mu \frac{\partial}{\partial x'^\mu} - m_0 c \mathbb{1}_4 \right) \psi'(x') = 0 \quad (240)$$

With x and x' the space-time 4-vector define as $x = \{x^\mu\} = \{x^0, x^1, x^2, x^3\}$. From the relativity principle the matrices $\hat{\gamma}'$ must satisfy the anticommutation conditions

$$[\hat{\gamma}'^\mu, \hat{\gamma}'^\nu]_+ = \hat{\gamma}'^\mu \hat{\gamma}'^\nu + \hat{\gamma}'^\nu \hat{\gamma}'^\mu = 2g^{\mu\nu} \mathbb{1}_4 \quad (241)$$

The hermiticity and antu-hermicity conditions are consequently preserved in all inertial reference frame

$$(\hat{\gamma}'^0)^\dagger = \hat{\gamma}'^0 \quad , \quad (\hat{\gamma}'^i)^\dagger = -\hat{\gamma}'^i \quad (242)$$

Let us rewrite the equation (240) in a Schrödinger-like form

$$i\hbar\hat{\gamma}'^0 \frac{\partial \psi'(x')}{\partial (ct')} = \left(-i\hbar\hat{\gamma}'^k \frac{\partial}{\partial x'^k} + m_0 c \mathbb{1}_4 \right) \psi'(x') \quad (243)$$

$$i\hbar \frac{\partial \psi'(x')}{\partial (t')} = \left(-i\hbar c \hat{\gamma}'^0 \hat{\gamma}'^k \frac{\partial}{\partial x'^k} + \hat{\gamma}'^0 m_0 c^2 \right) \psi'(x') \quad \Rightarrow \quad i\hbar \frac{\partial \psi'(x')}{\partial (t')} = \hat{H}' \psi'(x') \quad (244)$$

If the observer B measures real energies then the Hamiltonian must be hermitian

$$\hat{H}'^\dagger = \hat{H}' \quad (245)$$

This implies that the 4-momentum vector $\hat{p}' = \{\hat{p}_\mu\} = \{i\hbar \frac{\partial}{\partial x'^\mu}\}$ is hermitian and commutes with the matrices $\hat{\gamma}'$ because if we write \hat{H}'^\dagger these conditions are required

$$\hat{H}'^\dagger = (-c\hat{\gamma}'^0 \hat{\gamma}'^k \hat{p}'_k + \hat{\gamma}'^0 m_0 c^2)^\dagger = -c\hat{p}'_k{}^\dagger (\hat{\gamma}'^0 \hat{\gamma}'^k)^\dagger + \hat{\gamma}'^0 m_0 c^2 \quad (246)$$

thus

$$\hat{p}'_\mu = \hat{p}'_\mu{}^\dagger \quad , \quad [\hat{p}'_\mu, \hat{\gamma}'^\mu] = 0 \quad (247)$$

It is demonstrated in [?] that for every 4×4 -dimension matrices $\hat{\gamma}'^\mu$ which satisfy the conditions (241) and (242) are identical to the matrices $\hat{\gamma}^\mu$ *via* an unitary transformation \hat{U}

$$\hat{\gamma}'^\mu = \hat{U}^\dagger \hat{\gamma}^\mu \hat{U} \quad , \quad \hat{U}^\dagger = \hat{U}^{-1} \quad (248)$$

The unitary transformations are isomorphisms between two Hilberts spaces, *i.e.* it does not change the physics.

$$\left(i\hbar \hat{\gamma}'^\mu \frac{\partial}{\partial x'^\mu} - m_0 c \mathbb{1}_4 \right) \psi'(x') = 0 \quad \Rightarrow \quad \left(i\hbar \hat{\gamma}^\mu \frac{\partial}{\partial x'^\mu} - m_0 c \mathbb{1}_4 \right) \psi'(x') = 0 \quad (249)$$

There is no more reason to distinguish $\hat{\gamma}^\mu$ and $\hat{\gamma}'^\mu$.

We can now build a transformation between $\psi(x)$ and $\psi'(x')$. This transformation must be linear such as Dirac equations (249) and the Lorentz's transformation itself. We get the following expression

$$\psi'(x') = \psi'(\hat{a}x) = \hat{S}(\hat{a})\psi(x) = \hat{S}(\hat{a})\psi(\hat{a}^{-1}x') \quad (250)$$

With a_μ^ν Lorentz's transformation matrix and \hat{S} a 4×4 -dimension matrix which acts in the four components of the spinors $\psi(x)$.

$$\hat{a}x = \sum_{\mu=0}^3 a_\mu^\nu x^\mu = x' \quad (251)$$

\hat{S} will depend on \hat{a} and thus on the position and on the relative velocity between the two inertial reference frames \mathcal{R}_A and \mathcal{R}_B . The invariance of physics laws in every inertial reference frame arising from the relativity principle induces the existence of an inverse operator $\hat{S}^{-1}(\hat{a})$, the latter let the observer A to construct a wave function $\psi(x)$ from the wave function $\psi'(x')$ of the observer B .

$$\psi(x) = \hat{S}^{-1}(\hat{a})\psi'(x') = \hat{S}^{-1}(\hat{a})\psi'(\hat{a}x) \quad (252)$$

From (250)

$$\psi(x) = \hat{S}(\hat{a}^{-1})\psi'(x') \quad (253)$$

One can establish from (252) and (253) that

$$\hat{S}(\hat{a}^{-1}) = \hat{S}^{-1}(\hat{a}) \quad (254)$$

We will construct \hat{S} to satisfy the criteria (250-255). Let start from the equation (239)

$$\left(i\hbar\hat{\gamma}^\mu\frac{\partial}{\partial x^\mu} - m_0c\mathbb{1}_4\right)\hat{S}^{-1}(\hat{a})\psi'(x') = 0 \quad \Rightarrow \quad \left(i\hbar\hat{\gamma}^\mu\hat{S}^{-1}(\hat{a})\frac{\partial}{\partial x^\mu} - m_0c\hat{S}^{-1}(\hat{a})\right)\psi'(x') = 0 \quad (255)$$

By multiplying on the left with $\hat{S}(\hat{a})$ we get

$$\left(i\hbar\hat{S}(\hat{a})\hat{\gamma}^\mu\hat{S}^{-1}(\hat{a})\frac{\partial}{\partial x^\mu} - m_0c\mathbb{1}_4\right)\psi'(x') = 0 \quad (256)$$

Let us express the derivative with respect to the inertial reference frame \mathcal{R}_B 's coordinates with

$$\frac{\partial}{\partial x^\mu} = \frac{\partial x'^\nu}{\partial x^\mu} \frac{\partial}{\partial x'^\nu} = a_\mu^\nu \frac{\partial}{\partial x'^\nu}$$

$$\left(i\hbar\hat{S}(\hat{a})\hat{\gamma}^\mu\hat{S}^{-1}(\hat{a})a_\mu^\nu\frac{\partial}{\partial x'^\nu} - m_0c\mathbb{1}_4\right)\psi'(x') = 0 \quad (257)$$

The equation above (258) must be equivalent to the equation (249), this implies

$$\hat{S}(\hat{a})\hat{\gamma}^\mu\hat{S}^{-1}(\hat{a})a_\mu^\nu = \hat{\gamma}^\nu \quad (258)$$

We thus get

$$\left(i\hbar\hat{\gamma}^\nu\frac{\partial}{\partial x'^\nu} - m_0c\mathbb{1}_4\right)\psi'(x') = 0 \quad \Leftrightarrow \quad \left(i\hbar\hat{\gamma}^\mu\frac{\partial}{\partial x'^\mu} - m_0c\mathbb{1}_4\right)\psi'(x') = 0 \quad (259)$$

We succeed in recovering the \mathcal{R}_B 's wave function from the wave function constructed in \mathcal{R}_A . Thus demonstrates the Lorentz covariance of Dirac equation. (It is possible to construct the \hat{S} matrix, for more details about this the reader can look at the chapter 3.2 of [?])

B. The Dirac solution derivation

Let us turn to the Dirac equation solutions

$$i\hbar\frac{\partial\psi}{\partial t} = \hat{H}\psi = \left(c\hat{\boldsymbol{\alpha}} \cdot \hat{\mathbf{p}} + m_0c^2\hat{\beta}\right)\psi \quad \Leftrightarrow \quad \left(i\hbar\hat{\gamma}^\mu\frac{\partial}{\partial x^\mu} - m_0c\mathbb{1}_4\right)\psi = 0 \quad (260)$$

The pseudovector $\hat{\boldsymbol{\alpha}}$ is a 3-cartesian-component vector $\{\hat{\alpha}_1, \hat{\alpha}_2, \hat{\alpha}_3\}$.

1. The free particle

In this part we will study the Dirac equation solutions for the free particle, *i.e.* without external potential. The global operator $(i\hbar\hat{\gamma}^\mu\frac{\partial}{\partial x^\mu} - m_0c\mathbb{1}_4)$ in matrix form which acts on the wave function $\psi(x)$ can be written

$$\begin{pmatrix} i\hbar\frac{\partial}{\partial x^0} - m_0c & 0 & i\hbar\frac{\partial}{\partial x^3} & i\hbar\frac{\partial}{\partial x^1} + \hbar\frac{\partial}{\partial x^2} \\ 0 & i\hbar\frac{\partial}{\partial x^0} - m_0c & i\hbar\frac{\partial}{\partial x^1} - \hbar\frac{\partial}{\partial x^2} & -i\hbar\frac{\partial}{\partial x^3} \\ -i\hbar\frac{\partial}{\partial x^3} & -i\hbar\frac{\partial}{\partial x^1} - \hbar\frac{\partial}{\partial x^2} & -i\hbar\frac{\partial}{\partial x^0} - m_0c & 0 \\ -i\hbar\frac{\partial}{\partial x^1} + \hbar\frac{\partial}{\partial x^2} & i\hbar\frac{\partial}{\partial x^3} & 0 & -i\hbar\frac{\partial}{\partial x^0} - m_0c \end{pmatrix} \cdot \begin{pmatrix} \psi_1(x) \\ \psi_2(x) \\ \psi_3(x) \\ \psi_4(x) \end{pmatrix} = \begin{pmatrix} 0 \\ 0 \\ 0 \\ 0 \end{pmatrix} \quad (261)$$

To describe the free particle we can use the plane wave equation

$$\psi(x) = \mathcal{U}(\hat{p})e^{-\frac{i}{\hbar}\hat{p}_\mu x^\mu} \quad (262)$$

With $\mathcal{U}(\hat{p})$ a 4-dimension column vector with the components $u_i(\hat{p})$ which are relativistic momentum scalar functions. One can reformulates (261) to exhibit the components of the four momentum vector (contravariant form).

$$\hat{p} = \{\hat{p}^\mu\} = g^{\mu\nu} \{\hat{p}_\nu\} = g^{\mu\nu} \left\{ i\hbar\frac{\partial}{\partial x^\nu} \right\}$$

$$\begin{pmatrix} -p^0 + m_0c & 0 & p^3 & p^1 - ip^2 \\ 0 & -p^0 + m_0c & p^1 + ip^2 & -p^3 \\ -p^3 & -p^1 + ip^2 & p^0 + m_0c & 0 \\ -p^1 - ip^2 & p^3 & 0 & p^0 + m_0c \end{pmatrix} \cdot \begin{pmatrix} u_1(\hat{p}) \\ u_2(\hat{p}) \\ u_3(\hat{p}) \\ u_4(\hat{p}) \end{pmatrix} = \begin{pmatrix} 0 \\ 0 \\ 0 \\ 0 \end{pmatrix} \quad (263)$$

(We multiply the whole equation with -1 to reduce the number of minus sign)

The determinant of this matrix is then zero

$$\det(\hat{\gamma}^\mu\hat{p}_\mu - m_0c\mathbb{1}_4) = 0 \quad (264)$$

By developing explicitly the determinant, we get the following factorized form

$$\left[\left(\sqrt{\mathbf{p}^2 + m_0c^2} + p^0 \right) \left(\sqrt{\mathbf{p}^2 + m_0c^2} - p^0 \right) \right]^2 = 0 \quad (265)$$

It exhibits two times two solutions

$$p^0 = \pm \sqrt{\mathbf{p}^2 + m_0c^2} \quad (266)$$

By using the fact that $p^0 = \frac{E}{c}$ one can express (266) as the particle energy

$$E = \pm \sqrt{\mathbf{p}^2 c^2 + m_0 c^4} \quad (267)$$

The latter (267) is in perfect adequacy with the special relativity theory of a particle. Besides there are two solutions of negative energy which describe mainly the associated antiparticle.

2. The bi-spinor reformulation

The 4-component Dirac equation can be reformulate to ease analytical developments, implementation and some 2-component approximations. For this purpose let us write

$$u_A(\hat{p}) = \begin{pmatrix} u_1(\hat{p}) \\ u_2(\hat{p}) \end{pmatrix} \quad \text{et} \quad u_B(\hat{p}) = \begin{pmatrix} u_3(\hat{p}) \\ u_4(\hat{p}) \end{pmatrix} \quad (268)$$

In the equation (260), we introduce the bi-spinors to reformulate in pseudo 2-dimension the Dirac equation.

$$-(\hat{\gamma}^\mu \hat{p}_\mu - m_0 c \mathbb{I}_4) \begin{pmatrix} u_A(\hat{p}) \\ u_B(\hat{p}) \end{pmatrix} = 0 \quad (269)$$

We develop in (269) the Einstein summation by expressing the matrices $\hat{\gamma}$ (except $\hat{\gamma}^0$) in function of the Paul matrices $\hat{\sigma}_i$ (215)

$$-\left[\begin{pmatrix} \mathbb{I}_2 & 0 \\ 0 & -\mathbb{I}_2 \end{pmatrix} \cdot p^0 - \begin{pmatrix} 0 & \hat{\sigma}_1 \\ -\hat{\sigma}_1 & 0 \end{pmatrix} \cdot p^1 - \begin{pmatrix} 0 & \hat{\sigma}_2 \\ -\hat{\sigma}_2 & 0 \end{pmatrix} \cdot p^2 - \begin{pmatrix} 0 & \hat{\sigma}_3 \\ -\hat{\sigma}_3 & 0 \end{pmatrix} \cdot p^3 - m_0 c \begin{pmatrix} \mathbb{I}_2 & 0 \\ 0 & \mathbb{I}_2 \end{pmatrix} \right] \begin{pmatrix} u_A(\hat{p}) \\ u_B(\hat{p}) \end{pmatrix} = 0 \quad (270)$$

If we introduce the pseudovector $\hat{\boldsymbol{\sigma}} = \{\hat{\sigma}_1, \hat{\sigma}_2, \hat{\sigma}_3\}$ and the momentum $\hat{\mathbf{p}} = \{p^1, p^2, p^3\}$ we can write in a shorter way

$$\begin{pmatrix} (-p^0 + m_0 c) \mathbb{I}_2 & \hat{\boldsymbol{\sigma}} \cdot \hat{\mathbf{p}} \\ -\hat{\boldsymbol{\sigma}} \cdot \hat{\mathbf{p}} & (p^0 + m_0 c) \mathbb{I}_2 \end{pmatrix} \begin{pmatrix} u_A(\hat{p}) \\ u_B(\hat{p}) \end{pmatrix} = 0 \quad (271)$$

The equation (271) is the bi-spinor form of the Dirac equation (with $p^0 = \frac{E}{c}$). One can also obtain the solution from this form by considering these two coupled equations

$$\begin{cases} (-p^0 + m_0 c) \mathbb{I}_2 u_A(\hat{p}) + \hat{\boldsymbol{\sigma}} \cdot \hat{\mathbf{p}} u_B(\hat{p}) = 0 \\ -\hat{\boldsymbol{\sigma}} \cdot \hat{\mathbf{p}} u_A(\hat{p}) + (p^0 + m_0 c) \mathbb{I}_2 u_B(\hat{p}) = 0 \end{cases} \quad (272)$$

We obtain the following solutions

$$u_A(\hat{p}) = -\frac{\hat{\boldsymbol{\sigma}} \cdot \hat{\mathbf{p}}}{-p^0 + m_0 c} u_B(\hat{p}) \quad (273)$$

$$u_B(\hat{p}) = \frac{\hat{\boldsymbol{\sigma}} \cdot \hat{\mathbf{p}}}{p^0 + m_0 c} u_A(\hat{p}) \quad (274)$$

We use the Dirac relation

$$(\hat{\boldsymbol{\sigma}} \cdot \hat{\mathbf{a}}) \cdot (\hat{\boldsymbol{\sigma}} \cdot \hat{\mathbf{b}}) = (\hat{\mathbf{a}} \cdot \hat{\mathbf{b}}) \mathbb{1}_2 + i \hat{\boldsymbol{\sigma}} \cdot (\hat{\mathbf{a}} \times \hat{\mathbf{b}}) \quad (275)$$

By using (275) in the equation (273) and (274) we get

$$\left[- (p^0)^2 + m_0^2 c^2 + \mathbf{p}^2 \right] \mathbb{1}_2 u_A(\hat{p}) = 0 \quad (276)$$

$$\left[- (p^0)^2 + m_0^2 c^2 + \mathbf{p}^2 \right] \mathbb{1}_2 u_B(\hat{p}) = 0 \quad (277)$$

The term in brackets is zero and with $p^0 = \frac{E}{c}$ we get the Dirac equation solutions (267) *i.e.* $E = \pm \sqrt{\mathbf{p}^2 c^2 + m_0^2 c^4}$. To keep only one energy per spinor we can consider the limiting case where $\hat{\mathbf{p}} \rightarrow 0$, so we can eliminate the negative solution $E = -m_0 c^2$ for u_B and the positive solution $E = m_0 c^2$ for u_A .

We introduce now a vector space $\left\{ \begin{pmatrix} 1 \\ 0 \end{pmatrix}, \begin{pmatrix} 0 \\ 1 \end{pmatrix} \right\}$ for u_A and u_B and we evaluate

$$\hat{\boldsymbol{\sigma}} \cdot \hat{\mathbf{p}} = \begin{pmatrix} 0 & p^1 \\ p^1 & 0 \end{pmatrix} + \begin{pmatrix} 0 & -ip^2 \\ ip^2 & 0 \end{pmatrix} + \begin{pmatrix} p^3 & 0 \\ 0 & -p^3 \end{pmatrix} = \begin{pmatrix} p^3 & p^1 - ip^2 \\ p^1 + ip^2 & -p^3 \end{pmatrix} \quad (278)$$

If we take $u_A(\hat{p}) = \begin{pmatrix} 1 \\ 0 \end{pmatrix}$ then (274) gives

$$u_B(\hat{p}) = \frac{1}{p^0 + m_0 c} \begin{pmatrix} p^3 \\ p^1 + ip^2 \end{pmatrix} \quad (279)$$

We thus find a first 4-vector $\mathcal{U}(\hat{p}) = \begin{pmatrix} u_A(\hat{p}) \\ u_B(\hat{p}) \end{pmatrix}$

$$\mathcal{U}^{(1)}(\hat{p}) = \begin{pmatrix} 1 \\ 0 \\ \frac{p^3}{p^0 + m_0 c} \\ \frac{p^1 + ip^2}{p^0 + m_0 c} \end{pmatrix} \quad \text{avec } E > 0 \quad (280)$$

If we take $u_A(\hat{p}) = \begin{pmatrix} 0 \\ 1 \end{pmatrix}$ then (274) gives

$$u_B(\hat{p}) = \frac{1}{p^0 + m_0 c} \begin{pmatrix} p^1 - ip^2 \\ -p^3 \end{pmatrix} \quad (281)$$

We find a second 4-vector $\mathbf{u}(\hat{p})$

$$\mathbf{u}^{(2)}(\hat{p}) = \begin{pmatrix} 0 \\ 1 \\ \frac{p^1 - ip^2}{p^0 + m_0 c} \\ \frac{-p^3}{p^0 + m_0 c} \end{pmatrix} \quad \text{avec } E > 0 \quad (282)$$

By using the equation (273) and $u_B = \left\{ \begin{pmatrix} 0 \\ 1 \end{pmatrix}, \begin{pmatrix} 1 \\ 0 \end{pmatrix} \right\}$ we get the two other 4-vector $\mathbf{u}(\hat{p})$

$$\mathbf{u}^{(3)}(\hat{p}) = \begin{pmatrix} \frac{p^3}{p^0 - m_0 c} \\ \frac{p^1 + ip^2}{p^0 - m_0 c} \\ 1 \\ 0 \end{pmatrix} \quad \text{avec } E < 0 \quad (283)$$

$$\mathbf{u}^{(4)}(\hat{p}) = \begin{pmatrix} \frac{p^1 - ip^2}{p^0 - m_0 c} \\ \frac{-p^3}{p^0 - m_0 c} \\ 0 \\ 1 \end{pmatrix} \quad \text{avec } E < 0 \quad (284)$$

From now we can inject these 4-spinors \mathbf{u} in the plane wave function (262) in order to get the exact electronic solutions ψ of the free particle

$$\psi_+^{(1)}(x) = \mathcal{N} \begin{pmatrix} 1 \\ 0 \\ \frac{p^3}{p^0 + m_0 c} \\ \frac{p^1 + ip^2}{p^0 + m_0 c} \end{pmatrix} e^{-\frac{i}{\hbar} \hat{p}_\mu x^\mu} \quad \text{and} \quad \psi_+^{(2)}(x) = \mathcal{N} \begin{pmatrix} 0 \\ 1 \\ \frac{p^1 - ip^2}{p^0 + m_0 c} \\ \frac{-p^3}{p^0 + m_0 c} \end{pmatrix} e^{-\frac{i}{\hbar} \hat{p}_\mu x^\mu} \quad (285)$$

$\psi_+^{(1)}(x)$ and $\psi_+^{(2)}(x)$ are associated to a positive energy $E = \sqrt{\mathbf{p}^2 c^2 + m_0^2 c^4}$

$$\psi_-^{(3)}(x) = \mathcal{N} \begin{pmatrix} \frac{p^3}{p^0 - m_0 c} \\ \frac{p^1 + ip^2}{p^0 - m_0 c} \\ 1 \\ 0 \end{pmatrix} e^{-\frac{i}{\hbar} \hat{p}_\mu x^\mu} \quad \text{and} \quad \psi_-^{(4)}(x) = \mathcal{N} \begin{pmatrix} \frac{p^1 - ip^2}{p^0 - m_0 c} \\ \frac{-p^3}{p^0 - m_0 c} \\ 0 \\ 1 \end{pmatrix} e^{-\frac{i}{\hbar} \hat{p}_\mu x^\mu} \quad (286)$$

$\psi_-^{(3)}(x)$ and $\psi_-^{(4)}(x)$ are associated to a negative energy $E = -\sqrt{\mathbf{p}^2 c^2 + m_0^2 c^4}$

\mathcal{N} is a normalization factor such as $\mathcal{N} = \sqrt{\frac{|E| + m_0 c^2}{2|E|}}$

3. Probability density

The free particle solutions ψ determined above all have a positive probability density ρ .

$$\rho_+^{(1)}(x) \geq 0 \quad , \quad \rho_+^{(2)}(x) \geq 0 \quad , \quad \rho_-^{(3)}(x) \geq 0 \quad , \quad \rho_-^{(4)}(x) \geq 0 \quad (287)$$

The negative probability density problem present in Klein-Gordon equation is solved with the Dirac equation.

From now we can define the probability density 4-vector \mathbf{J} such as

$$\mathbf{J} = \begin{pmatrix} c\rho \\ \mathbf{j} \end{pmatrix} = \begin{pmatrix} c\psi^\dagger\psi \\ c\psi^\dagger\hat{\boldsymbol{\alpha}}\psi \end{pmatrix} \quad (288)$$

C. The Hydrogen-like problem

This part aims to give some calculation details about the one electron atom.

1. Equations of the problem

We want to establish the Dirac equation solutions for the stationary states of the hydrogen atom, as discussed in IB2 it is possible to separate the space and time variables of the wave function $\psi(x)$ to get a product of function (10). We use this product with the Hamiltonian form of Dirac with a scalar potential $V = -\frac{Ze}{r}$, r is the electron-nucleus distance and Z the number of proton in the nucleus. Since there is no magnetic field $\mathbf{A} = 0$, we get the following

$$\left[c\hat{\boldsymbol{\alpha}} \cdot \hat{\mathbf{p}} - \frac{Ze^2}{r} \mathbb{1}_4 + \hat{\beta}m_0c^2 \right] \psi(\mathbf{x})e^{-\frac{i}{\hbar}Et} = i\hbar \frac{\partial}{\partial t} \left(\psi(\mathbf{x})e^{-\frac{i}{\hbar}Et} \right) \quad (289)$$

The time dependent term vanish and we get the stationary Dirac equation

$$\left[c\hat{\boldsymbol{\alpha}} \cdot \hat{\mathbf{p}} - \frac{Ze^2}{r} \mathbb{1}_4 + \hat{\beta}m_0c^2 \right] \psi(\mathbf{x}) = E\psi(\mathbf{x}) \quad \Leftrightarrow \quad \hat{h}^D\psi = E\psi \quad (290)$$

The potential contains the r coordinate so the equation (290) must be written in spherical coordinates (r, θ, φ) . The mathematical details of the cartesian to spherical conversion can be found in plenty of books including [34]. Let us express the Hamiltonian as the following

$$\hat{h}^D = \begin{pmatrix} \left[m_0c^2 - \frac{Ze^2}{r} \right] \mathbb{1}_2 & c\hat{\boldsymbol{\sigma}} \cdot \hat{\mathbf{p}} \\ c\hat{\boldsymbol{\sigma}} \cdot \hat{\mathbf{p}} & \left[-m_0c^2 - \frac{Ze^2}{r} \right] \mathbb{1}_2 \end{pmatrix} \quad (291)$$

We must introduce the total angular momentum \hat{j} and study in detail the operator $\hat{\sigma} \cdot \hat{\mathbf{p}}$

2. The total angular momentum

We need to generalize the angular momentum and the spin to the 4-component formalism, let us introduce the generalized 4-component angular momentum

$$\hat{\mathbf{l}}_4 = \hat{\mathbf{l}} \mathbb{1}_4 = (\hat{l}_x \mathbb{1}_4, \hat{l}_y \mathbb{1}_4, \hat{l}_z \mathbb{1}_4) \quad (292)$$

Let us introduce the pseudovector $\hat{\Sigma}$ a 4-component generalization of the Pauli matrices

$$\hat{\Sigma} = \begin{pmatrix} \hat{\sigma} & 0 \\ 0 & \hat{\sigma} \end{pmatrix} = \left[\begin{pmatrix} \hat{\sigma}_x & 0 \\ 0 & \hat{\sigma}_x \end{pmatrix}, \begin{pmatrix} \hat{\sigma}_y & 0 \\ 0 & \hat{\sigma}_y \end{pmatrix}, \begin{pmatrix} \hat{\sigma}_z & 0 \\ 0 & \hat{\sigma}_z \end{pmatrix} \right] \quad (293)$$

We can now express the generalized 4-component spin operator $\hat{\mathbf{s}}_4$ from (293)

$$\hat{\mathbf{s}}_4 = \frac{\hbar}{2} \hat{\Sigma} \quad (294)$$

The 4-component total angular momentum operator can thus be written as the sum of (294) and (292)

$$\hat{\mathbf{j}}_4 = \hat{\mathbf{l}}_4 + \hat{\mathbf{s}}_4 = \hat{\mathbf{l}} \mathbb{1}_4 + \frac{\hbar}{2} \hat{\Sigma} \quad , \quad \hat{\mathbf{j}}_4 = \left\{ \hat{j}_4^1, \hat{j}_4^2, \hat{j}_4^3 \right\} \quad (295)$$

The operators \hat{j}_4^2 and \hat{j}_4^i commute with the Hamiltonian \hat{h}^D (291)

$$\left[\hat{h}^D, \hat{j}_4^2 \right] = \left[\hat{h}^D, \hat{j}_4^i \right] = 0 \quad \text{avec} \quad i \in \{1, 2, 3\} \quad (296)$$

One can find the commutation relations between the components of $\hat{\mathbf{j}}_4$

$$\left[\hat{j}_3^i, \hat{j}_4^j \right] = i\hbar \epsilon_{ijk} j_4^k \quad (297)$$

With ϵ_{ijk} the Levi-Civita tensor such as $\begin{cases} \epsilon_{123} = \epsilon_{231} = \epsilon_{312} = 1 \\ \epsilon_{132} = \epsilon_{213} = \epsilon_{321} = -1 \end{cases}$

3. The spin-orbit coupling

We turn on the operator $\hat{\sigma} \cdot \hat{\mathbf{p}}$, it is possible to express it in function of the angular momentum $\hat{\mathbf{l}}$ and the spin $\hat{\mathbf{s}}$. By using the Dirac relation (275) one can establish

$$\frac{1}{r^2} (\hat{\sigma} \cdot \mathbf{r}) (\hat{\sigma} \cdot \mathbf{r}) = \mathbb{1}_2 \quad (298)$$

We deduce the following development

$$(\hat{\sigma} \cdot \hat{\mathbf{p}}) = \mathbb{1}_2 \cdot (\hat{\sigma} \cdot \hat{\mathbf{p}}) = \frac{1}{r^2} (\hat{\sigma} \cdot \mathbf{r}) (\hat{\sigma} \cdot \mathbf{r}) (\hat{\sigma} \cdot \hat{\mathbf{p}}) \quad (299)$$

We reuse again the Dirac relation for

$$(\hat{\sigma} \cdot \mathbf{r}) (\hat{\sigma} \cdot \hat{\mathbf{p}}) = \mathbf{r} \cdot \hat{\mathbf{p}} + i\hat{\sigma} \cdot (\mathbf{r} \times \hat{\mathbf{p}}) \quad (300)$$

We get

$$(\hat{\sigma} \cdot \hat{\mathbf{p}}) = \frac{1}{r^2} (\hat{\sigma} \cdot \mathbf{r}) [\mathbf{r} \cdot \hat{\mathbf{p}} + i\hat{\sigma} \cdot (\mathbf{r} \times \hat{\mathbf{p}})] \quad (301)$$

$$(\hat{\sigma} \cdot \hat{\mathbf{p}}) = \frac{1}{r^2} (\hat{\sigma} \cdot \mathbf{r}) \left[-i\hbar r \frac{\partial}{\partial r} + i(\hat{\sigma} \cdot \hat{\mathbf{l}}) \right] \quad (302)$$

The latter expression above (302) exhibits the spin-orbit operator $(\hat{\sigma} \cdot \hat{\mathbf{l}})$ which is the only one in function of the angular variables (θ, φ) , the other contributions are radial. Let us express the spin-orbit operator in function of the quantum operators $\hat{\mathbf{j}}^2$, $\hat{\mathbf{l}}^2$ and $\hat{\mathbf{s}}^2$

$$\hat{\mathbf{j}}^2 = (\hat{\mathbf{l}}\mathbb{1}_2 + \hat{\mathbf{s}})^2 = \hat{\mathbf{l}}^2\mathbb{1}_2 + 2(\hat{\mathbf{s}} \cdot \hat{\mathbf{l}}) + \hat{\mathbf{s}}^2 = \hat{\mathbf{l}}^2\mathbb{1}_2 + \hbar(\hat{\sigma} \cdot \hat{\mathbf{l}}) + \hat{\mathbf{s}}^2 \quad (303)$$

In (303) we use the fact that the angular momentum and the spin operator commute, we can now establish the following relation

$$\hat{\sigma} \cdot \hat{\mathbf{l}} = \frac{1}{\hbar} (\hat{\mathbf{j}}^2 - \hat{\mathbf{l}}^2\mathbb{1}_2 - \hat{\mathbf{s}}^2) \quad (304)$$

The relation (304) allow us to write the eigenvalue equation of the spin-orbit operator by using the eigenvalue equations of the operators $\hat{\mathbf{l}}^2$, $\hat{\mathbf{s}}^2$ and $\hat{\mathbf{j}}^2$

$$\begin{aligned} \hat{\mathbf{l}}^2 |\chi_{j,m_j}\rangle &= l(l+1)\hbar^2 |\chi_{j,m_j}\rangle & l \in \mathbb{N} \\ \hat{\mathbf{s}}^2 |\chi_{j,m_j}\rangle &= s(s+1)\hbar^2 |\chi_{j,m_j}\rangle & s = \frac{1}{2} \\ \hat{\mathbf{j}}^2 |\chi_{j,m_j}\rangle &= j(j+1)\hbar^2 |\chi_{j,m_j}\rangle & |l-s| \leq j \leq l+s \end{aligned} \quad (305)$$

With l , s and j the associated quantum numbers and $|\chi_{j,m_j}\rangle$ an eigenfunction which depends on angular coordinates (θ, φ) . It should be noticed that only j is a good quantum number because we mentionned in (296) that its associated operator $\hat{\mathbf{j}}^2$ commutes with \hat{h}^D . Thus the spin-orbit eigenvalue equation is

$$\begin{aligned} (\hat{\sigma} \cdot \hat{\mathbf{l}}) |\chi_{j,m_j}\rangle &= \frac{1}{\hbar} (\hat{\mathbf{j}}^2 - \hat{\mathbf{l}}^2 - \hat{\mathbf{s}}^2) |\chi_{j,m_j}\rangle \\ &= \hbar \left[j(j+1) - l(l+1) - \frac{3}{4} \right] |\chi_{j,m_j}\rangle \end{aligned} \quad (306)$$

The quantum number j can take the values $j = l + \frac{1}{2}$ or $j = l - \frac{1}{2}$ if $l \neq 0$, we must distinguish two cases for the eigenfunction, respectively $\left| \chi_{j,m_j}^{(+)} \right\rangle$ and $\left| \chi_{j,m_j}^{(-)} \right\rangle$. By exploiting thus fact one can express the eigenvalue equation of the operator $\hat{\mathbf{l}}^2$ (305) in function of the quantum number j for these two cases

$$\begin{aligned} \hat{\mathbf{l}}^2 \left| \chi_{j,m_j}^{(+)} \right\rangle &= \left(j - \frac{1}{2} \right) \left(j + \frac{1}{2} \right) \hbar^2 \left| \chi_{j,m_j}^{(+)} \right\rangle & l = j - \frac{1}{2} \\ \hat{\mathbf{l}}^2 \left| \chi_{j,m_j}^{(-)} \right\rangle &= \left(j + \frac{1}{2} \right) \left(j + 1 \right) \hbar^2 \left| \chi_{j,m_j}^{(-)} \right\rangle & l = j + \frac{1}{2} \end{aligned} \quad (307)$$

Consequently we can express the eigenvalue equation (306) in function only of the quantum number j

$$\begin{aligned} (\hat{\boldsymbol{\sigma}} \cdot \hat{\mathbf{l}}) \left| \chi_{j,m_j}^{(+)} \right\rangle &= \hbar l \left| \chi_{j,m_j}^{(+)} \right\rangle = \hbar \left[-1 + \left(j + \frac{1}{2} \right) \right] \left| \chi_{j,m_j}^{(+)} \right\rangle \\ (\hat{\boldsymbol{\sigma}} \cdot \hat{\mathbf{l}}) \left| \chi_{j,m_j}^{(-)} \right\rangle &= -\hbar(l+1) \left| \chi_{j,m_j}^{(-)} \right\rangle = \hbar \left[-1 - \left(j + \frac{1}{2} \right) \right] \left| \chi_{j,m_j}^{(-)} \right\rangle \end{aligned} \quad (308)$$

4. The relativistic analog of the azimuthal quantum number : κ

The equations (308) can be slightly simplified by adding $\hbar \mathbb{1}_2$, we can introduce a new operator $\hat{\mathbf{k}}$ such as

$$\hat{\mathbf{k}} \equiv (\hat{\boldsymbol{\sigma}} \cdot \hat{\mathbf{l}}) + \hbar \mathbb{1}_2 \quad (309)$$

This new operator allow us to establish a simpler eigenvalue equation with a new quantum number κ

$$\hat{\mathbf{k}} \left| \chi_{j,m_j}^{(\pm)} \right\rangle = \pm \hbar \left(j + \frac{1}{2} \right) \left| \chi_{j,m_j}^{(\pm)} \right\rangle = \hbar \kappa^{(\pm)} \left| \chi_{j,m_j}^{(\pm)} \right\rangle \quad (310)$$

With $\kappa^{(+)} = j + \frac{1}{2}$ and $\kappa^{(-)} = -\kappa^{(+)} = -j - \frac{1}{2}$. This quantum number is very usefull in spectroscopy to distinguish the differents j states, it can also be used to qualify the eigenfunction

$$\begin{aligned} \left| \chi_{\kappa,m_j} \right\rangle &= \left| \chi_{j,m_j}^{(+)} \right\rangle \\ \left| \chi_{-\kappa,m_j} \right\rangle &= \left| \chi_{j,m_j}^{(-)} \right\rangle \end{aligned} \quad (311)$$

TABLE V. Summary table of quantum numbers and symbols used in atom spectroscopy

Symbols	$s_{1/2}$	$p_{1/2}$	$p_{3/2}$	$d_{3/2}$	$d_{5/2}$	$f_{5/2}$	$f_{7/2}$	$g_{7/2}$	$g_{9/2}$
κ	-1	1	-2	2	-3	3	-4	4	-5
l	0	1	1	2	2	3	3	4	4
$j = \kappa - \frac{1}{2}$	1/2	1/2	3/2	3/2	5/2	5/2	7/2	7/2	9/2
Parity $(-1)^l$	+	-	-	+	+	-	-	+	+
Degeneracy	2	2	4	4	6	6	8	8	10
$(2 \kappa = 2j + 1)$									

5. Operator 4-component generalization

We come back on the stationary Dirac Hamiltonian (290)

$$\left[c\hat{\boldsymbol{\alpha}} \cdot \hat{\mathbf{p}} - \frac{Ze^2}{r} \mathbb{1}_4 + \hat{\beta} m_0 c^2 \right] \boldsymbol{\psi}(\mathbf{x}) = E \boldsymbol{\psi}(\mathbf{x}) \quad \Leftrightarrow \quad \hat{h}^D \boldsymbol{\psi} = E \boldsymbol{\psi}$$

Based on the developments established in VIC 3 for the spin-orbit operator and for the operator $\hat{\mathbf{k}}$ defined in (309), we will make more explicit the operator

$$\hat{\boldsymbol{\alpha}} \cdot \hat{\mathbf{p}} = \begin{pmatrix} 0 & \hat{\boldsymbol{\sigma}} \cdot \hat{\mathbf{p}} \\ \hat{\boldsymbol{\sigma}} \cdot \hat{\mathbf{p}} & 0 \end{pmatrix} \quad (312)$$

Analogously to (300) we can write

$$(\hat{\boldsymbol{\alpha}} \cdot \mathbf{r}) \cdot (\hat{\boldsymbol{\alpha}} \cdot \hat{\mathbf{p}}) = \mathbb{1}_2 \otimes [\mathbf{r} \cdot \hat{\mathbf{p}} + i \hat{\boldsymbol{\sigma}} \cdot (\mathbf{r} \times \hat{\mathbf{p}})] \quad (313)$$

We introduce the radial momentum \hat{p}_r such as

$$\mathbf{r} \cdot \hat{\mathbf{p}} = r \hat{p}_r + i \hbar \quad (314)$$

We can express the equation (313) with (314)

$$(\hat{\boldsymbol{\alpha}} \cdot \mathbf{r}) \cdot (\hat{\boldsymbol{\alpha}} \cdot \hat{\mathbf{p}}) = \mathbb{1}_2 \otimes [r \hat{p}_r \mathbb{1}_2 + i(\hbar \mathbb{1}_2 + \hat{\boldsymbol{\sigma}} \cdot \hat{\mathbf{l}})] \quad (315)$$

Let us define $\hat{\alpha}_r$ the scalar product between the vector $\hat{\boldsymbol{\alpha}}$ and the unitary radial vector $\mathbf{e}_r = \frac{\mathbf{r}}{r}$ (with $\|\mathbf{e}_r\| = 1$)

$$\hat{\alpha}_r = \hat{\boldsymbol{\alpha}} \cdot \mathbf{e}_r = \frac{(\hat{\boldsymbol{\alpha}} \cdot \mathbf{r})}{r} = \frac{1}{r} \begin{pmatrix} 0 & \hat{\boldsymbol{\sigma}} \cdot \mathbf{r} \\ \hat{\boldsymbol{\sigma}} \cdot \mathbf{r} & 0 \end{pmatrix} \quad (316)$$

Its square is from (298) equal to

$$(\hat{\alpha}_r)^2 = \frac{1}{r^2}(\hat{\alpha} \cdot \mathbf{r}) \cdot (\hat{\alpha} \cdot \mathbf{r}) = \frac{1}{r^2} \begin{pmatrix} (\hat{\sigma} \cdot \mathbf{r}) \cdot (\hat{\sigma} \cdot \mathbf{r}) & 0 \\ 0 & (\hat{\sigma} \cdot \mathbf{r}) \cdot (\hat{\sigma} \cdot \mathbf{r}) \end{pmatrix} = \mathbb{1}_4 \quad (317)$$

So from (317) and (316)

$$(\hat{\alpha} \cdot \mathbf{r}) \cdot (\hat{\alpha} \cdot \hat{\mathbf{p}}) = \hat{\alpha}_r r (\hat{\alpha} \cdot \hat{\mathbf{p}}) \quad (318)$$

By using (318) we multiply to the left the equation (315) with $\frac{1}{r}\hat{\alpha}_r$ and we get

$$(\hat{\alpha} \cdot \hat{\mathbf{p}}) = \hat{\alpha}_r \cdot \left[\hat{p}_r \mathbb{1}_4 + \frac{i}{r} \left[\hbar \mathbb{1}_4 + \mathbb{1}_2 \otimes (\hat{\sigma} \cdot \hat{\mathbf{l}}) \right] \right] \quad (319)$$

Let us define the analog to the operator $\hat{\mathbf{k}}$ introduced in (309) : the operator $\hat{\mathbf{K}}$

$$\hat{\mathbf{K}} \equiv \hat{\beta}(\hbar \mathbb{1}_4 + \hat{\Sigma} \cdot \hat{\mathbf{l}}) = \hat{\beta} \cdot \left[\mathbb{1}_2 \otimes (\hat{\sigma} \cdot \hat{\mathbf{l}} + \hbar \mathbb{1}_2) \right] = \hat{\beta} \cdot (\mathbb{1}_2 \otimes \hat{\mathbf{k}}) = \begin{pmatrix} \hat{\mathbf{k}} & 0 \\ 0 & -\hat{\mathbf{k}} \end{pmatrix} \quad (320)$$

The use of the $\hat{\beta}$ matrix in the $\hat{\mathbf{K}}$ operator will become clearer in the following. Thus the eigenvalue equation of the operator $\hat{\mathbf{K}}$ is

$$\hat{\mathbf{K}} \begin{pmatrix} \chi_{\kappa, m_j} \\ \chi_{-\kappa, m_j} \end{pmatrix} = \begin{pmatrix} \hat{\mathbf{k}} & 0 \\ 0 & -\hat{\mathbf{k}} \end{pmatrix} \begin{pmatrix} \chi_{\kappa, m_j} \\ \chi_{-\kappa, m_j} \end{pmatrix} = \hbar \kappa \begin{pmatrix} \chi_{\kappa, m_j} \\ \chi_{-\kappa, m_j} \end{pmatrix} \quad (321)$$

6. The 4-spinor ansatz

The 2x2 blocks structure of the Hamiltonian \hat{h}^D (291) requires an appropriate ansatz to describe the stationary state represented by the wave function $\psi(\mathbf{r})$

$$\psi(\mathbf{r}) = \begin{pmatrix} F(r) \chi_{\kappa, m_j}(\theta, \varphi) \\ iG(r) \chi_{-\kappa, m_j}(\theta, \varphi) \end{pmatrix} \quad (322)$$

$F(r)$ and $G(r)$ are the pure real radial parts, the angular parts are represented by the functions $\chi_{\kappa, m_j}(\theta, \varphi)$ and $\chi_{-\kappa, m_j}(\theta, \varphi)$, these are the four functions to determine by solving the stationary Dirac equation (290) $\hat{h}^D \psi(\mathbf{r}) = E \psi(\mathbf{r})$. The wave function is separable with respect to radial coordinates r and angular coordinates (θ, φ) as well as the Hamiltonian \hat{h}^D . So, $\psi(\mathbf{r})$ will be an eigenstate of the operators $\hat{\mathbf{j}}^2$ and $\hat{j}_4^3 = \hat{j}_{4,z}$, in the following we will establish the general solution for the Dirac hydrogen atom.

7. The angular wave functions

The Pauli spinors $\chi(\theta, \varphi)$ can be decomposed in three products, a Clebsch-Gordan coefficient, the usual spherical harmonics $Y_l^{m_l}(\theta, \varphi)$ and a Pauli-spinors $\omega(m_s)$.

$$\chi_{j,m_j}(\theta, \varphi) = \sum_{m_l, m_s} \langle l, m_l, s, m_s | j, m_j \rangle Y_l^{m_l}(\theta, \varphi) \omega(m_s) \quad (323)$$

The spherical harmonics $Y_l^{m_l}(\theta, \varphi)$ are obtained from standard quantum mechanics, one can find more details about the construction of spherical harmonics through the definition of ladder operators in [109] (phase factor could be different in other presentations).

$$Y_l^{m_l} = (-1)^{m_l} \sqrt{\frac{(2l+1)(l-m_l)!}{4\pi(l+m_l)!}} P_l^{m_l}(\cos \theta) e^{im_l \varphi} \quad (324)$$

where we introduced the associated Legendre polynomials given by

$$P_l^{m_l}(\cos \theta) = (1 - \cos^2 \theta)^{\frac{m_l}{2}} \frac{d^{m_l}}{d(\cos \theta)^{m_l}} \left[\frac{(-1)^l d^l (\cos^2 \theta - 1)^l}{2^l l! d(\cos \theta)^l} \right] \quad (325)$$

The Clebsch-Gordan vector coupling coefficients between \mathbf{l} and \mathbf{s} is given by

$$\langle l, m_l, s, m_s | j, m_j \rangle = \sqrt{\frac{(2l)!(2s)!}{(2j)!}} \sqrt{\frac{(j+m_j)!(j-m_j)!}{(l+m_l)!(l-m_l)!(s+m_s)!(s-m_s)!}} \quad (326)$$

The Pauli-spinors $\omega(m_s)$ is just a bidimensionnal vector which projects on $m_s = \pm \frac{1}{2}$ defined as

$$\omega\left(\frac{1}{2}\right) = \begin{pmatrix} 1 \\ 0 \end{pmatrix} \quad \text{and} \quad \omega\left(-\frac{1}{2}\right) = \begin{pmatrix} 0 \\ 1 \end{pmatrix} \quad (327)$$

Now we have fully defined the four-component angular wave function

$$\begin{pmatrix} \chi_{\kappa, m_j}(\theta, \varphi) \\ \chi_{-\kappa, m_j}(\theta, \varphi) \end{pmatrix} = \begin{pmatrix} \langle j - \frac{1}{2}, m_j - \frac{1}{2}, \frac{1}{2}, \frac{1}{2} | j, m_j \rangle Y_{j-\frac{1}{2}}^{m_j-\frac{1}{2}}(\theta, \varphi) \\ \langle j - \frac{1}{2}, m_j + \frac{1}{2}, \frac{1}{2}, -\frac{1}{2} | j, m_j \rangle Y_{j-\frac{1}{2}}^{m_j-\frac{1}{2}}(\theta, \varphi) \\ \langle j + \frac{1}{2}, m_j - \frac{1}{2}, \frac{1}{2}, \frac{1}{2} | j, m_j \rangle Y_{j+\frac{1}{2}}^{m_j+\frac{1}{2}}(\theta, \varphi) \\ \langle j + \frac{1}{2}, m_j + \frac{1}{2}, \frac{1}{2}, -\frac{1}{2} | j, m_j \rangle Y_{j+\frac{1}{2}}^{m_j+\frac{1}{2}}(\theta, \varphi) \end{pmatrix} \quad (328)$$

8. The radial stationary Dirac equation

The separation between radial and angular coordinates allow us to solve the stationary Dirac equation for the hydrogen atom in two parts. If we turn to the

radial part, we established in (319) an explicit form for the operator $\hat{\alpha} \cdot \hat{\mathbf{p}}$, we can express it in the following manner

$$\hat{\alpha} \cdot \hat{\mathbf{p}} = \hat{\alpha}_r \hat{p}_r + \frac{i}{r} \hat{\alpha}_r \hat{\beta} \hat{\mathbf{k}} \quad (329)$$

Thus the Hamiltonian \hat{h}^D can be written such as

$$\hat{h}^D = c \hat{\alpha}_r \hat{p}_r + \frac{ic}{r} \hat{\alpha}_r \hat{\beta} \hat{\mathbf{K}} + m_0 c^2 \hat{\beta} - \frac{Ze^2}{r} \mathbb{1}_4 \quad (330)$$

Or under a matrix form by writting in a more explicit fashion the operator $\hat{p}_r = -i\hbar \left[\frac{\partial}{\partial r} + \frac{1}{r} \right] = -i\hbar \frac{1}{r} \frac{\partial}{\partial r} r$

$$\hat{h}^D = \begin{pmatrix} \left[m_0 c^2 - \frac{Ze^2}{r} \right] \mathbb{1}_2 & -ic \left(\frac{\hat{\sigma} \cdot \mathbf{r}}{r} \right) \left(\frac{\hbar}{r} \frac{\partial}{\partial r} r - \frac{\hat{\mathbf{k}}}{r} \right) \\ -ic \left(\frac{\hat{\sigma} \cdot \mathbf{r}}{r} \right) \left(\frac{\hbar}{r} \frac{\partial}{\partial r} r - \frac{\hat{\mathbf{k}}}{r} \right) & \left[-m_0 c^2 - \frac{Ze^2}{r} \right] \mathbb{1}_2 \end{pmatrix} \quad (331)$$

One should notice that the angular coordinates are only linked to the operator $\hat{\mathbf{k}}$. The radial functions $F(r)$ and $G(r)$ will describe a part of the stationary states characterized by the quantum numbers n, κ (thus j) and the angular function $\chi(\theta, \varphi)$ will describe the other part with the quantum numbers κ (thus j) and m_j . $\chi(\theta, \varphi)$

$$\boldsymbol{\psi}(\mathbf{r}) = \begin{pmatrix} F_{n\kappa}(r) \chi_{\kappa, m_j}(\theta, \varphi) \\ iG_{n\kappa}(r) \chi_{-\kappa, m_j}(\theta, \varphi) \end{pmatrix} \quad (332)$$

It is demonstrated in [34] that the radial function as well as the angular function are orthonormalized, *i.e.* are such as

$$\langle F_{n,\kappa} | F_{\tilde{n},\tilde{\kappa}} \rangle + \langle G_{n,\kappa} | G_{\tilde{n},\tilde{\kappa}} \rangle = \delta_{n,\tilde{n}} \delta_{\kappa,\tilde{\kappa}} \quad (333)$$

$$\langle \chi_{\kappa, m_j} | \chi_{\tilde{\kappa}, \tilde{m}_j} \rangle = \delta_{\kappa, \tilde{\kappa}} \delta_{m_j, \tilde{m}_j} \quad (334)$$

Consequently the wave function $\boldsymbol{\psi}(\mathbf{r})$ is orthonormalized

$$\langle \boldsymbol{\psi}_{n,\kappa, m_j} | \boldsymbol{\psi}_{\tilde{n},\tilde{\kappa}, \tilde{m}_j} \rangle = \delta_{n\tilde{n}} \delta_{\kappa, \tilde{\kappa}} \delta_{m_j, \tilde{m}_j} \quad (335)$$

We can evaluate the product $\hat{h}^D \boldsymbol{\psi}(\mathbf{r})$ form (331) and (332)

$$\hat{h}^D \boldsymbol{\psi}(\mathbf{r}) = \begin{pmatrix} \left[m_0 c^2 - \frac{Ze^2}{r} \right] F_{n,\kappa}(r) \chi_{\kappa, m_j}(\theta, \varphi) + c \left(\frac{\hat{\sigma} \cdot \mathbf{r}}{r} \right) \left(\frac{\hbar}{r} \frac{\partial}{\partial r} r - \frac{\hat{\mathbf{k}}}{r} \right) G_{n,\kappa}(r) \chi_{-\kappa, m_j}(\theta, \varphi) \\ -ic \left(\frac{\hat{\sigma} \cdot \mathbf{r}}{r} \right) \left(\frac{\hbar}{r} \frac{\partial}{\partial r} r - \frac{\hat{\mathbf{k}}}{r} \right) F_{n,\kappa}(r) \chi_{\kappa, m_j}(\theta, \varphi) + i \left[-m_0 c^2 - \frac{Ze^2}{r} \right] G_{n,\kappa}(r) \chi_{-\kappa, m_j}(\theta, \varphi) \end{pmatrix} \quad (336)$$

We first act with the operator $\hat{\mathbf{k}}$ on the angular part χ by applying (310), then we move χ beside the second operator which can act on it : $\frac{\hat{\boldsymbol{\sigma}} \cdot \mathbf{r}}{r}$

$$\hat{h}^D \psi(\mathbf{r}) = \begin{pmatrix} \left[m_0 c^2 - \frac{Ze^2}{r} \right] F_{n,\kappa}(r) \chi_{\kappa,m_j}(\theta, \varphi) + \hbar c \left(\frac{\hat{\boldsymbol{\sigma}} \cdot \mathbf{r}}{r} \right) \chi_{-\kappa,m_j}(\theta, \varphi) \left(\frac{1}{r} \frac{\partial}{\partial r} r + \frac{\kappa}{r} \right) G_{n,\kappa}(r) \\ -i \hbar c \left(\frac{\hat{\boldsymbol{\sigma}} \cdot \mathbf{r}}{r} \right) \chi_{\kappa,m_j}(\theta, \varphi) \left(\frac{1}{r} \frac{\partial}{\partial r} r - \frac{\kappa}{r} \right) F_{n,\kappa}(r) + \left[-m_0 c^2 - \frac{Ze^2}{r} \right] i G_{n,\kappa}(r) \chi_{-\kappa,m_j}(\theta, \varphi) \end{pmatrix} \quad (337)$$

It is shown in [34] that the operator $\frac{\hat{\boldsymbol{\sigma}} \cdot \mathbf{r}}{r}$ acts only on Pauli spinors $\chi(\theta, \varphi)$

$$\begin{aligned} \left(\frac{\hat{\boldsymbol{\sigma}} \cdot \mathbf{r}}{r} \right) \chi_{\kappa,m_j}(\theta, \varphi) &= -\chi_{-\kappa,m_j}(\theta, \varphi) \\ \left(\frac{\hat{\boldsymbol{\sigma}} \cdot \mathbf{r}}{r} \right) \chi_{-\kappa,m_j}(\theta, \varphi) &= -\chi_{\kappa,m_j}(\theta, \varphi) \end{aligned} \quad (338)$$

After applying (338) the resulting vector (337) becomes

$$\hat{h}^D \psi(\mathbf{r}) = \begin{pmatrix} \left[m_0 c^2 - \frac{Ze^2}{r} \right] F_{n,\kappa}(r) \chi_{\kappa,m_j}(\theta, \varphi) - \hbar c \chi_{\kappa,m_j}(\theta, \varphi) \left(\frac{1}{r} \frac{\partial}{\partial r} r + \frac{\kappa}{r} \right) G_{n,\kappa}(r) \\ i \hbar c \chi_{-\kappa,m_j}(\theta, \varphi) \left(\frac{1}{r} \frac{\partial}{\partial r} r - \frac{\kappa}{r} \right) F_{n,\kappa}(r) + \left[-m_0 c^2 - \frac{Ze^2}{r} \right] i G_{n,\kappa}(r) \chi_{-\kappa,m_j}(\theta, \varphi) \end{pmatrix} \quad (339)$$

We can now isolate the angular part

$$\hat{h}^D \psi(\mathbf{r}) = \begin{pmatrix} \left[\left(m_0 c^2 - \frac{Ze^2}{r} \right) F_{n,\kappa}(r) - \hbar c \left(\frac{1}{r} \frac{\partial}{\partial r} r + \frac{\kappa}{r} \right) G_{n,\kappa}(r) \right] \chi_{\kappa,m_j}(\theta, \varphi) \\ \left[\hbar c \left(\frac{1}{r} \frac{\partial}{\partial r} r - \frac{\kappa}{r} \right) F_{n,\kappa}(r) + \left(-m_0 c^2 - \frac{Ze^2}{r} \right) G_{n,\kappa}(r) \right] i \chi_{-\kappa,m_j}(\theta, \varphi) \end{pmatrix} = E \psi(\mathbf{r}) \quad (340)$$

If we multiply to the left by the bra $\langle \chi_{\kappa,m_j}, -i \chi_{-\kappa,m_j} |$ the two sides of the equation (340), we get a pure radial form (The Pauli spinors χ are orthonormalized (334))

$$\begin{pmatrix} \left(m_0 c^2 - \frac{Ze^2}{r} \right) F_{n,\kappa}(r) - \hbar c \left(\frac{1}{r} \frac{d}{dr} r + \frac{\kappa}{r} \right) G_{n,\kappa}(r) \\ \hbar c \left(\frac{1}{r} \frac{d}{dr} r - \frac{\kappa}{r} \right) F_{n,\kappa}(r) + \left(-m_0 c^2 - \frac{Ze^2}{r} \right) G_{n,\kappa}(r) \end{pmatrix} = E_{n,\kappa} \begin{pmatrix} F_{n,\kappa}(r) \\ G_{n,\kappa}(r) \end{pmatrix} \quad (341)$$

Let us introduce a second set of radial functions for convenience

$$\psi_{n,\kappa,m_j}(\mathbf{r}) = \begin{pmatrix} F_{n,\kappa}(r) \chi_{\kappa,m_j}(\theta, \varphi) \\ i G_{n,\kappa}(r) \chi_{-\kappa,m_j}(\theta, \varphi) \end{pmatrix} = \begin{pmatrix} \frac{1}{r} P_{n,\kappa}(r) \chi_{\kappa,m_j}(\theta, \varphi) \\ \frac{i}{r} Q_{n,\kappa}(r) \chi_{-\kappa,m_j}(\theta, \varphi) \end{pmatrix} \quad (342)$$

By putting the new set (342) into (341) we get

$$\begin{pmatrix} \left(m_0 c^2 - \frac{Ze^2}{r} \right) \frac{1}{r} P_{n,\kappa}(r) - \hbar c \left(\frac{1}{r} \frac{d}{dr} r + \frac{\kappa}{r} \right) \frac{1}{r} Q_{n,\kappa}(r) \\ \hbar c \left(\frac{1}{r} \frac{d}{dr} r - \frac{\kappa}{r} \right) \frac{1}{r} P_{n,\kappa}(r) + \left(-m_0 c^2 - \frac{Ze^2}{r} \right) \frac{1}{r} Q_{n,\kappa}(r) \end{pmatrix} = \frac{1}{r} E_{n,\kappa} \begin{pmatrix} P_{n,\kappa}(r) \\ Q_{n,\kappa}(r) \end{pmatrix} \quad (343)$$

and then

$$\begin{pmatrix} \left(m_0 c^2 - \frac{Ze^2}{r} \right) P_{n,\kappa}(r) - \hbar c \left(\frac{d}{dr} + \frac{\kappa}{r} \right) Q_{n,\kappa}(r) \\ \hbar c \left(\frac{d}{dr} - \frac{\kappa}{r} \right) P_{n,\kappa}(r) + \left(-m_0 c^2 - \frac{Ze^2}{r} \right) Q_{n,\kappa}(r) \end{pmatrix} = E_{n,\kappa} \begin{pmatrix} P_{n,\kappa}(r) \\ Q_{n,\kappa}(r) \end{pmatrix} \quad (344)$$

The differential equation system can be solved analytically, we will proceed for the analytical spinor of the hydrogen-like atoms ground states. Let us introduce some substitutions for sake of clarity

$$A^{\pm} \equiv \frac{m_0 c^2 \pm E}{\hbar c} \quad , \quad C \equiv \frac{Z e^2}{\hbar c} \quad (345)$$

Where the substitute C contains point nucleus charge information (we drops the indices n, κ for clarity). Inserting (345) in (344) we get the two differential equations

$$\left(A^- - \frac{C}{r}\right) P(r) + \left(-\frac{d}{dr} - \frac{\kappa}{r}\right) Q(r) = 0 \quad (346)$$

$$\left(\frac{d}{dr} - \frac{\kappa}{r}\right) P(r) - \left(A^+ + \frac{C}{r}\right) Q(r) = 0 \quad (347)$$

If we put these two equation together (346) and (347) we get a second order differential equation for $Q(r)$

$$\frac{d^2 Q(r)}{dr^2} - \frac{C}{r^2} \left(A^- - \frac{C}{r}\right)^{-1} \frac{dQ(r)}{dr} + \left[-\frac{\kappa(\kappa+1)}{r^2} - \frac{\kappa C}{r^3} \left(A^- - \frac{C}{r}\right)^{-1} - \left(A^+ + \frac{C}{r}\right) \left(A^- - \frac{C}{r}\right)\right] Q(r) = 0 \quad (348)$$

Solutions for large r will give an idea of an appropriate ansatz for the radial functions so if $r \rightarrow \infty$ then (348) becomes

$$\frac{d^2 Q(r)}{dr^2} - (A^+ A^-) Q(r) = 0 \quad \text{with a discriminant of } \Delta = 4A^+ A^- \quad (349)$$

$$\Delta = \frac{4(m_0^2 c^4 - E^2)}{\hbar^2 c^2} > 0 \quad \text{since } E < m_0 c^2 \quad (350)$$

The assumption in (350) is reasonable, to give an order of magnitude : the rest energy of the electron $m_0 c^2$ is approximately equal to 37560 times the ionization potential of hydrogen. These previous consideration allows us to set the following exponential forms for $P(r)$ and $Q(r)$

$$P(r) = p(r) e^{-Ar} \quad (351)$$

$$Q(r) = q(r) e^{-Ar} \quad (352)$$

With $A = \sqrt{A^+ A^-}$ deduced from (349). The short range behaviour ($r \rightarrow 0$) of the radial solutions can be studied if we assume it could be expanded in a Taylor series around 0 like $e^{-Ar} = \sum_{i=0}^{\infty} \frac{(-Ar)^i}{i!}$

$$p(r) = r^{\eta} \sum_{i=0}^{\infty} p_i r^i \quad (353)$$

$$q(r) = r^\eta \sum_{i=0}^{\infty} q_i r^i \quad (354)$$

Hence the product of $p(r)$ or $q(r)$ with e^{-Ar} will give a Taylor expansion around 0 of $P(r)$ or $Q(r)$. The unknown exponent η will be determined in the following, it is common to $p(r)$ and $q(r)$ to avoid a cancelation of first terms of $P(r)$ and $Q(r)$. We can now insert these new Taylor expendable radial functions into the differential equations (346) and (347)

$$\frac{dq(r)}{dr} - Aq(r) + \frac{\kappa}{r}q(r) + \left(\frac{C}{r} - A^-\right)p(r) = 0 \quad (355)$$

$$\frac{dp(r)}{dr} - Ap(r) - \frac{\kappa}{r}p(r) - \left(\frac{C}{r} + A^+\right)q(r) = 0 \quad (356)$$

Below the exponential vanishes and we multiplied the first equation (355) by (-1) . Let us now insert the Taylor expansion form of $p(r)$ (353) and $q(r)$ (354)

$$\sum_{i=0}^{\infty} (i+\eta) q_i r^{i+\eta-1} - A \sum_{i=0}^{\infty} q_i r^{i+\eta} + \kappa \sum_{i=0}^{\infty} q_i r^{i+\eta-1} + C \sum_{i=0}^{\infty} p_i r^{i+\eta-1} - A^- \sum_{i=0}^{\infty} p_i r^{i+\eta} = 0 \quad (357)$$

$$\sum_{i=0}^{\infty} (i+\eta) p_i r^{i+\eta-1} - A \sum_{i=0}^{\infty} p_i r^{i+\eta} - \kappa \sum_{i=0}^{\infty} p_i r^{i+\eta-1} - C \sum_{i=0}^{\infty} q_i r^{i+\eta-1} - A^+ \sum_{i=0}^{\infty} q_i r^{i+\eta} = 0 \quad (358)$$

If we multiply the two equation below by $r^{1-\eta}$ we can remove η from the various exponent

$$\sum_{i=0}^{\infty} (i+\eta) q_i r^i - A \sum_{i=0}^{\infty} q_i r^{i+1} + \kappa \sum_{i=0}^{\infty} q_i r^i + C \sum_{i=0}^{\infty} p_i r^i - A^- \sum_{i=0}^{\infty} p_i r^{i+1} = 0 \quad (359)$$

$$\sum_{i=0}^{\infty} (i+\eta) p_i r^i - A \sum_{i=0}^{\infty} p_i r^{i+1} - \kappa \sum_{i=0}^{\infty} p_i r^i - C \sum_{i=0}^{\infty} q_i r^i - A^+ \sum_{i=0}^{\infty} q_i r^{i+1} = 0 \quad (360)$$

Let us look at $r = 0$ equations, they are usefull to find an expression for η

$$\begin{cases} \eta q_0 + \kappa q_0 + C p_0 = 0 \\ \eta p_0 - \kappa p_0 - C q_0 = 0 \end{cases} \Rightarrow q_0 = \frac{\eta - \kappa}{C} p_0 = \frac{-C}{\eta + \kappa} p_0 \quad (361)$$

The latter leads to

$$\eta^2 - \kappa^2 = -C^2 \Rightarrow \eta = \pm \sqrt{\kappa^2 - C^2} \quad (362)$$

We need a positive exponent η in (353) and (354) in order to have quadratically integrable functions and then acceptable eigenfunctions, more precisely the integral

$$\int (|F(r)|^2 + |G(r)|^2) r^2 dr = \int (|P(r)|^2 + |Q(r)|^2) dr \quad (363)$$

must exist, consequently

$$\eta = \sqrt{\kappa^2 - \frac{Z^2 e^4}{\hbar^2 c^2}} \quad (364)$$

To deal with the unknowns p_i and q_i we can find a recursion relation between those by setting r^i as a common factor in equations (359) and (360)

$$\sum_{i=1}^{\infty} [(i + \eta + \kappa)q_i - Aq_{i-1} + Cp_i - A^-p_{i-1}] r^i = 0 \quad (365)$$

$$\sum_{i=1}^{\infty} [(i + \eta - \kappa)p_i - Ap_{i-1} - Cq_i - A^+q_{i-1}] r^i = 0 \quad (366)$$

Whose solutions are obtained if all coefficients vanish independently. $i = 0$ terms vanish because of the choice of η in (362)

$$(i + \eta + \kappa)q_i - Aq_{i-1} + Cp_i - A^-p_{i-1} = 0 \quad (367)$$

$$(i + \eta - \kappa)p_i - Ap_{i-1} - Cq_i - A^+q_{i-1} = 0 \quad (368)$$

First we multiply the first equation (367) by A and the second (368) by A^- , finally we subtract the two resulting equations

$$[A(i + \eta + \kappa) + A^-C] q_i + (-A^2 + A^-A^+)q_{i-1} + [AC - A^-(i + \eta - \kappa)] p_i + (-AA^- + A^-A)p_{i-1} = 0 \quad (369)$$

Then we multiply the first equation (367) by A^+ and the second (368) by A , finally we subtract the two resulting equations

$$[A^+(i + \eta + \kappa) + AC] q_i + (-A^+A + AA^+)q_{i-1} + [A^+C - A(i + \eta - \kappa)] p_i + (-A^+A^- + A^2)p_{i-1} = 0 \quad (370)$$

Since $A^+A^- = A^2$ in (351) and (352) the p_{i-1} and q_{i-1} terms vanish in both equations

$$[A(i + \eta + \kappa) + A^-C] q_i + [AC - A^-(i + \eta - \kappa)] p_i = 0 \quad (371)$$

$$[A^+(i + \eta + \kappa) + AC] q_i + [A^+C - A(i + \eta - \kappa)] p_i = 0 \quad (372)$$

Now we can finally express q_i in function of p_i in two different manners

$$q_i = \frac{-A^+C + A(i + \eta - \kappa)}{A^+(i + \eta + \kappa) + AC} p_i = \frac{-AC + A^-(i + \eta - \kappa)}{A(i + \eta + \kappa) + A^-C} p_i \quad (373)$$

The total 4-spinor must have a square integrable representation, therefore the radial functions $p(r)$ and $q(r)$ must terminate, to investigate this requirement we will look at long range behaviour ($r \rightarrow \infty$ and thus $i \rightarrow \infty$) of (373)

$$q_i = p_i \lim_{i \rightarrow \infty} \frac{-A^+C + A(i + \eta - \kappa)}{A^+(i + \eta + \kappa) + AC} = \left(\frac{A}{A^+} \right) p_i \quad (374)$$

For $(i \rightarrow \infty)$ equations (367) and (368) become

$$iq_i - Aq_{i-1} + Cp_i - A^-p_{i-1} = 0 \quad (375)$$

$$ip_i - Ap_{i-1} - Cq_i - A^+q_{i-1} = 0 \quad (376)$$

With $i \gg \kappa$ and $i \gg \eta$, we will establish a relation between q_i and q_{i-1} for $i \rightarrow \infty$ in (375) by replacing p_i and p_{i+1} in equation (376) with q_i and q_{i-1} using (374)

$$iq_i - Aq_{i-1} + C \left(\frac{A^+}{A} \right) q_i - A^- \left(\frac{A^+}{A} \right) q_{i-1} = 0 \quad (377)$$

which yields after simplification to

$$\left(i + C \frac{A^+}{A} \right) q_i - 2Aq_{i-1} = 0 \quad (378)$$

and then

$$q_{i-1} = \frac{1}{2} \left(\frac{i}{A} + \frac{CA^+}{A^2} \right) q_i \xrightarrow{i \rightarrow \infty} \frac{i}{2A} q_i \quad (379)$$

We have consequently a recursive relation between q_i and q_{i-1} for $i \rightarrow \infty$

$$q_i \xrightarrow{i \rightarrow \infty} \frac{2A}{i} q_{i-1} \quad (380)$$

Analogously we find one between p_i and p_{i-1}

$$p_i \xrightarrow{i \rightarrow \infty} \frac{2A}{i} p_{i-1} \quad (381)$$

By using (380) and (381) we can write $p(r)$ and $q(r)$ from (353) and (354) for $i \rightarrow \infty$

$$p(r) \xrightarrow{i \rightarrow \infty} \sum_{k=0}^{\infty} \frac{(2A)^k}{k!} r^k = e^{2Ar} \quad (382)$$

$$q(r) \xrightarrow{i \rightarrow \infty} \sum_{k=0}^{\infty} \frac{(2A)^k}{k!} r^k = e^{2Ar} \quad (383)$$

These latter equation (382) and (383) exhibit a wrong behaviour for large r (thus large i), they should vanish to yield to normalizable spinors. If we want square-integrable spinors $p(r)$ and $q(r)$ have to truncate, to proceed this aim let $(i-1) = n_r$ be the truncation rank then

$$p_{n_r} = q_{n_r} = 0 \quad (384)$$

The recursion relations in (375) and (376) give

$$-Aq_{n_r} - A^-p_{n_r} = 0 \quad \Leftrightarrow \quad q_{n_r} = -\frac{A^-}{A} p_{n_r} \quad (385)$$

$$-Ap_{n_r} - A^+q_{n_r} = 0 \quad \Leftrightarrow \quad p_{n_r} = -\frac{A^+}{A}q_{n_r} \quad (386)$$

Now we can use the (385) above combined with the first equation of (373) to get

$$-\frac{A^-}{A}p_{n_r} = \frac{-A^+C + A(n_r + \eta - \kappa)}{A^+(n_r + \eta + \kappa) + AC}p_{n_r} \quad (387)$$

Then we find a relation which have to be fulfilled for any p_{n_r}

$$-\frac{A^-}{A} [A^+(n_r + \eta + \kappa) + AC] = -A^+C + A(n_r + \eta - \kappa) \quad (388)$$

which simplify into

$$-A(n_r + \eta + \kappa) - A^-C = -A^+C + A(n_r + \eta - \kappa) \quad (389)$$

$$(A^+ - A^-)C = 2A(n_r + \eta) \quad (390)$$

9. Energy Eigenvalue

We can finally obtain from (390) with the substitution from (345) and η from (362) this energy equation

$$\left(\frac{m_0c^2 + E}{\hbar c} - \frac{m_0c^2 - E}{\hbar c} \right) \frac{Ze^2}{\hbar c} = 2 \frac{\sqrt{m_0^2c^4 - E^2}}{\hbar c} \left(n_r + \sqrt{\kappa^2 - \frac{Z^2e^4}{\hbar^2c^2}} \right) \quad (391)$$

We multiply by $\frac{\hbar c}{2}$ and then take the square of (391)

$$E^2 \frac{Z^2e^4}{\hbar^2c^2} = [m_0^2c^4 - E^2] \left(n_r + \sqrt{\kappa^2 - \frac{Z^2e^4}{\hbar^2c^2}} \right)^2 \quad (392)$$

If we isolate the energy E we get this expression

$$E = \pm m_0c^2 \sqrt{\frac{\left(n_r + \sqrt{\kappa^2 - \frac{Z^2e^4}{\hbar^2c^2}} \right)^2}{\frac{Z^2e^4}{\hbar^2c^2} + \left(n_r + \sqrt{\kappa^2 - \frac{Z^2e^4}{\hbar^2c^2}} \right)^2}} \quad (393)$$

$$E = \pm m_0c^2 \left[1 + \frac{\frac{Z^2e^4}{\hbar^2c^2}}{\left(n_r + \sqrt{\kappa^2 - \frac{Z^2e^4}{\hbar^2c^2}} \right)^2} \right]^{-\frac{1}{2}} \quad (394)$$

A first comment about the equation above (394), a pair of spinor $(-\kappa, \kappa)$ lead to the same energy and are thus degenerate. A second one will be about the truncation

rank integer n_r defined in (384) which can take any integer values : $n_r \in \mathbb{N}$. It is also called the radial quantum number and is related to the principal quantum number n and κ , from the truncation condition (385) we can find for $n_r = 0$

$$\frac{q_0}{p_0} = -\frac{A^-}{A} = -\frac{m_0c^2 - E}{\sqrt{m_0^2c^4 - E^2}} < 0 \quad \text{since} \quad E < m_0c^2 \quad (395)$$

We can rewrite (395) for ($r \rightarrow 0$) by using the equation (361)

$$\frac{q_0}{p_0} = \frac{-C}{\eta + \kappa} = \frac{\frac{-Ze^2}{\hbar c}}{\sqrt{\kappa^2 - \frac{Z^2e^4}{\hbar^2c^2}} + \kappa} \quad \begin{cases} < 0 \text{ if } \kappa > 0 \\ > 0 \text{ if } \kappa < 0 \end{cases} \quad (396)$$

Equation (395) and (396) together imply we must reject the $\kappa < 0$ case if $n_r = 0$, then the principal quantum number n can be defined as

$$n = n_r + |\kappa| = n_r + j + \frac{1}{2} \quad (397)$$

The final form for energy eigenvalue (394) for the electronic bound state in Dirac hydrogen-like atoms can be obtained, let us introduce the Sommerfeld's fine-structure constant $\alpha = \frac{e^2}{\hbar c}$

$$E = \frac{m_0c^2}{\sqrt{1 + \frac{Z^2\alpha^2}{(n-|\kappa|+\sqrt{\kappa^2-Z^2\alpha^2})^2}}} = \frac{m_0c^2}{\sqrt{1 + \frac{Z^2\alpha^2}{(n-j-\frac{1}{2}+\frac{1}{2}\sqrt{4j^2+4j+1-4Z^2\alpha^2})^2}}} \quad (398)$$

All the hydrogen-like state energy can be determined since they are characterized their quantum number : $E(n, j)$. For example the ground state energy of the hydrogen atom ($Z = 1$) will be

$$E\left(1, \frac{1}{2}\right) = m_0c^2\sqrt{1-\alpha^2} \quad (399)$$

D. The Pauli Equation

In this section we bring more details about the derivation of the Pauli equation. We start from the bispinor form of the Dirac equation with an external electric field, without magnetic field ($\mathbf{A} = 0$) since for atoms and molecules we only need the nucleus electric field.

$$\begin{pmatrix} [m_0c^2 + V - E] \mathbb{1}_2 & c\hat{\boldsymbol{\sigma}} \cdot \hat{\mathbf{p}} \\ c\hat{\boldsymbol{\sigma}} \cdot \hat{\mathbf{p}} & [-m_0c^2 + V - E] \mathbb{1}_2 \end{pmatrix} \begin{pmatrix} \psi^L(\mathbf{x}) \\ \psi^S(\mathbf{x}) \end{pmatrix} = 0 \quad (400)$$

We need to redefine the energy reference to have an energy equal to zero instead of m_0c^2 for the lowest possible energy value like with Schrödinger equation, let us introduce

$$E_0 = E - m_0c^2 \quad (401)$$

We get the following equation system

$$(V - E_0)\psi^L(\mathbf{x}) + c\hat{\boldsymbol{\sigma}} \cdot \hat{\mathbf{p}}\psi^S(\mathbf{x}) = 0 \quad (402)$$

$$c\hat{\boldsymbol{\sigma}} \cdot \hat{\mathbf{p}}\psi^L(\mathbf{x}) + (V - E_0 - 2m_0c^2)\psi^S(\mathbf{x}) = 0 \quad (403)$$

From the equation (403) we can express the small component in function of the large component

$$\psi^S(\mathbf{x}) = -\frac{c\hat{\boldsymbol{\sigma}} \cdot \hat{\mathbf{p}}}{V - E_0 - 2m_0c^2}\psi^L(\mathbf{x}) \quad (404)$$

By inserting the equation (404) in the equation (402) we obtain the following equation for the large component

$$(V - E_0)\psi^L(\mathbf{x}) - c\hat{\boldsymbol{\sigma}} \cdot \hat{\mathbf{p}} \left[\frac{1}{V - E_0 - 2m_0c^2} \right] c\hat{\boldsymbol{\sigma}} \cdot \hat{\mathbf{p}} \psi^L(\mathbf{x}) = 0 \quad (405)$$

and (406) can be rewritten into

$$(V - E_0)\psi^L(\mathbf{x}) + \frac{c^2}{2m_0c^2} \hat{\boldsymbol{\sigma}} \cdot \hat{\mathbf{p}} \left[1 - \frac{V - E_0}{2m_0c^2} \right]^{-1} \hat{\boldsymbol{\sigma}} \cdot \hat{\mathbf{p}} \psi^L(\mathbf{x}) = 0 \quad (406)$$

The equation (406) will be Taylor expanded $\left(\frac{1}{(1-x)} = 1 + x + x^2 + \dots \right)$ since $\frac{V-E_0}{2m_0c^2} \rightarrow 0$ for low-energy physics, the expanded term becomes

$$\left[1 - \frac{V - E_0}{2m_0c^2} \right]^{-1} = 1 + \frac{(V - E_0)}{2m_0c^2} + \frac{(V - E_0)^2}{4m_0^2c^4} + \dots \quad (407)$$

Substituting (407) in the equation (406) we get

$$\left[(V - E_0) + \frac{1}{2m_0}(\hat{\boldsymbol{\sigma}} \cdot \hat{\mathbf{p}})(\hat{\boldsymbol{\sigma}} \cdot \hat{\mathbf{p}}) + \frac{1}{4m_0^2c^2}(\hat{\boldsymbol{\sigma}} \cdot \hat{\mathbf{p}})(V - E_0)(\hat{\boldsymbol{\sigma}} \cdot \hat{\mathbf{p}}) + \dots \right] \psi^L(\mathbf{x}) = 0 \quad (408)$$

From the Dirac relation introduced in (300) the second term in (408) simplifies in

$$(\hat{\boldsymbol{\sigma}} \cdot \hat{\mathbf{p}})(\hat{\boldsymbol{\sigma}} \cdot \hat{\mathbf{p}}) = \mathbf{p}^2 \quad (409)$$

The third term in (408) is also expanded from the Dirac relation

$$(\hat{\boldsymbol{\sigma}} \cdot \hat{\mathbf{p}})(V - E_0)(\hat{\boldsymbol{\sigma}} \cdot \hat{\mathbf{p}}) = (V - E_0)(\hat{\boldsymbol{\sigma}} \cdot \hat{\mathbf{p}})(\hat{\boldsymbol{\sigma}} \cdot \hat{\mathbf{p}}) + (\hat{\boldsymbol{\sigma}} \cdot \hat{\mathbf{p}}V)(\hat{\boldsymbol{\sigma}} \cdot \hat{\mathbf{p}}) \quad (410)$$

$$= (V - E_0)\mathbf{p}^2 + \hat{\mathbf{p}}V \cdot \hat{\mathbf{p}} + i\hat{\boldsymbol{\sigma}} \cdot (\hat{\mathbf{p}}V \times \hat{\mathbf{p}}) \quad (411)$$

$$= (V - E_0)\mathbf{p}^2 + \hbar[-i(\nabla V) \cdot \hat{\mathbf{p}} + \hat{\boldsymbol{\sigma}} \cdot (\nabla V) \times \hat{\mathbf{p}}] \quad (412)$$

The 4-component ψ is normalized but not the large component ψ^L alone, we need to renormalize the large component in order to have a consistent hamiltonian and then we make the replacement

$$\psi^N = \hat{O}\psi^L \quad (413)$$

where ψ^N is normalized, *i.e.*

$$1 = \int d\mathbf{x} \psi^{N\dagger} \psi^N = \int d\mathbf{x} \psi^{L\dagger} \hat{O}^\dagger \hat{O} \psi^L = \int d\mathbf{x} [\psi^{L\dagger} \psi^L + \psi^{S\dagger} \psi^S] \quad (414)$$

If we insert the relation between the large and the small component (404) we get

$$\begin{aligned} 1 &= \int d\mathbf{x} \psi^{L\dagger} \hat{O}^\dagger \hat{O} \psi^L = \int d\mathbf{x} \left[\psi^{L\dagger} \psi^L + \psi^{L\dagger} (\hat{\boldsymbol{\sigma}} \cdot \hat{\mathbf{p}}) \frac{c^2}{(V - E_0 - 2m_0 c^2)^2} (\hat{\boldsymbol{\sigma}} \cdot \hat{\mathbf{p}}) \psi^L \right] \\ &= \int d\mathbf{x} \psi^{L\dagger} \left[1 + \frac{1}{4m_0^2 c^2} (\hat{\boldsymbol{\sigma}} \cdot \hat{\mathbf{p}}) \left[1 - \frac{V - E_0}{2m_0 c^2} \right]^{-2} (\hat{\boldsymbol{\sigma}} \cdot \hat{\mathbf{p}}) \right] \psi^L \end{aligned} \quad (415)$$

We deduce by identification in (415) that

$$\hat{O}^\dagger \hat{O} = 1 + \frac{1}{4m_0^2 c^2} (\hat{\boldsymbol{\sigma}} \cdot \hat{\mathbf{p}}) \left[1 - \frac{V - E_0}{2m_0 c^2} \right]^{-2} (\hat{\boldsymbol{\sigma}} \cdot \hat{\mathbf{p}}) \quad (416)$$

Since we choose \hat{O} hermitian, the square root of (416) gives the transformation operator \hat{O}

$$\hat{O} = \sqrt{1 + \frac{1}{4m_0^2 c^2} (\hat{\boldsymbol{\sigma}} \cdot \hat{\mathbf{p}}) \left[1 - \frac{V - E_0}{2m_0 c^2} \right]^{-2} (\hat{\boldsymbol{\sigma}} \cdot \hat{\mathbf{p}})} \quad (417)$$

The square root can be expanded in a Taylor serie ($\sqrt{1+x} = 1 + \frac{x}{2} + \dots$)

$$\hat{O} = 1 + \frac{1}{8m_0^2 c^2} (\hat{\boldsymbol{\sigma}} \cdot \hat{\mathbf{p}}) \left[1 - \frac{V - E_0}{2m_0 c^2} \right]^{-2} (\hat{\boldsymbol{\sigma}} \cdot \hat{\mathbf{p}}) + \dots \quad (418)$$

Then the square term in bracket is also Taylor expanded ($\frac{1}{(1-x)^2} = 1 + 2x + \dots$)

$$\begin{aligned} \hat{O} &= 1 + \frac{1}{8m_0^2 c^2} (\hat{\boldsymbol{\sigma}} \cdot \hat{\mathbf{p}}) \left[1 + \frac{V - E_0}{m_0 c^2} + \dots \right] (\hat{\boldsymbol{\sigma}} \cdot \hat{\mathbf{p}}) + \dots \\ &= 1 + \frac{1}{8m_0^2 c^2} \mathbf{p}^2 + \dots \end{aligned} \quad (419)$$

We truncate the expansion before c^{-4} since we want an approximated Hamiltonian at the c^{-2} order, so we write \hat{O} and also \hat{O}^{-1} deduced from the inverse square root in (417) with the same procedure

$$\hat{O} \simeq 1 + \frac{1}{8m_0^2 c^2} \mathbf{p}^2 \quad (420)$$

$$\hat{\mathcal{O}}^{-1} \simeq 1 - \frac{1}{8m_0^2 c^2} \mathbf{p}^2 \quad (421)$$

Now we come back on the expression (408) which can be expressed

$$\left[\hat{\mathcal{H}} - E_0 \right] \psi^L = 0 \quad \Rightarrow \quad \hat{\mathcal{H}} \psi^L = E_0 \psi^L \quad (422)$$

$\hat{\mathcal{H}}$ is the c^{-2} order approximated Hamiltonian we want to build. By inserting in (422) $\hat{\mathcal{O}}^{-1} \hat{\mathcal{O}}$ after the Hamiltonian and by multiplying to left by $\hat{\mathcal{O}}$ the normalized wave function can appear

$$\hat{\mathcal{O}} \hat{\mathcal{H}} \hat{\mathcal{O}}^{-1} \hat{\mathcal{O}} \psi^L = E_0 \hat{\mathcal{O}} \psi^L \quad (423)$$

$$\hat{\mathcal{O}} \hat{\mathcal{H}} \hat{\mathcal{O}}^{-1} \psi^N = E_0 \psi^N \quad (424)$$

The equation (424) is not consistent in this form, the Hamiltonian will still contain the energy, to avoid this problem we can multiply to the left with $\hat{\mathcal{O}}^{-2}$ to obtain

$$\hat{\mathcal{O}}^{-1} \hat{\mathcal{H}} \hat{\mathcal{O}}^{-1} \psi^N = E_0 \hat{\mathcal{O}}^{-2} \psi^N \quad (425)$$

From the equation (408) we can write $\hat{\mathcal{H}}$ as

$$\hat{\mathcal{H}} = V + \hat{T} + \frac{1}{4m_0^2 c^2} (\hat{\boldsymbol{\sigma}} \cdot \hat{\mathbf{p}}) (V - E_0) (\hat{\boldsymbol{\sigma}} \cdot \hat{\mathbf{p}}) \quad (426)$$

With $\hat{T} = \frac{\mathbf{p}^2}{2m_0}$ the nonrelativistic kinetic energy operator. We can substitute $\hat{\mathcal{H}}$ in the expression (425) and we get

$$\hat{\mathcal{O}}^{-1} \left[V + \hat{T} + \frac{1}{4m_0^2 c^2} (\hat{\boldsymbol{\sigma}} \cdot \hat{\mathbf{p}}) (V - E_0) (\hat{\boldsymbol{\sigma}} \cdot \hat{\mathbf{p}}) \right] \hat{\mathcal{O}}^{-1} \psi^N = E_0 \hat{\mathcal{O}}^{-2} \psi^N \quad (427)$$

Applying $\hat{\mathcal{O}}^{-1}$ and keeping only the term of the order c^{-2} it comes

$$\left(1 - \frac{1}{8m_0^2 c^2} \mathbf{p}^2 \right) \left[V + \hat{T} + \frac{1}{4m_0^2 c^2} (\hat{\boldsymbol{\sigma}} \cdot \hat{\mathbf{p}}) (V - E_0) (\hat{\boldsymbol{\sigma}} \cdot \hat{\mathbf{p}}) \right] \left(1 - \frac{1}{8m_0^2 c^2} \mathbf{p}^2 \right) \psi^N = E_0 \left(1 - \frac{1}{8m_0^2 c^2} \mathbf{p}^2 \right)^2 \psi^N \quad (428)$$

$$\left\{ V + \hat{T} + \frac{1}{4m_0^2 c^2} \left[(\hat{\boldsymbol{\sigma}} \cdot \hat{\mathbf{p}}) V (\hat{\boldsymbol{\sigma}} \cdot \hat{\mathbf{p}}) - E_0 \mathbf{p}^2 - \hat{T} \mathbf{p}^2 - \frac{1}{2} (\mathbf{p}^2 V + V \mathbf{p}^2) \right] \right\} \psi^N = \left(E_0 - \frac{E_0}{4m_0^2 c^2} \mathbf{p}^2 \right) \psi^N \quad (429)$$

On the left and right hand site of (429) the extra problematic energy term vanishes, there is no more an energy dependence on the Hamiltonian side. The last term on the left hand side can be expanded to

$$\frac{1}{2} (\mathbf{p}^2 V + V \mathbf{p}^2) = -\hbar^2 \left[\frac{1}{2} (\nabla^2 V) + (\nabla V) \cdot \nabla + V \nabla^2 \right] \quad (430)$$

and the first term in the brackets in (429) expands to

$$(\hat{\boldsymbol{\sigma}} \cdot \hat{\mathbf{p}})V(\hat{\boldsymbol{\sigma}} \cdot \hat{\mathbf{p}}) = -\hbar^2 [(\nabla V) \cdot \nabla + V \nabla^2] + \hbar \hat{\boldsymbol{\sigma}} \cdot (\nabla V) \times \hat{\mathbf{p}} \quad (431)$$

If we subtract (430) to (431) some terms vanish and by substituting this subtraction into (429) we finally find the Pauli equation

$$\left[V + \hat{T} - \frac{1}{8m_0^3c^2} \mathbf{p}^4 + \frac{\hbar^2}{8m_0^2c^2} (\nabla^2 V) + \frac{\hbar}{4m_0^2c^2} \hat{\boldsymbol{\sigma}} \cdot (\nabla V) \times \hat{\mathbf{p}} \right] \psi^N(\mathbf{x}) = E_0 \psi^N(\mathbf{x}) \quad (432)$$

Appendix II

VII. APPENDIX FOR RELATIVISTIC MANY BODY THEORY

In this second appendix, the reader can find details about many body (chapter II) derivations.

A. The pure correlation electronic Hamiltonian

In this appendix we recover the pure correlation normal-ordered electronic Hamiltonian from the original electronic Hamiltonian with the particle-hole formalism and the Wick theorem

$$\hat{H}_{\text{el}} = \sum_{pq}^{\mathbb{H} \oplus \mathbb{P}} h_{pq} \hat{p}^\dagger \hat{q} + \frac{1}{4} \sum_{pqrs}^{\mathbb{H} \oplus \mathbb{P}} \langle pq || rs \rangle \hat{p}^\dagger \hat{q}^\dagger \hat{s} \hat{r} \quad (433)$$

The first step is to rewrite the Hamiltonian into a normal-ordered form by using the relation introduced in (75), (76), let us start from the one-electron operator

$$\hat{p}^\dagger \hat{q} = \{\hat{p}^\dagger \hat{q}\} + \overline{\hat{p}^\dagger \hat{q}}. \quad (434)$$

The only non-vanishing terms are

$$\hat{p}^\dagger \hat{q} = \{\hat{p}^\dagger \hat{q}\} + \delta_{ij}, \quad (435)$$

then the one-electron part is

$$\sum_{pq}^{\mathbb{H} \oplus \mathbb{P}} h_{pq} \hat{p}^\dagger \hat{q} = \sum_{pq}^{\mathbb{H} \oplus \mathbb{P}} h_{pq} \{\hat{p}^\dagger \hat{q}\} + \sum_i^{\mathbb{H}} h_{ii}. \quad (436)$$

The two-electron string can be expanded with the Wick theorem introduced in (78)

$$\begin{aligned} \hat{p}^\dagger \hat{q}^\dagger \hat{s} \hat{r} &= \{\hat{p}^\dagger \hat{q}^\dagger \hat{s} \hat{r}\} + \{\overline{\hat{p}^\dagger \hat{q}^\dagger \hat{s} \hat{r}}\} + \{\overline{\hat{p}^\dagger \hat{q}^\dagger \hat{s} \hat{r}}\} + \{\overline{\hat{p}^\dagger \hat{q}^\dagger \hat{s} \hat{r}}\} + \{\overline{\hat{p}^\dagger \hat{q}^\dagger \hat{s} \hat{r}}\} \\ &+ \{\overline{\overline{\hat{p}^\dagger \hat{q}^\dagger \hat{s} \hat{r}}}\} + \{\overline{\overline{\hat{p}^\dagger \hat{q}^\dagger \hat{s} \hat{r}}}\} \end{aligned} \quad (437)$$

and by performing the particle-hole contractions, it simplifies to

$$\begin{aligned} \hat{p}^\dagger \hat{q}^\dagger \hat{s} \hat{r} &= \{\hat{p}^\dagger \hat{q}^\dagger \hat{s} \hat{r}\} - \delta_{p \in \mathbb{H}} \delta_{ps} \{\hat{q}^\dagger \hat{r}\} + \delta_{p \in \mathbb{H}} \delta_{pr} \{\hat{q}^\dagger \hat{s}\} + \delta_{q \in \mathbb{H}} \delta_{qs} \{\hat{p}^\dagger \hat{r}\} \\ &- \delta_{q \in \mathbb{H}} \delta_{qr} \{\hat{p}^\dagger \hat{s}\} - \delta_{p \in \mathbb{H}} \delta_{ps} \delta_{q \in \mathbb{H}} \delta_{qr} + \delta_{p \in \mathbb{H}} \delta_{pr} \delta_{q \in \mathbb{H}} \delta_{qs} \end{aligned} \quad (438)$$

where the notation $\delta_{p \in \mathbb{H}}$ means that p must be in the hole space \mathbb{H} , in other words $p = i$. Note that, the second and the fifth term get a minus sign because an odd number of permutation is needed to perform the contraction. The sixth term get

a minus sign due to an odd number of contraction bar crossing. If we insert the expression above (438) in the two-electron term in the Hamiltonian (433) we obtain

$$\begin{aligned}
\frac{1}{4} \sum_{pqrs}^{\mathbb{H} \oplus \mathbb{P}} \langle pq || rs \rangle \hat{p}^\dagger \hat{q}^\dagger \hat{s} \hat{r} &= \frac{1}{4} \sum_{pqrs}^{\mathbb{H} \oplus \mathbb{P}} \langle pq || rs \rangle \{ \hat{p}^\dagger \hat{q}^\dagger \hat{s} \hat{r} \} - \frac{1}{4} \sum_{iqr}^{\mathbb{H} \oplus \mathbb{P}} \langle iq || ri \rangle \{ \hat{q}^\dagger \hat{r} \} \\
&+ \frac{1}{4} \sum_{iqs}^{\mathbb{H} \oplus \mathbb{P}} \langle iq || is \rangle \{ \hat{q}^\dagger \hat{s} \} + \frac{1}{4} \sum_{ipr}^{\mathbb{H} \oplus \mathbb{P}} \langle pi || ri \rangle \{ \hat{p}^\dagger \hat{r} \} \\
&- \frac{1}{4} \sum_{ips}^{\mathbb{H} \oplus \mathbb{P}} \langle pi || is \rangle \{ \hat{p}^\dagger \hat{s} \} - \frac{1}{4} \sum_{ij}^{\mathbb{H}} \langle ij || ji \rangle + \frac{1}{4} \sum_{ij}^{\mathbb{H}} \langle ij || ij \rangle.
\end{aligned} \tag{439}$$

Some terms can be gathered by using these relations between antisymmetrized integrals

$$\langle pq || rs \rangle = -\langle pq || sr \rangle = -\langle qp || rs \rangle = \langle qp || sr \rangle, \tag{440}$$

and re-indexing, then the electronic Hamiltonian can be written as

$$\begin{aligned}
\hat{H}_{\text{el}} &= \sum_{pq}^{\mathbb{H} \oplus \mathbb{P}} h_{pq} \{ \hat{p}^\dagger \hat{q} \} + \sum_{ipq}^{\mathbb{H} \oplus \mathbb{P}} \langle pi || qi \rangle \{ \hat{p}^\dagger \hat{q} \} + \frac{1}{4} \sum_{pqrs}^{\mathbb{H} \oplus \mathbb{P}} \langle pq || rs \rangle \{ \hat{p}^\dagger \hat{q}^\dagger \hat{s} \hat{r} \} \\
&+ \sum_i^{\mathbb{H}} h_{ii} + \frac{1}{2} \sum_{ij}^{\mathbb{H}} \langle ij || ij \rangle.
\end{aligned} \tag{441}$$

The first two term in (441) are the Fock operator

$$\hat{F} = \sum_{pq}^{\mathbb{H} \oplus \mathbb{P}} \left[h_{pq} + \sum_i^{\mathbb{H}} \langle pi || ri \rangle \right] \{ \hat{p}^\dagger \hat{q} \} = \sum_{pq}^{\mathbb{H} \oplus \mathbb{P}} f_{pq} \{ \hat{p}^\dagger \hat{q} \} \tag{442}$$

and the two last terms are the Hartree-Fock energy

$$\langle \Phi | \hat{H}^{\text{el}} | \Phi \rangle = \sum_i^{\mathbb{H}} h_{ii} + \frac{1}{2} \sum_{ij}^{\mathbb{H}} \langle ij || ij \rangle = E^{\text{HF}}. \tag{443}$$

Finally the correlation electronic Hamiltonian \hat{H} is obtained by removing the Hartree-Fock energy (443)

$$\hat{H} = \sum_{pq}^{\mathbb{H} \oplus \mathbb{P}} f_{pq} \{ \hat{p}^\dagger \hat{q} \} + \frac{1}{4} \sum_{pqrs}^{\mathbb{H} \oplus \mathbb{P}} \langle pq || rs \rangle \{ \hat{p}^\dagger \hat{q}^\dagger \hat{s} \hat{r} \} \tag{444}$$

Appendix III

VIII. APPENDIX FOR COUPLED CLUSTER THEORY

A. The Baker-Campbell-Haussdorf truncation

Since the Hamiltonian operator \hat{H} and the excitation operators \hat{T} are constructed from creator and annihilator strings we introduce the up and down rank of \hat{H}

$$s_{\hat{H}}^+ = \frac{1}{2} (n_p^c + n_h^a) \quad (445)$$

$$s_{\hat{H}}^- = \frac{1}{2} (n_h^c + n_p^a) \quad (446)$$

where n_p^c and n_h^c are respectively the number of creator of particle and of hole, n_p^a and n_h^a are respectively the number of annihilator of particle and of hole in the operator \hat{H} . Let us define the particle rank $m_{\hat{H}}$ and the excitation rank $s_{\hat{H}}$

$$m_{\hat{H}} = s_{\hat{H}}^+ + s_{\hat{H}}^- \quad (447)$$

$$s_{\hat{H}} = s_{\hat{H}}^+ - s_{\hat{H}}^- \quad (448)$$

If $s_{\hat{H}}$ is positive, then $\hat{H} |\Phi\rangle$ represents an excited determinant of excitation rank $s_{\hat{H}}$ relative to the Fermi vacuum $|\Phi\rangle$. If $s_{\hat{H}}$ is negative, then $\hat{H}^\dagger |\Phi\rangle$ represents an excited determinant of excitation rank $|s_{\hat{H}}|$. We now examine the nested commutator of the strings \hat{H} with k excitation operators \hat{T}_{n_i} such as those in (94), the subindex n_i refers to cluster order.

$$\Omega = \left[\left[\dots \left[\left[\hat{H}, \hat{T}_{n_1} \right], \hat{T}_{n_2} \right], \dots \right], \hat{T}_{n_k} \right] \quad (449)$$

For each excitation operator \hat{T}_{n_i} , the particle rank and the excitation rank are both equal to n_i . If the commutator does not vanish, then its particle and excitation ranks are given by

$$m_{\Omega} = m_{\hat{H}} + \sum_{i=1}^k n_i - k \quad (450)$$

$$s_{\Omega} = s_{\hat{H}} + \sum_{i=1}^k n_i \quad (451)$$

In calculating the particle rank m_{Ω} , we have added the particle ranks of all the operators and subtracted k since each commutator in (449) reduces the rank by 1. (see the first chapter of [50]). In calculating the excitation rank s_{Ω} , we have added

the excitation ranks of all operators, noting that commutation does not change the excitation tank of the operators. Substracting (450) to (451), we obtain

$$m_{\Omega} - s_{\Omega} = m_{\hat{H}} - s_{\hat{H}} - k \quad (452)$$

Inserting (447) and (448) on both sides, we find that the down ranks of the commutator Ω and the operator \hat{H} are related by

$$2s_{\Omega}^{-} = 2s_{\hat{H}}^{-} - k \quad \Rightarrow \quad s_{\Omega}^{-} = s_{\hat{H}}^{-} - \frac{k}{2} \quad (453)$$

From (453) we read that each commutator reduces the down rank of the operator Ω by one-half and increases the up rank by the same amount. Since the down rank of Ω cannot be negative, we obtain the following condition on the down rank of \hat{H}

$$2s_{\hat{H}}^{-} \geq k \quad (454)$$

for the commutator expansion Ω not to vanish, since the operator \hat{H} from (36) is a two-particle operator its maximum down rank is 2 so $k \leq 4$. These conditions are generalized for all number-conserving n -particle operator in [50] if one want to work with 3-body nuclear Hamiltonian or for other purposes.

The amplitude equation can thus be written

$$\Omega_{\mu} = \langle \Phi | \hat{\tau}_{\mu}^{\dagger} \left(\hat{H} + [\hat{H}, \hat{T}] + \frac{1}{2} [[\hat{H}, \hat{T}], \hat{T}] + \frac{1}{6} [[[\hat{H}, \hat{T}], \hat{T}], \hat{T}] + \frac{1}{24} [[[[\hat{H}, \hat{T}], \hat{T}], \hat{T}], \hat{T}] \right) | \Phi \rangle \quad (455)$$

-
- [1] J. Doyle, B. Friedrich, R. V. Krems, and F. Masnou-Seeuws. Quo vadis, cold molecules? *Eur. Phys. J. D*, 31 :149, 2004.
 - [2] W. C. Stwalley, P. L. Gould, and E. E. Eyler. Ultracold Molecule Formation by Photoassociation. In R. V. Krems, W. C. Stwalley, and B. Friedrich, editors, *Cold Molecules*, chapter 5. CRC Press, Taylor & Francis Group, Boca Raton, FL, U.S.A., 2009. ISBN : 978-1-4200-5903-8.
 - [3] M Asplund, N Grevesse, A J Sauval, and P Scott. The Chemical Composition of the Sun. *Annu. Rev. Astron. Astrophys.*, 47 :481, 2009.
 - [4] P S Barklem, A K Belyaev, M Guitou, N Feautrier, F X Gadéa, and A Spielfiedel. On inelastic hydrogen atom collisions in stellar atmospheres. *Astron. Astrophys.*, 530 :A94, 2011.
 - [5] E D Commins. Electric Dipole Moments of Leptons. *Adv. Mol. Opt. Phys.*, 40 :1, 1999.
 - [6] A E Leanhardt, J L Bohn, H Loh, P Maletinsky, E R Meyer, L C Sinclair, R P Stutz, and E A Cornell. On Measuring the Electron Electric Dipole Moment in Trapped Molecular Ions, 2010. arXiv :1008.2997v2 [physics.atom-ph].
 - [7] C van Wüllen. in : M. barysz, y. ishikawa (eds.), relativistic density functional theory, relativistic methods for chemists, vol. 10, springer, heidelberg germany, 2010, isbn 978-1-4020-9974-8 (chapter 5).
 - [8] T Fleig. Relativistic Wave-Function Based Electron Correlation Methods. *Chem. Phys.*, 395 :2, 2012.
 - [9] V. V. Ivanov, D. I. Lyakh, and L. Adamowicz. Electronic Excited States in the State-Specific Multireference Coupled Cluster Theory with a Complete-Active-Space Reference. In P Čársky, J Paldus, and J Pittner, editors, *Recent Progress in Coupled Cluster Methods*, volume 11, chapter 9. Springer, Heidelberg, Germany, 2010. ISBN : 978-90-481-2884-6.
 - [10] P Čársky, J Paldus, and J Pittner, editors. *Recent Progress in Coupled Cluster Methods*. Springer, Heidelberg, Germany, 2010. ISBN : 978-90-481-2884-6.
 - [11] M. Musial and R. J. Bartlett. Intermediate Hamiltonian Fock-space multireference coupled-cluster method with full triples for calculation of excitation energies. *J.*

- Chem. Phys.*, 129 :044101, 2008.
- [12] S Hirata. Higher-order equation-of-motion coupled-cluster methods. *J. Chem. Phys.*, 121 :51, 2004.
 - [13] V. V. Ivanov, L. Adamowicz, and D. I. Lyakh. Excited states in the multireference state-specific coupled-cluster theory with the complete active space reference. *J. Chem. Phys.*, 124 :184302, 2006.
 - [14] O. Christiansen, H. Koch, and P. Jørgensen. Response functions in the CC3 iterative triple excitation model. *J. Chem. Phys.*, 103 :7429, 1995.
 - [15] H. Fliegl, C. Hättig, and W. Klopper. Coupled-cluster response theory with linear- r_{12} corrections : The CC2-R12 model for excitation energies. *J. Chem. Phys.*, 124 :044112, 2006.
 - [16] M Kállay and P Surján. Computing coupled-cluster wave functions with arbitrary excitations. *J. Chem. Phys.*, 115 :2945, 2001.
 - [17] S. Hirata M. Nooijen and R. J. Bartlett. High-order determinantal equation-of-motion coupled-cluster calculations for ionized and electron-attached states. *Chem. Phys. Lett.*, 328 :459, 2000.
 - [18] Sørensen, L. K., Fleig, T., and Olsen, J. Spectroscopic and electric properties of the LiCs molecule : a coupled cluster study including higher excitations. *J. Phys. B*, 42 :165102, 2009.
 - [19] A Köhn and J Olsen. Coupled-cluster with active space selected higher amplitudes : Performance of seminatural orbitals for ground and excited state calculations. *J. Chem. Phys.*, 125 :174110, 2006.
 - [20] L Visscher, E Eliav, and U Kaldor. Formulation and implementation of the relativistic Fock-space coupled-cluster method for molecules. *J. Chem. Phys.*, 115 :9720, 2001.
 - [21] E Eliav, M J Vilkas, Y Ishikawa, and U Kaldor. Extrapolated intermediate Hamiltonian coupled-cluster approach : Theory and pilot application to electron affinities of alkali atoms. *J. Chem. Phys.*, 122 :224113, 2005.
 - [22] S Hirata, T Yanai, R J Harrison, M Kamiya, and P-D Fang. High-order electron-correlation methods with scalar relativistic and spin-orbit corrections. *J. Chem. Phys.*, 126 :024104, 2007.
 - [23] J F Stanton and R J Bartlett. the equation of motion coupled-cluster method. A

- systematic biorthogonal approach to molecular excitation energies, transition probabilities, and excited state properties. *J. Chem. Phys.*, 98 :7029, 1993.
- [24] M. Musial and R. J. Bartlett. Multireference Fock-space coupled-cluster and equation-of-motion coupled-cluster theories : The detailed interconnections. *J. Chem. Phys.*, 129 :134105, 2008.
- [25] P A Christiansen and K S Pitzer. Electronic structure for the ground state of TIH from relativistic multiconfiguration SCF calculations. *J. Chem. Phys.*, 73 :5160, 1980.
- [26] T Fleig. Relativistic String-Based Electron Correlation Methods. In M Barysz and Y Ishikawa, editors, *Relativistic Methods for Chemists*, volume 10, chapter 10. Springer, Heidelberg, Germany, 2010. ISBN : 978-1-4020-9974-8.
- [27] J. Olsen, B. O. Roos, P. Jørgensen, and H. J. Aa. Jensen. Determinant based configuration interaction algorithms for complete and restricted configuration interaction spaces. *J. Chem. Phys.*, 89 :2185, 1988.
- [28] S Das, D Mukherjee, and M Kállay. Full implementation and benchmark studies of Mukherjee’s state-specific multi-reference coupled-cluster ansatz. *J. Chem. Phys.*, 132 :074103, 2010.
- [29] D Kedziera M Stanke and L Adamowicz. A generalization of the state-specific complete-active-space coupled-cluster method for calculating electronic excited states. *J. Chem. Phys.*, 128 :074101, 2008.
- [30] P A M Dirac. The Quantum Theory of the Electron. *Proc. Roy. Soc.*, 117 :610, 1928.
- [31] P A M Dirac. A theory of electrons and protons. *Proc. Roy. Soc.*, 126 :360, 1930.
- [32] C D Anderson. *Phys. Rev.*, 41 :405, 1932.
- [33] S Fritzsche. On the accuracy of valence-shell computations for heavy and super-heavy elements. *Eur. Phys. J. D*, 33 :15, 2005.
- [34] M Reiher and A Wolf. *Relativistic Quantum Chemistry*. Wiley-VCH, 2007.
- [35] H A Bethe and E E Salpeter. *Quantum Mechanics of One- and Two-Electron Atoms*. Springer-Verlag, Berlin, Göttingen, Heidelberg, 1957.
- [36] T.P. Das. *Relativistic Quantum Mechanics of Electrons*. Harper and Row, 1973.
- [37] P. Indelicato K.P. Ziolk J.P. Briand, P. Chevalier and D.D. Dietrich. Observation and measurement of $n=2$ to $n=1$ transitions of hydrogenlike and heliumlike uranium. *Phys. Rev. Lett.*, 65 :2761, 1990.

- [38] P. J. Mohr. Lamb shift in high- z atoms. In G.L. Malli, editor, *Relativistic Effects in Atoms, Molecules and Solids*. Plenum Press, 1983.
- [39] Kenneth G. Dyall and Knut Fægri, Jr. *Introduction to Relativistic Quantum Chemistry*. Oxford University Press, New York, 2007.
- [40] W. Greiner. *Relativistic quantum mechanics : Wave equations*. Springer, 2000.
- [41] L D Landau and E M Lifschitz. *Classical Theory of Fields*, volume II. 1939.
- [42] L D Landau and E M Lifschitz. *Quantenmechanik*, volume IV. Akademie-Verlag, Berlin, 6. auflage edition, 1989.
- [43] J J Sakurai. *Advanced Quantum Mechanics*. Addison-Wesley, Reading, Massachusetts, 1980.
- [44] J B Mann and W R Johnson. Breit Interaction in Multielectron Atoms. *Phys. Rev. A*, 4 :41, 1971.
- [45] Trond Saue. *Principles and Applications of Relativistic Molecular Calculations*. Dissertation, Department of Chemistry, Faculty of Mathematics and Natural Sciences, University of Oslo, Norway, 1995.
- [46] B. Swirles. *Proc. Roy. Soc. London A*, A152 :625, 1935.
- [47] Relativistic methods for chemists. In Y. Ishikawa M. Barysz, editor, *Challenges and advances in computational chemistry and physics*, volume 10. Springer, 2010.
- [48] H H Grelland. *J. Phys. B*, 13 :L389, 1980.
- [49] Jean-Marc Lévy-Leblond. Nonrelativistic Particles and Wave Equations. *Commun. math. Phys.*, 6 :286, 1967.
- [50] Trygve Helgaker, Poul Jørgensen, and Jeppe Olsen. *Molecular Electronic Structure Theory*. John Wiley & Sons, Chichester, 2000.
- [51] <http://www.emsl.pnl.gov/docs/global/>.
- [52] R. E. Stanton and S. Havriliak. *J. Chem. Phys.*, 81 :1910, 1984.
- [53] P Pulay. Analytical derivative techniques and the calculation of vibrational spectra. In D R Yarkony, editor, *Modern Electronic Structure Theory, Part II*, volume 2, page 1191. World Scientific Publishing Co. Pte. Ltd., Singapur, 1995.
- [54] L. Visscher, P. J. C. Aerts, O. Visser, and W. C. Nieuwpoort. Kinetic balance in contracted basis sets for relativistic calculations. *Int. J. Quantum Chem. Symp.*, 25 :131–139, 1991.

- [55] K G Dyall. Relativistic and nonrelativistic finite nucleus optimized triple zeta basis sets for the 4p, 5p and 6p elements (vol 108, pg 335, 2002). *Theoret. Chim. Acta*, 109 :284, 2003.
- [56] K G Dyall. Relativistic double-zeta, triple-zeta, and quadruple-zeta basis sets for the 5d elements Hf-Hg. *Theoret. Chim. Acta*, 112 :403, 2004.
- [57] K G Dyall. Relativistic quadruple-zeta and revised triple-zeta and double-zeta basis sets for the 4p, 5p, and 6p elements. *Theoret. Chem. Acc.*, 115 :441, 2006.
- [58] K.G. Dyall. Relativistic double-zeta, triple-zeta, and quadruple-zeta basis sets for the 4s, 5s, 6s, and 7s elements. *J. Phys. Chem. A*, page in press, 2009. (8 pages) Available online, DOI : 10.1021/jp905057q. Basis sets available from the Dirac web site, <http://dirac.chem.sdu.dk>.
- [59] K Balasubramanian. *Relativistic Effects in Chemistry Part A. Theory and techniques*. Wiley Interscience, New York, 1997.
- [60] H. A. Kramers. *Proc. Acad. Amsterdam*, 33 :959, 1930.
- [61] A. Messiah. *Quantum Mechanics*. North Holland, Amsterdam, 1967.
- [62] T Fleig. Time-reversal symmetry in general coupled cluster theory. *Phys. Rev. A*, 77 :062503, 2008.
- [63] G A Aucar, H J Aa Jensen, and J Oddershede. Operator representations in Kramers bases. *Chem. Phys. Lett.*, 232 :47, 1995.
- [64] N. Rösch. Time-reversal symmetry, kramers degeneracy and the algebraic eigenvalue problem. *Chem. Phys.*, 80 :1, 1983.
- [65] M Kállay and P Surján. Higher excitations in coupled-cluster theory. *J. Chem. Phys.*, 115 :2945, 2001.
- [66] MRCC, a string-based quantum-chemical program suite written by M. Kállay. <http://tc03.fkt.bme.hu/index.php?n=Main.HomePage>.
- [67] S Hirata. Symbolic algebra in quantum chemistry. *Theoret. Chim. Acta*, 116 :2, 2006.
- [68] R Ansaloni, G L Bendazzoli, S Evangelisti, and E Rossi. A parallel full-ci algorithm. *Comp. Phys. Commun.*, 128 :496, 2000.
- [69] J Olsen, P Jørgensen, and J Simons. Passing the one-billion limit in full configuration interaction (FCI) calculations. *Chem. Phys. Lett.*, 169 :463, 1990.
- [70] T Fleig, J Olsen, and C M Marian. The generalized active space concept for the

- relativistic treatment of electron correlation. I. Kramers-restricted two-component configuration interaction. *J. Chem. Phys.*, 114 :4775, 2001.
- [71] J Thyssen, T Fleig, and H J Aa Jensen. A direct relativistic four-component multi-configuration self-consistent-field method for molecules. *J. Chem. Phys.*, 129 :034109, 2008.
- [72] T Fleig, L K Sørensen, and J Olsen. A relativistic 4-component general-order multi-reference coupled cluster method : Initial implementation and application to HBr. *Theoret. Chem. Acc.*, 118 :347, 2007. Erratum : *Theo. Chem. Acc.*, 118 :979, 2007.
- [73] J D Talman. Minimax Principle for the Dirac Equation. *Phys. Rev. Lett.*, 57 :1091, 1986.
- [74] L Visscher. The dirac equation in quantum chemistry : Strategies to overcome the current computational problems. *j. comp. chem.* 23, 759 (2002). *J. Comp. Chem.*, 23 :759, 2002.
- [75] T. Saue. Relativistic Hamiltonians for Chemistry : A Primer. *Comp. Phys. Commun.*, 12 :3077, 2011.
- [76] Recent progress in coupled cluster methods. theory and applications. In J. Paldus J. Pittner J. Leszczynski, P. Čársky, editor, *Challenges and advances in computational chemistry and physics*, volume 11. Springer, 2010.
- [77] L K Sørensen, J Olsen, and T Fleig. Two- and four-component relativistic generalized active space coupled cluster method. Implementation and application to BiH. *J. Chem. Phys.*, 134 :214102, 2011.
- [78] Program LUCIA, a general CI code written by J Olsen, University of Aarhus, with contributions from H. Larsen and M. Fülcher.
- [79] J Olsen, B O Roos, P Jørgensen, and H J Aa Jensen. Determinant based configuration interaction algorithms for complete and restricted configuration interaction spaces. *J. Chem. Phys.*, 89 :2185, 1988.
- [80] M Hubert, L K Sørensen, J Olsen, and T Fleig. Excitation energies from relativistic coupled cluster of general excitation rank : Initial implementation and application to the silicaon atom and to the molecules XH, X =(As, Sb, Bi). *Phys. Rev. A*, 86 :012503, 2012.
- [81] T D Crawford and H F Schaefer III. An Introduction to Coupled Cluster Theory

- for Computational Chemists. In K B Lipkowitz and D B Boyd, editors, *Reviews in Computational Chemistry*, volume 14. Wiley-VCH, John Wiley and Sons, Inc., New York, 2000.
- [82] I Lindgren and J Morrison. *Atomic Many-Body Theory*, volume 3. Springer-Verlag, Berlin, 1986.
 - [83] I Shavitt and R J Bartlett. *Many-Body Methods in Chemistry and Physics. MBPT and Coupled-Cluster Theory*. Cambridge university press, 2009.
 - [84] G C Wick. The evaluation of the collision matrix. *Phys. Rev.*, 80 :268, 1950.
 - [85] N. G. Bochkarev. Molecules and their migration in the universe. *Paleototological Journal*, 44 :778, 2010.
 - [86] J. Ulmanis, J. Deiglmayr, M. Repp, R. Wester, and M Weidemüller. Ultracold Molecules formed by Photoassociation : Heteronuclear Dimers, Inelastic Collisions, and Interactions with Ultrashort Laser Pulses. *Chem. Rev.*, 112 :4890, 2012.
 - [87] C. Chin, M. G. Kozlov, and V. V. Flambaum. Ultracold molecules : new probes on the variation of fundamental constants. *New J. Phys.*, 11 :055048, 2009.
 - [88] E. R. Meyer and J. L. Bohn. Prospects for an electron electric-dipole moment search in metastable ThO and ThF⁺. *Phys. Rev. A*, 78 :010502, 2008.
 - [89] Coesterl and Kümmel. 17 :477, 1960.
 - [90] U S Mahapatra, B Datta, and D Mukherjee. A size-consistent state-specific multi-reference coupled cluster theory : Formal developments and molecular applications. *J. Chem. Phys.*, 110 :6171, 1999.
 - [91] J Olsen. The initial implementation and applications of a general active space coupled cluster method. *J. Chem. Phys.*, 113 :7140, 2000.
 - [92] L K Sørensen and T Fleig and J Olsen. A Relativistic Four- and Two-Component Generalized-Active-Space Coupled Cluster Method. *Z. Phys. Chem.*, 224 :671, 2010.
 - [93] A Szabo and N S Ostlund. *Modern Quantum Chemistry*. McGraw Hill, New York, 1982.
 - [94] Lasse K. Sørensen. *General Order Coupled-Cluster in the 4-Component Framework*. Dissertation, Mathematisch-Naturwissenschaftliche Fakultät, Heinrich-Heine-Universität Düsseldorf, 2009.
 - [95] P. Pulay. *Chem. Phys. Lett.*, 73 :393, 1980.

- [96] J Olsen and P Jørgensen. Linear and non-linear response functions for an exact state and for an MCSCF state. *J. Chem. Phys.*, 82 :3235, 1984.
- [97] H Koch and P Jørgensen. Coupled cluster response functions. *J. Chem. Phys.*, 93 :3333, 1990.
- [98] O Christiansen, P Jørgensen, and C Hättig. Response Functions from Fourier Component Variational Perturbation Theory Applied to a Time-Averaged Quasienergy. *Int. J. Quantum Chem.*, 68 :1, 1998.
- [99] P Jørgensen K Kristensen J Olsen T Helgaker, S Coriani and K Ruud.
- [100] K Hald, P Jørgensen, J Olsen, and M Jaszuński. An analysis and implementation of a general coupled cluster approach to excitation energies with application to the B₂ molecule. *J. Chem. Phys.*, 115 :671, 2001.
- [101] C Hättig K Hald and P Jørgensen. Cc3 triplet excitation energies using an explicit spin coupled excitation. *J. Chem. Phys.*, 115 :3545, 2001.
- [102] J. Olsen. Unpublished.
- [103] O Christiansen, H Koch, A Halkier, P Jørgensen, T Helgaker, and A Sánchez de Merás. Large-scale calculations of excitation energies in coupled cluster theory : The singlet excited states of benzene. *J. Chem. Phys.*, 105 :6921, 1996.
- [104] P. J. Knowles and N. Handy. *Chem. Phys. Lett.*, 111 :313, 1984.
- [105] L K Sørensen, S Knecht, T Fleig, and C Marian. Four-Component Relativistic Coupled Cluster and Configuration Interaction Calculations on the Ground and Excited States of the RbYb Molecule. *J. Phys. Chem. A*, 113 :12607, 2009.
- [106] Ralchenko, Yu ; Kramida, A E ; Reader, J. and NIST ASD Team (2008). NIST Atomic Spectra Database (version 3.1.5). Available : <http://physics.nist.gov/asd3> (2009, May 3). National Institute of Standards and Technology, Gaithersburg, MD.
- [107] LUCIAREL is a direct, relativistic double group CI program written by T Fleig and J Olsen, *MOLCAS* interface by T Fleig, 2000.
- [108] T. Fleig and M. K. Nayak. Enhanced electron electric dipole moment P,T -odd constant for HfF⁺ from relativistic correlated all-electron theory, 2013. submitted to *Phys. Rev. Lett.*, under revision.
- [109] A. R. Edmonds. Angular momentum in quantum mechanics. Princeton University Press, 1957.